



University  
of Glasgow

Tochel, Claire (2001) *Evaluation of contrast threshold measurements and simultaneous brightness ratios in the diagnosis of glaucoma*. PhD thesis.

<http://theses.gla.ac.uk/4879/>

Copyright and moral rights for this thesis are retained by the author

A copy can be downloaded for personal non-commercial research or study, without prior permission or charge

This thesis cannot be reproduced or quoted extensively from without first obtaining permission in writing from the Author

The content must not be changed in any way or sold commercially in any format or medium without the formal permission of the Author

When referring to this work, full bibliographic details including the author, title, awarding institution and date of the thesis must be given

Evaluation of contrast threshold measurements  
and simultaneous brightness ratios  
in the diagnosis of glaucoma

A thesis submitted for the degree of Doctor of Philosophy  
University of Glasgow

By

Claire Tochel

July 2001



Neuroscience and Biomedical Systems  
Institute of Biomedical and Life Sciences  
University of Glasgow

Tennent Institute of Ophthalmology  
Gartnavel General Hospital  
Glasgow

© Claire Tochel July 2001

**BEST COPY**

**AVAILABLE**

Variable print quality

## Acknowledgements

First and foremost sincere thanks go to all the friends, relatives, colleagues and strangers who volunteered their time to this project. Research like this would just not happen without people like them.

Thanks to my supervisor Dr. J.D. Morrison for his consistent support throughout the last four years, and to Dr. J.L. Jay for regular clinical back up and access to the glaucoma clinic at Gartnavel General Hospital. I am extremely grateful to both for assistance in the production of the thesis.

I am indebted to Prof. J.C. McGrath and Prof. C. Kirkness for the use of departmental facilities in IBLS and the Tennent's Institute, respectively. Thanks also to Prof. McGrath for his help as my project assessor and to Dr. D. Miller for his advice.

Thanks to Bill Biddlecombe for offering his time and expert eye to resolving one of the project's technical difficulties; to the staff of the IBLS workshop for regular technical support to the project; to Prof. Aitchison, Daniel Ortega, and others in the Department of Electronics and Electrical Engineering for their attempts to assist me with the OptiCAD software, unfortunately it was in vain.

Deepest thanks to Maureen at Gartnavel General Hospital for help acquiring case notes and patient information again and again and again – always with a smile.

Thanks also to colleagues who became friends during my last few years at the West Medical Building, especially my office-mate Sarah and to Caroline and Martin. Thanks also to Gemma for being such a good friend to me.

Special thanks to mum and dad for giving me support every step of the (very long) way, I couldn't have done this without them. Also to Lucy for putting me up (and putting up with me) all those nights when I was working too late to get home.

And finally to Gerry, thanks for the support, companionship, encouragement, understanding, patience, enthusiasm and praise you've given me, I hope I can return it with interest.

## Abstract

There is considerable dissatisfaction with the reliability and sensitivity of the methods used to assess the glaucomatous visual field. Two types of visual field test, which have been proposed as having potential in diagnosing glaucomatous visual field defects, have been modified and tested on a group of patients from a glaucoma clinic, a group of age-matched control subjects and a younger control group.

1. A grating pattern was generated using a laser interferometer which projected a large diameter image onto the retina independent of the subject's refractive error. The experimental set up which produced the most reliable and consistently low contrast threshold values in normal subjects was sought. The display characteristics which were examined included different orientations for the field quadrants as projected to the subject; stationary and flickering patterns using a variety of flicker generation methods; red and green light sources; and concentric or vertical sinusoidal grating patterns. Ultimately the optimal display was found to be a stationary image consisting of a green, vertical sinusoidal grating pattern. Arcuate regions of the visual field (at 10 to 20° from fixation) were stimulated in 4 distinct, obliquely oriented quadrants and a low spatial frequency (one cycle per degree) was chosen.
2. Normal limits were obtained from age-matched control subjects for comparison with the results for the patients from the glaucoma clinic. In the patient group, of the 13 who completed the test, 9 individuals were identified as abnormal with one or more of their contrast threshold scores exceeding that limit. The patients' Friedmann visual field plots were analysed and the amount of loss in each quadrant was quantified. There was a positive correlation between the quantified visual field loss and contrast threshold scores in 6 patients, a statistically borderline correlation in 2 patients and the absence of a correlation was found in 5 patient's results. The results for a subgroup of 6 visually abnormal eyes (not affected by glaucoma) excluded from the age-matched control group are also described. Their visual defects included mild cataract, amblyopia and retinal detachment. There were no clear abnormal results in 5 of the eyes in this group; however, in one subject with retinal scarring due to an infection, there was a distinct elevation of contrast threshold in the affected eye. Humphrey visual field plots were obtained for all but one of the age-matched control subjects.

3. Simultaneous brightness ratios (SBR) have previously been shown to provide an indication of glaucomatous damage. The same subject groups as described above were tested. SBRs were obtained for central vision in both eyes of subjects (inter-ocular ratio). This technique was now extended for the first time to paired regions within each eye (intra-ocular ratios) producing 'nasal / temporal' and 'upper / lower' ratios. In each test the subject controlled the brightness ratio which was changed in a smoothly graduated and continuous way. The most effective procedure for recording repeatable SBRs was first explored, and it was determined that these could be best obtained by alternating the start point of the graduated filter position. For each subject, 5 ratios were obtained: inter-ocular SBR; upper / lower intra-ocular SBR for right eye and left eye; and nasal / temporal intra-ocular SBR for right eye and left eye.
4. Normal limits were obtained from age-matched control subjects for comparison with the results for the patients from the glaucoma clinic. In each of the 5 SBR tests carried out, these limits were wide, reflecting considerable variation in the normal results. Of the 14 patients who completed the tests, 5 were identified as abnormal by one or more of their SBRs being outside normal limits. Three of these were identified as abnormal by their inter-ocular SBRs alone, one was abnormal according to his upper / lower intra-ocular SBR alone and one patient had an abnormal inter-ocular SBR and an abnormal intra-ocular SBR. The corresponding regions of the patients' Friedmann visual fields were quantified, and these values were used to calculate visual field loss ratios. There was a positive correlation between the visual field loss ratios and SBRs in 3 patients, but no correlation in 11 patients. In the sub-group of 6 visually abnormal eyes without glaucoma, mild cataract appeared not to adversely affect SBR. Mean SBRs were normal in the subject with retinal detachment but there was evidence of an enhanced amount of variation in the readings. Two subjects with a damaged retina and one with an amblyopic eye did produce abnormal inter-ocular SBRs, with the normal eye being significantly more sensitive in both cases.

Abstract	i
Table of Contents	iv
Table of Figures	xii
Table of Tables	xxii
Table of Equations	xxiv
Abbreviations	xxv
Chapter 1 - Introduction	1
Chapter 2 - Methods	71
Chapter 3 - Results	120
Chapter 4 - Discussion	196
Chapter 5 - Appendix	222
Chapter 6 - Bibliography	236

# Table of Contents

<b>1 Introduction</b>	<b>1</b>
<b>1.1 Problems in making the diagnosis of glaucoma</b>	<b>2</b>
<b>1.2 The healthy eye</b>	<b>3</b>
<b>1.2.1 Structure</b>	<b>3</b>
<b>1.2.2 Aqueous humour production and drainage</b>	<b>4</b>
<b>1.2.3 Retina</b>	<b>6</b>
<b>1.2.4 Ganglion cells and the optic nerve</b>	<b>7</b>
<b>1.2.5 Vascular supply</b>	<b>11</b>
<b>1.3 Clinical definition of glaucoma</b>	<b>13</b>
<b>1.3.1 Classification</b>	<b>16</b>
<b>1.4 Pathophysiology of glaucoma</b>	<b>19</b>
<b>1.4.1 Pressure mechanisms</b>	<b>19</b>
<b>1.4.2 Vasogenic mechanisms</b>	<b>22</b>
<b>1.4.2.1 Circulation defects</b>	<b>23</b>
<b>1.4.3 Cellular changes in glaucoma</b>	<b>26</b>
<b>1.4.3.1 Retinal neurones</b>	<b>26</b>
<b>1.4.3.2 Magnocellular (or large diameter) ganglion cells</b>	<b>27</b>
<b>1.4.3.3 Magnocellular LGN cells</b>	<b>29</b>
<b>1.5 Visual Field Defects</b>	<b>31</b>
<b>1.5.1 Pattern of defects</b>	<b>31</b>

<b>1.5.2 Visual field defects in relation to other glaucomatous signs</b>	<b>32</b>
<b>1.6 Glaucoma diagnosis</b>	<b>34</b>
<b>1.6.1 Diagnosis using IOP measurement</b>	<b>35</b>
<b>1.6.2 Diagnosis using optic nerve evaluation</b>	<b>36</b>
<b>1.6.3 Diagnosis using visual field examination</b>	<b>37</b>
<b>1.6.3.1 Printed sinusoidal grating patterns</b>	<b>44</b>
<b>1.6.3.2 Grating patterns externally generated by CRT or TV monitor</b>	<b>45</b>
<b>1.6.3.3 Gratings generated by laser interferometry</b>	<b>48</b>
<b>1.6.4 Diagnosis using electrophysiology</b>	<b>55</b>
<b>1.6.4.1 Electroretinogram (ERG)</b>	<b>55</b>
<b>1.6.4.2 Pattern ERG</b>	<b>56</b>
<b>1.6.4.3 Multifocal ERG</b>	<b>58</b>
<b>1.6.4.4 Visual Evoked Response (VER)</b>	<b>59</b>
<b>1.7 Effect of different definitions on prevalence</b>	<b>61</b>
<b>1.8 Risk factors for glaucoma</b>	<b>62</b>
<b>1.9 Demography</b>	<b>64</b>
<b>1.10 Treatment</b>	<b>65</b>
<b>1.11 Aims of project</b>	<b>69</b>

<b>2 Methods</b>	<b>71</b>
<b>2.1 Contrast threshold methods</b>	<b>71</b>
<b>2.1.1 Initial format of apparatus</b>	<b>71</b>
2.1.1.1 Maxwellian view	74
2.1.1.2 Intensity of light beams	75
2.1.1.3 Measurement of the field size	76
<b>2.1.2 Exploratory experiments with concentric ring pattern</b>	<b>78</b>
2.1.2.1 Peripheral rings	78
2.1.2.2 Central occlusion and quadrant	80
2.1.2.3 Psychophysical testing of illuminance of quadrants	81
2.1.2.4 Green and red diffraction patterns	83
2.1.2.5 Contrast thresholds to red versus green display	84
2.1.2.6 Stationary versus flicker	86
2.1.2.7 Quadrant orientation	90
2.1.2.8 Vertical sinusoidal grating pattern	92
<b>2.1.3 Final protocol</b>	<b>96</b>
<b>2.1.4 Conventional visual field analysis</b>	<b>99</b>
<b>2.1.5 Analysis of results</b>	<b>102</b>
<b>2.2 Simultaneous Brightness Ratios (SBR) methods</b>	<b>103</b>
<b>2.2.1 Development of apparatus</b>	<b>103</b>
2.2.1.1 Light intensity measurements	104

2.2.1.2 Apparatus	106
2.2.1.3 Pupil diameter measurements	111
<b>2.2.2 <i>Experimental protocol</i></b>	<b>112</b>
2.2.2.1 Inter-ocular SBR	113
2.2.2.2 Intra-ocular SBR	114
2.2.2.3 Repeatability of SBR measurements	115
<b>2.2.3 <i>Conventional visual field analysis</i></b>	<b>117</b>
<b>2.2.4 <i>Analysis of results</i></b>	<b>119</b>

<b>3 Results</b>	<b>120</b>
<b>3.1 Contrast threshold results</b>	<b>120</b>
<b><i>3.1.1 Stationary versus flickering display</i></b>	<b>120</b>
<b><i>3.1.2 Final protocol</i></b>	<b>124</b>
<b>3.1.2.1 Older control group subject details</b>	<b>125</b>
<b>3.1.2.2 Older control group contrast threshold determinations</b>	<b>129</b>
<b>3.1.2.3 Glaucoma group patient details</b>	<b>132</b>
<b>3.1.2.4 Glaucoma patients contrast threshold determinations</b>	<b>135</b>
<b>3.1.2.5 Young control group subject details</b>	<b>148</b>
<b>3.1.2.6 Young control group contrast threshold determinations</b>	<b>149</b>
<b>3.1.2.7 Older control group (abnormal eyes) subject details</b>	<b>154</b>
<b>3.1.2.8 Older control group (abnormal eyes) contrast threshold determinations</b>	<b>156</b>
<b><i>3.1.3 Apparatus investigations</i></b>	<b>162</b>
<b>3.1.3.1 Light intensity and contrast threshold</b>	<b>162</b>
<b>3.1.3.2 Psychophysical testing of illuminance of quadrants</b>	<b>164</b>
<b>3.1.3.3 Repeatability</b>	<b>165</b>
<b>3.2 SBR results</b>	<b>166</b>
<b><i>3.2.1 Older control group subject details</i></b>	<b>166</b>
<b><i>3.2.2 Older control group SBR determinations</i></b>	<b>166</b>
<b><i>3.2.3 Glaucoma patient group details</i></b>	<b>173</b>

<b>3.2.4 Glaucoma patient group SBR determinations</b>	<b>173</b>
<b>3.2.5 Young control group subject details</b>	<b>184</b>
<b>3.2.6 Young control group SBR determinations</b>	<b>184</b>
<b>3.2.6.1 Comparison with older control group</b>	<b>189</b>
<b>3.2.7 Older control group (abnormal eyes) SBR determinations</b>	<b>190</b>

<b>4 Discussion</b>	<b>196</b>
<b>4.1 Contrast thresholds</b>	<b>196</b>
<i>4.1.1 Concentric ring pattern</i>	196
<i>4.1.2 Stationary versus flickering grating pattern</i>	197
<i>4.1.3 Final protocol</i>	199
4.1.3.1 Older and young control groups	200
4.1.3.2 Glaucoma patient group	202
4.1.3.3 Older control group (abnormal eyes)	207
<i>4.1.4 Contrast threshold as a screening device</i>	209
<b>4.2 Simultaneous Brightness Ratio</b>	<b>211</b>
<i>4.2.1 Inter-ocular SBR</i>	211
4.2.1.1 Older and young control groups	211
4.2.1.2 Glaucoma patient group	212
<i>4.2.2 Intra-ocular SBR</i>	213
4.2.2.1 Older and young control groups	213
4.2.2.2 Glaucoma patient group	215
4.2.2.3 Older control group (abnormal eyes)	215
<i>4.2.3 SBR as a screening device</i>	217
<b>4.3 Conclusions</b>	<b>220</b>

<b>5 Appendix</b>	<b>222</b>
5.1 Lens equations	222
5.2 Humphrey Visual Field plots – older control subjects	222
5.3 Calculation of blind spot as fraction of quadrant area	231
5.4 Conversion equations for SBR readings	232
5.5 Glaucoma patient details	234
5.6 Equations used in Discussion	235
5.7 Additional analysis – monocular data	235a
5.7.1 <i>Contrast threshold</i>	235a
5.7.2 <i>Simultaneous Brightness Ratio</i>	235c
<b>6 Bibliography</b>	<b>236</b>

## Table of Figures (with page numbers)

### Chapter 1 - Introduction

- Figure 1.2-1 *Schematic representation of cross section of optic nerve head. Top: small physiological cup, a = nerve fibre layer, b = prelaminar layer, c = optic nerve. Middle: large physiological cup. Bottom: total glaucomatous cupping (taken from Kanski, McAllister and Salmon, 1995, page 21).* 8
- Figure 1.2-2 *Vascular supply and drainage of optic nerve, (taken from Anderson, in Moses and Hart, 1987 fig 20-2).* 12
- Figure 1.2-3 *Superior arcuate defect, result from kinetic perimetry examination, (taken from Henson, 1993 fig 7.5), numbers indicate degrees from fovea.* 15
- Figure 1.4-1 *Schematic representation of typical hourglass arrangement of pores in human lamina cribrosa presented 'en face'. The largest pores are found in the superior and inferior quadrants, (redrawn from Fechtner and Weinreb, 1994, fig 2).* 20
- Figure 1.4-2 *Schematic representation of the anatomical basis of visual field loss pattern caused by a nerve fibre bundle defect, (redrawn from Parr, 1989, fig 1-12).* 33

### Chapter 2 - Methods

- Figure 2.1-1 *Schematic representation of the set up for initial experiments (viewed from above), showing the combination of the green laser beam passed through a multifocal lens to produce an interference pattern of concentric rings, and the diffuse green background from the tungsten lamp, HeNe = Helium Neon.* 72
- Figure 2.1-2 *Schematic representation of the projection of the interference pattern onto the retina in the Maxwellian view, (the actual combination of lenses is simplified to a single lens for the purposes of the diagram).* 74
- Figure 2.1-3 *Plot of intensity of tungsten background light (open symbols) and laser light (filled symbols) against time.* 75
- Figure 2.1-4 *Schematic representation of the apparatus used to measure the distance of the blind spot from central fixation (at the level of the image) with respect to right eye viewing.* 77
- Figure 2.1-5 *Schematic representation of concentric light / dark ring pattern at high contrast, showing a central illuminated disc surrounded by 2 diffraction rings (left) and 3 diffraction rings (right). Fine lines appearing within the bright regions were attributed to the machining process used to etch the diffraction rings.* 78
- Figure 2.1-6 *Individual example of mean contrast threshold  $\pm$  SE to one, 2, 3, 4 and 5 diffraction rings.* 79

- Figure 2.1-7 Schematic representation of diffraction pattern consisting of 2 rings and central occluder. Mask for; A: superior temporal, B: superior nasal, C: inferior temporal, and D: inferior nasal quadrants, with reference to left eye viewing. 81
- Figure 2.1-8 Individual example of mean contrast threshold  $\pm$  SE with and without the central occluder, for field containing 2 bold peripheral diffraction rings in each of 4 quadrants. 82
- Figure 2.1-9 Schematic representation of the set up (viewed from above), used to generate interference pattern of red concentric rings. N.B. New lenses are in place above viewing position. 83
- Figure 2.1-10 Plot of tungsten background (open symbols) and laser light (filled symbols) for red display. 84
- Figure 2.1-11 Mean contrast threshold  $\pm$  SE to red and green stationary image for one subject. 85
- Figure 2.1-12 Schematic representation of set up (viewed from above) used to generate flickering stimulus, using motorised rotating polarizer. 87
- Figure 2.1-13 Schematic representation of set up (viewed from above) indicating the position of the windmill used to generate a flickering stimulus by intermittently interrupting the laser beam. N.B. Features not annotated are identical to Figure 2.1-12. 88
- Figure 2.1-14 Schematic representation of Perspex windmill (viewed from front). 89
- Figure 2.1-15 Schematic representation of windmill (viewed from front) with diffuser vanes designed to disrupt the interference pattern in order to cause flicker but allow transmission of light. 90
- Figure 2.1-16 Schematic representation of the oblique quadrant positions showing two bold diffraction rings outside central occluder; A: superior, B: nasal, C: temporal, D: inferior, with respect to left eye viewing. 91
- Figure 2.1-17 Left graph: mean contrast thresholds ( $\pm$  SE) in response to rectilinear (left) and oblique (right) quadrants. Right graph: aggregated contrast threshold data for rectilinear and oblique quadrants. 92
- Figure 2.1-18 Schematic representation of the set up (viewed from above) used to generate a sinusoidal interference grating pattern. As before features not annotated are identical to Figure 2.1-12. 94
- Figure 2.1-19 Schematic representation of the production of a laser interference pattern in the Maxwellian view with two laser beams (one lens rather than two shown for simplicity). 95
- Figure 2.1-20 Schematic representation of superior quadrant and nasal quadrant as viewed by the subject's left eye at minimal contrast, i.e. no grating pattern visible. The dimensions of the display and the fixation point are shown. 96

- Figure 2.1-21 Schematic representation of inferior quadrant and temporal quadrant, as viewed by subject's left eye, with grating pattern at high contrast. A reduced number of grating cycles is shown for simplicity. 97
- Figure 2.1-22 Friedmann visual field for patient 5-g's left eye (A) and right eye (B). Left eye field was superimposed with mask which revealed an aperture corresponding to the truncated superior quadrant of the contrast threshold test; this could be rotated to reveal the nasal, inferior and temporal quadrants. The full right eye field is shown: this was then analysed with the mask in place, as for the left eye field. 100
- Figure 2.1-23 Plot of percentage visual field loss as measured by Friedmann visual field analyser in each contrast threshold oblique quadrant region and quantified by simplified Sponsel method, for patient 5-g. 101
- Figure 2.2-1 Schematic representation of 3 black cardboard masks, created to reveal 2 squares of light of equal intensity for SBR testing. A: inter-ocular comparison B: nasal / temporal intra-ocular comparison, and C: upper / lower intra-ocular comparison. All squares have side lengths of 5cm, the bar between upper / lower and nasal / temporal squares is 0.75cm. These displays were viewed from a distance of 30cm, resulting in angular subtenses for the squares of  $10^\circ$ . 104
- Figure 2.2-2 3-D plot of the luminance of the light box output measured across the face of the box in  $\text{cd/m}^2$ . The vertical and horizontal co-ordinates are shown in mm from the top of the box and from the left edge of the box, respectively. 105
- Figure 2.2-3 Plot of light intensity (in  $\text{cd/m}^2$ ) at 6 test sites measured over 3 hours plotted against time, individual points are joined for each site, this is not a continuous recording. 105
- Figure 2.2-4 Schematic representation of counter wedge, viewed separately from graduated wedge. 106
- Figure 2.2-5 Schematic representation of filter unit (viewed from front), in the orientation used to test upper / lower intra-ocular SBR, showing fixed filter on top, and graduated density filter below the fixation point with the counter wedge in front of it. 107
- Figure 2.2-6 Schematic representation of equipment (viewed from front), used to test nasal / temporal intra-ocular SBR, showing fixed filter to left, and graduated density filter to right of fixation point. 107
- Figure 2.2-7 Schematic representation of the equipment (viewed from above) used to test inter-ocular SBR, showing fixed density filter on left, graduated filter on right, and the prisms in the Wheatstone stereoscope which divert gaze through the appropriate filters. 108
- Figure 2.2-8 Plot of log luminance plotted against the position of the graduated filter in mm, including a zero position where filter was absent. 108
- Figure 2.2-9 Calibration graph of the attenuation in log units against the position of the graduated filter, showing best fit straight line. 109
- Figure 2.2-10 Schematic representation of SBR equipment (viewed from side) showing the position of the light box and filters through which subjects viewed the squares of light at 30cm, encased by light proof hood. 112

- Figure 2.2-11 Sketch of test squares for inter-ocular SBR testing - double-sided arrow indicates that the graduated filter was positioned over the square stimulating right eye. This will be used later for clarity on graphs and tables. 113
- Figure 2.2-12 Sketch of test squares for nasal / temporal intra-ocular SBR testing - double-sided arrow indicates that the graduated filter was positioned over the square stimulating the temporal field (T) for the right eye, and the nasal field (N) for the left eye. These will be used later for clarity on graphs and tables. 114
- Figure 2.2-13 Sketch of test squares for upper / lower intra-ocular SBR testing - double-sided arrow indicates that the graduated filter was positioned over the square stimulating the lower field (L), (U indicates squares stimulating the upper field). These will be used later for clarity on graphs and tables. 115
- Figure 2.2-14 Mean inter-ocular SBR  $\pm$  SE, repeated every 10 to 15 minutes over 65 minutes, dotted line indicates the point of absolute match of the brightness sensitivity of each eye 116
- Figure 2.2-15 Friedmann plots for patient 15-g, indicating masks used to reveal points falling within SBR test regions. A: nasal / temporal comparison in left eye, B: upper / lower comparison in right eye. 117
- Figure 2.2-16 Mean percentage differences in sensitivity in Friedmann visual field plot for regions of visual field stimulated in SBR testing, for patient 15-g (R = right eye, L = left eye). 118
- ## Chapter 3 - Results
- Figure 3.1-1 Mean contrast threshold  $\pm$  SE to a stationary image and an image flickering at 4Hz and 10 Hz using the rotating mirror / polarizer for two different subjects, left shows increased contrast thresholds to both 4Hz and 10Hz, right shows reduced contrast thresholds in response to both 4Hz and 10Hz. 121
- Figure 3.1-2 Mean contrast threshold  $\pm$  SE to a stationary image and an image flickering at 4Hz and 8Hz using the solid vane windmill for two different subjects, left shows reduced contrast threshold in response to 4Hz and similar contrast threshold in response to 10Hz, right shows increased contrast thresholds in response to both 4Hz and 8Hz. 122
- Figure 3.1-3 Mean contrast threshold  $\pm$  SE to a stationary image and an image flickering at 4Hz, using the diffuser windmill showing a small but statistically significant increased contrast threshold in response to 4Hz. 123
- Figure 3.1-4 Distribution of ages for age-matched control group (i.e. older control group excluding the 3 youngest subjects: 16-n, 17-n and 18-n),  $n = 21$ . (Compare with age distribution of glaucoma group: Figure 3.1-8.) 125
- Figure 3.1-5 Four individual examples of mean contrast threshold  $\pm$  SE in control subjects for the named truncated quadrants, A: 1-n, 70 year old male, B: 5-n, 59 year old female, C: 11-n, 66 year old male, D: 14-n, 73 year old male. 129

- Figure 3.1-6 Mean contrast threshold  $\pm$  SE for age-matched control group, i.e. older control group excluding 3 youngest subjects. 130
- Figure 3.1-7 Mean contrast threshold plotted against MD for each eye of each control subject, visually abnormal eyes marked as filled symbols. Regression best-fit line is marked:  $y = 0.03 - 0.001x$ ,  $R^2 = 0.7\%$ ,  $P = 0.6$ . 131
- Figure 3.1-8 Distribution of ages for glaucoma patient group ( $n = 17$ ). 132
- Figure 3.1-9 Four individual examples of mean contrast threshold  $\pm$  SE in patients with glaucoma for the named truncated quadrants, A: 2-g, 54 year old male with LTG in right eye, B: 8-g, 55 year old female with glaucoma in right eye, C: 12-g, 70 year old male with OHT in both eyes, D: 16-g, 71 year old male with POAG in both eyes. 136
- Figure 3.1-10 Mean contrast threshold in each quadrant for both eyes of all patients in glaucoma group. Dashed line indicates a contrast threshold value of 0.073 – the upper prediction limit for normal. Open symbol indicates patients who did not complete the experiment: asterisk indicates patients for whom all mean contrast threshold values were within normal limits, triangles indicate default scores of 1.0. 137
- Figure 3.1-11 Top: mean contrast thresholds  $\pm$  SE. Middle: Friedmann Visual Field plots (left = left eye, right = right eye). Bottom: regression plot of mean contrast thresholds against quantified visual field loss, regression equation:  $y = 0.01 + 0.0003x$ ,  $R^2 = 79\%$ ,  $P = 0.003$ , for patient 1-g, a 72 year old male with POAG in both eyes. 141
- Figure 3.1-12 Top: mean contrast thresholds  $\pm$  SE. Middle: Friedmann Visual Field plots (left = left eye, right = right eye). Bottom: regression plot of mean contrast thresholds against quantified visual field loss, regression equation:  $y = 0.08 - 0.0003x$ ,  $R^2 = 0.1\%$ ,  $P = 0.9$ , for patient 16-g, a 71 year old male with POAG in both eyes. 142
- Figure 3.1-13 Top: mean contrast thresholds  $\pm$  SE. Middle: Friedmann Visual Field plots (left = left eye, right = right eye). Bottom: regression plot of mean contrast thresholds against quantified visual field loss, regression equation:  $y = 0.02 + 0.0002x$ ,  $R^2 = 49\%$ ,  $P = 0.05$ , for patient 17-g, a 73 year old male with glaucoma in left eye and a normal right eye. 143
- Figure 3.1-14 Top: mean contrast thresholds  $\pm$  SE. Middle: Friedmann Visual Field plots (left = left eye, right = right eye). Bottom: regression plot of mean contrast thresholds against quantified visual field loss – data unsuitable for regression analysis, for patient 12-g, a 70 year old male who has OHT in both eyes. 144
- Figure 3.1-15 Plot of mean contrast threshold for each quadrant in each eye of patients in glaucoma group against percentage visual field loss in same quadrant as measured by Friedmann perimetry, dotted line indicates upper prediction limit for normal. 147
- Figure 3.1-16 Distribution of ages for young control group ( $n = 20$ ). 148
- Figure 3.1-17 Four individual examples of mean contrast threshold  $\pm$  SE in young control subjects for the named truncated quadrants, A: 3-y, 21 year old female, B: 10-y, 29 year old female, C: 14-y 29 year old male, D: 18-y, 26 year old female. 150

- Figure 3.1-18 Box plots of the range of contrast thresholds in the young control group, the top of each box indicates the first quartile, the mid-line indicates the median and the bottom of the box indicates the third quartile. Note unusual spread of results for subjects 1-y and 5-y. 151
- Figure 3.1-19 Mean contrast threshold  $\pm$  SE for the named truncated quadrants in the young control group ( $n = 18$ ). 152
- Figure 3.1-20 Aggregated mean contrast thresholds  $\pm$  SE for young and older control groups. 153
- Figure 3.1-21 Mean contrast threshold  $\pm$  SE for subject 2-n (70 year old female with retinal scarring in left eye). 156
- Figure 3.1-22 Mean contrast threshold  $\pm$  SE for subject 6-n (63 year old male with surgically treated retinal detachment in right eye). 157
- Figure 3.1-23 Mean contrast threshold  $\pm$  SE for subject 7-n (69 year old female with a mild cataract in her left eye). 158
- Figure 3.1-24 Mean contrast threshold  $\pm$  SE for subject 9-n (76 year old male with poorer vision in his right eye). 159
- Figure 3.1-25 Mean contrast threshold  $\pm$  SE for subject 15-n (73 year old female with a macular hole in her right eye). 160
- Figure 3.1-26 Mean contrast threshold  $\pm$  SE for subject 23-n (59 year old female with amblyopia in her right eye). 161
- Figure 3.1-27 Regression plot for contrast threshold (in response to the vertical sinusoidal grating pattern) against the respective value for the percentage difference in intensity between background and laser beams. Regression equation is:  $y = 0.03 + 0.0002x$ ,  $R^2 = 4\%$ ,  $P = 0.004$ ,  $F = 8$ . 163
- Figure 3.1-28 Regression plot of mean foveal contrast threshold against mean peripheral contrast threshold for subjects in final protocol in each quadrant. Regression equation:  $y = 0.04 + 0.09x$ ,  $R^2 = 0\%$ ,  $P = 0.7$ , ( $n = 200$ ). 164
- Figure 3.1-29 Mean contrast threshold in response to a stationary concentric grating pattern, 4 peripheral quadrants measured hourly for 6 hours (only 3 results are visible at each test time as one result is hidden by another). 165
- Figure 3.2-1 Four individual examples of mean SBRs  $\pm$  SE for upper / lower, nasal / temporal intra-ocular comparisons and inter-ocular central comparisons in older control group subjects. A: 3-n, 70 year old male, B: 4-n, 65 year old female, C: 8-n, 61 year old female, D: 10-n, 71 year old male. R = right eye, L = left eye. 167

Figure 3.2-2 Graphs showing all mean SBR values for older control group by test; A: upper / lower right eye, B: upper / lower left eye, C: nasal / temporal right eye, D: nasal / temporal left eye, E: right / left inter-ocular. Crosses indicate subjects with visually abnormal eyes whose results are analysed in Results section 3.2.7. Open symbols on graph E indicate subjects for whom inter-pupillary difference > 0.5mm. U = upper, L = lower, N = nasal, T = temporal. 169

Figure 3.2-3 Inter-ocular mean SBR for older control subjects plotted against inter-pupillary difference. Regression equation is:  $y = 0.9 + 0.4x$ ,  $R^2 = 0\%$ ,  $P = 0.98$ . 170

Figure 3.2-4 Mean SBR  $\pm$  SE for age-matched control group, R = right eye, L = left eye. 171

Figure 3.2-5 Four individual examples of mean SBRs  $\pm$  SE for upper / lower, nasal / temporal intra-ocular comparisons and inter-ocular central comparisons in glaucoma patients. A: 2-g, 54 year old male with LTG in right eye, B: 5-g, 67 year old male with POAG in his left eye and LTG in his right eye, C: 15-g, 79 year old male with glaucoma in his left eye, D: 16-g, 71 year old male with POAG in both eyes, R = right eye, L = left eye. 173

Figure 3.2-6 Graphs showing all mean SBR values for glaucoma patients (filled symbols) and prediction limits for normal subjects marked as dashed lines, (A): upper / lower right eye, (B): upper / lower left eye, (C): nasal / temporal right eye, (D): nasal / temporal left eye, (E): right / left eye inter-ocular. N.B. Y-scales have been adjusted to include large positive and negative values – not same on all 5 graphs. Crosses indicate patients who did not complete the test. U = upper, L = lower, N = nasal, T = temporal, broken axis on Graph A used to show default score without obscuring other values. More details in text. 175

Figure 3.2-7 Top: mean SBR  $\pm$  SE for each of the 5 tests. Middle: Friedmann visual fields, Bottom: regression plot of mean SBR plotted against the ratio of visual fields (%), regression equation is:  $y = 17 + 0.3x$ ,  $R^2 = 63\%$ ,  $P = 0.1$ . All for patient 3-g, 73 year old male with POAG in both eyes. 178

Figure 3.2-8 Top: mean SBR  $\pm$  SE for each of the 5 tests. Middle: Friedmann visual fields, Bottom: regression plot of mean SBR plotted against the ratio of visual fields (%), regression equation is:  $y = 9 + 0.8x$ ,  $R^2 = 73.3\%$ ,  $P = 0.064$ . All for patient 7-g, an 83 year old male with glaucoma in both eyes. N.B. this graph includes default SBR and VF loss values of -700% for area of total visual field loss. 179

Figure 3.2-9 Top: mean SBR  $\pm$  SE for each of the 5 tests. Middle: Friedmann visual fields, Bottom: mean SBRs plotted against ratio of visual fields (%) of related areas from visual fields, data is not suitable for regression analysis, for patient 12-g, 70 year old male with OHT in both eyes. 180

Figure 3.2-10 Four individual examples of mean SBRs  $\pm$  SE for upper / lower and nasal / temporal intra-ocular comparisons, and central inter-ocular comparisons in young control subjects. A: 1-y, 24 year old female, B: 5-y, 27 year old female, C: 14-y, 29 year old male, D: 15-y, 27 year old female. R = right eye, L = left eye. 184

Figure 3.2-11 Mean SBR values for young control group by test, A: upper / lower right eye, B: upper / lower left eye, C: nasal / temporal right eye, D: nasal / temporal left eye, E: right / left eye inter-ocular. N.B. The y-axis scale is extended on graph D to include an outlying point. 186

Figure 3.2-12 Mean SBR  $\pm$  SE for young control group, R = right eye, L = left eye 187

- Figure 3.2-13 Mean SBR  $\pm$  SE for both young and older control groups for each test, R = right eye, L = left eye. 189
- Figure 3.2-14 Mean SBR  $\pm$  SE for subject 2-n (70 year old female with retinal scarring in left eye), R = right eye, L = left eye. 190
- Figure 3.2-15 Mean SBR  $\pm$  SE for subject 6-n (63 year old male with retinal detachment in right eye), R = right eye, L = left eye. 191
- Figure 3.2-16 Mean SBR  $\pm$  SE for subject 7-n (69 year old female with mild cataract in her left eye), R = right eye, L = left eye. 192
- Figure 3.2-17 Mean SBR  $\pm$  SE for subject 9-n (76 year old male with poorer vision in his right eye), R = right eye, L = left eye. 193
- Figure 3.2-18 Mean SBR  $\pm$  SE for subject 15-n (73 year old female with a macular hole in her right eye), R = right eye, L = left eye. 194
- Figure 3.2-19 Mean SBR  $\pm$  SE for subject 23-n (59 year old female with amblyopia in her right eye), R = right eye, L = left eye. 195

## Chapter 5 - Appendix

- Figure 5.2-1 Humphrey visual field plot using the Central 24-2 programme for subject 1-n, 70 year old male, MD = +0.2dB, -2.1dB, L = left eye, R = right eye. 223
- Figure 5.2-2 Humphrey visual field plot using the Central 24-2 programme for subject 2-n, 78 year old female with retinal scarring in left eye, MD = -2.2dB, -0.5dB, L = left eye, R = right eye. 223
- Figure 5.2-3 Humphrey visual field plot using the Central 24-2 programme for subject 3-n, 70 year old male, MD = 0.0dB, -1.0dB, L = left eye, R = right eye. 223
- Figure 5.2-4 Humphrey visual field plot using the Central 24-2 programme for subject 4-n, 65 year old female, MD = +1.3dB, +1.1dB, L = left eye, R = right eye. 224
- Figure 5.2-5 Humphrey visual field plot using the Central 24-2 programme for subject 5-n, 59 year old female, MD = 0.0dB, +0.8dB, L = left eye, R = right eye. 224
- Figure 5.2-6 Humphrey visual field plot using the Central 24-2 programme for subject 6-n, 63 year old male with surgically treated retinal detachment in right eye, MD = -0.7dB, -1.5dB, L = left eye, R = right eye. 224
- Figure 5.2-7 Humphrey visual field plot using the Central 24-2 programme for subject 7-n, 69 year old female with mild cataract in left eye, MD = -1.6dB, -0.7dB, L = left eye, R = right eye. 225
- Figure 5.2-8 Humphrey visual field plot using the Central 24-2 programme for subject 8-n, 61 year old female, MD = +0.2dB, +1.1dB, L = left eye, R = right eye. 225
- Figure 5.2-9 Humphrey visual field plot using the Central 24-2 programme for subject 9-n, 76 year old male with poorer vision in right eye, MD = -2.5dB, -0.9dB, L = left eye, R = right eye. Left eye shows loss of sensitivity in upper field. 225

- Figure 5.2-10 Humphrey visual field plot using the Central 24-2 programme for subject 10-n, 71 year old male, MD = -1.4dB, -0.5dB, L = left eye, R = right eye. 226
- Figure 5.2-11 Humphrey visual field plot using the Central 24-2 programme for subject 11-n, 66 year old male, MD = +0.9dB, +1.2dB, L = left eye, R = right eye. 226
- Figure 5.2-12 Humphrey visual field plot using the Central 24-2 programme for subject 13-n, 69 year old female, MD = +2.3dB, -0.6dB, L = left eye, R = right eye. Left eye shows hypersensitivity, right eye shows area of reduced sensitivity. 226
- Figure 5.2-13 Humphrey visual field plot using the Central 24-2 programme for subject 14-n, 73 year old female, MD = -1.0dB, +0.4dB, L = left eye, R = right eye. 227
- Figure 5.2-14 Humphrey visual field plot using the Central 24-2 programme for subject 15-n, 73 year old female with a macular hole in right eye - therefore unable to fixate, MD = +1.4dB, L = left eye. 227
- Figure 5.2-15 Humphrey visual field plot using the Central 24-2 programme for subject 16-n, 51 year old male, MD = 0.0dB, +1.0dB, L = left eye, R = right eye. 227
- Figure 5.2-16 Humphrey visual field plot using the Central 24-2 programme for subject 17-n, 69 year old female, MD = +0.8dB, +0.6dB, L = left eye, R = right eye. 228
- Figure 5.2-17 Humphrey visual field plot using the Central 30-2 programme for subject 18-n, 49 year old male, MD = -1.2dB, -1.3dB, L = left eye, R = right eye. 228
- Figure 5.2-18 Humphrey visual field plot using the Central 24-2 programme for subject 19-n, 52 year old male, MD = +0.9dB, 0.0dB, L = left eye, R = right eye. 228
- Figure 5.2-19 Humphrey visual field plot using the Central 24-2 programme for subject 20-n, 66 year old male, MD = -2.2dB, -3.5dB, L = left eye, R = right eye. 229
- Figure 5.2-20 Humphrey visual field plot using the Central 24-2 programme for subject 21-n, 65 year old male, MD = -0.2dB, +2.1dB, L = left eye, R = right eye. 229
- Figure 5.2-21 Humphrey visual field plot using the Central 24-2 programme for subject 22-n, 55 year old male, MD = -2.8dB, -0.8dB, L = left eye, R = right eye. 229
- Figure 5.2-22 Humphrey visual field plot using the Central 24-2 programme for subject 23-n, 59 year old female with amblyopia in her right eye, MD = 2.0dB, -2.1dB, L = left eye, R = right eye. 230
- Figure 5.2-23 Humphrey visual field plot using the Central 30-2 programme for subject 24-n, 59 year old male showing loss of sensitivity in upper field (especially in left eye), repeat testing showed similar results, but ophthalmologic examination identified no abnormality, MD = -1.7dB, -0.3dB, L = left eye, R = right eye. 230
- Figure 5.7-1 Contrast threshold readings for one eye each of patient group as compared to the upper confidence limit for age-matched normal group (dotted line), default score of 1.0 indicated by triangle, open circles indicate subjects who did not complete the experiment, asterisks indicate readings which are all within normal range 235a
- Figure 5.7-2 Mean contrast threshold ( $\pm$ SE) in older control group and young control group using monocular data. 235b

*Figure 5.7-3 . Mean intra-ocular SBRs for upper / lower (left) and nasal / temporal (right) comparisons in one eye each of glaucoma patients. Prediction limits marked by dotted lines – hatched area on right graph indicates both right and left eye limits. Crosses indicate those SBRs which fall outside confidence limit for age-matched group for that eye, open circles indicate those who didn't complete this test.*

235d

*Figure 5.7-4 Mean SBRs  $\pm$  SE of young and older control group*

235e

# Table of Tables

## Chapter 1 - Introduction

<i>Table 1.6-1 Summary of several studies (in chronological order) which have used contrast sensitivity in relation to glaucoma.</i>	51
--	----

## Chapter 3 - Results

<i>Table 3.1-1 Subject details for older control group</i>	126
<i>Table 3.1-2 Humphrey visual field analysis for older control group.</i>	128
<i>Table 3.1-3 Patient details for glaucoma group including specified diagnosis of glaucoma type from case notes</i>	134
<i>Table 3.1-4 Patient's ID with indication of whether relationship between contrast thresholds and visual field is positive (<math>P &lt; 0.05</math>), negative (<math>P &gt; 0.05</math>) or borderline (<math>P = 0.05</math>) using regression analysis, number of mean contrast thresholds which exceeded the normal limit, visual health and severity of visual field loss in each eye for all patients who completed contrast threshold experiments (i.e. not 4-g, 10-g, 11-g or 14-g).</i>	146
<i>Table 3.1-5 Subject details for young control group</i>	149
<i>Table 3.1-6 Subject details for those control subjects with visually abnormal eyes (subject identifiers relate to listing for older control group).</i>	154
<i>Table 3.1-7 Humphrey visual field analysis for each subject in control group with abnormal eyes</i>	155
<i>Table 3.2-1 Mean SBRs for age-matched control group with prediction limits and P-value for difference between mean and zero using one-sample t-test.</i>	172
<i>Table 3.2-2 Patient group's normal and abnormal SBRs, and whether relationship between SBRs and visual field is positive (<math>P &lt; 0.05</math>) or negative (<math>P &gt; 0.05</math>).</i>	181
<i>Table 3.2-3 Visual health and the severity of the imbalance in ratio of visual field loss (as measured by the Friedmann Visual Field Analyser) in paired regions relating to SBR tests of all patients who completed the SBR experiments (i.e. not 8-g, 13-g or 14-g), patient 10-g did not complete the inter-ocular test (R/L).</i>	182
<i>Table 3.2-4 Mean SBR values for young control group with prediction limits and P-values for difference between mean and zero using one-sample t-test.</i>	188

## Chapter 5 - Appendix

*Table 5.4-1 Mean SBRs for older control group with prediction limits and P-value for difference between mean and zero using one-sample t-test.* 233

*Table 5.5-1 Further details of patients' glaucoma: medications specific to glaucoma at the time of the experiments, surgery for glaucoma prior to the experiments, recorded cup to disc ratio and IOP history, and any other details from case notes relevant to visual health.* 234

*Table 5.7-1 Mean SBRs for age-matched control group with prediction limits and P-value for difference between mean and zero using one-sample t-test.* 235c

*Table 5.7-2 Mean SBRs for older and young control groups with prediction limits and P-value for difference between mean and zero using one-sample t-test.* 235d

# Table of Equations

## Chapter 1 - Introduction

*Equation 1.2-1 Goldmann equation for the factors determining IOP* 14

*Equation 1.6-1 Imbert-Fick principle for a dry, thin-walled sphere* 35

## Chapter 2 - Methods

*Equation 2.1-1 Calculation of contrast threshold value from angle of rotation of calibrated rotatable polarizer.* 73

*Equation 2.1-2 Michelson contrast value from intensity of grating pattern* 73

*Equation 2.2-1 Calibration equation for the conversion of the graduated filter position into a log value for the filter strength.* 109

## Chapter 5 - Appendix

*Equation 5.1-1 To calculate combined power of 2 lenses* 222

*Equation 5.1-2 To calculate combined power of 3 lenses* 222

*Equation 5.3-1 To convert NDF difference into a percentage difference in sensitivity* 232

## Abbreviations

°	degrees	K <sup>+</sup>	Potassium ion
μl	microlitres	LGN	lateral geniculate nucleus
μm	micrometres	LTG	low tension glaucoma
μV	microvolt	M	male
ACG	angle closure glaucoma	M-cell	magnocellular cell
BSR	brightness sense ratio	mm	millimetres
CAG	closed angle glaucoma	mmHg	millimetres of Mercury
c/deg	cycles per degree	mm <sup>2</sup>	square millimetres
cd/m <sup>2</sup>	candelas per square metre	ms	millisecond
cGMP	cyclic GMP	Na <sup>+</sup>	Sodium ion
Cl	chloride ion	nm	nanometres
CRT	cathode ray tube	NTG	normal tension glaucoma
CS	contrast sensitivity	nW	nanowatts
dB	decibels	OAG	open angle glaucoma
D	dioptries	OHT	ocular hypertension
ERG	electroretinogram	<i>P</i>	level of statistical significance
F	female	P-cell	parvocellular cell
FPR	false positive rate	POAG	primary open angle glaucoma
GLM	general linear model	POBF	pulsatile ocular blood flow
Hz	Hertz	SBR	simultaneous brightness ratio
ID	identifier	SE	standard error
IOP	intra-ocular pressure	SD	standard deviation

# 1 Introduction

Glaucoma is the end stage of several eye conditions in which damage occurs to the nerve fibres at and around the optic nerve head, causing characteristic and progressive loss of the visual field. Glaucoma itself cannot be measured as an independent variable, but is defined by the occurrence of three quantifiable clinical signs; elevated intra-ocular pressure (IOP), physical changes at the optic nerve head (e.g. increased cup to disc ratio), and visual field defects. There is considerable variation in the occurrence of these signs and the rate and extent of their pathological progression between patients. As yet, there is no precise standardised point at which clinicians or scientists agree that glaucoma begins which can be applied in all patients. Furthermore, its definition has changed from one intrinsically linked to elevated IOP, 30 or more years ago, to a more complex one which includes the 13% to 50% of patients who have glaucomatous damage and have an IOP within the 'normal' range at primary screening (Leske, 1983; Sommer *et al.*, 1991; Henson, 1993; Tuck and Crick, 1997 (a)).

This lack of universal consensus over the start of the disease is matched by a lack of understanding of the underlying causes and pathophysiological processes involved in glaucoma, despite extensive research. However, it is widely accepted that one key area in need of improvement in the management of glaucoma is that of its initial identification in patients. It is with this in mind that this project was undertaken.

## 1.1 Problems in making the diagnosis of glaucoma

As there is a lack of consensus on the defined point at which glaucoma begins in terms of extent of the visual field loss, the IOP or the amount of optic nerve head neuropathy, (Lewis, Johnson and Quigley, 1985), the moment of diagnosis of glaucoma in a patient may fall into a 'grey' area (which is confounded by the inevitable inconsistency between clinicians' interpretation of clinical signs). Clinicians may be cautious in their diagnosis due to the common and unpleasant side effects of many medications and yet, if diagnosis is delayed, there is serious risk of permanent impairment to the patient's visual field. The fact that diagnosis of glaucoma often *follows* definite visual field losses revealed by perimetry which, as will be discussed in detail later, only occurs when considerable loss of optic nerve axons has occurred, means that initiation of treatment may be delayed, albeit with the best of intentions. This delay may in fact be deliberate, where the low risk of disease progression in the mildly affected or borderline patient is outweighed by the likely high risk of treatment side effects in that patient. The known fluctuation of visual field sensitivity in glaucoma (Gloor and Vökt, 1985), exaggerated daily oscillations of IOP (Moses, in Moses and Hart, 1987), in addition to the possible inaccuracies in tonometry (Sudesh, Moseley and Thompson, 1993) and optic disc analysis (Abrams *et al.*, 1994) have all hindered the development of a more precise diagnostic method.

The relative importance of the diagnostic signs in glaucoma and which of them is the earliest sign of glaucomatous damage have been the subject of debate for over two decades. Patients may be referred to a specialist on the appearance of one of the three recognised clinical signs (elevated IOP, optic nerve head neuropathy, visual field defect) but as yet there is no standardised and recognisable severity of these signs (or combination of signs) at which glaucoma is said to begin. Thus, two or three of the above may be clearly apparent before treatment is considered (O'Brien, 1998 (b)). Therefore, there is undoubtedly variation amongst health professionals regarding the appropriate time to commence treatment. The unpredictable nature of glaucoma progression is reflected in the Royal College of Ophthalmologists guidelines which refer to the management of glaucoma in terms of using treatment to achieve an 'acceptable IOP' in the patient, coupled with adequately frequent and detailed monitoring in order for that treatment to be routinely re-evaluated (Royal College of Ophthalmologists, 1997).

## 1.2 The healthy eye

### 1.2.1 Structure

The globe of the eye is made up of three layers. The sclera is the structural, external fibrous coat which includes the cornea. Internal to this is the vascular coat, the uvea, which includes the iris, choroid and ciliary body, and finally internal to the uvea is the neural layer which consists of the retina (Davson, 1990).

The cornea forms the transparent anterior surface of the eye, which transmits light and contributes about 42 dioptres (D) to the refraction of the transmitted image. Behind this is the anterior chamber which contains aqueous humour, described in detail in the next section. Between the iris and lens is the posterior chamber, and posterior to the lens is the jelly-like vitreous humour. The vitreous humour is a clear, semisolid mass, which fills the posterior cavity of the eye, and allows light transmission and diffusion of nutrients from the ciliary body to the retina. It consists of over 99% water and dissolved salts, and contains several inorganic constituents e.g.  $\text{Na}^+$  ions,  $\text{K}^+$  ions,  $\text{Cl}^-$  ions,  $\text{HCO}_3^-$  ions and organic constituents e.g. proteins, glucose, mucopolysaccharides and collagen (Gloor, in Moses and Hart, 1987). It is held together by a fine fibrillar network composed primarily of elongated proteoglycan molecules. Substances can diffuse slowly into the vitreous humour but there is little flow of fluid (Guyton and Hall, 1996).

The shape of the lens is altered by contraction and relaxation of the ciliary muscles, such that the refractive power of the lens in a young person can vary between about 13D and 26D, allowing the focussing of images at both far and near distances, respectively (Davson, 1990).

### **1.2.2 Aqueous humour production and drainage**

The rate of aqueous humour production, together with the rate of outflow and the episcleral venous pressure, determine the level of IOP within the eyeball.

At the angle between the iris and the cornea is a drainage channel known as Schlemm's canal, through which aqueous humour is reabsorbed into the venous system. Schlemm's canal is an extremely porous, thin-walled vein which extends circumferentially all the way around the eye (Guyton and Hall, 1996). On the side nearest the aqueous humour, Schlemm's canal is covered by a meshwork of endothelium-covered trabeculae (the trabecular meshwork), through which the aqueous humour percolates before entering the canal.

Aqueous humour is formed continuously by the ciliary body in the posterior chamber, normally at a rate of around 2 microlitres ( $\mu\text{l}$ ) per minute. The epithelial cells of the ciliary body actively transport of  $\text{Na}^+$  ions into the intercellular spaces. The movement of the  $\text{Na}^+$  ions attracts  $\text{Cl}^-$  and  $\text{HCO}_3^-$  with them, maintaining electrical neutrality. The movement of these ions causes osmosis of water from the sublying tissue into the epithelial intercellular spaces. This solution travels from the spaces onto the surfaces of the ciliary processes (Guyton and Hall, 1996). Several nutrients are transported by active transport or facilitated diffusion across the epithelium including amino acids, ascorbic acid and glucose (Guyton and Hall, 1996). The active transport processes are independent of the level of IOP, but are adversely affected by hypoxia and other factors which alter metabolic rate. These processes account for 80% of the production of aqueous humour (Davson, 1990). The remaining 20% of aqueous humour production is made up of (non-energy dependent) ultra filtration. Ultra filtration (i.e. movement down a pressure gradient) occurs in the ciliary body, consisting of fluid movement from plasma into the ciliary stroma.

Diffusion (i.e. movement of a substance down a concentration gradient) allows aqueous humour to donate glucose, amino acids, oxygen, lactate and pyruvate and to remove waste products from the adjacent avascular tissues of the eye (Hoskins and Kass, 1989).

Diffusion and ultra filtration, as non-energy dependent processes, are dependent on the level of IOP, ciliary capillary blood pressure and plasma oncotic pressure (Kanski, McAllister and Salmon, 1996).

Aqueous humour passes through the pupil into the anterior chamber and is drained away into the venous system at the angle of the anterior chamber via Schlemm's canal. There is a complete turnover of aqueous humour approximately every 100 minutes (Brandt and O'Donnell, 1999).

Aqueous humour contains all the proteins present in plasma but reduced in concentration (0.02% as compared to 7% in plasma in humans). This has been interpreted as evidence for the production of at least part of the aqueous humour by the filtration of plasma, rather than being a fluid produced from constituent parts (Hoskins and Kass, 1989). It is higher in ascorbate and pyruvate, and lower in urea and glucose than plasma. Aqueous humour production reduces with increasing age and reduced ciliary muscle tone. The age-related decrease was matched by a decrease in uveoscleral out-flow in a study of visually normal subjects; consequently IOP was shown not to rise significantly with age in this sample (Toris *et al.*, 1999).

Aqueous humour production fluctuates with heart rate, respiration and may fluctuate diurnally. Hoskins and Kass report that most authors attribute diurnal variations in IOP to a variation in aqueous humour production, but some noted that drainage rate also varies through the day (Hoskins and Kass, 1989). A circadian rhythm in IOP has been recognised for many years: Davson quotes from Köllner who, in 1916, identified a peak in the early morning and a trough at about midnight (Davson, 1990). Although studies published subsequently have identified differing times for the peaks and troughs, there is general agreement that regular variation does occur naturally. For example, Liu and colleagues found a trough at the end of the day (or waking) period and a peak after the beginning of the night (or sleeping) period in a group of elderly subjects (Liu *et al.*, 1999). Pointer studied two groups of healthy subjects of the same age, one of which behaved normally (i.e. upright during day and supine at night) and another which stayed awake and upright in light conditions all night. The first group displayed a night time peak in IOP, while the second group did not, suggesting that the fluctuation is linked with body posture (Pointer, 1999).

### 1.2.3 Retina

The retina is made up of neural layers and an outer layer of pigment epithelium. The neural layers contain 2 types of light sensitive cells, known as rods and cones reflecting their shape. Photoreceptors cover the entire retina except at the blind spot, the area at which the optic nerve leaves the eye. The human retina is estimated to contain between 5 and 7 million cone photoreceptors and 75 to 150 million rod photoreceptors (Østerberg, 1935; Willis in Berne & Levy, 2000). The density of rods and cones per unit area varies across the retina. There are no rods within the central 2°. Fifty percent of cones are within  $\pm 18^\circ$  of central retina, and they peak in density at the fovea where there are approximately 140,000 per square millimetre ( $\text{mm}^2$ ) (Davson and Maida, 1984). This falls off dramatically with eccentricity such that at beyond 10° from the centre of the fovea there are relatively few cones and many more rods. The rods peak at around 20° eccentricity where there are approximately 160,000 per  $\text{mm}^2$ .

Both rod and cone photoreceptors respond to light by hyperpolarization due to a reduction in the  $\text{Na}^+$  influx into their outer segments. Cone photoreceptors can be classified as blue, green or red, according to the part of the visible spectrum to which they are most sensitive. Each class of receptor has a bandwidth at half amplitude of about 100 nanometres (nm) and a range of sensitivities to one part of the spectrum of visible light, peaking at a characteristic wavelength (420nm for blue cones, 534nm for green cones, and 563nm for red cones) (Bowmaker and Dartnall, 1980). Cone photoreceptors form synapses with the dendrites of bipolar cells which in turn synapse with ganglion cells. In the central retina, these show no convergence. Connections between these ganglion cells underlie acuity and spectral tuning. Rod photoreceptors connect to rod bipolar cells, which connect in turn to amacrine cells and ganglion cells. There is a great deal of convergence in this pathway, which underlies visual sensitivity. In addition, lateral pathways exist in the outer retina via horizontal cells which mediate inhibitory interactions between photoreceptors and in the inner retina where lateral inhibitory interactions are mediated by amacrine cells between bipolar cells and ganglion cells (Davson, 1990).

### **1.2.4 Ganglion cells and the optic nerve**

It has generally been accepted that ganglion cells subserve luminance contrast and chromatic contrast detection, although recent work by Dacey *et al.* suggests that these characteristics may initially be encoded by bipolar cells (Dacey *et al.*, 2000). Ganglion cells project information from the retina through the optic nerve towards the higher visual centres, including the lateral geniculate nucleus (LGN) and superior colliculus. There are approximately one million axons in the human optic nerve at birth, each arising from a single retinal ganglion cell (Kanski *et al.*, 1996).

The axons exit the eyeball at the optic disc through the scleral ring via holes in a laminar plate called the lamina cribrosa (indicated at the top of Figure 1.2-2). The plate is made up of collagenous connective tissue and is thought to provide mechanical support for the nerve axons. The surface of the optic nerve viewed from the front of the eye forms a disc, and within it there is an optic cup defined as 'a three-dimensional pale depression in the centre of the optic nerve head which is not occupied by neural disc tissue' (Kanski *et al.*, 1996). This is shown schematically at the top of Figure 1.2-1.

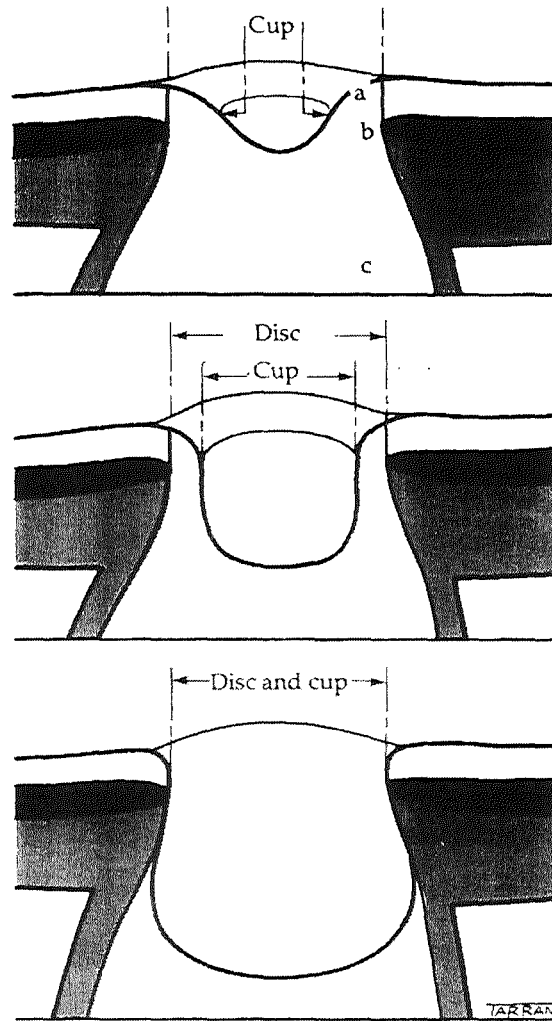


Figure 1.2-1 Schematic representation of cross section of optic nerve head. Top: small physiological cup, a = nerve fibre layer, b = prelaminar layer, c = optic nerve. Middle: large physiological cup. Bottom: total glaucomatous cupping (taken from Kanski *et al.*, 1996, page 21).

The path of the axons continues via the optic chiasma through the optic tract to arborize mainly in the LGN while some pass via the superior brachium to the superior colliculus.

The number of optic nerve axons in normal subjects can vary considerably. In a group of 13 controls with a mean age of  $69.2 \pm 11.5$  years (mean  $\pm$  standard deviation (SD)), the mean number of fibres was  $689,500 \pm 136,300$  (mean  $\pm$  SD) (i.e.  $\pm 20\%$ ) (Quigley, Dunkelberger, and Green, 1988). However it is not clear whether this is a true variation in retinae or is due to differences in preservation techniques, as the samples described in this paper were preserved by a variety of methods. Johnson *et al.* compared the total axon population and mean axon diameter in two groups of different ages (64 to 81 years and 31 to 42 years), and found that the respective means were 759,000 and 1,685,000, but that the mean axon diameter was independent of age (Johnson, Miao and Sadun, 1987). Balazsi

and colleagues found that there was a significant fall in optic nerve fibre number with age but noted that numbers also fell with time following removal of the eye (Balazsi, Rootman, Drance, Schulzer and Douglas, 1984). The number of optic fibres in each nerve decreases throughout life in a non-uniform rate of decline. In a study by Gao and Hollyfield using 35 post-mortem eyes from patients aged 18 to 95 years, the rate of loss was shown to be fastest between the second and fourth decades. The time to fixation for these eyes ranged from 20 to 180 minutes (mean  $75.5 \pm 46.9$  minutes SD) (Gao and Hollyfield, 1992).

The majority of ganglion cells can be defined by their stimulus response characteristics, receptive field size and type of LGN connections. The latter categorisation is commonly used because it encompasses ganglion cells which fall into two clearly distinct groups of cell which project to the parvocellular and magnocellular layers of the LGN and are known as parvocellular (or midget) and magnocellular (or parasol) ganglion cells which are morphologically and physiologically distinct (reviewed by Sample, Madrid and Weinreb, 1994). In the primate, the LGN cell population consists of about 75-80% parvocellular and about 10% magnocellular cells (Schiller and Malpeli, 1977; Sample, *et al.*, 1994; Lee, 1996) and a third class which contains all those not definable as magnocellular or parvocellular and which project to the superior colliculus – sometimes referred to as ‘rarely encountered cells’ (Schiller and Malpeli, 1977). The main type of midget ganglion cells, which is probably the morphological counterpart of the type I concentric single opponent cell type, is red / green sensitive. Bistratified ganglion cells are probably blue / yellow sensitive cells. Parasol ganglion cells are mainly type III concentric broadband cells and type IV red inhibitory off cells (Schiller and Malpeli, 1977). Type II cells, which are rarely encountered, are non-concentric single opponent cells (DeMonasterio, 1978). More recently, Dacey has recently reviewed the evidence that bistratified (blue / yellow sensitive) ganglion cells project to a cell population in the LGN which is intercalated between the main cellular layers (Dacey, 2000). This constitutes part of what is now termed the K or koniocellular pathway (Hendry and Reid, 2000).

The characteristics of the known types of ganglion cell and their central projections are further expanded below:

- Cytochrome-rich midget ganglion cells have very small dendritic fields in the central retina of man (5 – 10 micrometres ( $\mu\text{m}$ )) increasing in the periphery ( $225\mu\text{m}$  at  $75^\circ$  eccentricity) (Dacey, 2000). These ganglion cells are spectrally tuned, have low

luminance contrast sensitivity, respond to high spectral frequencies of sinusoidal grating patterns, generate sustained responses which dictates low temporal resolution and show linear spatial summation (Shapley and Perry, 1986). Midget cells project axons to the 4 most dorsal laminae of the LGN (the parvocellular layers), and do not project to the superior colliculus (Schiller and Malpeli, 1977). Sample *et al.* reviewed several studies and reported projections of LGN P-cells to layer 4C $\beta$  of striate cortex, to the cytochrome oxidase rich blobs and inter blobs of layers II and III, and to extra striate cortex (Sample, *et al.*, 1994).

- Parasol ganglion cells have larger dendritic fields (35–50 $\mu\text{m}$  in central retina and up to 200–1000 $\mu\text{m}$  in peripheral retina), high luminance contrast sensitivity, respond only to low spatial frequencies (although this is not agreed by all workers in this field), generate transient responses which confers high temporal resolution and may show linear spatial summation (analogous to cat X cells) or non-linear spatial summation (analogous to cat Y cells). In the LGN, the ratio of X:Y properties is 3:1. Their axons project mainly to the magnocellular layers of the LGN (the 2 ventral layers) and possibly also in a smaller proportion to the superior colliculus (Shapley and Perry, 1986; Schiller and Malpeli, 1977). Parasol ganglion cells tend to have faster conduction velocities than midget ganglion cells, but there is considerable overlap between the two groups (Schiller and Malpeli, 1977).
- Bistratified ganglion cells project to the K cells which lie in intercalated layers of the LGN which project, respectively, to the cytochrome oxidase-rich blobs of layers 2 and 3 of the primary visual cortex, to layer 1 of the primary visual cortex (relaying low-acuity visual information) and to the superior colliculus. According to recent work there may be in the order of 30,000 K-cells innervating each blob, although the concept of the blob as discrete regions with defining characteristics, has been disputed by some authors (reviewed by Hendry and Reid, 2000).
- Finally type V and VI ganglion cells project to the superior colliculus and have complex receptive field characteristics (Schiller and Malpeli, 1977; Shapley and Perry, 1986).

Both parasol and midget ganglion cells occur across the retina, with a high density of midget cells at the fovea and a greater proportion of parasol cells in the periphery. The dendritic field size of parasol cells increases with eccentricity while for midget cells there is no increase in size between zero degrees and up to 5° to 10° from the centre of the fovea (Shapley and Perry, 1986). Within each class of retinal ganglion cell, there is a minimum

overlap of dendritic fields across the retina. Each class of cell has been estimated to cover the retina fully by between 3 and 5 times, where the coverage factor indicates the number of cell centres covering a given point in visual space (Lee, 1996). Of these categories, the parasol ganglion cells have been proposed as being the most vulnerable to the effects of raised IOP (e.g. Quigley *et al.*, 1988). This will be described in more detail in later sections.

### **1.2.5 Vascular supply**

There are two separate vascular systems which supply the eye; via the retinal and the ciliary vessels (Alm and Bill, in Moses and Hart, 1987). Ciliary vessels include the vascular beds of the iris, ciliary body and the choroid. In humans the retina depends on both retinal vessels and the choroid. Human ocular blood vessels are derived from the ophthalmic artery (which arises from the internal carotid artery) and gives rise to the central retinal artery, 2 or 3 long posterior ciliary arteries and several anterior ciliary arteries. The central retinal artery enters the optic nerve about 10 millimetres (mm) behind the eye and branches into 4 vessels at the optic disc, each supplying one quadrant of the retina. The retinal vessels are distributed within the inner two-thirds of the retina. The choroidal circulation is served by the short posterior ciliary arteries. A capillary layer ('choriocapillaris') lies adjacent to the retina, separated by Bruch's membrane, and is thought to supply the avascular outer layers (including photoreceptors, pigment epithelium, bipolar cells), but may also supply the innermost layer. The optic nerve and disc are thought to be supplied by 3 major sources: retinal arterioles, the peripapillary choroid, and the centripetal branches of the short posterior ciliary arteries (see Figure 1.2-2 for schematic diagram).

The retinal venous blood is drained by a central retinal vein which leaves the eye through the optic nerve, whereas choroidal blood leaves the eye via the vortex veins. Blood from the anterior uvea is drained mainly through the vortex veins but also through anterior episcleral vessels which collect aqueous humour leaving the canal of Schlemm (Alm and Bill in Moses & Hart, 1987).

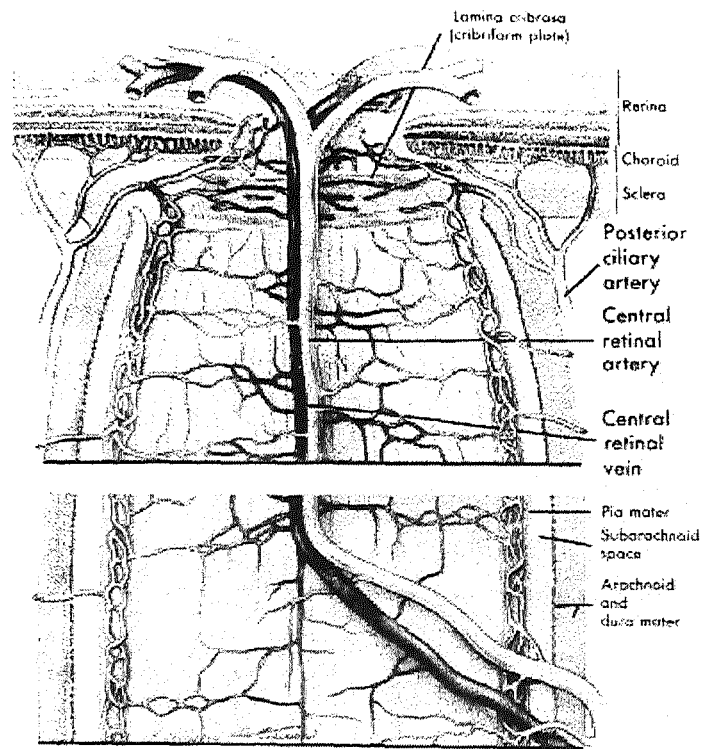


Figure 1.2-2 Vascular supply and drainage of optic nerve, (taken from Anderson, in Moses & Hart, 1987 fig 20-2)

The actual layout of the vascular supply of the human eye shows variation even in healthy individuals, with some authors reporting significant differences within a population (Fechtner and Weinreb, 1994). At the lamina cribrosa, the blood supply is thought to be from centripetal branches of the short posterior ciliary arteries, although capillary branches arising from the central retinal artery have also been identified (Fechtner and Weinreb, 1994). Interpretation of the vascular supply *in vivo* are made more controversial by disagreement over the use of different techniques and the overall difficulty in investigating such a system (Fechtner and Weinreb, 1994).

## 1.3 Clinical definition of glaucoma

Glaucoma is defined clinically by the presence (to some degree) of three measurable signs: elevated IOP, optic disc abnormality and visual field defects.

### 1. Elevated IOP

The mean IOP in a Western population is 16.5mmHg. Evaluation of the IOP in a population has shown that 95.5% of healthy eyes have an IOP between 10.5mmHg and 20.5mmHg, and 1% have an IOP of 24mmHg or greater (Davson, 1990). Two SD above the population mean (21mmHg), has therefore been long used as a 'cut off' point for 'normal' IOP, which is perhaps unhelpful as the population distribution is **not** normal, being skewed towards higher values. Some authors have stated that the quantitative analysis of IOP in glaucoma and its categorisation as 'normal' or 'abnormal' has been unwise. The clinical definition of IOP and the concept of a specific value above which IOP is defined as *abnormal* has become increasingly controversial over the last decade (Schumer and Podos, 1994; Liesegang, 1996; Drance, 1996; Sommer, 1996; Hitchings, 1997). Sommer pointed out that the *relative* risk of glaucomatous optic nerve damage may be one sixth when IOP is lower than 22mmHg of the risk when IOP is above this level, but that the number of people with IOP below 22mmHg is 20 times as great than the number with IOP above it (Sommer, 1989). This would suggest that the relative numbers of people at risk of glaucoma above and below this cut-off point is 3 to 10, respectively\*. Therefore it is not safe to ignore low IOPs in a population as there is still a risk of glaucoma. The distribution of 'normal' IOP is also population specific. A survey published in 1991 found that the mean IOP in Japan was actually lower in the older age groups: the mean IOP at ages 30 to 39 years was 13.7mmHg; at ages 50 to 59 years it was 13.4mmHg; and at ages 70 to 79 years it was 12.8mmHg. However, despite this, the prevalence of glaucoma (both angle closure glaucoma (ACG) and open angle glaucoma (OAG)) still rose with age (Shiose *et al.*, 1991).

---

\* i.e.  $1 / 6 \times 20 = 3.33$ , or roughly a 3 in 10 ratio

The factors determining IOP are shown by the Goldmann Equation:

$$\text{Equation 1.2-1} \quad P_o = F/C + P_v$$

$P_o$  = IOP (mmHg)

F = rate of aqueous production ( $\mu$ l/min)

C = ease of outflow ( $\mu$ l/min/mmHg)

$P_v$  = episcleral venous pressure (mmHg)

(Kanski *et al.*, 1996).

Toris *et al.* compared IOP and various ocular dynamic factors in the eyes of healthy subjects in two age groups (20 to 30 years, and 60 years and older). It was shown that in these subjects (with no ophthalmic disorders, and therefore not a representative sample of the population as a whole), there was no difference in IOP between the two age groups. A reduction in uveoscleral outflow of aqueous humour was present in the older group but was matched by a reduced aqueous humour production; therefore there was no resulting increase in IOP (Toris *et al.*, 1999). This suggests that the age-related increase in glaucoma prevalence (described later) is not a simple factor of IOP.

## 2. Optic disc abnormality

The optic disc consists of ganglion cell axons at the point which they exit the eye ball via the optic nerve. As glaucoma progresses, these fibres atrophy and die. As the number of fibres decreases, the optic cup, as defined in Introduction section 1.2.4, is seen to be enlarged with respect to the optic disc as a whole, as the neuroretinal rim becomes smaller (see Figure 1.2-1). Most normal eyes have a cup to disc ratio of 0.3 or less (Quigley, Addicks, Green and Maumenee, 1981; Kanski, *et al.*, 1996). Glaucomatous abnormalities of the optic nerve head can include: notching of the neural rim caused by focal fibre loss; reduced neuroretinal rim area caused by diffuse loss of fibres; cup to disc ratio greater than 0.5; and pallor of the disc (caused by loss of glial tissue) (Hoskins and Kass, 1989; Kanski *et al.*, 1996).

## 3. Visual field defects

In primary open angle glaucoma (POAG), loss of a patch of the visual field may be the first apparent symptom to the patient; however, since the typical early field loss is peripherally located, this may exist unnoticed. Common early glaucomatous defects take the form of characteristic arcuate shapes of reduced retinal sensitivity (known as

scotomata). An example of a glaucomatous visual field is shown in Figure 1.2-3, with the blindspot shown as the black oval shape and the shaded area indicating the scotomatous region of the visual field, which loops around the fovea but does not encroach on it. This may also arise in the lower hemifield, and in both cases the horizontal meridian is not crossed.

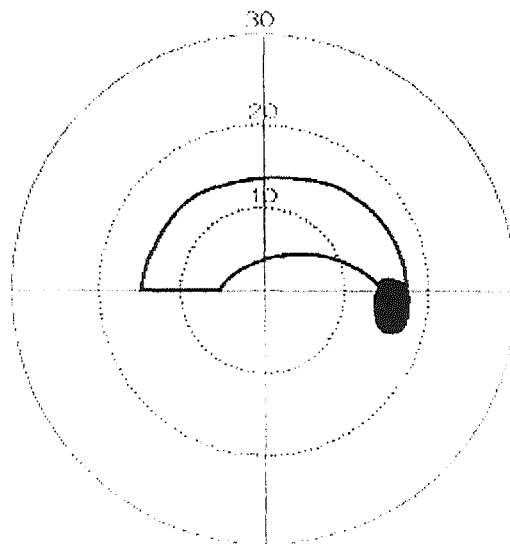


Figure 1.2-3. Superior arcuate defect, result from kinetic perimetry examination (taken from Henson 1993 fig 7.5). Numbers indicate degrees from fovea.

Other visual field defects in glaucoma include other shapes of paracentral defect, nasal step and generalised depression of sensitivity (summarised by Kitazawa and Yamamoto, 1997). However, generalised depression of visual field sensitivity that could not be explained by non-glaucomatous reasons was found in only 2 of 1582 eyes (Asman and Heijl, 1994). The latter study has been criticised for not comparing visual thresholds of glaucoma patients with those of true age-matched values (Mutlukan, 1995). Generalised depression of visual field sensitivity is also not specific to glaucoma, but can occur as a result of cataractous changes in the lens, and also as a result of the normal ageing process (Henson, 1993). Quigley *et al.* have indicated that visual field defects occur subsequent to optic nerve damage, which means that the distinction of glaucoma patients in relation to their visual field status relates to different degrees of optic nerve damage: it is not a distinction between those with and without optic nerve damage, (Quigley *et al.*, 1981).

As has already been mentioned, the occurrence and severity of these three signs (elevated IOP, optic nerve head abnormality, visual field defect) vary considerably between patients and have contributed to the lack of standardisation over the definitive point at which a patient can be said to have glaucoma. The variation has also added to the debate over whether glaucoma can be subdivided into high and low (or normal) pressure categories and there is some confusion over the use of the term *glaucoma suspect* – this will be discussed in more detail later.

### 1.3.1 Classification

Although the end result of optic nerve damage and pattern of vision loss are virtually the same for the different types of glaucoma, their relative occurrence and aetiology vary. The following breakdown has been taken from a standard glaucoma textbook (Henson, 1983):

- 5% of glaucoma is secondary to another condition e.g. trauma, or pigment dispersion syndrome, among many others.
- 95% is primary glaucoma, and of this;
  - 66% is primary open angle glaucoma (POAG). POAG is caused by impaired outflow of aqueous humour through the trabecular meshwork and Schlemm's canal. It is an insidious disease process, often with no recognisable symptoms until at a late stage, when parts of the visual field may already be lost irreversibly. A review of 15 population-based glaucoma prevalence studies found that the rate of newly detected POAG, was **at least** 46% (Tuck and Crick, 1997 (b)): in other words, almost half of the POAG cases only came to light during these population studies. It must be stressed, therefore, that one of the major problems in preventing severe visual impairment by glaucoma is detection at an early enough stage to implement effective treatment.
  - 33% is closed angle glaucoma (CAG) (or angle closure glaucoma, ACG). ACG is caused by an increase in the resistance to outflow of aqueous humour by the peripheral iris, partially or fully, blocking the trabecular meshwork resulting in an elevated IOP. This may present periodically, giving rise to symptoms which come and go. Acute ACG causes a rapid rise of IOP and severe pain, and must be treated immediately to avoid permanent damage; otherwise, the visual field may be seriously compromised within a matter of hours and blindness can occur within days (Moses in Moses & Hart, 1987).

- 1% is developmental (congenital) glaucoma, caused by a malformation of the aqueous drainage route from the eye, leading to a raised IOP (Henson, 1993).

Normal tension glaucoma (NTG) (or low tension glaucoma, LTG) may be diagnosed when optic disc changes and visual field defects are found in patients with IOP within the normal range at repeated consultations. It is not generally considered to be a distinct category of glaucoma, as all the above types may involve high or low ocular pressures. NTG is considered by some investigators to be a misleading distinction in glaucoma (Schumer and Podos, 1994; Drance, 1996). Other investigators have attempted to describe characteristics of NTG that differ from 'high tension' glaucoma. The visual field defects found in NTG were analysed by Araie *et al.* and compared to those in high-tension glaucoma. In one area of the visual field, the sensitivity in NTG patients was significantly lower than in the high tension patients 'for a given amount of visual field damage'. However, the stage of the disease process was estimated by the authors, who stated that they could not be sure that they were comparing equivalent stages of the disease in the two groups, (Araie, Yamagami and Suzuki, 1993). Hence the significance of that finding remains unclear.

The relative proportions of glaucoma described above (at the beginning of Introduction section 1.3.1) are highly population specific. In the USA, POAG accounted for 82% of the definite or probable cases of glaucoma identified in the initial screening of a population-based study (Tielsch, Katz, Singh, Quigley, Gottsch, Javitt and Sommer, 1991). People of Afro-Caribbean descent are at greater risk of developing POAG by around 4 times (Sommer, Tielsch, Katz, Quigley, Gottsch, Javitt, Singh, 1991; Wormwald, Basauri, Wright and Evans, 1994), although some authors have put the relative risk as high as 8 times (Leske, 1983). In a Japanese glaucoma survey which categorised NTG separately, the authors noted that 98% of the Japanese population is normotensive (i.e. IOP is less than 21mmHg). Of all the cases of glaucoma diagnosed in this survey, POAG accounted for 16%, NTG accounted for 57%, and ACG 10% (Shiose *et al.*, 1991). This implies that the age-related development of glaucoma is independent of IOP increases, which may be characteristic of Western populations, but not of *all* elderly people.

Another group of patients who are linked with glaucoma are those diagnosed as having ocular hypertension (OHT). OHT patients have an IOP greater than 21mmHg at more than one consultation, an absence of glaucomatous change at the optic disc and no detectable visual field defect (Kanski *et al.*, 1996). It is not clear what percentage of OHT patients

will go on to develop glaucomatous damage, and this is another area of debate. Most OHT patients (96.7%) were shown not to develop visual field defects over a 5 to 7 year follow-up period (Perkins, 1973 (a)). However, more recently it has been shown that between 3.2% and 35% of OHT patients eventually develop glaucoma (Shields 1987; Quigley *et al.*, 1994). The rate and percentage of progression of glaucomatous visual field defects is directly related to level of IOP and the duration of follow up, i.e. the longer a group of people at risk of glaucoma is followed, the more likely it is that some of them will have developed glaucomatous defects in the intervening time period. It has been estimated that between 0.1% and 1% of OHT patients incur glaucomatous damage per year (Quigley, 1990; Rasker, van den Ender, Bakker and Hoyng, 1997).

## 1.4 Pathophysiology of glaucoma

The mechanisms that cause glaucoma are still not fully understood. The contributions of mechanical, vascular and cellular changes associated with glaucoma are reviewed below.

### 1.4.1 Pressure mechanisms

While the development or occurrence of glaucoma is no longer considered to be a linear function of IOP, there is ongoing debate about whether elevated IOP causes mechanical compression of axons directly or indirectly. The level of pressure certainly does affect the functioning of the eye and the incidence of glaucomatous field defects increases with increasing pressures (Leske, 1983). Sommer evaluated the relative risk of developing glaucomatous damage in people with different levels of base-line IOP over a follow-up period of one to 13 years. The risk of developing glaucomatous damage for the subjects with an original IOP of less than 16mmHg had a relative risk was taken to be 1.0; the relative risk for those whose IOP was between 16mmHg and 19mmHg was taken to be 1.7; between 20mmHg and 23mmHg, the risk was 4.0 and those whose initial IOP was greater than or equal to 24mmHg had a relative risk of 10.5 (Sommer, 1989).

The rate of glaucomatous vision loss also increases with increasing IOP (Jay and Murdoch, 1993). The estimated time to end stage field loss (defined as the presence of absolute scotoma within 5° of fixation) in untreated eyes with POAG is 14.4 years at IOP of 21mmHg to 25mmHg, 6.5 years at 25mmHg to 30mmHg and just 2.9 years at IOP over 30mmHg (Jay and Murdoch, 1993). In acute ACG, IOP may rise to around 55mmHg to 60mmHg in hours and total field loss may occur in a few days (Moses in Moses & Hart, 1987).

In a normal population free from glaucoma and optic nerve disease, every 10mmHg increase in IOP has been found to correlate with an increase in optic cup diameter of 0.01mm; an increase in cup / disc ratio of 0.04; and a decrease in neural rim width of 0.07mm, which, the authors conclude, suggests a causal link between IOP and loss of neural tissue (Healey, Mitchell, Smith and Wang, 1997). However, it has been stated that despite extensive efforts to establish a definite link between IOP and visual field loss in

OAG, this has not been possible in individuals whose IOP is lower than 30mmHg (Cockburn, 1985, quoted in Sponsel, 1985).

The actual effect of IOP on the eye is not yet fully understood; however as IOP increases, the lamina cribrosa is thought to bow posteriorly causing the laminar plates to collapse on each other. This is thought to cause loss of nerve fibres and possibly glial cells and capillaries, thus produce cupping and pallor of the optic disc (Moses and Hart, 1987). Emery *et al.* first produced visual evidence, in the form of scanning electron micrographs of 6 eyes, with acute or chronic glaucoma and 24 normal controls, to support the theory that axon compression is a pathological event in the process of glaucomatous damage (Emery, Landis, Paton, Boniuk and Craig, 1974). Two years later, 20 eyes with glaucoma were obtained immediately following either enucleation or autopsy, and cut into sections of 40µm to 60µm thickness. They were stained, thus allowing the path of their retinal axons to be examined. This led to the statement that the 'breaking point' of the retinal ganglion cell axons could be specifically identified as the lamina cribrosa region of the optic nerve head (Vrabec, 1976). This has been confirmed by studies published subsequently (Fechtner and Weinreb, 1994; Quigley, 1995).

At the upper and lower polar quadrants, shown in Figure 1.4-1 as the dotted areas, it has been shown that there is less connective tissue, i.e. the laminar pores are larger (Fechtner and Weinreb, 1994; Quigley, 1995).

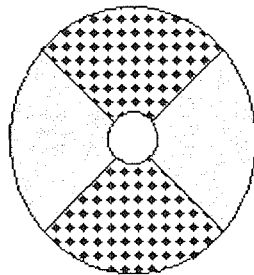


Figure 1.4-1 Schematic representation of typical hourglass arrangement of pores in human lamina cribrosa presented 'en face'. The largest pores are found in the superior and inferior quadrants (redrawn from Fechtner and Weinreb, 1994, fig. 2).

Regional differences in the density of support may be responsible for rendering fibres in the upper and lower quadrants of the lamina cribrosa more susceptible to pressure related injury (Quigley, 1995).

Findings that there are differences in the amounts of connective tissue in the lamina cribrosa in different individuals has led to hypotheses to account for the apparent different tolerances to raised IOP in people, for example in OHT patients and those with so-called NTG. Theoretically, if the former group had more substantial connective tissue at the lamina cribrosa, this may enable them to withstand greater IOP than the average person. Likewise, it has been postulated that individuals with NTG have less connective tissue in their lamina cribrosa, and therefore are less able to withstand even moderately high IOP. Quigley has presented photographic evidence to support this theory. Two humans with the same severity of visual field defects prior to death had lived with different levels of IOP in their affected eye, which averaged at about 19mmHg in one, and between 28mmHg and 35mmHg for the other over the last few years of life. The patient whose eye had the lower pressure was found on post-mortem to have a less dense laminar structure (Quigley, Addicks, Green and Maumenee, 1981).

Lampert *et al.* noted an accumulation of organelles, vesicles etc. in all damaged axons at the lamina cribrosa of monkeys with experimentally induced glaucoma. The glaucoma was induced by the injection of chymotrypsin into the posterior chamber. The optic disc and nerve were dissected out within minutes of sacrifice, and fixed in phosphate-buffered osmium tetroxide solution. Sections (2µm thick) of the nerve anterior and posterior to the lamina cribrosa were obtained using a dissecting microscope, stained using paraphenylenediamine, and screened with light microscopy. The effect of the elevated IOP (raised to 40 - 80mmHg) occurred within 12 hours and was more pronounced in eyes subjected to longer periods of elevated IOP. They postulated that the observed organelle accumulation (using electron microscopy) was due to passive aggregation caused by the restriction of axoplasmic flow. They went on to postulate further that moderately high IOP might interfere with axonal flow in advance of ischaemic axonal damage caused by reduced blood flow (Lampert, Vogel and Zimmerman, 1968).

The obstruction of axonal transport in response to elevated IOP is postulated to cause cell death (Quigley, 1995). This has been shown to be the case in experimental conditions by Minckler *et al.* who showed that horseradish peroxidase injected into the optic tract and

dorsal LGN of ocular hypertensive monkeys, accumulated at the lamina cribrosa (referred to as the lamina scleralis in this publication) when IOP was maintained above 25mmHg for 12 to 28 hours by cannulation of the anterior chamber. This, they said, indicated blockages in retrograde axoplasmic transport. <sup>3</sup>H-amino acids were injected intra-vitreally and incorporated into retinal ganglion cell proteins and, subsequent to the same IOP conditions, were shown to accumulate at the lamina cribrosa, indicating a blockage to orthograde transport. The analysis of orthograde and retrograde transport was undertaken by autoradiography and peroxidase cytochemistry, respectively. The accumulations occurred most prominently in the temporal quadrants of the optic nerve head (Minckler, Bunt and Johansen, 1977) which is at variance with the respect to the hour glass pattern of less dense support seen in humans described above and shown in Figure 1.4-1.

Gaasterland *et al.* induced glaucoma by argon laser treatment to the anterior chamber angle of monkeys for 3 to 11 weeks before sacrifice. Using light and electron microscopy they showed the accumulation of mitochondria and dense bodies both anterior and posterior to the collagenous septae of the lamina cribrosa. The authors stated that this pattern of accumulation was consistent with a local block of axoplasmic transport (Gaasterland, Tanishima and Kuwabara, 1978).

Diurnal fluctuations in IOP have been shown to play a possible role in glaucoma by Gonzalez and colleagues, who noted that 64% of OHT patients whose IOP fluctuated by more than 5mmHg, had developed visual field defects 4 to 5 years later. Of those who did not have this 'positive diurnal fluctuation', 82% had a normal visual field 5 years later (Gonzalez, Pablo, Ferrer, Melcon, Abecia and Honrubia, 1997).

### **1.4.2 Vasogenic mechanisms**

A significant effect of elevated IOP is that of disrupting the vascular systems of the eye. It is still under dispute, however, whether vascular disruptions cause glaucomatous damage or occur secondary to it (Anderson in Moses & Hart, 1987).

Minckler's experimental ocular hypertensive monkeys, in which modestly high IOP (between 25mmHg and 50mmHg) was induced, displayed evidence of blockage of

axoplasmic transport in the optic nerve head at the level of the lamina cribrosa. This occurred despite an intact nerve head capillary circulation. The authors postulated that this may discount a direct role for tissue hypoxia in causing axoplasmic disruption in the optic nerve (Minckler, Bunt and Johanson, 1977). Quigley found that capillaries were still present in the lamina cribrosa at the optic nerve head in 15 eyes of 9 humans each with a long glaucomatous history. This may suggest the maintenance of blood flow until the later stages of disc atrophy; however they could not comment on the viability of the vessels, as this was a histological study (Quigley *et al.*, 1981).

#### 1.4.2.1 Circulation defects

Findl and colleagues studied normal volunteers using a suction cup pneumatically connected to the eye and the subsequent application of a vacuum in order to temporarily elevate IOP. This raises IOP by the occlusion of the intrascleral and episcleral venous drainage (Hoskins and Kass, 1989). In the study by Findl *et al.*, 10 healthy volunteers underwent IOP increases of 10mmHg and 20mmHg. IOP was measured by Goldmann applanation tonometry, although the authors did not describe how this was achieved with the presence of the suction cup. Blood flow at the back of the eye was measured by Doppler ultrasound sonography. The subjects displayed reductions in choroidal flow, with no change noted in the ophthalmic artery flow (Findl, Strenn, Wolzt, Menapace, Vass, Eichler and Schmetterer, 1997). Ophthalmic artery blood flow defects have been found, however, in the majority of NTG patients and some POAG patients (numbers not specified), in whom ocular pulse amplitude and pulsatile ocular flow have been found to be slower than normal (reviewed by Fechtner and Weinreb, 1994).

Other circulation defects are described below:

- In a review of various qualitative analyses of ocular blood flow, Geijssen and Greve have highlighted that at least 50% of NTG patients and up to 50% of high tension glaucoma patients were shown to have a disturbance of blood flow in the posterior pole of the eye (Geijssen and Greve, 1995). These studies included some using measurements of ocular blood flow by scanning laser angiography, scanning laser Doppler flowmetry and pulsatile ocular blood flow (POBF) measurements. The authors postulated that the cases identified were 'true vascular glaucoma'. Fontana and

colleagues provided further evidence that POBF was abnormal in NTG patients with respect to normal, and also in the NTG patients' eyes with field loss with respect to those without field loss (Fontana *et al.*, 1998). Perhaps most significantly, however, Kerr *et al.* have demonstrated a difference in the POBF between normal controls, patients with POAG and those with OHT while IOP, age and blood pressure were matched between the groups, none of whom were taking glaucoma medication (Kerr, Nelson and O'Brien, 1998).

- A disturbance in the distribution of choroidal blood flow has been described in glaucoma patients by some authors. Regional differences in the distribution of posterior ciliary arteries in different individuals (including visually normal individuals) have also been described. These were interpreted to mean that some optic nerves may be more susceptible to compromise (as choroidal vessels have little or no auto regulation) (reviewed by Fechtner and Weinreb, 1994).
- Abnormalities in retinal blood flow have been highlighted by several Fluorescein angiography studies which have been reviewed by Fechtner and Weinreb. For example in patients with bilateral glaucoma but unequal levels of damage a slower retinal blood flow was found in the eye with more advanced glaucomatous damage (Fechtner and Weinreb, 1994). It is not clear, however, whether these observed defects cause glaucomatous changes or occur as a consequence of them.
- The auto-regulation of retinal blood flow has been shown to be abnormal in glaucoma patients. A review by Grunwald cites a study in which normal blood flow could not be maintained above an induced IOP of 25mmHg in patients with OAG (as opposed to 30mmHg in normals). Clearly, at such an elevated IOP the normal supply of nutrients to and removal of metabolites from retinal ganglion cells and the inner retina would be compromised (Grunwald, 1994). This may be in part due to endothelin levels in the aqueous humour or plasma - discussed in more detail below.
- Haemorrhages at the optic nerve head may occur as a result of loss of the support by the lamina cribrosa resulting in stretching and rupture of vessels (Quigley, Addicks, Green and Maumenee, 1981). However, whether local haemorrhages are primary or secondary to glaucoma is still not clear. The presence of disc haemorrhages in patients with NTG, OHT and POAG has been shown to be associated with a greater occurrence of visual field deterioration. Thirty two percent of NTG patients without disc haemorrhages had visual field deterioration while 80% of those with haemorrhages had visual field deterioration, over an average follow up of 9 years. In OHT patients, the incidence of visual field loss increased from 6% to 14% for those without and with disc

haemorrhages, respectively, while in the two equivalent groups of POAG patients the incidence was 32% and 89%, respectively (Rasker *et al.*, 1997).

- Vasoactive factors may play a role in glaucoma. Sugiyama and colleagues have investigated endothelin, a potent vasoacting peptide, and showed it to be at significantly higher plasma levels in 52 NTG patients, when compared with 10 controls (Sugiyama, Moriy, Oky and Azuma, 1995). Azuma went on to test the effect of systemic and intra vitreal injections of endothelin on the rabbit eye. Both caused a fall in IOP and in blood flow in the optic nerve head. Azuma postulated that raised endothelin levels may be related to impaired autoregulation of blood flow, leading to NTG (Azuma, 1996). Tezel *et al.* found plasma endothelin levels in POAG patients to be at normal levels, but aqueous humour endothelin levels were significantly higher than normal. The ratio of aqueous to plasma endothelin levels was 10% higher in POAG patients than in normals (Tezel *et al.*, 1997). However, the authors pointed out that they could not completely discount the effects of the patients' glaucoma medication on alterations in endothelin levels; therefore the actual link between endothelin and glaucoma, if indeed there is one, is not yet understood.

### 1.4.3 Cellular changes in glaucoma

Although the visual neurones thought to be primarily affected by glaucoma are retinal ganglion cells, other cell types have been studied.

#### 1.4.3.1 Retinal neurones

Kendal *et al.* examined human retinae taken from 14 post-mortem donations to eye banks, in which POAG had been documented and compared them to 9 age-matched eyes with no ophthalmic disease. They found no significant difference in the total number of photoreceptors, outer nuclear layer depth or number of photoreceptors per 0.1mm of retina between glaucomatous and normal eyes, measured at specific points around the fovea, (Kendall *et al.*, 1995). Janssen and colleagues showed that horizontal cells in 2 human glaucomatous retinae were 26% larger than 4 normal retinae and had dendrites which were swollen with additional varicosities. The authors postulated that these changes preceded retinal ganglion cell degeneration (Janssen *et al.*, 1997). They also noted a 'clear loss of photoreceptor outer segments', but this was not quantified or further described beyond reference to one photograph. In this study the glaucomatous eyes were both removed from patients suffering from pain due to therapy-resistant secondary glaucoma and may have represented the result of more severe compression in the retina.

Maraffa *et al.*, examined the retina with confocal laser scanning ophthalmoscopy and found that the retinal nerve fibre layer was significantly thinner in glaucoma patients than in normals. The authors identified a patient subgroup they described as having 'glaucoma' but *normal* visual fields and found the nerve fibre layer was also significantly thinner than in normals. (Maraffa *et al.*, 1997).\*

---

\* Maraffa defined glaucomatous eyes as those having at least 2 out of 3 of the following signs: IOP greater than 23mmHg without treatment; optic disc change apparent by ophthalmoscopy and visual field defects. This group of so-called glaucoma patients could therefore include NTG patients and what other authors would refer to as glaucoma suspects; this will be discussed in more detail later.

### 1.4.3.2 Magnocellular (or large diameter) ganglion cells

The selective loss of magnocellular (parasol) ganglion cells and, less specifically, larger retinal ganglion cells of all types early in the glaucomatous process has been proposed by several authors (Dandona, Hendrickson and Quigley, 1991; Glovinsky, Quigley and Dunkelberger, 1991; Anderson and O'Brien, 1997) and disputed by several others (Morgan, 1994; Johnson, 1994; Graham, 1997; Crawford *et al.*, 2000; Morgan, Uchida and Caprioli, 2000).

Quigley and colleagues showed that, when chronic experimental glaucoma was induced by laser damage to the trabecular meshwork in monkeys for a duration of 6 to 16 months, the mean ganglion cell axon diameter across the retina was significantly reduced. The mean diameter of axons in the 'normal' eye was  $0.85\mu\text{m}$  compared with  $0.74\mu\text{m}$  in the experimental glaucomatous eye, a statistically significant difference (Quigley *et al.*, 1987). Quigley and his colleagues proposed that the larger cells atrophied more rapidly (although all sizes were affected), partly due to their relative higher proportion in the superior and inferior quadrants of the optic nerve, but noted that they were also more susceptible in other areas of the optic nerve. In 1988, Quigley and colleagues showed similar effects of chronic elevated IOP in human retinae which had been obtained by enucleation and had been stored at an eye bank. Fibres were lost 2 to 3 times more rapidly in the superior and inferior peripheral sectors of the optic nerve compared with age-matched normal controls – this relates to the 'hour glass' image in Figure 1.4-1. They also found that fibres larger than  $0.7\mu\text{m}$  diameter showed disproportionately greater loss than narrower fibres (Quigley *et al.*, 1988).

Further evidence from experimental glaucoma studies in 1991 indicated that the magnitude of size dependent cell loss was related to the stage of glaucoma. Four monkeys had glaucoma induced by argon laser trabecular treatment creating an IOP of between 24 and 55mmHg. They were sacrificed between 6 and 24 months later displaying a range of glaucomatous damage to the optic nerve. Ganglion cell size and distribution was calculated at 6 sites in each optic nerve and it was found that large cells were preferentially lost at each stage of damage, but in varying relative amounts. The ganglion cell counts from the corresponding area of the paired (normal) eye were used to define the number of ganglion cells lost and by implication the stage of glaucoma in each test site, e.g. early, intermediate or advanced. In areas of retina with glaucoma in its early stages and advanced

stages there was a moderate size-dependent loss of ganglion cells. The greatest amount of size-dependent loss occurred at intermediate stages when around 50% of the total number of ganglion cells remained (Glovinsky *et al.*, 1991).

The theory of selective loss of large diameter ganglion cells view has been challenged by Morgan with the suggestion that non-selective cell shrinkage of retinal ganglion cells in glaucoma, before cell death would leave a general trend towards remaining cell sizes being smaller (Morgan, 1994). He pointed out that a decrease in the number of cells in a particular part of the cell size distribution pattern does not equate to a selective loss of one class of cell. Quigley replied by stating that, in the experiments quoted from, the process of cell death was fast enough to suggest that shrinkage did not account for the number of fibre losses (Quigley, 1994).

Johnson reviewed the topic of size (or type) selective loss and argued that, despite evidence for selective loss of larger diameter ganglion cells, the hypothesis should be interpreted with caution for a number of reasons:

- most of the main studies had small sample sizes,
- mild glaucomatous damage does not cause size selective losses according to some authors,
- histo-pathological studies are unable to identify functional cell types.

This latter point has been addressed by Anderson and O'Brien who provided psychophysical evidence for the selective loss of magnocellular ganglion cells in 1997. They tested the acuity of normal subjects, patients with OHT and POAG using sinusoidal grating patterns at 10° and 20° eccentricity. The authors state that using stationary and flickering stimuli target parvocellular and magnocellular ganglion cells, respectively. They demonstrated that the reduction in the acuity which was found for patients with OHT and POAG was greater when magnocellular ganglion cells were preferentially stimulated (Anderson and O'Brien, 1997).

The authors who question the theory of size selective loss do not generally reject it outright; rather they suggest that working exclusively to the theory may hinder the development of early, accurate detection of defects in glaucoma. Johnson developed the theory of 'reduced redundancy' (previously proposed by Glovinsky *et al.* in terms of the 'functional reserve' of the magnocellular system which has a greater coverage of each

retinal point than the parvocellular – 3.4 times compared to 1.9 times), which stresses that the greatest relative loss from a single subpopulation of cells may not yield the earliest defects, due to the remaining overlap of receptive fields. Thus, when considering the development of new tests for diagnosing early glaucomatous damage, one must take into account which populations of ganglion cells have both reduced redundancy as well as a fall in total number (Johnson, 1994; Glovinsky *et al.*, 1991).

The effects of IOP elevation on optic nerve fibres have also been studied in non-primates. Brief pressure elevation to moderate and severe levels (actual levels not defined) applied to the cat optic nerve was shown, when examined several weeks later, to have caused alterations to the proportions of ganglion cell types. The incidence of recorded Y cells (also known as brisk transient cells) fell from 77% of the total number of axonal recordings from the optic nerve to 68.8% in moderate pressure and to 5.2% in severe pressure (Rose, Levick and Burke, 1997). A study published in early 1998 has shown that raising IOP in the rat to 1.5-1.8 times normal by episcleral vein cauterization (which leaves retinal blood flow intact) caused retinal ganglion cells to die uniformly across the retina at about 4% per week for the first two weeks. Beyond this point however, the ratio of peripheral retinal ganglion cells increased relative to the middle and central retina. At 10 weeks, the peripheral loss of 63.2% contrasted with a middle and central retinal ganglion cell loss of 37.2% and 36.5%, respectively (Laquis, Chaudhary and Sharma, 1998).

#### **1.4.3.3 Magnocellular LGN cells**

Dandona *et al.* used <sup>3</sup>H-proline labelling of monkey optic nerves to monitor the amount of axonal transport to the LGN. Thereafter, IOP was elevated by argon laser treatment of the trabecular meshwork. Chronic IOP elevation involved holding IOP at 35 - 48mmHg for 2 to 44 weeks and acute elevation involved IOP held at 40 - 100mmHg for 12 hours. The magnocellular layers of the LGN in the eye with chronic elevation were shown to have a significantly reduced amount of labelling when compared to the normal eye. Acute elevation of IOP, however, did not produce a consistent difference in the relative labelling of the parvocellular and magnocellular layers (Dandona *et al.*, 1991).

Morgan noted that although there is a greater number of parvocellular ganglion cells, the magnocellular cells tend to have larger terminal axons. He suggests that the same

percentage of shrinkage in such cells would give a greater absolute volume change in the magnocellular layers (Morgan, 1994).

Functionally, one might expect the proposed early, disproportionately great loss of magnocellular cells in glaucoma to show up as deficits in tests using low spatial frequency or high temporal frequency stimuli, but not as deficits in colour sensitivity, high spatial frequency discrimination and in low temporal frequency tests. However, as Sample and colleagues note, deficits have been identified in glaucoma patients which encompass both magnocellular and parvocellular pathways (Sample *et al.*, 1994). Johnson quotes motion coherence, flicker and temporal-modulation sensitivity as tests able to isolate magnocellular responses and show deficits in glaucoma. He also quotes high pass resolution perimetry and short-wavelength automated perimetry as tests which show deficits in glaucoma which are believed to be mediated by the parvocellular system (Johnson, 1994). Merigan *et al.*, 1991 have shown that luminance detection to low spatial frequency stimuli presented at 10Hz flicker is mediated by both magnocellular and parvocellular pathways (Merigan, Katz and Maunsell, 1991).

## 1.5 Visual Field Defects

### 1.5.1 Pattern of defects

Aulhorn and Karmeyer have characterised early glaucomatous visual field defects by recording their size and location on a circular mesh which encompassed 228 regularly shaped areas within  $\pm 30^\circ$  from the fovea (Aulhorn and Karmeyer, 1977). This was used to standardise the visual field results of 400 patients with definite or suspected glaucoma. They were tested with various perimeters (not specified in the article) in order to characterise common patterns of glaucomatous visual field defects in terms of the frequency of defects in specific areas. They identified several features of defects in early glaucoma:

- lower hemifield defects tended to arise further from the centre of the visual field than upper hemifield defects,
- the frequency of scotomata was roughly the same in upper and lower hemifields,
- in the upper half of the visual field, scotomata were roughly symmetrically distributed, lying arcuately around the centre, while in the lower half they lay predominantly in the nasal quadrant (Aulhorn and Karmeyer, 1977).

Also the relative occurrence of peripheral and central field defects has been compared in the right eyes of 100 glaucoma patients and suspects (Ballon, Echelman, Shields and Ollie, 1992). The central fields were tested with a static target at points extending to  $24^\circ$  from fixation in all quadrants, except in the nasal quadrant which extended to  $30^\circ$ . Peripheral fields were tested with kinetic targets presented between  $60^\circ$  and  $70^\circ$ . Ballon *et al.* noted that virtually all the peripheral visual field defects recorded with the Humphrey Visual Field Analyser occurred in the nasal quadrant. In 69 eyes, defects in the peripheral field were found where the central fields were either questionable or glaucomatous. However, 4 eyes had a normal central field and a glaucomatous peripheral field, and the peripheral field was normal in spite of questionable or definite central defects in 10 eyes (Ballon *et al.*, 1992).

### **1.5.2 Visual field defects in relation to other glaucomatous signs**

Drance has proposed that other psychophysical disturbances (such as colour and contrast sensitivity) in glaucoma precede relative scotomata (relative scotomata occur when visual thresholds are increased, though the area of retina is still responsive to stronger stimuli) (Drance, 1985). He suggested that fluctuations in the patient's threshold for such tests may occur, i.e. the patient's sensitivity thresholds may oscillate, rather than simply increase over time (Drance, 1985). He also postulated that glaucomatous damage develops by more than one mechanism due to the fact that all the signs of glaucomatous damage were not found in all patients. For example, one quarter of patients with glaucoma had normal colour vision and one third of asymmetric OAG patients had a contracted central isopter (the boundary of the most sensitive region of the retina) in the eye without the nerve fibre bundle defect (Drance, 1985). In other words, various visual modalities fail first and deteriorate at different rates among individual patients.

Although foveal vision usually survives until late in the development of glaucoma, this does not mean that the foveal ganglion cells are not damaged. Experimental models in the monkey have shown that the amount of the loss of cells at the fovea is indistinguishable from the loss at 10° to 12° into the periphery. The impact of early visual defects on vision is said to be delayed by the retina's functional reserve which is quite considerable especially at the fovea (Desatnik, Quigley and Glovinsky, 1996). For example, it has been widely cited that one human eye used in a study by Quigley *et al.* had lost 44% of optic nerve axons relative to the mean of the age-matched control group, despite Goldmann visual field testing showing no defect shortly before removal of the eye (Quigley *et al.*, 1988).

The pattern of field loss correlates with the location and extent of optic nerve fibre losses. Loss of fibres at the superior and inferior quadrants of the optic nerve correlates with the nature of typical glaucomatous field losses, which often include areas served by arcuate fibres (Quigley, Addicks and Green, 1982).

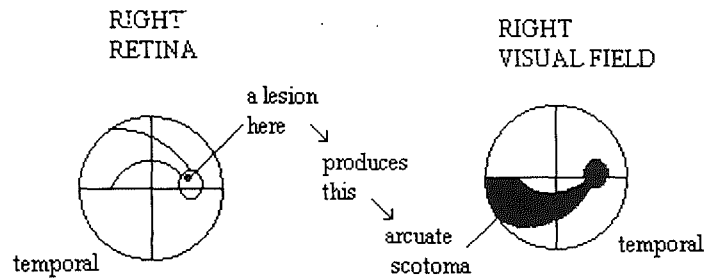


*Figure 1.4-2 Schematic representation of the anatomical basis of visual field loss pattern caused by a nerve fibre bundle defect (redrawn from Parr, 1989, fig 1-12)*

Figure 1.4-2 shows a schematic representation of the retina and the associated visual field defect that would occur with a lesion of the optic disc as marked. This would occur due to the detrimental effect of pressure on the ganglion cell axons in a nerve bundle which enters the optic nerve at the supero-temporal aspect of the optic disc (Parr, 1989).

## 1.6 Glaucoma diagnosis

As already indicated, when a population is screened for glaucoma, one new case is generally found for each one already diagnosed. When investigating the question of why glaucoma is underdetected, Tuck and Crick investigated different patterns of primary screening techniques used by optometrists. They showed that optometrists who used tonometry on more than half of their patients and visual field tests on more than 15% of patient eye tests detected several times more cases of glaucoma (which were confirmed at referral) than optometrists who used tonometry and visual field testing less regularly, (Tuck and Crick, 1997 (a)).

As discussed in Introduction section 1.4.3, the proposed loss of different types of cell with distinct functional properties would suggest that tests which target the appropriate population of ganglion cell may be able to identify early defects. This has driven the investigations of motion detection threshold, temporal and spatial contrast sensitivity, colour discrimination, short wavelength automated perimetry and high pass resolution perimetry as potential glaucomatous screening tests. These have all been tested primarily on the central visual field and are discussed in more detail in Introduction section 1.6.3. These may be used to pick up the earliest signs of glaucoma in the visual field, which standard perimetry fails to identify. However, in the clinical context, no new test has been accepted as efficient and quick enough to replace the standard Goldmann, Friedmann or Humphrey Visual Field Analysers. This may be a serious shortfall in the diagnostic procedure as considerable evidence has indicated that, by the time glaucoma has been diagnosed on the basis of a characteristic optic disc and visual field changes (as measured by the above mentioned perimeters) together with a possible rise in IOP, several visual functions have already been compromised. The limitations of the standard diagnostic procedures have led the search for a new more effective diagnostic tool.

The debate over which glaucomatous change occurs first continues to be paramount as early diagnosis and treatment of glaucoma is the only way of ensuring protection of the visual field. Perimetry is still used clinically along with IOP measurements to diagnose glaucoma, both of which can be quantified and thus compared to previous data. It has been suggested by Lewis and Johnson that psycho-physical disturbances revealed by automated perimetry, colour vision testing, contrast sensitivity determinations and flicker detection, and abnormal electrophysiological recordings are the most useful tools in diagnosing

glaucoma. They consider them to be more reliable and reproducible than the subjective optic disc evaluation (Lewis *et al.*, 1985). Whereas Quigley, who wrote the second half of the same article, however, indicated that by the time visual field disturbances have become manifest, there is already considerable loss of nerve fibre axons and that cupping of the optic disc should in fact be considered as the most appropriate diagnostic sign for glaucoma (Lewis *et al.*, 1985). The beginning of the damage, however, is almost certain to be earlier than the manifestation of a cupped optic disc and, indeed, it has been shown that between 15% and 50% of ganglion cells can be lost before significant excavation of the optic disc occurs (Quigley, 1995). It has also been shown that up to 40% of *diffuse* axon loss can occur without a localised visual field defect (Quigley, Addicks and Green, 1982).

### **1.6.1 Diagnosis using IOP measurement**

The measurement of IOP clinically is usually done by applanation tonometry, which flattens the cornea and measures the force applied per unit area, by the Imbert-Fick principle for an ideal dry, thin walled sphere.

Equation 1.6-1

$$P = F/A$$

P = pressure inside the sphere

F = force necessary to flatten its surface

A = area of flattening

The human eye is not an ideal sphere, and the cornea resists flattening. The tear meniscus tends to cause the tonometer to adhere to the cornea by surface tension. However, all these factors are estimated to cancel each other out when a Goldmann tonometer is used (approximately 3mm in diameter). This is considered the most accurate tonometer (Kanski *et al.*, 1996).

IOP is proportional to the pressure applied to the curvature of the cornea and is affected by the corneal thickness (Kanski *et al.*, 1996). The central corneal thickness, therefore, will have an effect on the accuracy of IOP measurement. A study of a group of normals, glaucoma patients and OHT patients suggested that artificially high readings may be

occurring in OHT patients as a result of a significantly greater central corneal thickness than in normals or glaucoma patients (between whom there was no significant difference) (Herndon *et al.*, 1997).

Successive measurements of IOP by individual practitioners have been shown not to vary significantly. The mean of a second set of readings taken, however, was significantly lower than the mean of the first set, but it is not clear whether this came about due to relaxation of the subject or a physical effect of repeated tonometry. It emerged from this study that more experienced practitioners obtained readings that were lower than their less experienced colleagues. This may be a consequence of their ability to avoid sources of error, which can include the patient breath-holding, squeezing the eye lid, converging, or an effect of the observer's fingers. Inter-practitioner differences were under 2mmHg (Sudesh *et al.*, 1993).

It is well recognised that using a single IOP reading measured by tonometry to predict glaucoma in individuals has a very poor sensitivity and specificity. In a study by Mundorf *et al.*, it was noted that the use of tonometry alone would have diagnosed only 20% of the glaucoma patients (defined as having an abnormal cup to disc ratio **and** abnormal visual fields) and identified only 14% of the glaucoma suspects (defined as having either an abnormal cup to disc ratio **or** abnormal IOP) (Mundorf *et al.*, 1989). Therefore IOP measurement must be used in conjunction with other testing methods for accurate diagnosis of glaucoma.

### **1.6.2 Diagnosis using optic nerve evaluation**

The ability of physicians to accurately identify glaucoma by ophthalmoscopic fundus photography has been shown to have poor or, at the least variable, specificity<sup>\*</sup>. Abrams and colleagues calculated that the respective specificities for correctly identifying normal individuals using fundus photographs was 47%, 53% and 60% for ophthalmology residents, optometrists and general ophthalmologists, respectively, while the related

---

\* specificity is the ability of a test to produce a negative test result in an individual who does not have the disease

sensitivity\* scores were 78%, 56% and 78% respectively (Abrams *et al.*, 1994). It was also noted in this paper that intra-observer correlation was much higher than inter-observer correlation for each group. This suggests that observers use different anatomical cues when determining cup to disc ratio, rather than there simply being inaccuracies in the measurements.

Miglior *et al.* have demonstrated that optic disc analysis (i.e. shape, size and cup to disc ratio) may be more sensitive in detecting early glaucomatous changes than visual field examination, but that the reverse was true for detecting more advanced changes (Miglior *et al.*, 1996).

Despite the limitations described above, some authors do cite the analysis of the optic disc as a key area in the improvement of glaucoma management. If an accurate, objective test becomes a reality, possibly through the use of confocal laser scanning ophthalmoscopy, significant improvements may lie in this area (O'Brien, 1998 (a)).

### **1.6.3 Diagnosis using visual field examination**

Numerous reviews of psychophysical testing methods for glaucoma have been written over the last few years (Ruben *et al.*, 1994; Sample *et al.*, 1994; Bodis-Wollner and Brannan, 1994; Stewart and Chauhan, 1995; Nordmann, 1996), all of which have deemed conventional perimetry to be among the least effective methods of early detection of functional loss of vision. This is due to the fact that it is a non-specific test for light sensitivity, rather than one that isolates one particular modality of visual function. Most reviewers suggest, without conclusive evidence, that colour or motion testing, in combination with one or more other psycho-visual tests may be the answer to the problem of distinguishing most glaucoma patients from normals. One test alone has not, so far, been shown to be entirely satisfactory. Ruben and colleagues examined the multi-factorial nature of glaucoma using pattern ERG (pERG), colour contrast threshold, motion detection, and Humphrey automated perimetry. Of glaucoma patients with abnormal pERG, 36% had abnormal colour contrast discrimination, 32% had abnormal motion detection threshold, while only 15% were abnormal on both tests. They postulated that the

---

\* sensitivity is the ability of a test to produce a positive result in an individual who has the disease

lack of intra-patient correlation between these tests suggested that more than one pathological mechanism may be at work (Ruben *et al.*, 1994).

Several of these methods of visual field analysis are described on the following pages.

### **CONVENTIONAL TESTS: PERIMETERS AND OTHERS**

The Friedmann and other visual field analysers test specific field locations within the central 50° ( $\pm 25^\circ$  from the fovea), which are associated with the typical early glaucomatous visual field losses. The Humphrey and Goldmann visual field analysers can measure up to  $\pm 90^\circ$ , but more commonly the central  $\pm 30^\circ$  region is tested. Since these test the ability to detect light they are not pathway specific i.e. do not isolate magnocellular or parvocellular cell functions (Sample *et al.*, 1994; Nordmann, 1996). The stimulus involves the projection of a small white dot of light at specific locations within the visual field. This will lead to stimulation of those retinal ganglion cells subserving that location in the retina. A defect will only become apparent therefore when very marked loss of retinal ganglion cell function has occurred at that point, since so long as some retinal function persists, the target will be detected with a sufficiently bright stimulus.

Lustgarten *et al.* compared the results from two automated perimeters (Humphrey and Octopus) using a static stimulus and one manual perimeter (Goldmann) using a kinetic stimulus in both eyes of 29 OHT patients or early OAG (except for one patient in whom one eye was excluded, hence 57 eyes in study). The authors showed that the different types of visual field analysers differed in the number of abnormal visual fields which were detected. The Humphrey perimeter identified 24 eyes as abnormal, the Octopus perimeter identified 20 eyes as abnormal and the Goldmann identified 14 eyes as abnormal out of the total of 57 eyes tested. The authors of this study defined a defect as having a depth of 8 decibels (dB), 5dB as suggestive of a defect and 10dB as definitely significant. They found that Humphrey and Octopus analysers were not significantly different in the proportion of normal and abnormal results obtained within the group, but that significantly fewer defects were identified by the Goldmann perimeter (Lustgarten *et al.*, 1990). It was not clear from the paper if the same patients were identified as being abnormal, or different patients were identified by the different tests used.

New systems of evaluating the results of existing psycho-visual tests (including computerised automated perimetry and advanced mathematical analysis) continue to be presented as potential solutions to the problem of accurately diagnosing and monitoring glaucomatous change in the visual field (Glovinsky *et al.*, 1992; Fitzke *et al.*, 1996; Nouri-Mahdavi *et al.*, 1997). However, these have yet to be accepted as useful by many clinicians since reservations have been expressed about their complexity. They may not actually help in improving the signal to noise ratio \* (Jay, 1994).

The Damato visual field test is a printed chart with a small central black dot of 2mm in diameter (Chia, Goldberg and Bauman, 1999). A hinged arm held at the level of the closed eye sets the head at 40 centimetres (cm) from the chart. Gaze is checked by viewing a letter 'L' or 'R' (for left or right eye) at which point the central black dot should disappear into the blind spot. The subject then fixates the printed numbers of one to 26, in turn. The task is to state whether the dot is visible or disappears from view as would be the case if the spot fell on a scotomatous region of the retina. The numbers which are arranged in a spiral around the central dot from approximately 5° to approximately 12° from fixation. The sensitivity of this test has been found to be between 86% and 53%, and the specificity was found to be between 56% and 90% by the following two studies respectively (Chia, Goldberg and Bauman, 1999; Yamada, Chen, Mills, Leen, Lieberman, Stamper and Stanford, 1999). However, its value may lie in its simplicity, inexpensive form, portability, and speed of use which some authors have stated make it a useful adjunctive technique in addition to other glaucoma tests, particularly when used by non-ophthalmologists (Chia *et al.*, 1999).

The following tests have all been used experimentally on normal and pathological visual fields but none has yet been accepted as accurate or useful enough to become routinely used in the clinical setting.

### **SHORT WAVELENGTH AUTOMATED PERIMETRY (SWAP)**

This perimetric test produces a violet spot of light on a yellow background and has found deficits in 47% of glaucoma suspects. When the results of 17 patients with POAG were compared with those of 30 age-matched normal controls, 16 produced abnormal results

---

\* Noise includes the patient learning process and short and long term fluctuations in sensitivity; and signal is the true pathological change in the visual field.

(Sample, Bosworth and Weinreb, 1997). This implies that parvocellular ganglion cells are also affected in early glaucoma. The relative scarcity of blue sensitive cones (around 6% of the total in primates), and thus of blue / yellow ganglion cells (Marc and Sperling, 1977), means that the retina of glaucoma patients may display abnormal colour discrimination between blue and yellow due to the disproportionate effects of the loss of these ganglion cells. Some authors have stated that blue / yellow ganglion cells make up 15% of primate ganglion cells (Lee, 1996; Dacey, 2000). However, the possibility of selective post-receptoral pre-ganglion cell damage (e.g. bipolar cells) in early glaucoma has not been ruled out.

It is suggested by most reviewers of visual and psychophysical techniques that SWAP is a useful adjunct technique in glaucoma diagnosis. It must be noted, though, that the normal age-related changes in the lens can cause colour vision anomalies, namely a rise in threshold of the short wavelength mechanism (Weale, 1992). Therefore SWAP may not be suitable in populations of advanced age (in whom glaucoma is most prevalent) without careful comparisons with age-related normal subjects and allowances for patients with lens implants (Stewart and Chauhan, 1995).

### **HIGH PASS RESOLUTION PERIMETRY**

This is a specific measure of the resolution ability of the visual system which is another parvocellular function (Stewart and Chauhan, 1995). It presents visual targets in ring shapes with dark borders and a bright core in the peripheral field. The space-averaged luminance of these rings is equiluminant with the background and they must thus be resolved for detection. It has detection results comparable to standard perimetry in terms of sensitivity and specificity for glaucoma, but has detected abnormalities in a greater proportion of suspects. The test can be completed in 6 to 8 minutes, which has been quoted as one of its main appeals (Sample *et al.*, 1994).

### **MOTION PERCEPTION**

These tests involve a computer-generated display of random dots that move in a certain direction. The proportion of the dots moving together determines the percentage of coherent motion in the image. An individual's threshold is the percentage of coherence at

which they correctly identify the direction of motion of the dots 75% of the time (Sample *et al.*, 1994). This is said to target magnocellular function and has led to the identification of 15% to 36% of OHT patients as abnormal - the percentage identified as abnormal depended on the velocity of the target viewed. The test stimulus was viewed directly with one eye at a time. This study showed that there was a significant elevation of motion threshold in both the POAG and OHT groups relative to normal (by 70% and 44% respectively), however there was considerable overlap between the groups (Silverman, Trick and Hart, 1990).

### **FLICKER SENSITIVITY**

This usually refers to testing the subject's sensitivity to a spatially uniform field of light at a range of flicker speeds, i.e. their luminance sensitivity. It has been shown that flicker sensitivity falls with age despite retinal illumination and pupil size being accounted for, suggesting that the deficit has a neural basis (Kuyk and Wesson, 1991). Deficits in flicker sensitivity in individuals with glaucoma have also been identified. Breton and colleagues presented a 5° diameter spatially uniform field to the central vision of glaucoma patients and suspects. The field flickered sinusoidally after being passed through a rotatable polarizer, mounted against a fixed polarizer, which rotated at between 5 Hertz (Hz) and 30Hz. They found a significant sensitivity loss at 15Hz in glaucoma patients and noted that 12% of glaucoma suspects were indistinguishable from the glaucoma patients (Breton *et al.*, 1991). Tyler found that the proportion of OHT patients and glaucoma patients who showed significant deficits in flicker sensitivity was 83% and 77% respectively (the test was most sensitive at 30Hz to 40Hz). At 20° eccentricity the equivalent proportions were 86% and 100% (Tyler, 1981). Vo Van Toi *et al.* showed that temporary increases in IOP in humans, created by use of an 'ophthalmodynamometer' which exerted pressure on the eye ball through the eyelids controlled by a manual pump, induced reversible flicker sensitivity losses. Temporal frequencies between 5 and 30Hz were tested. The losses were 'significant' for frequencies under 20Hz for medium increases in IOP (+13.5mmHg), and 'significant' for all frequencies over 5Hz during larger increases in IOP (+27mmHg) (Vo Van Toi, Grounauer and Burckhardt, 1990).

## **BRIGHTNESS SENSE TESTING OR SIMULTANEOUS BRIGHTNESS RATIOS**

This test involves presenting a light stimulus to each eye, the level of brightness of one being adjustable. The stimuli projected to each eye begin at different levels of brightness and the subject's task is to match them. From this is derived the brightness ratio. Brightness sense is thought to be a functional test of the integrity of the optic nerve, which may be impaired by disease (Sadun and Lessell, 1985). It can be determined by covering the eyes with polarizers, one of which is at a fixed position, and another which can be rotated. The subject views a source of polarized light and the rotatable polarizer is turned until they report that the light viewed via the rotatable polarizer is equally bright with that viewed via the fixed polarizer. However the method used varies between studies.

By testing the brightness ratio of the two eyes, it has been shown in a number of studies that abnormalities arise in a large proportion of glaucomatous eyes (Teoh, Allan, Dutton and Foulds, 1990; Cummins, MacMillan, Heron and Dutton, 1994) and those affected by optic neuritis (especially unilaterally) and optic neuropathy (Sadun and Lessell, 1985). Brightness sense ratio testing has been demonstrated to be more sensitive in detecting optic neuropathies than tests of visual acuity, colour sensitivity, the relative afferent pupillary defect or optic disc appearance (Preston, Bernstein and Sadun, 1988). Sadun *et al.* showed the effect of unilateral cataract on brightness sense not to be significantly different from normal subjects. This has been disputed by Peter *et al.*, who showed that the presence of a cataract in subjects increased brightness sense ratio two-fold (Peter, Thomas and Muliylil, 1996).

Anisocoria has been said to have no effect on brightness sense ratio values (Sadun and Lessell, 1985) following their study of 102 subjects (29 normals, the remaining 73 included patients with maculopathy, cataract and optic neuritis among others). This was tested directly by MacMillan and colleagues in 1994, by the instillation of a mydriatic agent (0.5% tropicamide) into one eye each of two young subjects. Brightness sense ratio was measured repeatedly as interpupillary difference decreased from approximately 3mm difference to being equal in size and was shown to be highly sensitive to inter-ocular pupil differences greater than 0.5mm (MacMillan, Cummins, Heron and Dutton, 1994). Subsequent studies by the same authors have excluded subjects with anisocoria greater than 0.5mm.

The sensitivity and specificity of brightness sense testing in identifying patients with glaucoma has been cited as 67% and 93%, respectively, by Peter and colleagues who employed sequential presentation of the stimulus to each eye in turn (Peter, Thomas and Muliyl, 1996). However Cummins and colleagues had previously developed a technique for simultaneous brightness sense testing, and they obtained sensitivity and specificity values of 100% and 95% respectively (Cummins *et al.*, 1994). The difference may be attributed to the differences in methodology.

The optimum technique for taking readings, with regard to the filters placed over each eye at the start of the determination has also been examined. It was found that beginning with maximum transmission of light through both polarizers each time gave the least reproducibility as compared to their optimal start points, where one polarizer was set for maximum transmission paired with the other set for the mid-point (Borgmann, Steiner and Dutton, 1991). These factors (simultaneous versus consecutive testing, and initial maximum transmission of light) may have influenced the results obtained by Peter *et al.* who did, in fact, begin with maximum transmission in each eye for each reading, and did employ consecutive testing. Therefore their conclusion that poor values for sensitivity and specificity in detecting a significant visual field defect (53% and 76% respectively) rendered their test unsuitable as a screening test for glaucoma may not extend to all forms of brightness sense testing (Peter *et al.*, 1996).

### **CONTRAST SENSITIVITY**

Since 1978, measurement of contrast sensitivity has been explored as a potential tool in glaucoma diagnosis (Arden and Jacobson, 1978) and this continues to the present day. Contrast sensitivity is the reciprocal of contrast threshold, which is the amount of contrast between the dark and light cycles of a grating pattern required for detection of the pattern. The greater the contrast needed before the pattern is perceived, the higher is the subject's contrast threshold, and thus the lower is their contrast sensitivity.

The majority of contrast sensitivity studies use a circular field of around 5° presented centrally, but some tests of peripheral retina and larger test areas have been undertaken. Almost every study uses a unique stimulus in terms of field size and shape, position in the visual field, pattern generated, spatial frequency, method of generation, whether stationary

or temporally modulated. The fact that the experimental protocols differ makes it difficult to compare results or make an overall conclusion of the effectiveness of contrast sensitivity in identifying glaucomatous visual field defects. Almost without exception, studies have shown some sort of deficit in contrast sensitivity in glaucoma patients and in a significant proportion of suspects. Table 1.6-1 (on pages 51 - 54) contains a summary of 17 studies that have explored contrast sensitivity measurements in glaucoma patients and normal controls. Contrast sensitivity testing has also been used to identify sub-groups of glaucoma suspects and OHT patients who may be at increased risk of developing visual field impairment. The results have not yet been proven by long-term follow up studies. The following sections (1.6.3.1 to 1.6.3.3) describe the studies referred to in Table 1.6-1 categorised by the generation method of the grating pattern.

### **1.6.3.1 Printed sinusoidal grating patterns**

The original study using the Arden printed grating patterns showed a distinction between normal controls and glaucoma patients with visual field defects of differing severity (Arden and Jacobson, 1978). A score, directly related to the amount of contrast required to view each pattern, was given to each subject or patient. The authors identified a cut off score of 82 as a point of separation between the two groups. No normal subjects scored above this level and only 4 out of 43 subjects in the glaucoma group scored below it. However, the authors reported that their controls were not age-matched and that pupil size was smaller in most glaucoma patients (Arden and Jacobson, 1978). They also found that the severity of the patient's glaucomatous damage (rated as early, moderate or severe by the cup to disc ratio and extent of visual field loss) related positively to their score.

A few years later, printed grating patterns were tested on 387 eyes of 200 patients attending a glaucoma family screening unit (Hitchings *et al.*, 1981). Of these eyes, 38% exceeded the upper score for normality despite most having normal visual acuity and IOP. Between 20% and 40% showed one or more signs of glaucoma (IOP greater than 21mmHg, cup to disc ratio greater than 0.5, abnormal visual field, narrow anterior chamber depth or presence of angle pigment) so clearly this was not a normal population. Only 4 people were diagnosed as having POAG (2%) (Hitchings *et al.*, 1981). In 1982, a forced choice method of measuring contrast sensitivity with printed grating patterns was shown to give improved results in identifying abnormalities; however, the amount of time by which this

increased the testing procedure was not specified (Vaegan and Halliday, 1982). The overlap between glaucoma suspects (with and without visual field defects) and normals in studies using Vistech grating patterns proved to be too large to satisfactorily distinguish between them (Sponsel *et al.*, 1991). This result is not dissimilar from most other attempts to distinguish glaucoma suspects from normal. It is important, however, that the quality of the materials, the printing process and the storage of the cards are adequate, as the resolution of the grating depends on the maintenance of accurate levels of contrast which may not be accurately calibrated as with oscilloscopes or TV monitor displays.

### **1.6.3.2 Grating patterns externally generated by CRT or TV monitor**

Studies using patterns generated by monitors or CRTs have been shown to be considerably more successful at identifying glaucomatous damage than the printed gratings. In 1981 Lundh and Lennerstrand completed a study which showed that contrast sensitivity in response to static and dynamic patterns discriminated between normal and glaucoma subjects equally well (Lundh and Lennerstrand, 1981). Since then contrast sensitivity in response to stationary (Ross, Bron and Clarke, 1984) and temporally modulated (Lundh, 1985) grating patterns have each been identified as being more sensitive than the other in identifying glaucomatous deficits. Differences in results to stationary and flickering stimuli leave the topic open to further exploration and debate.

Lundh and Lennerstrand presented gratings between 0.3 and 6 cycles per degree (c/deg), centrally and paracentrally (10° above and below fixation). The field size was about 5° in diameter and it was viewed stationary and at 2Hz flicker. In 8 of 12 glaucomatous eyes tested there was a reduction in contrast sensitivity well below normal for areas already defined as having visual field defects. The level of that reduction in contrast sensitivity was similar with stationary and flickering patterns, and tended to be greater in the parafoveal regions compared to the central regions (Lundh and Lennerstrand, 1981).

Visual acuity measured (by determining the highest spatial frequency visible) at high contrast was shown not to be adversely affected in OHT patients or patients with glaucoma. However contrast sensitivity in response to grating patterns which were of low spatial frequency was reduced (Neima, LeBlanc and Regan, 1984). The authors speculated that the outer extremities of the larger dendritic trees of retinal ganglion cells were

defective in some patients. They surmised that since this process may be unrelated to that which causes actual cell loss, contrast sensitivity defects in OHT patients may be a precursor to glaucomatous visual field defects which are detectable by perimetry. For all 10 glaucoma patients tested, the defects in contrast sensitivity corresponded to the patient's visual field defect as measured conventionally, and additional defects were revealed by contrast sensitivity measurements in 4 of the 10 patients (Neima *et al.*, 1984).

Ross and colleagues presented gratings of between 0.4 and 19.2 c/deg, both stationary and flickering at 0.8Hz and 10Hz. Of 50 glaucoma patients, 94% had a statistically significantly reduced contrast sensitivity, compared to age-matched controls, at 2.9 c/deg. They found the contrast sensitivity in response to the stationary stimulus was more sensitive in identifying glaucoma patients as abnormal than either of the flickering stimuli. In early glaucoma, only spatial frequencies of 2.9 c/deg and above were affected by glaucoma but, in late glaucoma, contrast sensitivity in response to all spatial frequencies were abnormal (Ross *et al.*, 1984).

Lundh repeated his 1981 protocol in 1985 (omitting 6 c/deg). For this study 14 glaucoma patients were tested and it was shown that flickering stimuli were more discriminatory than stationary stimuli and that peripheral locations were preferable to central ones. Also when used together (i.e. a flickering stimulus viewed peripherally) they were effective in identifying glaucomatous damage (Lundh, 1985). As the number of patients who had normal or abnormal contrast sensitivity was not specified, it is assumed that the described defects were present in all 14 patients.

Spatial frequencies of 2.3 c/deg or greater (termed 'medium high' by Lustgarten *et al.* in 1990) have been noted to be most susceptible to a contrast sensitivity deficiency in early glaucoma. Contrast sensitivities in response to a grating pattern flickering at 0.3Hz were measured at spatial frequencies between 0.5 and 32 c/deg in 57 eyes of 29 OHT or early glaucoma patients for comparison with perimetry results (perimetry results described in Introduction section 1.6.2). They showed that abnormal contrast sensitivity occurred in patients at either spatial frequencies above 9.2 c/deg (19 eyes) or above 2.3 c/deg (27 eyes). The authors concluded that, in early glaucoma, spatial frequency-specific losses occurred which may be dependent on temporal frequency, and that contrast sensitivity measurements were more sensitive than kinetic perimetry in detecting visual field loss (Lustgarten *et al.*, 1990).

Teoh and colleagues measured contrast sensitivity in 28 patients with POAG and compared them with 41 age-matched controls in response to spatial frequencies of between 0.5 and 23 c/deg. They identified 39% of the patients as abnormal by this test, with low and medium spatial frequencies more commonly affected than high (Teoh *et al.*, 1990).

Patients with OHT, considered not to be high risk\*, were shown to be indistinguishable from normal when contrast sensitivities were measured both centrally and peripherally (sinusoidal grating of 1.9 c/deg, flickering at 1Hz). However, high risk OHT patients, and patients with POAG had abnormal contrast sensitivities when measured at 20° and 25° into the periphery despite normal central contrast sensitivity (Falcão-Reis, O'Donoghue, Buceti, Hitchings and Arden, 1990).

Zulauf and Flammer calculated the correlation between contrast sensitivity and perimetric evaluation of the visual field in one eye each of 60 glaucoma patients and suspects. They found that the correlation was strongest when comparing the patient's central mean sensitivity (as measured by the Octopus automated perimeter) with the mean contrast sensitivity, and slightly less well with mean sensitivity of the visual field as a whole. However it was poorly correlated with other measures of field sensitivity, e.g. short-term fluctuation (Zulauf and Flammer, 1993).

Horn and colleagues tested the central contrast sensitivity of 19 LTG, 30 POAG, and 10 secondary OAG patients. They used 3 spatial frequencies between 0.6 and 12 c/deg which were presented statically, and one c/deg which was presented at 2.5Hz in the lower nasal field. They correlated the results with the patient's mean visual sensitivity from the Octopus perimeter, and their level of optic nerve damage estimated from fundus photographs. The best correlation was between mean sensitivity and the peripheral flickering contrast sensitivity, which was statistically significant. For central stationary contrast sensitivity 3 c/deg gave the best correlation with mean sensitivity but, overall, the correlation was poorer when compared with peripheral contrast sensitivity. Central contrast sensitivity showed very poor correlation with the estimated amount of optic disc damage (Horn, Korth and Martus, 1995).

---

\* High risk OHT was defined as having an IOP greater than 26mmHg, and a vertical cup to disc ratio of greater than 0.6.

Lundh and Gottvall described a diffuse depression of contrast sensitivity in patients with 'early glaucoma' (N.B. these patients did not have established visual field defects and therefore may be interpreted as glaucoma suspects). They tested 3 spatial frequencies between 0.5 and 2 c/deg within a 5° circular field viewed at 6 positions which were all 7.5° from fixation, 3 in the upper hemifield and 3 in the lower hemifield (i.e. 24 tests in total). The glaucoma patients all had decreased contrast sensitivity for all tests, and the differences from normal values were statistically significant in 20 of the 24 location / spatial frequency combinations. The lower hemifield was found to be affected by deficiencies in contrast sensitivity earlier than the upper hemifield (Lundh and Gottvall, 1995).

### 1.6.3.3 Gratings generated by laser interferometry

Studies using laser generated grating patterns are much fewer in number and are often not referred to in reviews of psychophysical testing methods (Sample *et al.*, 1994; Bodis-Wollner and Brannan, 1994).

As an English translation is not available, little can be taken from the paper by Isayama and colleagues; however it appears that a 5° field was viewed centrally by 42 eyes of patients with optic neuropathies, and 12 eyes of patients with suspected glaucoma. The abstract states that there was a fall in contrast sensitivity at 3 to 4 c/deg for those who had suspected glaucoma with a normal visual field (as measured by Goldmann perimetry) and a normal optic nerve. When central visual field was affected and nerve atrophy was noted, contrast sensitivity was significantly reduced at all spatial frequencies tested (1.5 to 30 c/deg) (Isayama, Mizokami and Tagami, 1980).

Tagami and colleagues used a laser interferometer to generate a circular test field of 5° consisting of a red, vertical grating pattern. The spatial frequencies tested ranged from 1.5 to 30 c/deg. They obtained contrast sensitivities from 6 eyes of 6 OHT patients and 12 eyes of 12 patients with POAG. They found no significant difference between OHT patients and normal subjects (who were not described in the paper). There was a

depression of sensitivity in POAG patients with respect to normal values which was statistically significant at 3 to 4 c/deg (Tagami *et al.*, 1981).

Motolko and Phelps compared contrast sensitivity in both eyes of 27 patients with asymmetric symptoms of glaucoma (including 6 with LTG, 13 with POAG and 5 with OHT) and used 10 normal subjects of similar ages for comparison. The test field was 5° in diameter and was viewed centrally in the Maxwellian view. They projected grating patterns of different orientations to the subject between the spatial frequency range of 0.4 to 40 cycles per degree. They found that in 10 patients there was no difference in contrast sensitivity between the eyes, in 15 patients the eye with more damage (as measured conventionally) produced a lower contrast sensitivity, and the reverse was true in the remaining 2 patients. For the latter 2 patients, there was evidence of glaucoma in the eye which produced the lower contrast sensitivity, albeit less than in the companion eye (Motolko and Phelps, 1984).

### **CONTRAST SENSITIVITY SUMMARY**

Potential problems with contrast sensitivity testing for glaucoma diagnosis are the current lack of standardisation and its susceptibility to be affected by other factors e.g. cataract, disease of the companion eye, amblyopia, refractive error (Sample *et al.*, 1994, Bodis-Wollner, 1979). Refractive correction is not required, however, when the pattern is created with coherent light in the Maxwellian view. It is important that control subjects are of a similar age to the patient subjects, as age-related deterioration of contrast sensitivity is well-documented (McGrath and Morrison, 1981). The optimal form of contrast sensitivity testing for identifying glaucoma has therefore not yet been settled: however as the studies mentioned above indicate contrast sensitivity does seem to be successful, to a degree, in identifying glaucomatous visual field loss. Several studies imply that peripheral testing may be more sensitive than central testing. The difference between the diagnostic sensitivity using dynamic and statically generated patterns is not clear, with many contradictions in the reported results. Presentation of a small circular or square field is one aspect of the above studies which does not vary. Therefore there may be scope to increase understanding of the contrast sensitivity in previously unexplored areas of retina. Attempts to correlate contrast sensitivity with visual field loss as measured by conventional analysis,

usually using mean sensitivity values from visual field analysis and mean contrast sensitivity values, have tended to produce a low correlation (Zulauf and Flammer, 1993).

Its usefulness as a diagnostic tool has not yet been confirmed, as cross study results vary in their interpretation of the optimal form of testing and the proportion of patients identified as abnormal. The difficulty may arise because some reviewers, when comparing contrast sensitivity to other tests, use the least useful printed gratings, thus contributing to a lack of real progress.

It would appear that the most useful or appropriate test characteristics for glaucoma would be a low spatial frequency, but the results from stationary and flickering stimuli seem equivocal. Testing central regions of retina can highlight defects, although peripheral locations tend to be preferable. When centrally viewed the most useful spatial frequencies are around 2 to 4 c/deg, i.e. at the peak to the contrast sensitivity function, suggesting that for peripheral viewing a spatial frequency of around 1 c/deg may be appropriate. Additionally, if the subjects view the grating at very low contrast, this is likely to preferentially stimulate magnocellular ganglion cells.

**PAGES  
MISSING  
IN  
ORIGINAL**

<b>Zulauf, and Flammer (1993)</b>	44 glaucoma patients and 16 suspects	2° field size viewed centrally, above, below and either side of the fovea at a distance of 2°, presented in the Maxwellian view	horizontal and vertical static gratings, on the Moiré Visometer	1.5 - 24 c/d	CS correlates well with central mean sensitivity measured by perimetry in the glaucoma patients. In both groups mean CS did not correlate significantly with two other visual field indices (corrected loss variance or short term fluctuation). Glaucoma suspects have significantly better correlation between CS and VF at low than high SF.
<b>Horn, Korth and Martus (1994)</b>	59 glaucoma patients with optic disc damage and visual field defects, 31 age matched normals	5.3 x 4.3° field size presented centrally and in the lower nasal field 13.8° horizontally and 4.2° vertically from fixation,	computer generated striped pattern, central test viewed stationary, peripheral test viewed at 2.5 Hz	Central pattern = 0.6, 3.0 and 12 c/d, peripheral pattern = 1 c/d	A statistically significant correlation was found between mean sensitivity and peripheral flickering CS. For static, central CS, 3c/deg gave the best correlation with mean sensitivity.
<b>Lundh, and Gottvall (1995)</b>	16 with early 'glaucoma', without definite VF deficits, 16 age and sex-matched controls	5° circular field viewed at 3 eccentric positions in each hemifield, all 7.5° from fixation, left middle and right positions in both the upper and lower field	dynamic (2 Hz), computer-generated display, sinusoidal grating pattern (maximum contrast was 41%)	0.5, 1, 2 c/d	CS was depressed in glaucoma patients at all 3 SFs, significantly different from normals in 6 of 9 combinations (3 SFs tested at 3 positions) tested in the upper hemifield and 8 of 9 in the lower hemifield. Results suggest an early diffuse effect on VF, better picked up by CS testing than perimetry. CS less useful for glaucoma detection in the individual, due to large overlaps in group measurements.

Abbreviations used in Table

c/d = cycles per degree  
CS = contrast sensitivity  
Hz = Hertz

SF = spatial frequency/frequencies  
VF = visual field

## **1.6.4 Diagnosis using electrophysiology**

As glaucomatous field loss has been attributed to ganglion cell atrophy, over the past three decades many investigators have examined the electrophysiological responses of the retina to gain further insight into the pathophysiological effects of glaucoma. Several of the electrical responses of the visual pathways have been identified as defective in early stages of glaucoma, however this is not the case for all patients.

### **1.6.4.1 Electroretinogram (ERG)**

The electroretinogram (ERG) is a massed retinal response to a temporally modulated light stimulus. The photoisomerisation of visual pigments in the discs of the outer segments of the photoreceptors leads to the reduction in cGMP levels which causes the closure of  $\text{Na}^+$  channels. This in turn causes the photoreceptor to hyperpolarize, the commencement of which can be recorded as the negative 'a-wave'. The hyperpolarized photoreceptors then release reduced amounts of neurotransmitter (glutamate) from synaptic terminals which leads to depolarization or hyperpolarization of bipolar cells (depending on their type) and hyperpolarization of horizontal cells. The depolarizing action arises from the reduced activation of  $\text{Cl}^-$  channels by the reduced release of glutamate which, in this case, acts as an inhibitory neurotransmitter. The hyperpolarizing action arises from reduced activation of cationic channels by the reduced glutamate release which in this case acts as an excitatory neurotransmitter. Measurements with  $\text{K}^+$  sensitive electrodes have shown the accumulation of  $\text{K}^+$  in the extracellular space at the level of the border of the outer plexiform layer and the outer nuclear layer in skate retina (Kline, Ripps, Dowling, 1978). The inward flow of these  $\text{K}^+$  ions into the Müller glial cells leads to radial current flow through the retina, which generates the rapid phase of the positive phase of the 'b' wave and cuts short the 'a' wave. Within the inner retina, the ganglion cells are driven by glutamate release from bipolar cell terminals, which is always excitatory, thus show response patterns reflecting the bipolar cell responses. Hence, ganglion cells generating an ON response to light are driven by depolarizing bipolar cells while ganglion cells generating an OFF response to light (otherwise an ON response to dark) are driven by hyperpolarizing bipolar cells. Another site of  $\text{K}^+$  accumulation has been identified at the border of the inner nuclear and the inner plexiform layer border, which again leads to radial current flow through the retina and into the Müller glial cells at this site, thus leading to the

sustained positive component of the 'b' wave (the DC component). A resulting increase in extracellular  $K^+$  causes a depolarisation of Müller cells and a current flow, principally towards the inner retina. A decrease in  $K^+$  extracellularly around the photoreceptor outer segments which arises due to the hyperpolarization of the photoreceptors, in turn, leads to hyperpolarization of the retinal pigment epithelial cells. This is manifest as a corneal positive potential: the 'c' wave (Oakley and Green, 1976). For longer duration light stimuli in the photopic range, there is an off-response, probably originating from the recovery of the photoreceptors and the hyperpolarizing bipolars, which causes the 'd-wave' (Graham and Klistorner, 1998).

#### 1.6.4.2 Pattern ERG (pERG)

The pERG is generated in response to contrast modulation. Commonly used patterns are a checker board or grating pattern of  $10^\circ$  to  $30^\circ$  degrees in diameter, the black and white regions of which alternate temporally. This means that the total amount of light projected to the eye does not change; therefore the stimulus display generates a constant amount of scattered light, which may be excluded as a causal factor in the generation of the ERG which can therefore be attributed to changes in contrast (Dodt, 1987). Refractive error, small pupil size and media opacities affect the response. The pERG is considerably smaller in magnitude (one micro Volt ( $\mu V$ ) compared to  $20\mu V$  to  $30\mu V$  for the flash ERG) originates in the inner retina, i.e. retinal ganglion cells and neighbouring structures (reviewed in Muir, Barlow and Morrison, 1996). This led to the conclusion that the pERG arose as the summed response of the retinal ganglion cells to contrast modulation. A small negative component occurs at roughly 25 milliseconds (ms) ( $N_1$ ) and is followed by a large positive component at around 50ms ( $P_1$ ). A further negative wave occurs at roughly 95ms after stimulation ( $N_2$ ) unless the pattern reversal is occurring at greater than 10Hz, whereby the subsequent  $P_1$  obscures it and the response produced is a steady state one (Graham and Klistorner, 1998). The pERG was observed to be abolished in a patient, 3 months after suffering trauma to her left optic nerve while the flash ERG remained normal (Gronenberg and Tepping, 1980, quoted in Muir *et al.*, 1996). This led to the conclusion that the pERG arose as the summed response of the retinal ganglion cells to contrast modulation. Muir and colleagues found that if young and elderly subjects were tested at a level of display luminance which was a fixed factor of their own luminance threshold, the pERG implicit time was not different between the two groups (pupil size was also taken into account)

(Muir *et al.*, 1996). This was inferred to mean that retinal ganglion cell responsiveness was not a major factor in the age-related loss of contrast sensitivity.

In a study on 8 OHT patients, eyes with IOP greater than 30mmHg had a decreased amplitude in the pERG despite their luminance ERG being normal. The amplitude was greater at lower levels of pressure. This was interpreted by the authors to indicate that high IOP had impaired the blood flow to the inner retinal layers and reduced retinal ganglion cell responsiveness (Papst, Bopp and Schnaudigel, 1984 (b)). In another study, the pERG was recorded in 15 patients with glaucomatous field loss due to POAG, but who had IOP in the range of 10mmHg to 22mmHg without the use of miotics. Of 28 eyes tested, the pERG amplitude was reduced in all of them when compared to 30 healthy eyes (Papst, Bopp and Schnaudigel, 1984 (a)). Other studies have found comparable results for glaucoma patients, i.e. 96% to 100% of eyes had a significantly reduced pERG amplitude, and 43% to 92% of OHT patients had abnormally low amplitudes (Bach and Speidl-fiaux, 1989; Porciatti, Falsini, Brunori, Colotto and Moretti, 1987). Porciatti *et al.* also found that the pERG amplitude reduction was greater as the IOP increased. They identified that reductions were greater at spatial frequencies between 1.2 and 1.7 c/deg than those at high or low ones (the range tested extended from 0.6 to 6.8 c/deg). Trick found that if OHT patients were subdivided into low risk or high risk groups, on the grounds of age, family history, mean IOP over preceding 12 months, and cup to disc ratio, the proportion of patients showing reductions in pERG amplitude varied accordingly. They found that 50% of the high risk group had reduced pERG amplitude, compared with 8% in the low risk group when tested with a display of check size 30 mins arc (Trick, 1987). However, Hawlina *et al.* report that the pattern ERG amplitude was normal in 5 eyes of 11 in patients with established visual field defects, and 27 eyes of 30 in patients with either glaucoma or ocular hypertension (Hawlina *et al.*, 1989).

From these studies, it may be concluded, that while pERG recordings can undoubtedly identify glaucomatous defects, the technique has its limitations (especially the overlap between normal individuals and OHT patients and between OHT patients and those with glaucoma), especially in the context of the difficulty in making these recordings, which require substantial signal averaging.

### 1.6.4.3 Multifocal ERG

The multifocal ERG (mERG) was developed in 1992 by E.E. Sutter (Hood *et al.*, 2000). It allows the calculation of up to 100 focal ERG signals from the retina from one recording site using multiple sites of stimulation. The function of the outer retinal layers can be mapped for a visual field of up to 60° in diameter. It is obtained by recording the subject's ERG while viewing an array of hexagons which are arranged to stimulate the visual field in a specific way. The shape and size of the hexagons are designed such that they increase in size and elongate in shape as eccentricity increases, thus stimulating areas of retina adjusted for the changing levels of visual sensitivity in peripheral retina. The hexagons flicker on and off following a known algorithmic pattern, each of them beginning that same algorithm at different points, and repeating it in cycles. The result is a complex image made up of elongated hexagons that appear to flicker between black and white randomly; however as the algorithm of flicker is known, use of the appropriate computer software can allow the differentiation of the individual discrete retinal responses to each stimulus.

There have been conflicting reports over whether the mERG is abnormal in patients with glaucoma. One recent study by Hood and colleagues have attempted to discriminate between 18 glaucoma patients, 4 glaucoma suspects and 13 normal controls. They found that the most sensitive measure in identifying OAG patients was the ratio of the amplitude at 8ms after the peak response to the amplitude at the peak. However this ratio was outwith the statistical normal limit in only 6 of 18 patients. They also found that the correlation with local field loss (by Humphrey Visual Field Analysis) was poor. The authors described that mERG deficiencies, although clear in some glaucoma patients, do not appear to be present in some others, despite local visual field defects. They have suggested that the optimal method of obtaining mERG responses is yet to be found (Hood *et al.*, 2000).

#### 1.6.4.4 Visual Evoked Response (VER)

The VER, or visually evoked cortical potential (VECP), is an electrical response to a temporally modulated visual stimulus (flash of light or pattern) generated by the visual cortex. The central 2° of the retina is thought to be responsible for 65% of the recorded signal, since it is primarily derived from the macular region. Full responses are evoked by slow stimulus frequencies e.g. 0.5Hz, and consist of the following constituent parts:  $N_1$ , the primary response which may occur around 70ms and is thought to arise in striate cortex, and  $P_1$  or  $P_{100}$ , the secondary response which may occur around 100ms, and is thought to originate in the extra striate areas 18 and 19 (reviewed by Graham and Klistorner, 1998). However, these results are not universally agreed and other authors have identified the following response times:  $N_1$  at 90ms,  $P_1$  at 100ms,  $N_2$  at about 120ms, and  $P_2$  at about 150ms for a high contrast sinusoidal grating pattern (Morrison and Reilly, 1989). They have interpreted  $N_1$  and  $N_2$  as being generated by the striate cortex and  $P_1$  and  $P_2$  as being generated by prestriate cortex. By contrast, a rapidly modulated stimulus generates the steady state response which, for sinusoidal temporal modulation, consists of a sine wave response following the stimulus after a time delay (phase-lag) response is obtained to an 8Hz flickering stimulus with a spatial frequency of 10 to 20 minutes of arc (Graham and Klistorner, 1998).

The VER is affected by macular disorders and optic nerve disease. Abe *et al.* found that the peak latency of the VER was prolonged in 15% of early glaucoma patients, 28% of patients whose glaucoma was moderately advanced and 40% with advanced glaucoma. They noted that this was not as sensitive as visual field measurement or fundus photography in detecting early glaucoma (Abe, Hasegawa and Iwata, 1987). Sano and Adachi-Usami found a significant delay in the  $P_1$  peak latency in a group of 24 NTG patients compared to normal subjects in response to a check size of 60 minutes of arc (or one c/deg) (Sano and Adachi-Usami, 1997). VERs were obtained for 28 eyes of 28 patients which had been surgically treated for high IOP at least a year earlier. The  $P_{100}$  latency of the VER showed greater variation in patients with both optic disc and visual field damage (110ms to 160ms) than in patients with normal optic discs and visual fields (115ms to 125ms). The  $P_{100}$  latency for all patients in the group with glaucomatous damage was outwith normal limits, and all of the latter group fell within normal limits. The authors reported that the amplitude in the patient group as a whole overlapped considerably with the normal group (Papst *et al.*, 1984 (a)). The amplitude was recorded in

the response to temporal frequencies between 10Hz and 50Hz in POAG patients, OHT patients and controls. The P<sub>1</sub> amplitude in OHT patients was not significantly different from the normal controls. However there was a significant reduction in POAG patients when compared to control levels and this reduction was exacerbated with increasing temporal frequency (Holopigian *et al.*, 1990).

In summary, the VER, like the ERG is time consuming and requires careful refraction and positioning of the stimulus field. It is necessary to stimulate the upper or lower half of the field only; as if the whole central field is stimulated the averaging effect of the generated currents in the lower and upper cortex make it impossible to distinguish a useful signal.

## 1.7 Effect of different definitions on prevalence

Glaucoma is defined in Becker-Shaffer's *Diagnosis and Therapy of the Glaucomas* as "a disturbance of the structural or functional integrity of the eye that can be arrested or diminished by adequate lowering of IOP" (Hoskins and Kass, 1989); however there are different definitions in almost every textbook and research paper.

A review of 182 articles, spanning the years 1980 to 1995, was undertaken by Bathija and colleagues to determine the level of consistency in defining OAG. They found that 34% of the articles did not provide a definition using the optic disc, visual field or IOP (their method of describing glaucoma is not further explained in the review). Of the others 5% defined using an optic disc abnormality only, 13% used the optic disc abnormality or a visual field defect, 20% used elevated IOP only, 26% used a visual field defect only, and 36% used an optic disc abnormality or a visual field defect. Of all the articles that specified an elevated IOP as a diagnostic feature of OAG, in 46% it was defined as greater than or equal to 22mmHg (Bathija, Gupta, Zangwill and Weinreb, 1998).

Kahn and Milton, using visual data from the Framingham Heart Study of 1977, have evaluated the effect of different definitions of glaucoma on its prevalence in a population. Their definitions were based on combinations of the following: history of glaucoma; IOP greater or equal to 22mmHg or inter-ocular IOP difference greater than or equal to 3mmHg; inter-ocular difference in the horizontal or vertical cup to disc ratio of 0.2 or more; visual field defects with or without the presence of blind spot enlargement. They found that depending on the combination of these defining characteristics, the prevalence rate varied from 0.4% to 11.2% of the population (Kahn and Milton, 1980). In a follow up of the Baltimore Eye Survey of 1991, which examined the racial variations in POAG prevalence, the criteria for a diagnosis of POAG was made irrespective of the subject's IOP. Rather 'evidence of glaucomatous damage' was specified although subjects with IOP greater than 21mmHg were referred for further examination, so clearly this was an investigative distinction rather than a clinical one (Tielsch, Sommer, Katz, Royall, Quigley and Javitt, 1991). The results have been described in Introduction section 1.3.1.

## 1.8 Risk factors for glaucoma

Risk factors for glaucoma were described by Quigley and colleagues in 1994 following a 12 year prospective study on the relative importance of factors which were present at OHT patients' initial examination (Quigley *et al.*, 1994). Unexpectedly, some of the factors usually associated with glaucoma were shown not to confer any statistically significant greater risk of developing visual field loss: e.g. gender, family history of glaucoma, and race. Therefore these risk factors may not be as predictive of the progression of glaucoma as OHT or the initial appearance of glaucomatous signs. However, they did identify several risk factors which did confer a significantly increased risk of the development of glaucoma: older age, larger cup / disc ratio, larger cup asymmetry, and higher IOP. The most significant correlation with the risk of developing visual field loss was nerve fibre layer atrophy which, when moderate or severe, conferred an increased risk of developing visual field defects of 7 to 8 times the normal rate. The unusually weak association in this study between race and the incidence of visual field defects in OHT patients was suggested by the authors to be at least partially due to the fact that black people tend to get glaucoma at an earlier age than white people and it progresses faster. Thus, as this study excluded those with visual field defects at the initial screening, a greater proportion of them would be missing (Quigley *et al.*, 1994). Alternatively, it may suggest that black people with OHT may have the same risk of progression of glaucoma once the condition is established, therefore race itself would not confer any additional levels of risk of visual field progression.

Risk factors for glaucoma cited by other authors include race, age and a positive family history (20% to 25% of glaucoma is thought to be hereditary) (Leske, 1983). Refractive error is also thought to relate in some way to the development of glaucoma, with myopics being at greater risk. This may be due to the greater axial length of the eye ball in myopia which may offer less mechanical support to the optic nerve fibres than normal at the exit-point of the optic nerve from the eye ball (Hoskins and Kass, 1989; Fechtner and Weinreb, 1994). Several systemic conditions have been cited as being linked with glaucoma including diabetes and various cardiovascular abnormalities (Leske, 1983). However, Quigley proposed that the apparent link between diabetes and glaucoma may have been overestimated in the past. He postulated that the regular and life-long health screening of diabetics in specialist clinics has perhaps led to the identification of more cases of glaucoma than would normally have been detected in a population (Quigley *et al.*, 1994).

In the interpretation of any glaucoma study, consideration must be given to the effects of increasing age. Increasing age itself is associated with many changes which must be taken into account in the evaluation of glaucomatous signs, i.e. decreasing neuro-retinal rim area (Healey *et al.*, 1997); increasing cup area and cup / disc ratio (Garway-Heath, Wollstein and Hitchings, 1997); flicker sensitivity deficits (Kuyk and Wesson, 1991); contrast sensitivity deficits (McGrath and Morrison, 1981); increasing mean IOP (Kanski *et al.*, 1996); decreased mean sensitivity and a contraction of the visual field (Weale, 1992). This creates the need in studies on glaucoma to compare any results against a control group that has been matched for age.

## 1.9 Demography

Glaucoma is rare in the under 40-year age group. Thereafter, the prevalence of POAG and ACG rises with increasing age. The prevalence of POAG increases from under 1% in the under 65-year age group to roughly 3% in the over 75-year age group in a Western population (Leske, 1983). Glaucoma was estimated to be responsible for 11% of all reported cases of registered blindness in the USA in 1970 and 13% in the UK; however differences in definitions, in the methods of data collection and in the ages of the populations make it difficult to compare rates between studies and countries (Leske, 1983).

The influence of socio-economic factors on the prevalence of glaucoma was also considered by Leske who noted that labourers, farmers and those with more outdoor exposure were reported to be at greater risk of developing OAG in some studies, though it was noted that racial differences between the groups had not been taken into account (Leske, 1983). A geographical factor on the prevalence of glaucoma was considered by Leske, who surmised that it was more likely to be the effect of genetic subpopulations within a geographical area which made the difference, i.e. a greater number of people of African descent within a population will lead to a higher rate of OAG (Leske, 1983). People of African descent may have a prevalence of 4 times that of white people (Kahn and Milton, 1980; Wormwald *et al.*, 1994, Garway-Heath *et al.*, 1997). Garway-Heath *et al.* state in their 1997 study of the optic nerve head that 1% of white subjects have OAG at 50 years and 4% at 80 years, while black subjects have a prevalence for OAG of 3% and 13%, respectively (Garway-Heath *et al.*, 1997). The higher risk of OAG in black people occurs despite white and black people of the same age having similar IOP (Sommer *et al.*, 1991). NTG has been found to have a higher incidence in Japan than elsewhere in the world (Shiose *et al.*, 1991).

## 1.10 Treatment

All forms of glaucoma treatment aim to reduce IOP. The three most commonly used in the United Kingdom are pharmacological therapy, laser trabeculoplasty and trabeculectomy (Jay, 1992 (a)); these are described below.

### PHARMACOLOGICAL THERAPY (I.E. TOPICAL OR SYSTEMIC DRUGS) FOR POAG

Cholinergic drugs (miotic agents) (e.g. pilocarpine, carbachol) increase aqueous outflow via the trabecular meshwork, by stimulation of the ciliary muscle. This puts traction on the scleral spur and the trabecular meshwork, separating the trabecular sheets and preventing Schlemm's canal from collapsing (Hoskins and Kass, 1989). Side effects include smaller pupil size, brow ache and exacerbation of the symptoms of cataract. It is reported that the use of these drugs has declined since the introduction of the newer drugs described below, which tend to have less 'troublesome' side effects (reviewed by Migdal, 2000).

Beta-blockers (e.g. Timolol, Levobunolol). These have been described as the 'mainstay' of medical therapy for glaucoma (Migdal, 2000). They decrease the rate at which aqueous humour is produced, by an unknown mechanism (Hoskins and Kass, 1989). They can have adverse cardiovascular and pulmonary side effects, so must be prescribed with care.

Carbonic anhydrase inhibitors (e.g. Dorzolamide) are thought to decrease both the rate of  $\text{HCO}_3^-$  entry into aqueous humour and the rate of water entry into the posterior chamber, thus reducing aqueous humour formation. Again the exact mechanism, or mechanisms, involved are not fully understood (Hoskins and Kass, 1989). Side effects which have been reported include a bitter taste after drop instillation and topical discomfort (Migdal, 2000).

Prostaglandin analogues (e.g. Latanoprost) decrease IOP by increasing aqueous humour outflow by the uveoscleral route. This is thought to occur via relaxation of the ciliary muscle, creating spaces between ciliary muscle bundles, and also by causing alteration

to the metabolism of the extracellular matrix surrounding ciliary muscle cells (Migdal, 2000). Side effects appear to be relatively common and may include conjunctival hyperaemia, increased iris pigmentation, discomfort in the eyes and blurred vision (Migdal, 2000).

Alpha agonists (e.g. Brimonidine) reduce IOP by a combination of aqueous reduction and increase in uveoscleral outflow (Migdal, 2000). Side effects may include dry mouth, fatigue or drowsiness. These tend to have a high rate of allergy in patients, occurring in around 13% of patients per annum (Migdal, 2000).

Conventional management for glaucoma usually involves pharmacological therapy administered via eye drops every few hours to lower IOP followed by trabeculectomy for individuals who do not respond satisfactorily (Jay, 1992 (b)). The IOP-lowering effect of trabeculectomy has been shown to be proportional to pre-operative IOP, bringing it down to between 16mmHg and 20mmHg in the vast majority of cases (Jay and Murray, 1980). However, it has been noted that the prolonged pharmacological treatment for patients with raised IOP in the lower range actually puts them at greater risk of visual field loss than eyes with more severe disease, who tend to be operated on more quickly. It is now recommended by some that surgery takes place sooner rather than later (Jay, 1992 (b)).

## **LASER SURGERY**

Argon laser trabeculoplasty involves the application of laser energy to the trabeculum at the drainage angle in order to enhance aqueous outflow (Kanski *et al.*, 1996).

## **CONVENTIONAL SURGERY**

Trabeculectomy, although devised to create an opening in Schlemm's canal, functions as a non-specific corneal scleral fistula protected by a scleral flap for aqueous humour to drain into the subconjunctival space (Jay, 1992 (a)). Trabeculectomy has been identified as the most effective of the three most common methods for treatment of glaucoma (Jay, 1992 (a)).

## **ALTERNATIVE THERAPIES**

These are mainly aimed at relieving stress, maintaining collagen levels in the body and replenishing nutrient deficiencies. Techniques such as acupuncture, reflexology, and herbal or dietary supplements (e.g. vitamin C-containing or anti-oxidant foods) have been proposed, but not scientifically or clinically investigated. There is no evidence proving their effectiveness in lowering IOP or preventing glaucomatous damage; therefore these are all considered to be complementary to traditional medicine used through personal choice, rather than a genuine 'alternative' to the conventional approach.

The effect of marijuana on IOP has been investigated more thoroughly and its pressure lowering properties (in both blood vessels and the eye) have been established (Merritt, Crawford and Alexander, 1980). However, the evidence for its therapeutic effectiveness has not superseded concerns over its safe use (Workshop on the Medical Utility of Marijuana, Report to the Director, National Institutes of Health; web site: <http://www.nih.gov/news/medmarijuana/MedicalMarijuana.htm#GLAUCOMA>).

## **NEW APPROACHES TO TREATMENT**

Since, to date, IOP is the only aspect of glaucoma which can be treated successfully, several researchers have proposed radically different approaches by attempting to find other modifiable aspects of glaucoma.

As previously discussed the obstruction of retrograde axonal transport to ganglion cells in glaucoma is thought to cause the deprivation of trophic factors, thus setting their apoptotic programme in motion (Quigley, 1995; Garcia-Valenzuela, Shareef, Walsh and Sharma, 1995). Therefore it has been proposed that the administration of trophic factors to ganglion cells which have been 'cut off' by the glaucomatous process may prevent the initiation of apoptosis (Quigley, 1995). It has also been proposed that altering the ganglion cell genetic composition may successfully inhibit apoptosis (Quigley, 1995) for example by administration of Selegiline (also known as 1-deprenyl, a monoamine oxidase inhibitor) which increases the gene expression related to the inhibition of apoptosis (Caprioli, 1997).

In his review of neuroprotective ideas with respect to glaucoma, Caprioli has also suggested that the administration of calcium channel blockers may interrupt the cascade of events leading to death from ischaemia (proposed to be particularly useful in NTG).

Neuronal injury from glutamate-mediated neurotoxicity has been implicated in many central nervous system diseases, and this neurotransmitter has been found to be in high concentrations in the vitreous of glaucomatous monkeys, but it is not clear if this is a cause or effect of damage, (Caprioli, 1997).

## 1.11 Aims of project

To date the only treatable aspect of glaucoma is IOP. In most patients it can be successfully lowered to a level at which the risk of damage to the optic nerve is adequately reduced. IOP measurement is also currently the most common means of identification of people at risk. However, as previously outlined its poor sensitivity and specificity for glaucoma means that another screening test is required. The presence and extent of optic nerve head abnormalities, as measured currently, do not seem to correlate precisely enough with the disease process to be useful as an accurate diagnostic measure. It is widely accepted that conventional visual field analysis only identifies damage at unacceptably late stages of the disease. At the point where perimetry finds abnormality, the visual field of the patient is already permanently damaged (within the limits of the fluctuation described previously). However as preservation of the visual field is the principal goal in glaucoma therapy, it is perhaps appropriate to persevere in using visual field testing as a key measure of the disease progress, and the success or otherwise of the treatment being administered.

What is needed, therefore, is a visual field test which can identify subtle defects in visual function to allow diagnosis and treatment when there is sufficient residual visual function to remain during the life of the patient. Until such times that optic nerve fibres may be restored or their life span extended, the improvement in the management of glaucoma is likely to come from the earlier and more accurate identification of individuals at risk. The demographics and numbers of people at risk place special requirements on such a screening test. The test should be straightforward to administer, simple to explain and complete, not be affected by refractive error, pupil size, or cataractous lens changes, and be quick, accurate and repeatable.

The aim of this project was to design and test a form of visual field analysis that would meet these specifications. A test which is simple to administer and complete is more likely to be utilised in primary health care settings, for example, the high street optician - a crucial screening location for glaucoma. This also makes it more likely to be used on large numbers of individuals, which is crucial for primary screening. A test that can be easily understood by the patient and performed quickly, thus reducing patient fatigue is preferable when the population at risk is large and includes elderly people. Most crucially the test must provide sensitive information on the visual field, ideally prior to the emergence of visual field loss which adversely affects the individual's quality of life.

We have developed and tested new forms of two psychophysical tests of the visual field, which have, in other forms, been proposed as having potential in identifying early glaucomatous defects. Contrast Thresholds (also commonly referred to by its reciprocal 'contrast sensitivity') and Simultaneous Brightness Ratios have been investigated and developed to an optimal format, then applied to controls and patients with glaucoma.

Contrast threshold testing in the format used in these experiments, namely by stimulating the retina at the lowest contrast perceivable, utilises the characteristics of the magnocellular ganglion cells, hence exploiting the theory of reduced redundancy discussed earlier. If the magnocellular ganglion cell population is affected early in the glaucomatous process, as some investigators have stated, then isolating this population may reveal deficits prior to actual functional loss of vision. However even if the magnocellular population is not *specifically* damaged early on in the process as some authors maintain, it is anticipated that, according to the theory of reduced redundancy that by targeting one population of ganglion cells, deficits may still be revealed early enough to initiate treatment to prolong useful visual function. This assumes, of course, that if one type of ganglion cell is not affected preferentially, that all types do deteriorate at the same rate, which may not in fact be true. This will be explored in more detail in the Discussion.

This thesis will take the form of individual descriptive sections of the development process involved in producing the optimal set up for each of the two tests described - Methods sections 2.1 and 2.2. The contrast threshold Methods section (2.1) includes results of preliminary experiments; however the results of all substantial groups of experiments are described in the Results section 3.1. All Simultaneous Brightness Ratio results are described in Results section 3.2. The significance and implications of the results of each test will be described separately in Discussion sections 4.1 and 4.2.

## 2 METHODS

The apparatus for the determination of contrast thresholds and of the simultaneous brightness ratios (SBR) passed through a series of developments until a final version was achieved which could be applied to patients with glaucoma and normal subjects.

### 2.1 Contrast threshold methods

Measurements of contrast threshold were determined in response to the detection of a grating pattern generated by laser interferometry. The optimal size, shape and form of that grating pattern were arrived at following a series of exploratory experiments.

#### 2.1.1 *Initial format of apparatus*

The apparatus used initially is shown schematically in Figure 2.1-1 as viewed from above the optical table on which all pieces of equipment were mounted. The beam of a green Helium / Neon laser of emission wavelength 543nm and output power 0.95mW (model UNIPHASE 1652P), which consisted of vertically polarized, coherent light, was passed through a spatial filter containing a x10 microscope objective and a pinhole of 50 $\mu$ m and then through a concave trial lens of power -10 D to increase the diameter of the beam. The beam was then passed through a collimating lens of +6.7 D to produce a parallel beam. After reflection through 90° from a front silvered mirror ( $\lambda / 20$  flatness), the beam passed through a sheet of polarizing film of extinction  $10^{-4}$ . It was then passed through an acrylic multifocal intra-ocular lens (3M Health Care, type 815LE, +23.5D), which has concentric grooves ground into its surface. This created an interference pattern consisting of a series of bold and fine concentric rings (shown schematically in Figure 2.1-5). The contrast of these rings decreased with increasing eccentricity. A cube beam splitter allowed addition of a green tungsten background beam from a Vickers microscope lamp that had a controllable output level. This beam consisted of a non-coherent light passed through a narrow band interference filter of peak emission 546nm (bandwidth 8.2nm at half amplitude), and was polarized with a sheet of polarizing film positioned at 90° to the

polarization plane of the laser beam. The final image consisting of a circular field comprised the laser interference pattern and the diffuse green background light. These two light beams were passed through a calibrated rotatable polarizer of extinction  $10^{-4}$  (Coherent-Ealing 22-9161) and the Maxwellian lens array (see section 2.1.1.1 for further details).

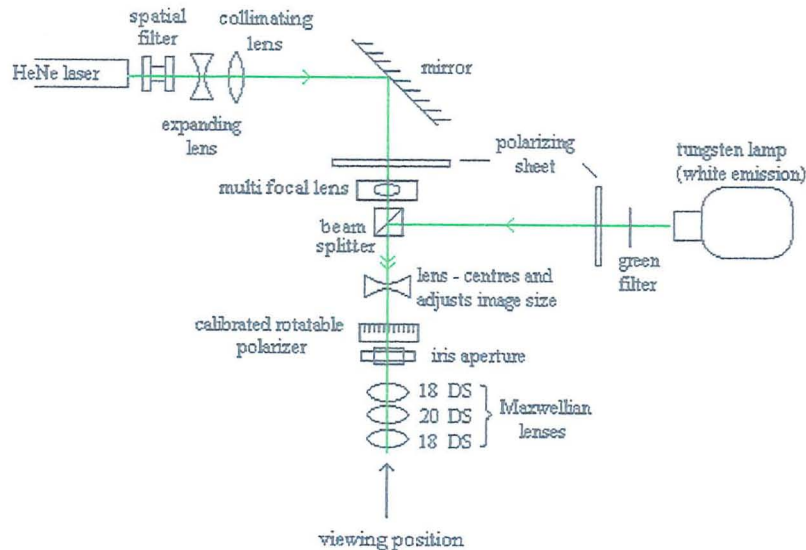


Figure 2.1-1 Schematic representation of the set up for initial experiments (viewed from above), showing the combination of the green laser beam passed through a multifocal lens to produce an interference pattern of concentric rings, and the diffuse green background from the tungsten lamp, HeNe = Helium Neon

Since it was not possible to use a single lens of sufficient power, in the first instance combinations of high power full aperture trial lenses were employed. The total power of these lens arrays was calculated from the procedure described by Freeman (1990), see details in Appendix section 5.1. The lens array initially consisted of 3 full aperture trial lenses of power +18D, +20D and +18D, which combined to give a total power of +44D. An adjustable aperture set the image diameter to the size required revealing a given number of interference rings. The subject viewed the image by looking directly into the Maxwellian lens array and controlled the relative proportions of background and laser light by turning the rotatable polarizer. This was initially set to zero degrees, at which position maximum transmission of background light and minimum transmission of laser light occurred. This corresponded to a field of diffuse green light with no interference pattern.

The subject then turned the rotatable polarizer towards 90° thereby increasing the proportion of laser light and reducing the proportion of background light, until there was sufficient contrast between the dark and light areas of the pattern for him or her to perceive the rings. Prior to the experiments, the lighting in the room was dimmed to a level, measured by the Optometer as 0.1 lux, in order to reduce reflection and glare from the lenses but precluding complete dark adaptation of the subject. Heaters were used in the room and the ambient temperature was monitored and maintained between 16 and 22 Centigrade, both for the comfort of the subject and the steady output of the light sources.

Contrast threshold was calculated by the conversion of the angle of rotation of the calibrated rotatable polarizer into a value for the contrast of light and dark in the interference pattern, using the formula:

$$\text{Equation 2.1-1} \quad \text{contrast threshold} = (\sin [\text{angle of rotation}])^2$$

The Michelson contrast value for the interference pattern was defined as:

$$\text{Equation 2.1-2} \quad (I_{\max} - I_{\min}) / (I_{\max} + I_{\min})$$

where I is the intensity of the laser light.

### 2.1.1.1 Maxwellian view

The interference pattern was passed through a Maxwellian lens array which focussed the rays of polarized light in the same plane as the posterior nodal point (Figure 2.1-2). Walsh described this method in terms of 'a lens being arranged to form an image of the source at the pupil of the eye' (Walsh, 1958).

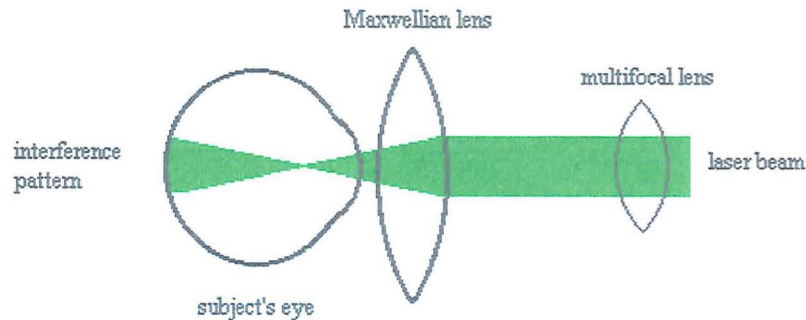


Figure 2.1-2 Schematic representation of the projection of the interference pattern onto the retina in the Maxwellian view, (the actual combination of lenses is simplified to a single lens for the purposes of the diagram).

This type of display has three major advantages over an externally viewed display such as produced by a cathode ray tube (CRT) or computer monitor. First, the laser pattern is transmitted unrefracted by the optical media of the subject's eye, which means that an uncorrected refractive error has no effect on the stimulus display. Therefore, prior correction of refractive errors or determination of a reading distance correction in the case of more elderly subjects is not required, which clearly has beneficial consequences for clinical testing of groups of subjects. Second, it is possible to arrange a patterned display which subtends a large angle. By contrast, a large externally viewed display is harder to arrange, and may entail moving the subject closer to an external display. Consequently this introduces problems of accommodation and the distortion of the image. Third, illumination is independent of pupil diameter since rays are transmitted through the pupil where they are at their narrowest. This may be particularly useful in testing for glaucoma in the older age-groups for whom senile miosis would reduce the retinal illumination of an external display (Weale, 1992).

### 2.1.1.2 Intensity of light beams

Before every experiment the intensity of the background and laser beams was measured with a UDT Optometer (S370 model 248) the sensor of which was placed at the viewing position marked on Figure 2.1-1. The laser and background beams were exposed in turn to allow an objective measurement of their individual illuminance at the position at which subjects viewed the image. The measurements were made with the rotatable polarizer at the appropriate position to transmit maximum light intensity: zero degrees for the background beam and 90° for the laser beam. Thereafter, the beams were adjusted, if necessary, to match their intensities to be as close as possible at their maximum levels (more details in Results section 3.1.3.1). This was achieved by altering the output of the tungsten lamp, or by the addition of appropriate neutral density filters to the laser beam.

In order to determine the stability of the two beams, an experiment was undertaken whereby measurements were made at 5-minute intervals over 3 hours. For simplicity during this experiment, no attempt was made to equalise the beams and measurements were made with the polarizer at 45°, meaning that repeated adjustments between zero degrees and 90° were not necessary (Figure 2.1-3).

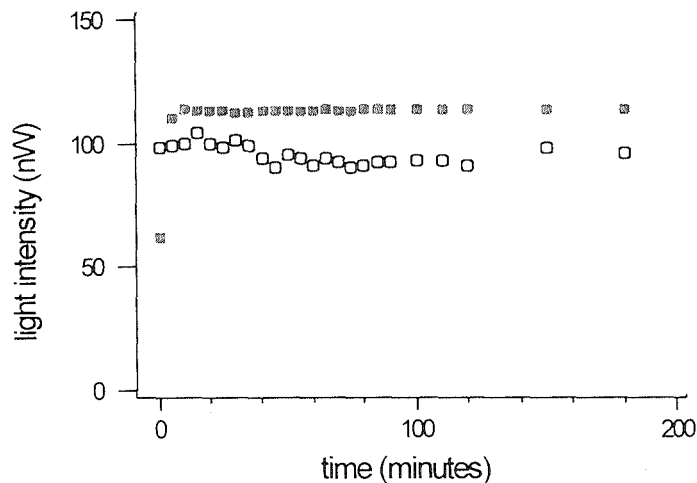


Figure 2.1-3 Plot of intensity of tungsten background light (open symbols) and laser light (filled symbols) against time.

Figure 2.1-3 shows that the output of the tungsten lamp fluctuated for about 60 minutes before settling to a reasonably steady level, of around 100nW. The laser light was found to settle within 15 minutes, at around 110nW. For this reason, prior to experimentation, each of the light beams was turned on for at least an hour to allow them to settle adequately. Once the beams were steady, the laser and tungsten output intensities at 90° and zero degrees (on the calibrated rotatable polarizer) respectively, were matched as outlined above.

### **2.1.1.3 Measurement of the field size**

Initially it was hoped that lens equations could be used to calculate the magnification and hence the angular subtense of the image field as observed in the Maxwellian view, as it cannot be measured directly. The basic problem was to determine the location of the position of the principal plane against which the equivalent focal length could be referenced. However the complex nature of the set up with a series of high power lenses of appreciable thickness and at different distances made this task extremely complex. Consequently a psychophysical method involving determination of the angular subtense of the blind spot was developed for its estimation.

The angular subtense of the blind spot from central fixation was first measured for external viewing. Using a rule to fix the distance of the head from a sheet of graph paper, the subject fixated monocularly straight ahead, where a point was marked on the graph paper. A target (the tip of a pencil) was moved out into the temporal field until it just disappeared into the blind spot: this point was marked. The target was then moved further out until it just reappeared from the blind spot: this point was also marked. This was repeated 3 times and the distances from the centre point were used to calculate the mean angular subtense between the start and end of the blind spot. The procedure was then repeated for the companion eye.

These measurements were repeated in the Maxwellian view. A pin mounted on a micromanipulator was placed in the plane of the aperture (Figure 2.1-4). In order to provide a fixation point, a fine thread was fixed across the centre of the field vertically and horizontally and the subject fixated at the crossover point (for simplicity this is marked with an X on Figure 2.1-4). With the needle initially at this point, the micromanipulator

reading was taken. The needle was then moved out into the subject's temporal field until its tip just disappeared into their blind spot, at which point a micromanipulator reading was taken, and then moved further until it reappeared, at which point a second reading was taken. Three measurements were taken for each eye and the mean distance to the start and end of the blindspot was calculated.

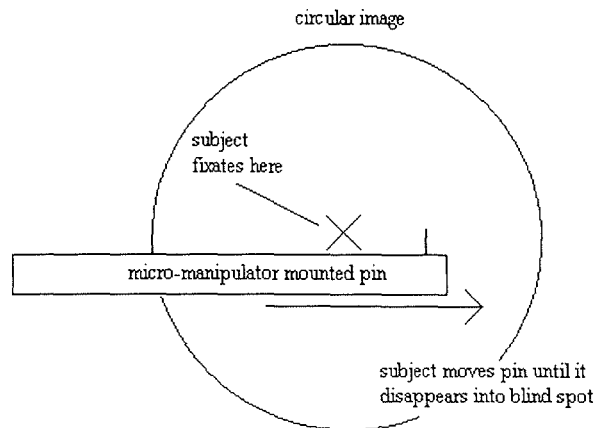


Figure 2.1-4 Schematic representation of the apparatus used to measure the distance of the blind spot from central fixation (at the level of the image) with respect to right eye viewing.

The angle subtended between central vision and the blind spot, obtained by the external measurements in each subject, were then used to convert the micromanipulator readings into a value for the number of degrees per mm. Three individuals completed this test and the results were averaged.

The mean value for the angle subtended per mm was  $4.3^\circ \pm 0.07$  standard error (SE). Since the diameter of the aperture that determines the field size could be measured in mm, it was opened to a diameter of 9.4mm to set the field diameter to  $40^\circ$ . This field size applies to all experiments which were undertaken using the final protocol, as described in Methods sections 2.1.2.7 and 2.1.3.

In experiments undertaken prior to this, when lower power Maxwellian lenses were used, the field size was estimated to be  $30^\circ$ .

## 2.1.2 Exploratory experiments with concentric ring pattern

At the start of every contrast threshold determination, the subject was instructed to look directly at the centre of the circular field with one eye. The other eye was closed or an eye patch was used if the subject preferred. The subject viewed the plain green field in the Maxwellian view and as contrast was increased the central disc became visible, then the first diffraction ring, then the second and so on. The subject was asked to increase the contrast by rotating the polarizer until they just perceived the outermost ring of the contrast pattern.

### 2.1.2.1 Peripheral rings

An investigation was undertaken to determine whether the contrast threshold would change in response to viewing an increasing number of concentric diffraction rings, seen in the Maxwellian view, by 7 subjects. Increasing the field of view by opening the aperture allowed the exposure of between one and 5 diffraction rings in addition to the central disc. The greater the number of rings, the further the outermost one extended into the peripheral field. Since for any given laser beam intensity, the progressively more peripheral rings have reduced contrast, therefore in order to detect them above the background, the laser beam intensity has to be increased. Figure 2.1-5 shows a schematic representation of 2 and 3 rings at high contrast.

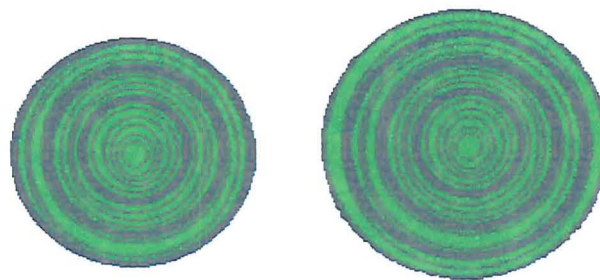


*Figure 2.1-5 Schematic representation of concentric light / dark ring pattern at high contrast, showing a central illuminated disc surrounded by 2 diffraction rings (left) and 3 diffraction rings (right). Fine lines appearing within the bright rings were attributed to the machining process used to etch the diffraction rings. In reality the peripheral rings had reduced contrast in relation to the more central ones.*

A spot of brightness was visible at the central disc from the laser pattern due to there being a finite extinction value of the rotatable polarizer ( $10^{-4}$ ). This provided a useful fixation point within the plain green field.

The subject was asked to look directly at the fixation spot, and rotate the polarizer until the outermost ring was visible. The required angle of rotation for the subject to perceive the outermost ring was noted and then the polarizer reset to zero prior to the subsequent determination. This was repeated 6 times and a mean value was calculated.

The mean contrast thresholds were therefore obtained for different numbers of diffraction rings ranging from one to 5 and are plotted with  $\pm$  one SE for one individual in Figure 2.1-6. This result was similar to those for all 7 subjects.

## RESULTS

Increasing the number of rings from one to 5 did not have a significant effect on contrast threshold, ( $P= 0.98$ , one-way ANOVA).

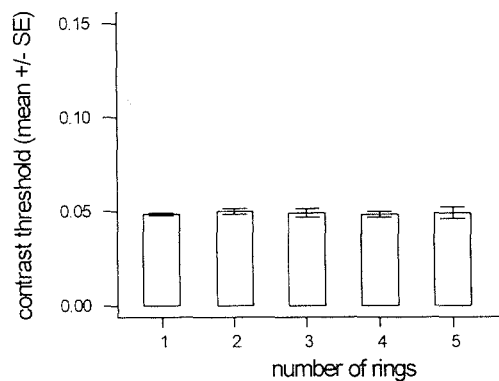


Figure 2.1-6 Individual example of mean contrast threshold  $\pm$  SE to one, 2, 3, 4 and 5 diffraction rings.

If the rings had been detected separately, the intuitive expectation was that the contrast threshold would increase. However, the invariance of the contrast threshold was clearly contrary to this expectation. This suggested that despite the instruction to determine contrast threshold to the outermost ring, the contrast threshold may have been determined primarily by perception of the first ring. It was, therefore, deemed impossible to resolve when each peripheral ring appeared separately while viewing clearly visible central rings.

### **2.1.2.2 Central occlusion and quadrants**

In order to confirm that the central rings determined contrast threshold, a 9mm-diameter central occluder was then incorporated into the stimulus field. This blocked out the central 3 rings of the display. The occluder contained a small hole at its centre (less than 1mm in diameter) to allow for central fixation.

Since the ultimate goal was to test different regions of the visual field, the circular image was subdivided into 4 equivalent quadrants, using occluders. These consisted of full aperture blanks and very low power lenses, which were partially blacked out leaving a single quadrant clear. They were placed in front of the central occluder. The test regions were thus limited to an arcuate shape in the peripheral field as shown schematically in Figure 2.1-7. Two peripheral bold diffraction rings were visible. This is the same quadrant format as used by Devos *et al.*, in their 1995 study on quadrant analysis using colour contrast thresholds in glaucoma (Devos *et al.*, 1995).

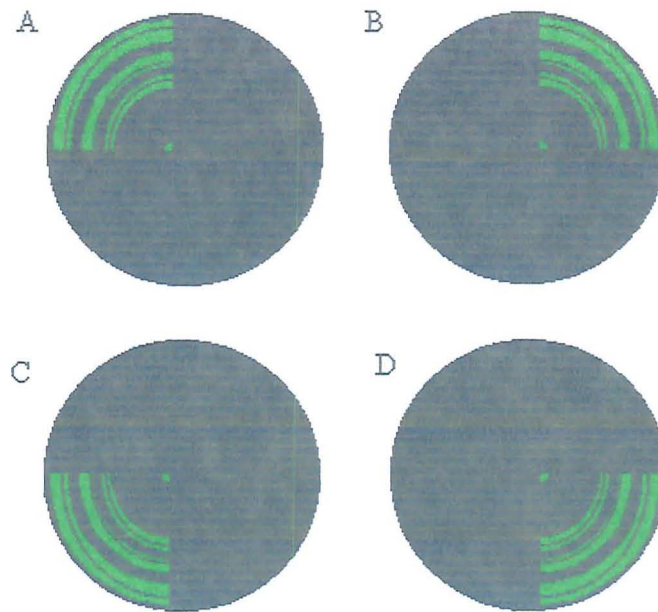


*Figure 2.1-7 Schematic representation of diffraction pattern consisting of 2 rings and central occluder. Mask for; A: superior temporal, B: superior nasal, C: inferior temporal, and D: inferior nasal quadrants, with reference to left eye viewing.*

The central occluder could then be removed to reveal the full quadrant, the contrast thresholds of which could be compared with those for the truncated arcuate quadrant. Five consecutive readings for contrast threshold were taken for each of the 4 quadrant positions for 11 subjects, with and without the central occluder. Quadrants were tested in random order for the subject's preferred eye. The subjects were instructed to look at the centre of the field and rotate the polarizer until the diffraction rings were just visible.

### **2.1.2.3 Psychophysical testing of illuminance of quadrants**

In addition to radiometric determinations of the illuminance of each quadrant using the Optometer, the relative brightness was confirmed psychophysically by determination of the contrast threshold for direct foveal vision. These were routinely made for each quadrant before every experiment by the author. Initially this was undertaken through a circular aperture placed within each quadrant in an attempt to avoid any effect on threshold caused by the different shapes of the stimulus. However, distortion of the circularity of this

aperture occurred due to the curvature of the lenses and so the aperture was abandoned. Thereafter, the attention was focussed on the centre of each quadrant and the contrast increased until the pattern was first perceived just as for the peripheral contrast threshold readings. Details of the results and an investigation of a relationship with peripheral contrast threshold are contained in Results section 3.1.3.2.

## RESULTS

An effect of the inclusion of central vision on the contrast threshold was confirmed for viewing the full quadrant. The contrast thresholds with the occluder present were consistently elevated with respect to those without the central occluder, ( $P < 0.02$ , ANOVA<sup>\*</sup>). A typical result for one individual is shown in Figure 2.1-8.

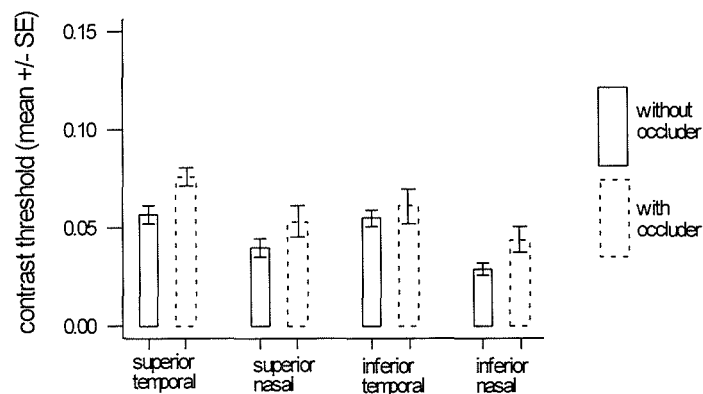


Figure 2.1-8 Individual example of mean contrast threshold  $\pm$  SE with and without the central occluder for field containing 2 bold peripheral diffraction rings in each of 4 quadrants.

These experiments vindicate the use of a central occluder in order to obtain a valid peripheral contrast threshold. From this point onwards, the central and quadrant occluders were employed in all experiments.

\* Where more than one factor was involved in the series of contrast threshold readings, a balanced ANOVA was used to determine statistical significance, or an unbalanced ANOVA (based on the General Linear Model) for sets of data which had uneven numbers. Significance was taken when  $P < 0.05$  in all cases.

### 2.1.2.4 Green and red diffraction patterns

The effect of the colour of image on contrast threshold was tested by comparison of contrast thresholds in response to red as well as green interference rings: the apparatus used is shown in Figure 2.1-9. A red laser interferometry pattern of concentric rings was generated using a Helium Neon laser (emission 632nm) of power 5mW (NEC – 9LG 5311). The background illumination was provided by a tungsten light passed through a red interference filter (peak transmission 630nm, 5.0nm at half amplitude). The trial lenses used to generate the Maxwellian view were dispensed with and replaced by a 38mm diameter high refractive index plano-convex lens of power +32 D,  $n = 1.7$  (Norville Optical Company, Livingstone) and 40mm diameter aspheric lens of +40 D (Coherent-Ealing 34-6338). The total power was +62 D.

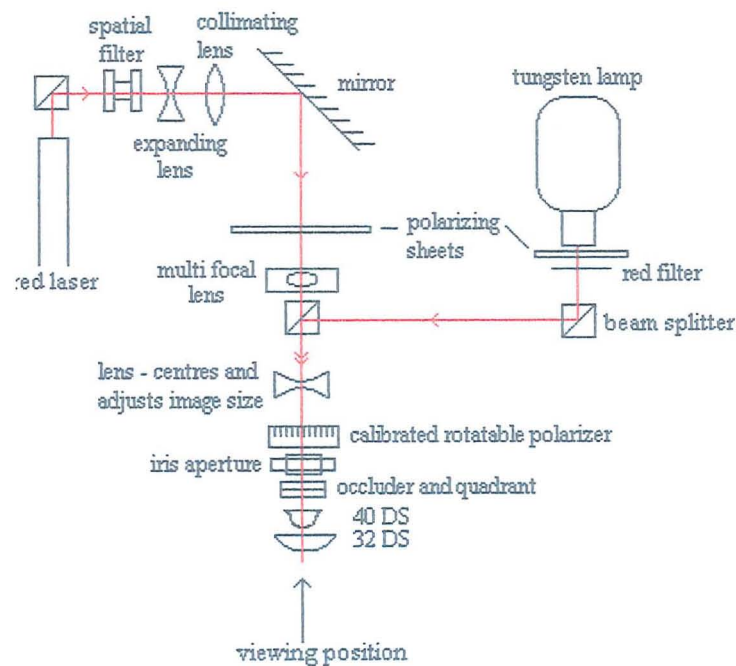


Figure 2.1-9 Schematic representation of the set up (viewed from above), used to generate interference pattern of red concentric rings. N.B. New lenses are in place above viewing position.

## INTENSITY OF LIGHT BEAMS

The intensities of the red background and laser beams were checked against time with the Optometer, using the same procedure as described for the green beams in Methods section 2.1.1.2. The results are shown in Figure 2.1-10. As with the equivalent green experiment, the laser and background beams were not equated prior to this experiment for simplicity.

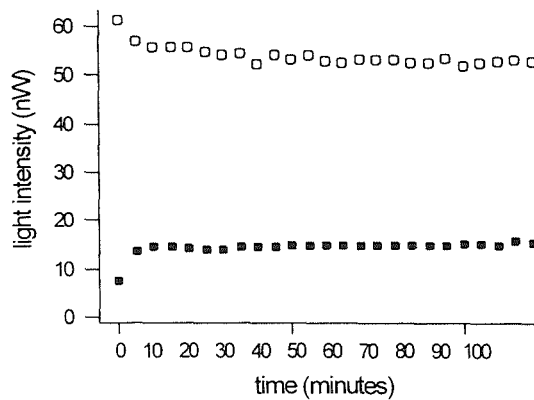


Figure 2.1-10 Plot of tungsten background light (open symbols) and laser light (filled symbols) for red display.

The laser beam settled around 15nW, while the background beam settled at around 55nW. Stable light outputs were reached after around 40 minutes for both the laser and background beams. Thereafter, the apparatus was turned on at least 40 minutes before any experiments were undertaken. The laser and background beams were equated in intensity at 90° and zero degrees respectively prior to further experiments.

### **2.1.2.5 Contrast thresholds to red versus green display**

For the purposes of the experiment, the intensity of the red laser beam (at the 90° position on the calibrated polarizer) was made equal to the intensity of the red background beam (at 0° position on the calibrated polarizer) as already described for the green display. It was not appropriate to match these two displays in terms of radiometric intensity since the visual system is much more sensitive to green than to red light. Accordingly, the intensity

of the two stimulus displays was determined psychophysically. The strength of neutral density filter necessary to reduce the beam intensity so that it was just visible and no more was determined as quickly as possible to avoid dark adaptive changes. The value of this neutral density is thus the amount by which the intensity exceeded the photopic threshold. For the red background beam this was 1.0 log units. Subsequently, the intensity of the red laser and the green laser and their background beams were equated to this level, i.e. one log unit above photopic threshold. Despite the relatively small amount of suprathreshold illuminance, both displays were clearly visible.

Six consecutive readings for contrast threshold were taken for each of 4 quadrant positions for 8 subjects with the central occluder in place, in response to both the red and green display. Quadrants were tested in pseudo random order for the subject's preferred eye. The subjects were instructed to look at the centre of the field and rotate the polarizer until the diffraction rings were just visible.

## RESULTS

The mean contrast threshold in response to the red diffraction ring display was significantly elevated compared with those for the green display in all 8 subjects in the 4 quadrants under study. The increase in contrast threshold in response to the red image was statistically significant, ( $P \leq 0.001$ , ANOVA). A typical example is shown in Figure 2.1-11.

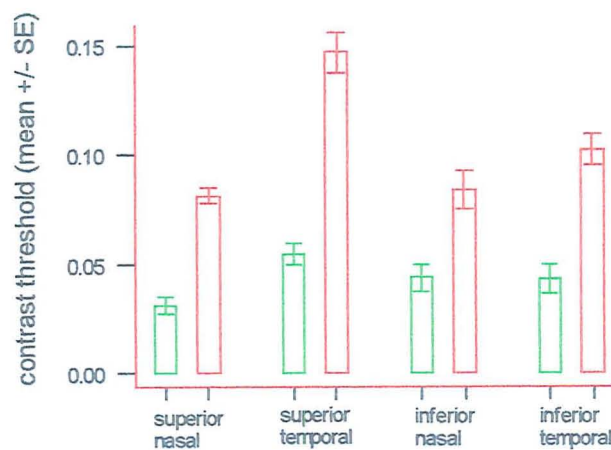


Figure 2.1-11 Mean contrast threshold  $\pm$ SE to red and green stationary image for one subject.

Subjects universally reported that the red image was less comfortable on the eye than the green display despite being psychophysically matched. On grounds of comfort and the need to have the lowest baseline contrast thresholds against which any anomalies may be compared, it was decided to employ only the green display in future experiments.

#### **2.1.2.6 Stationary versus flicker**

Since there is some evidence (as discussed in the Introduction) that the magnocellular pathway, which subserves movement detection, may be disproportionately adversely affected in glaucoma, comparisons were made of the contrast thresholds in response to different rates of flicker in addition to a stationary display for visually normal subjects. Unlike a CRT display with which a flickering stimulus can be readily effected electronically, this was not so straightforward with an optical table display, due to the intensity change which would arise on interruption of the laser beam. Consequently, the apparatus evolved through a series of modifications as the optimum method was sought.

In the first instance, flicker was achieved by reflection of the laser beam from a rotating front silvered mirror on which was mounted a sheet of polarizer as shown in Figure 2.1-12. In order to achieve this the laser beam was diverted using a cube beam splitter (B1 in Figure 2.1-12) onto the rotating mirror-polarizer. The rotating mirror-polarizer was mounted on a precision direct current (DC) motor (RS components 336 – 236), which was driven by a variable DC supply. The rate of rotation of the mirror-polarizer mount was calibrated by reflecting the incident beam onto an assembly consisting of a photodiode and amplifier, the output of which was displayed on an oscilloscope. As the mirror-polarizer rotated, the oscilloscope displayed a sine wave voltage change, representing the frequency of rotation. Hence, the required rate of rotation could then be arranged and the appropriate setting on the DC supply was noted.

As the mirror-polarizer rotated, the intensity of the laser beam changed sinusoidally. The flickering beam was redirected towards the subject's eye by beam splitter B2, and as in previous experiments the background beam was added using a beam splitter, marked as B3 on Figure 2.1-12.

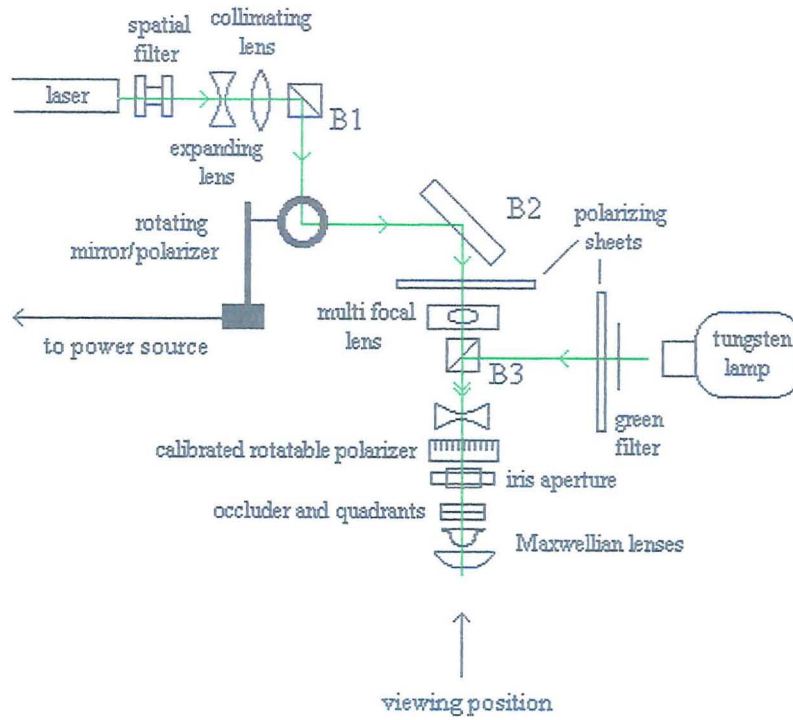


Figure 2.1-12 Schematic representation of set up (viewed from above) used to generate flickering stimulus, using motorised rotating polarizer.

The occluder and quadrants were used as in the previous experiments. As before, the subject centrally fixated and increased the contrast until their first perception of the grating pattern within the truncated quadrant, whether flickering (at 4Hz, 8Hz or 10 Hz) or stationary. The field size was 40° in diameter for both red and green displays. Six contrast threshold readings were taken for each quadrant position for both stationary and flickering stimuli, and quadrants were tested in pseudo random order.

The results (described in Results section 3.1.1) proved to be inconsistent, with depression, elevation and no effect on contrast threshold all occurring within the same subject group. A confounding factor became apparent in that the change in intensity was not perfectly sinusoidal. This arose because the incident and reflected beams from the rotating mirror-polarizer had a finite separation as the centres of the mirror and polarizer elements could not be identical. Given this shortcoming, we then sought to explore further methods of producing a flickering display with our apparatus. The experiments were continued on the basis that at just supra-threshold contrasts, the modulation in intensity would be small thus allowing any effects of the different temporal frequencies on contrast threshold to be discerned.

Simpler methods of generating flicker, in a non-sinusoidal form, were then explored:

1. A rotating windmill with vanes made of black cardboard was placed at the position marked by the asterisk on Figure 2.1-13. It was appreciated that this method of generating flicker would cause an illuminance flicker, however it was used in the investigations in anticipation of more consistent responses compared with the previous method. The rate of flicker was calibrated as for the rotating mirror-polarizer described above.

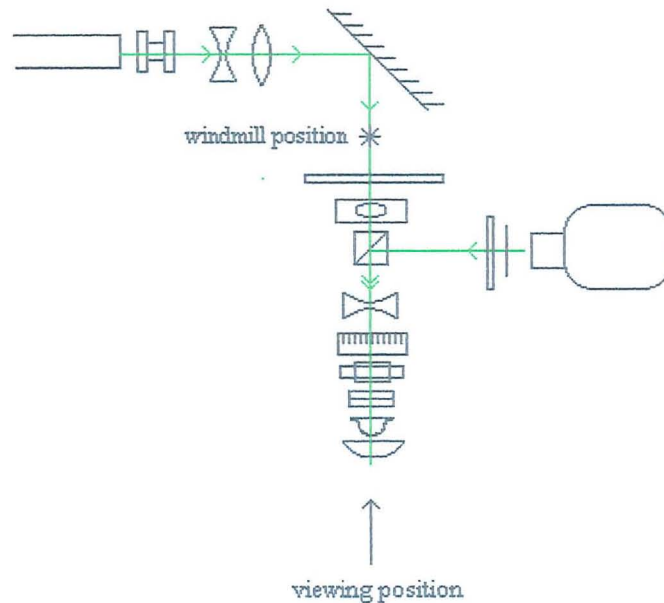


Figure 2.1-13 Schematic representation of set up (viewed from above) indicating the position of the windmill used to generate a flickering stimulus by intermittently interrupting the laser beam. N.B. Features not annotated are identical to Figure 2.1-12.

However, this also produced inconsistent results in different individuals (described in Results section 3.1.1); therefore it was abandoned.

2. A rotating disc of Perspex was designed with its surface made up of alternate, equally spaced vanes which were either smooth or abraded (Figure 2.1-14).

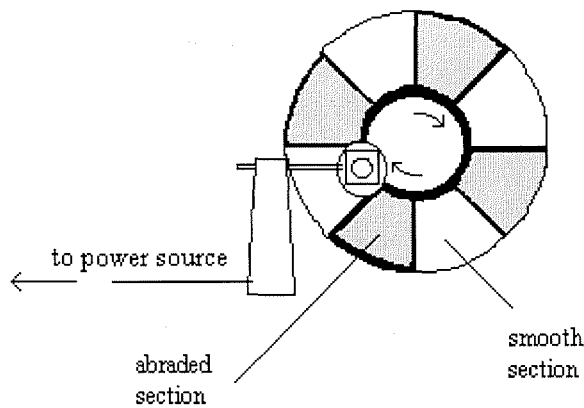


Figure 2.1-14 Schematic representation of Perspex windmill (viewed from front).

This was placed at the same position as in the previous method, marked by the asterisk on Figure 2.1-13. It was anticipated that the abraded sections would cause scattering of the interference pattern while still transmitting an appreciable amount of light, while the clear vanes would allow the generation of the interference pattern. This proved unsuccessful due to the phase shift of polarization caused by the two types of Perspex surface. This was discovered when calibrating the intensities of the beams. With the clear Perspex vane in place, the minimum laser intensity no longer occurred at zero degrees on the calibrated polarizer. When the abraded Perspex vane was placed in the path of the beam, the polarization minimum further changed. The outcome was a substantial flickering effect at the supposedly minimum setting on the calibrated polarizer. This approach was therefore discontinued without testing on any subjects.

3. Finally a rotating windmill was created whose frame was black cardboard in which the vanes consisted of thin tissue paper to scatter light but still allow some transmission. The areas of black card were kept to the minimum possible to limit the amount of complete blockage of the light sources, while still producing a rigid structure. The windmill was put in the same position as the previous method, as shown in Figure 2.1-13. The diffuser vanes were of equal size to the inter-vane spaces as shown in Figure 2.1-15.

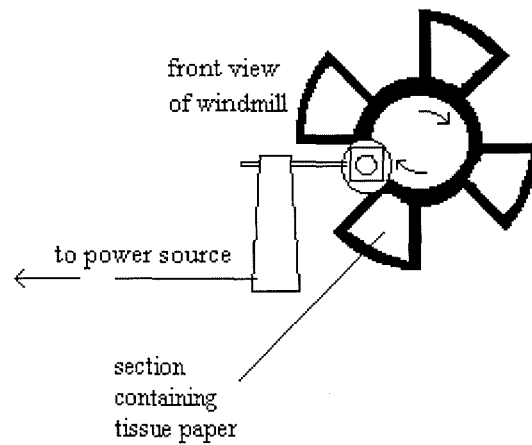
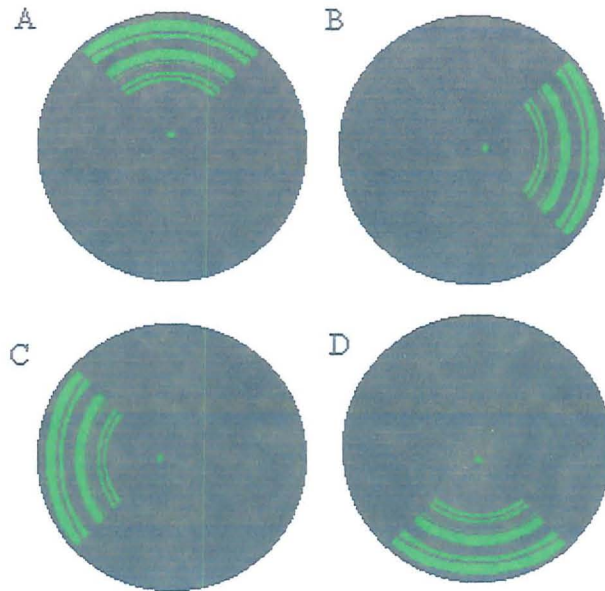


Figure 2.1-15 Schematic representation of windmill (viewed from front) with diffuser vanes designed to disrupt the interference pattern in order to cause flicker but allow transmission of light.

This windmill reduced the intensity of the laser beam to about 62%. As the protocol involved increasing the transmission of the laser beam by rotation of the calibrated polarizer, the contrast threshold values were dependent on the contrast of the display in addition to the change in the intensity of the display caused by the windmill. Despite the fact that the least amount of intensity change occurred using this method, the results produced were still unexpected, they are described in Results section 3.1.1. In subsequent experiments a stationary stimulus was used.

### 2.1.2.7 Quadrant orientation

The layout of the quadrants, which had initially been chosen with reference to another glaucoma study (Devos *et al.*, 1995), was then explored. It was reasoned that an oblique arrangement rather than the rectilinear one may be more appropriate for analysis of the glaucomatous visual field. As discussed in the introduction, glaucomatous visual field defects are most often found in the superior and inferior quadrants (Aulhorn and Karmeyer, 1977) and the nasal quadrant has also been identified as significant in glaucoma (Ballon *et al.*, 1992). This set up also allowed the blind spot to fall directly into the centre of the temporal quadrant, rather than at the border of the upper temporal and lower temporal quadrants. Figure 2.1-16 shows a schematic diagram of the oblique quadrant layout, in contrast to the rectilinear quadrants shown in Figure 2.1-7.



*Figure 2.1-16 Schematic representation of the oblique quadrant positions showing two bold diffraction rings outside central occluder; A: superior, B: nasal, C: temporal, D: inferior, with respect to left eye viewing.*

Contrast threshold determinations were obtained in two subjects in response to each of the 4 quadrants superimposed upon a central occluder in both rectilinear and oblique positions.

## **RESULTS**

The new position of the quadrant had no significant effect on contrast threshold in either of these subjects ( $P = 0.1$ , one-way ANOVA). Mean contrast thresholds for one subject are shown in Figure 2.1-17.

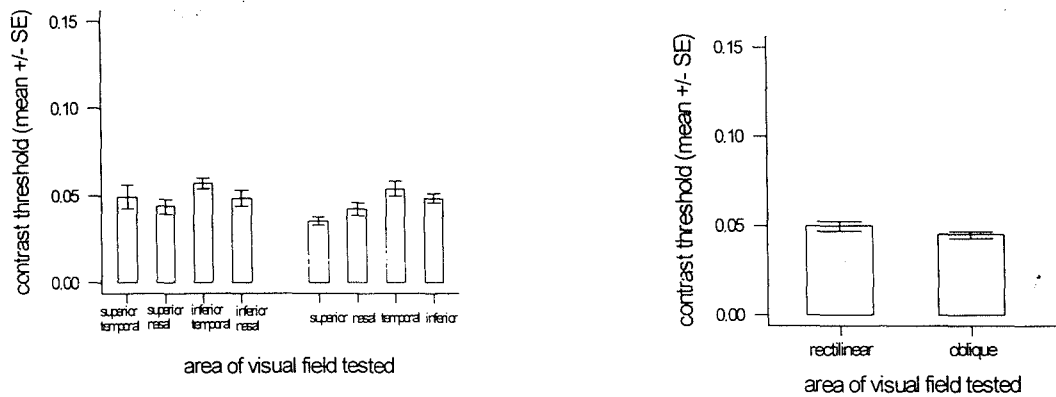


Figure 2.1-17 Left graph: mean contrast thresholds ( $\pm$  SE) in response to rectilinear (left) and oblique (right) quadrants. Right graph: aggregated contrast threshold data for rectilinear and oblique quadrants.

Both subjects tested reported a preference for the oblique quadrants. From this point onwards oblique quadrants were used.

### 2.1.2.8 Vertical sinusoidal grating pattern

The original concept of determining the contrast threshold of progressively more eccentric diffraction rings proved impracticable, though this form of stimulus had been persevered with due to its advantage in allowing truncated quadrants with the same stimulus pattern to be viewed. In the course of the exploratory investigations, however, subjects reported confusion concerning the specific aspects of the display which they were to use as the point of threshold. This confusion arose due to the presence of the very fine grooves superimposed on the larger, bold diffraction rings. This may have led to a lack of consistency in repeat measurements particularly with subjects completing the experiment for the first time. Therefore the decision was taken to remove the multifocal lens and its ring pattern in favour of a sinusoidal grating pattern, which was even and could thus be detected with more confidence.

Orientation and spatial frequency of such a pattern could be set at the required values using the following apparatus. The green laser beam was split into two by a cube beam splitter

marked as B1 on Figure 2.1-18. The diverted laser beam, after reflection from a front-silvered mirror (M1), was redirected towards the subject's eye by a beam splitter (B2). By translation of mirror M1, followed by appropriate rotation of the mirror to direct the half beam towards beam splitter B2, the path length of this beam could be changed. Consequently a phase shift relative to the half-beam transmitted by B1 was arranged. The recombined beams produced an interference pattern. The spatial frequency of the pattern was adjustable by alteration of the position and angle of mirror M1 on Figure 2.1-19. The angle of mirror M2 set the orientation of the interference pattern. The laser beam consisted of coherent, vertically polarized light, and the green background beam (which was added via beam splitter B3) consisted of non-coherent, horizontally polarized light. With the rotatable polarizer at  $90^\circ$ , the intensity of the two laser half-beams was adjusted to be as near as possible by addition of the appropriate neutral density filters. With the rotatable polarizer at zero degrees, the intensity of the background beam was adjusted to be as near as possible to the combined laser half-beams using the output control on the tungsten lamp.

The reflected half laser beam (reflected by B1) underwent a polarization shift which was compensated for by addition of rotatable sheet polarizer P1, this ensured that the two half-beams were of the same polarization. Rotatable sheet polarizer P2 was used to sharpen the polarization of the laser beams.

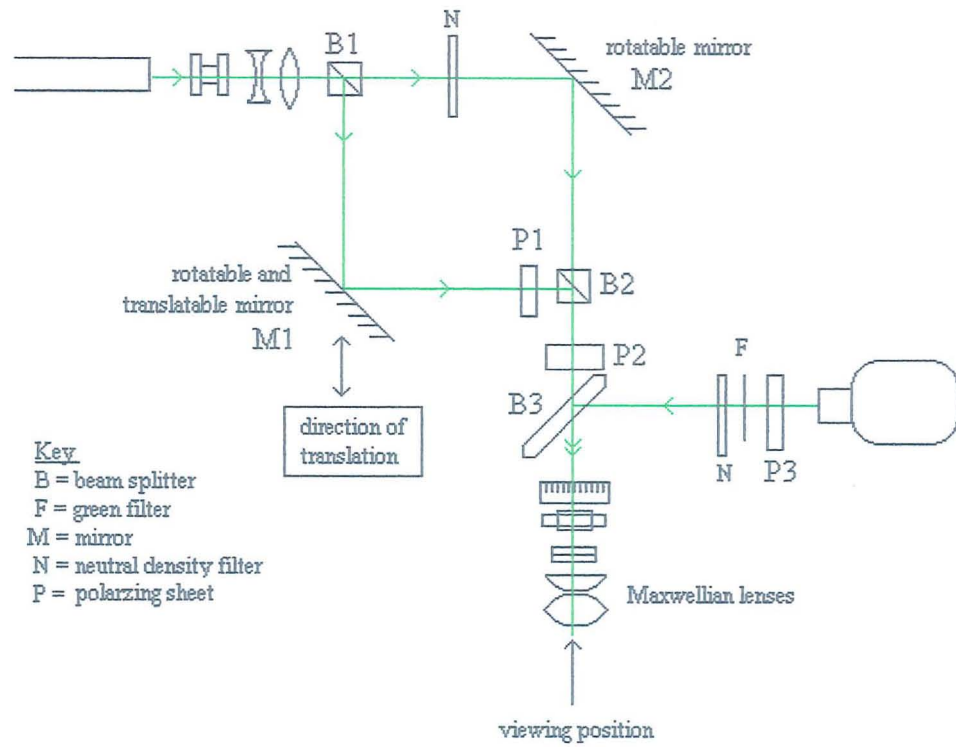
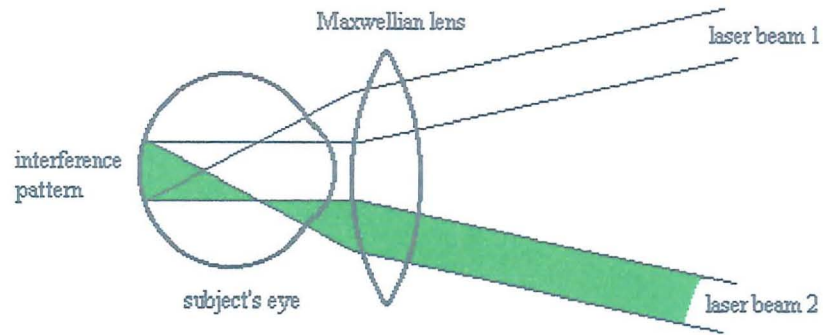


Figure 2.1-18 Schematic representation of the set up (viewed from above) used to generate a sinusoidal interference grating pattern. As before, features not annotated are identical to Figure 2.1-12.

The generated image of a vertical sinusoidal grating pattern was projected into the subject's eye via a pair of high power Maxwellian lenses shown at the bottom of Figure 2.1-18. The two laser half-beams enter the eye separately and diverge beyond the posterior nodal point. The interference pattern is therefore only generated beyond the level of the subject's refractive media, as shown schematically in Figure 2.1-19.



*Figure 2.1-19 Schematic representation of the production of a laser interference pattern in the Maxwellian view with two laser beams (one lens rather than two shown for simplicity).*

As previously discussed, this means the subject perceives the image in the Maxwellian view and the image is not degraded by the subject's refractive error. Maxwellian viewing gives the capacity to generate a display of large angular subtense, as the incoming rays are not limited by the subject's pupil to the same degree as an image viewed directly.

### 2.1.3 Final protocol

As before, the intensity of the laser and background beams was checked at the start of each experiment. The field was circular and was set to  $40^\circ$  in diameter with the aperture using the conversion factor for the angular subtense of the image, as described in Methods section 2.1.1.3. An annulus of  $20^\circ$  diameter (i.e. subtending  $\pm 10^\circ$  from fixation) was mounted concentrically and had a central hole of less than  $2^\circ$  diameter for fixation. The hole was covered with clear adhesive tape which allowed transmission of light for fixation but which disrupted the grating pattern, see Figure 2.1-20.

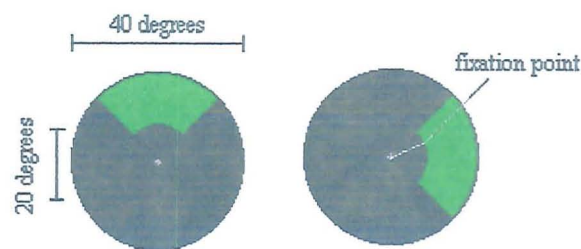
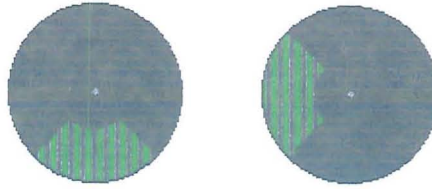


Figure 2.1-20 Schematic representation of superior quadrant and nasal quadrant as viewed by the subject's left eye at minimal contrast, i.e. no grating pattern visible. The dimensions of the display and the fixation point are shown.

A spatial frequency of one cycle per degree was chosen as it is near the peak of the human contrast sensitivity function for peripheral retina (Kelly, 1984), thus producing low contrast threshold values in the normal subject. As already mentioned it was also desirable to target one population of retinal ganglion cells, and in choosing a low spatial frequency grating, the response characteristics of magnocellular ganglion cells are specifically targeted. Also, Vaegan and Halliday noted that contrast threshold determinations are less variable at lower spatial frequencies (Vaegan and Halliday, 1982). For the size of field being used, 10 to 20 full gratings were visible in each quadrant, which is important for detecting a true contrast threshold unaffected by the number of cycles (Hoekstra *et al.*, 1974). A vertical pattern was chosen throughout the experiment for simplicity. High contrast gratings within two of the truncated quadrants are shown schematically in Figure 2.1-21.



*Figure 2.1-21 Schematic representation of inferior quadrant and temporal quadrant, as viewed by subject's left eye, with grating pattern at high contrast. A reduced number of grating cycles is shown for simplicity.*

As part of the ongoing development to improve the apparatus, in place of the trial frame used to support the lenses and apertures, an enclosed cylindrical unit was fabricated to support the Maxwellian lens array. It also had an in-built disc providing the quadrant and annulus occlusion: this could be rotated to reveal each test region as required. This was much more robust than the former method of lens mounted occluders. It was not prone to bumping by subjects or irregularities in positioning and was more efficient since simple rotation of the housing provided an accurate arcuate position. As the measurements of the laser and background beams used to match them before each experiment were previously done for the whole unoccluded field, one effect of this in-built rotatable quadrant occluder was that it was no longer possible to match the beams' intensities in the same way; thereafter it was measured individually for each quadrant position. This gave a more robust indication that each test region was well matched, rather than having one single measurement for the whole field.

Prior to the start of the experiment, the point of threshold was explained carefully using drawings showing grossly different levels of contrast. Subjects were encouraged to experiment initially, by turning up the contrast too far and observing the grating at supra-threshold contrast before beginning the experiment proper. Subjects were also encouraged to ask questions and describe the image, as they perceived it, until they became confident. As with the previous experiments, the rotatable polarizer was set to zero before each new reading. The subject fixated on the central dot then turned the rotatable polarizer slowly and smoothly, stopping when the grating pattern first became apparent in their peripheral vision. Several 'warm up' readings were taken before beginning the experiment. Once the experiment began, specific questions regarding the image and experiment were answered, but no further instruction was given in order to avoid influencing the readings. Subjects

were instructed to avoid staring at the image for too long, to prevent adaptation to the grating, and they were required to sit back from the apparatus after every reading.

## **SUMMARY**

The final protocol therefore consisted of a green, sinusoidal grating pattern of one cycle per degree presented as a stationary image. The contrast threshold in response to 4 obliquely oriented, truncated quadrants was taken with the stimulus viewed peripherally. These quadrants extended between  $10^\circ$  and  $20^\circ$  from fixation with a central occluder disc containing a fixation spot of  $2^\circ$  in diameter. Both eyes were tested individually, with the subject's preferred eye first. Six readings were taken for each quadrant, the first quadrant being repeated at end of experiment (further details of this are given in Results section 3.1.3.3). The order in which quadrants were tested was repeated for the second eye. In a co-operative subject this took no more than 30 minutes to complete, including time for instruction and initial practice readings.

**PAGE  
MISSING  
IN  
ORIGINAL**

analysis' used by Sponsel. We wanted to evaluate the sensitivity of retina stimulated by each truncated quadrant; therefore we have not excluded the points around the blind spot as Sponsel did in an attempt to increase the diagnostic sensitivity of his method.

Our scoring system involved masking off the points that fell outside the areas of visual field stimulated by our test. The mask revealing the points relating to the superior quadrant stimulus for contrast threshold testing was overlaid on the left eye chart (Figure 2.1-22, A). A full Friedmann Visual Field chart for the right eye of patient 5-g is shown in Figure 2.1-22 B. The right eye chart (Figure 2.1-22, B) includes filled circles which indicate points missed at all intensities, plain circled letters indicating points missed at intermediate intensities, and letters without annotation indicating test points which were perceived at all intensities.

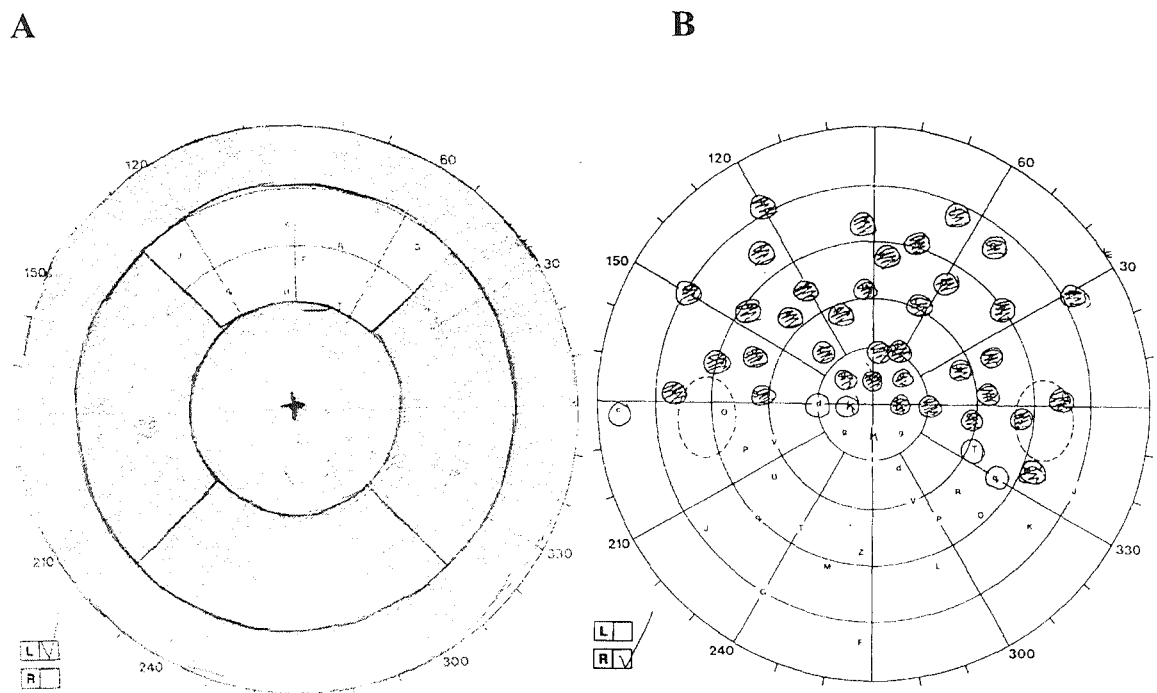


Figure 2.1-22 Friedmann visual field for patient 5-g's left eye (A) and right eye (B). Left eye field was superimposed with a mask which revealed an aperture corresponding to the truncated superior quadrant of the contrast threshold test; this could be rotated to reveal the nasal, inferior and temporal quadrants. The full right eye field is shown: this was then analysed with the mask in place, as for the left eye field.

For each of the points falling in the test region (between 6 and 12 points depending on the quadrant location), a value was allocated related to the intensity of the light at which it was perceived by the subject. A score of 3 was allocated for points perceived at the dimmest age-related intensity (stronger filter in place), a score of 2 when perceived with the weaker

filter, a score of one when perceived with no filter, and zero when not seen at all. These values were summed, divided by the maximum score possible and then multiplied by 100, to give a value of percentage sensitivity in that region. This value was then subtracted from 100 to give a percentage loss of sensitivity. The corresponding plot of percentage losses as quantified by our method for patient 5-g is shown in Figure 2.1-23.

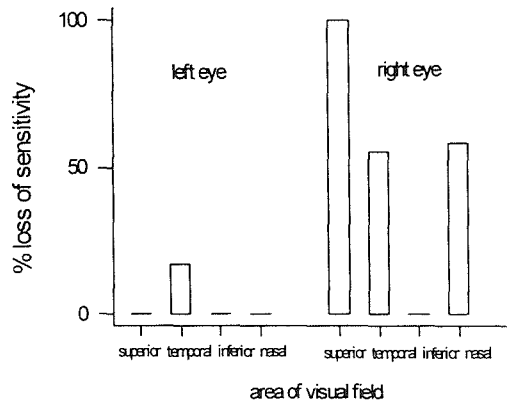


Figure 2.1-23 Plot of percentage visual field loss as measured by Friedmann visual field analyser in each contrast threshold oblique quadrant region and quantified by simplified Sponset method, for patient 5-g.

For this patient, the left eye has a full visual field, the only missed points being those which fell into the blind spot, which can be seen in Figure 2.1-23 as a slight loss of sensitivity in the temporal quadrant. The right eye has extensive sensitivity loss in the superior quadrant, moderate losses in the temporal and nasal quadrants, and full sensitivity in the inferior quadrant.

### **2.1.5 Analysis of results**

All calculations and statistical analysis were completed using Minitab 11 for Windows. For each subject who completed the experiment, a mean value for contrast threshold was calculated and plotted for each quadrant and both eyes. Graphs were plotted with error bars which indicated  $\pm$  one SE. One-way ANOVA tests were used on the effect of single factors on contrast threshold, e.g. quadrant layout. Where more than one factor was involved, i.e. both eyes of each subject; 4 quadrants within each eye; red or green colour of display or stationary versus flickering display; a balanced ANOVA was carried out (or an unbalanced ANOVA using the General Linear Model where the data sets were unbalanced).

Where groups of data were being compared, two-sample t-tests were used on parametric data, and Mann-Whitney tests on non-parametric data. In all cases statistical significance was taken when  $P < 0.05$ . For the purposes of defining a prediction limit for normal, we have used the convention of mean + 2 SD, which relates to a 97.7% confidence limit. In glaucoma patients, the mean contrast thresholds were plotted against the quantified visual field results from conventional analysis, as described above, and linear regression analysis was applied.

For assessing the usefulness or importance of a regression where a statistically significant result is obtained but for which the value of  $R^2$  was very low, we have adopted the standard procedure described by Draper and Smith, 1982. In such cases the slope of the regression line may be calculated to be non-zero, but the importance of the slope is deemed doubtful unless the F-value exceeds a multiple of the 'usual percentage point for the minimum level of proper representation'. Where  $n > 120$  (as is the case for the data concerned), the usual percentage point is 3.8, and the recommended multiple by Draper and Smith is 6, therefore where an F-value exceeds 22.8 the relationship will be considered to have significance in such cases.

## 2.2 Simultaneous Brightness Ratio (SBR) methods

A set of apparatus was designed and developed in order to be able to test inter-ocular SBR by a novel method, in addition to the previously unexplored intra-ocular SBR.

### 2.2.1 *Development of apparatus*

In order to determine the inter-ocular SBR, it was necessary to generate light stimuli that could be projected onto the central visual field of each eye simultaneously without fusion occurring. Authors who have already published results on inter-ocular SBRs have achieved this by placing a partition between the eyes (MacMillan *et al.*, 1994). We decided to use a Wheatstone stereoscope to divert the gaze towards the display (seen from above in Figure 2.2-7). In addition to inter-ocular SBR, we also explored intra-ocular differences in brightness sense by testing upper / lower and nasal / temporal SBR in the same eye. This does not appear to have been investigated previously; therefore to the best of the author's knowledge no literature is available on either methods or results.

Previous work on inter-ocular brightness sense testing (Sadun and Lessell, 1985; Preston, Bernstein and Sadun, 1988; Teoh, Allan, Dutton and Foulds, 1989; Borgmann *et al.*, 1991; MacMillan, *et al.*, 1994), often involved rotatable polarizers mounted on trial spectacle frames (controlled by the experimenter), and polarizing sheets covering the light sources. In contrast to this, we used a graduated neutral density filter wedge controlled by the subject to adjust the transmission of light into the eye. This allowed the greater flexibility required in order to adapt the equipment for testing both inter- and intra-ocular SBR testing, which is not possible with polarizers as used by previous authors. A photographic fluorescent light box (38cm by 30cm) positioned on its side was used as a light source. Three black cardboard masks of the about same dimensions as the light box were created each with two square apertures cut into them, as shown in Figure 2.2-1. These were affixed over the front of the box limiting the visibility of light for each test a pair of two identical squares, as required for each SBR.

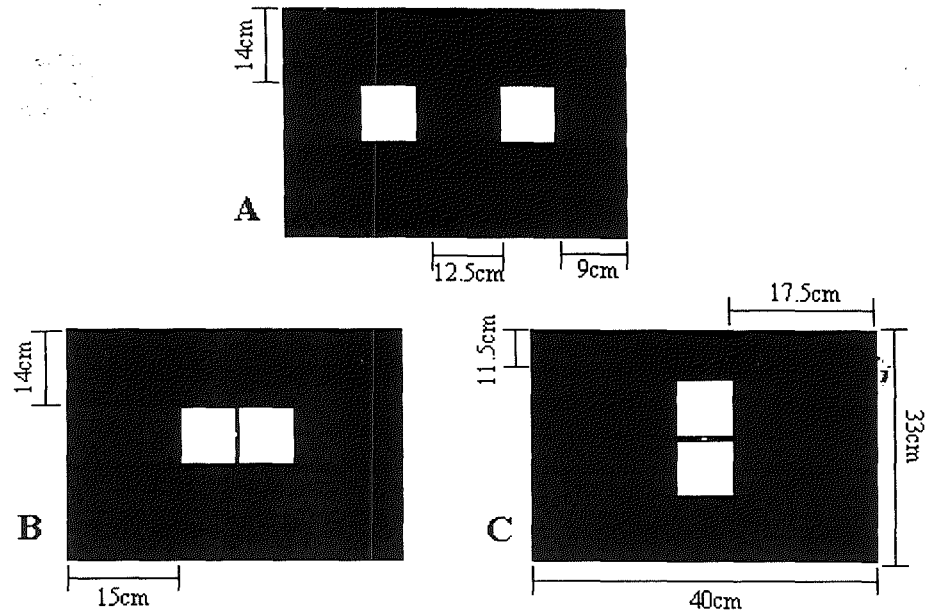


Figure 2.2-1 Schematic representation of three black cardboard masks, created to reveal two squares of light of equal intensity for SBR testing. A: inter-ocular comparison B: nasal / temporal intra-ocular comparison, and C: upper / lower intra-ocular comparison. All squares have side lengths of 5cm, the bar between upper / lower and nasal / temporal squares is 0.75cm. These displays were viewed from a distance of 30cm, resulting in angular subtenses for the squares of 10°.

### 2.2.1.1 Light intensity measurements

A series of measurements were taken across the whole face of the light box (using a UDT Optometer S370 model 248) with the sensor at the subject's viewing position. This revealed pronounced differences in illuminance related to the location of the lighting elements (Figure 2.2-2). This was taken into account when siting the positions of the squares within the masks, so that the luminance of the paired squares varied by no more than 5%.

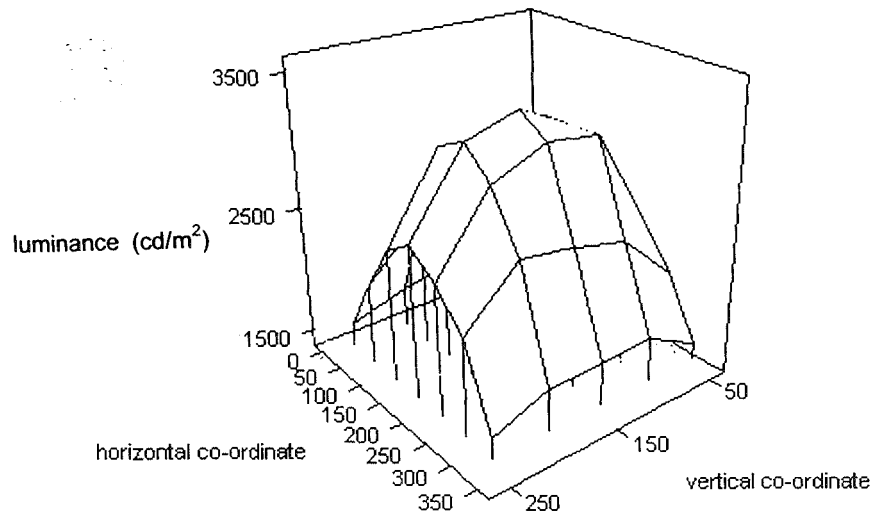


Figure 2.2-2 3-D plot of the luminance of the light box output measured across the face of the box in  $cd/m^2$ . The vertical and horizontal co-ordinates are shown in mm from the top of the box and from the left edge of the box respectively.

Measurement of the brightness of the test areas was done periodically thereafter to check for balance in the paired test regions. In addition to the spatial differences in luminance, temporally occurring differences were also anticipated. Therefore, measurements were taken at 6 test sites every 5 minutes for one hour, followed by every 10 minutes for a further hour, then every 30 minutes for one final hour. The results are shown in Figure 2.2-3 with each point joined as a continuous line in order to display the results from the 6 sites clearly.

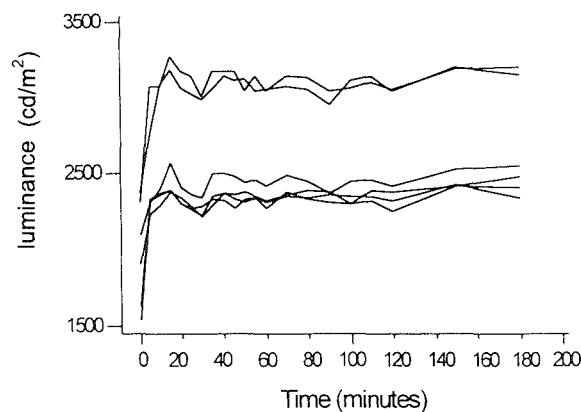
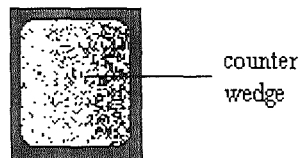


Figure 2.2-3 Plot of light intensity (in  $cd/m^2$ ) at 6 test sites measured over 3 hours plotted against time, individual points are joined for each site, this is not a continuous recording.

Irrespective of location, a reasonably stable luminance was measured after around 30 minutes after the light box had been switched on. This indicated that it was necessary to turn on the light box for at least half an hour before experiments began to allow the level of brightness to settle.

### 2.2.1.2 Apparatus

A graduated neutral density filter wedge, which had a density ranging from 0.2 to 1.1 log units was fitted against a 0.3 log unit counter wedge (Figure 2.2-4), which ensures a uniform density across its width.



*Figure 2.2-4 Schematic representation of counter wedge, viewed separately from graduated wedge.*

The paired graduated wedge and counter wedge (hereafter referred to jointly as the graduated filter) were fitted with a control dial attached to a rack and pinion action which allowed the subject to move the graduated wedge smoothly to alter the amount of light transmitted. For each pair of square apertures, the graduated density filter was mounted over one aperture, and a 0.6 log unit fixed strength neutral density filter was mounted over the other. A fixation point was located within the midpoint of the narrow strip between the two apertures. This was formed by a pinhole that transmitted light from the light box (Figures 2.2-5 and 2.2-6).

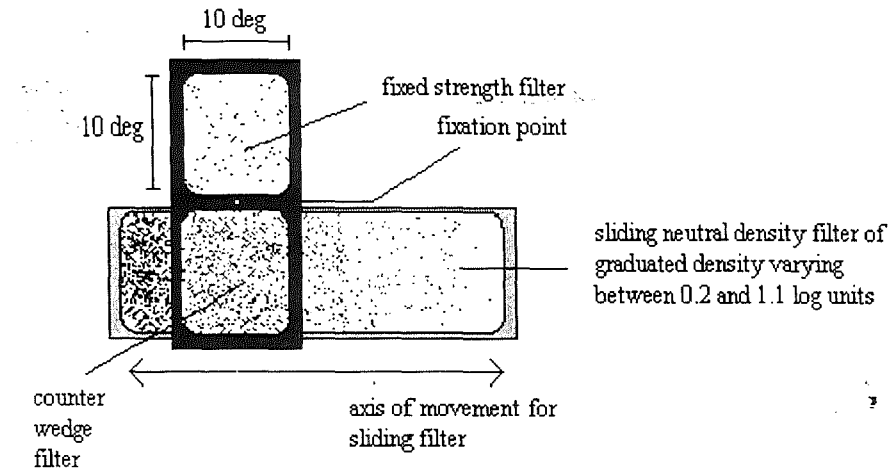


Figure 2.2-5 Schematic representation of filter unit (viewed from front), in the orientation used to test upper / lower intra-ocular SBR, showing fixed filter on top, and graduated density filter below the fixation point with the counter wedge in front of it.

This unit could be used in 3 different ways:

1. The graduated filter positioned horizontally as shown in Figure 2.2-5 for testing upper / lower intra-ocular SBR.
2. The graduated filter positioned vertically as shown in Figure 2.2-6 for testing nasal / temporal intra-ocular SBR.

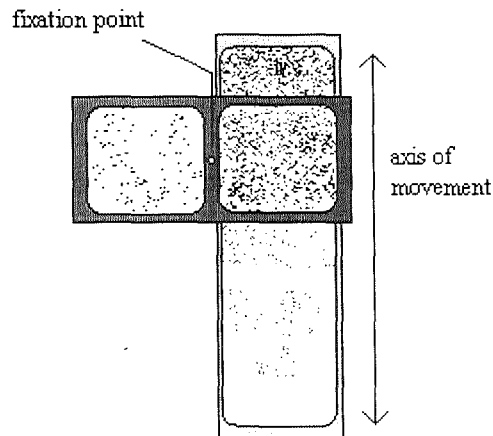


Figure 2.2-6 Schematic representation of equipment (viewed from front) used to test nasal / temporal intra-ocular SBR, showing fixed filter to left, and graduated density filter to right of fixation point.

3. The graduated filter positioned vertically (as in Figure 2.2-6) with a separate fixed strength filter displaced about 10cm to the left for inter-ocular comparisons, all shown as viewed from above in Figure 2.2-7.

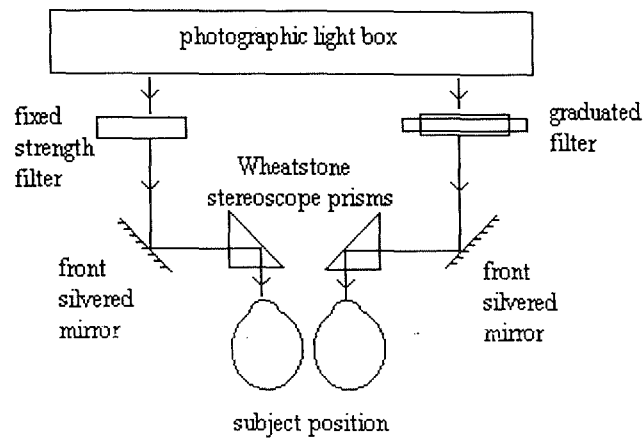


Figure 2.2-7 Schematic representation of the equipment (viewed from above) used to test inter-ocular SBR, showing fixed density filter on left, graduated filter on right, and the prisms in the Wheatstone stereoscope which divert gaze through the appropriate filters.

### CALIBRATION OF GRADUATED FILTER

The graduated filter unit was fitted with a scale, numbered from 1 to 104 (mm values). The value of the luminance through the graduated filter (measured with the Optometer through the centre of the counter wedge) throughout its full range of positions, including a 'zero' position which involved measuring the brightness from the light box at the same distance but without the filter. A graph of light intensity was plotted against the position of the graduated filter (Figure 2.2-8).

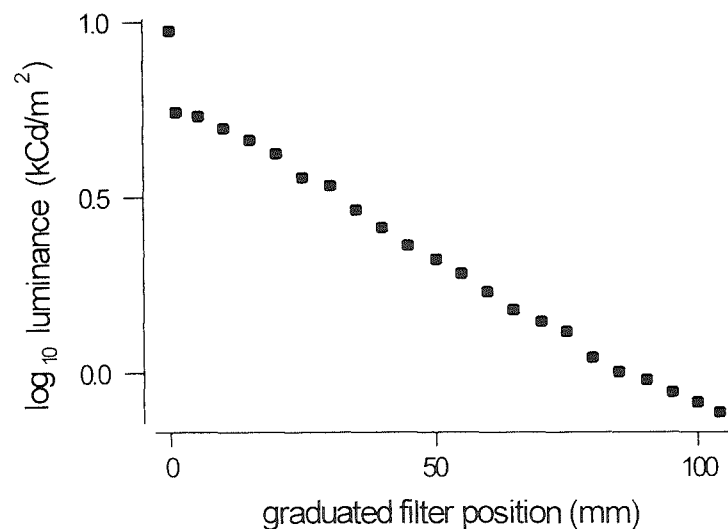


Figure 2.2-8 Plot of log luminance plotted against the position of the graduated filter in mm, including a zero position when filter was absent.

The value of the density of the filter at each position was then calculated by taking the difference of the log luminance with and without the filter. This value was plotted against position of the filter, (Figure 2.2-9), and a calibration equation for this relationship was derived. This was subsequently used for conversion of each filter position to a log value for the filter.

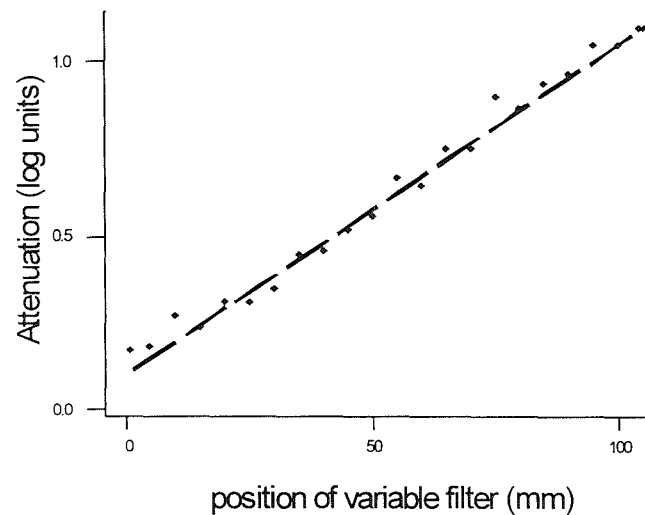


Figure 2.2-9 Calibration graph of the attenuation in log units against the position of the graduated filter showing best fit straight line.

The data were extremely well described by the best fit line, ( $R^2 = 99\%$ ), and the relationship was highly statistically significant ( $P < 0.001$ ). The calibration equation for conversion of the position of the graduated filter into a log value for the filter was given by Equation 2.2-1.

Equation 2.2-1 
$$y = 0.1 + 0.009 x$$

During the experiments the subject's chosen match point on the graduated filter could subsequently be converted to a log value which was used in the calculation of the SBR. The calculation is fully detailed in Appendix section 5.4. For each SBR the difference in the log value for the compared fields was calculated (right eye minus left eye, upper minus lower, nasal minus temporal) and the direction of this difference was noted. The modulus was then converted to a percentage difference by taking its antilog and multiplying it by 100. The percentage difference in sensitivity between the compared fields was obtained by

subtracting 100 from this figure, and the direction of the greater sensitivity was added by re-applying the sign.

It was therefore the case that at 0%, the two comparison areas were equally sensitive. Whereas, for example, at + 300% the first named field (i.e. right, upper or nasal) is three times the sensitivity of the second named field (i.e. left, lower or temporal). If the sign was negative then the second named field was more sensitive by the given percentage.

### 2.2.1.3 Pupil diameter measurements

A review of the literature available on inter-ocular SBR testing indicated that anisocoria of greater than 0.5mm had a significant effect on the ratio of brightness sense (MacMillan *et al.*, 1994). As part of the testing process therefore, we attempted to obtain accurate measurements of pupil diameter for our subjects. Without specialist equipment being available, we experimented with several methods. Initially, we tried to estimate pupil diameter by eye, using a rule held below the subject's eye, in ambient light. The subject was asked to look at a fixed distant point over the experimenter's shoulder, and an average of two or more measurements taken for each eye was recorded. However, the precision of this method was limited by problems of resolving the boundary between the pupil and iris. This was probably made more difficult by spontaneous movements of the iris and changes in pupil diameter if the subject's fixation altered. While measurement with a rule did exclude gross anisocoria, a more accurate technique was sought.

High contrast black and white photographs were then taken of the subject's eyes below which was affixed a millimetre scale, again in ambient light. However this method did not provide the accuracy required in a number of subjects due to the ill-defined contrast between the iris and pupil.

Finally, we employed the facility on the Humphrey Visual Field Analyser at Gartnavel General Hospital for measuring pupil diameter in standardised conditions during the fixation monitoring procedure. A camera is trained on the subject's pupil as they hold their gaze steady at the beginning of the test. The pupil measurement is arrived at 'using the camera image data and the differences of contrast between adjacent pixels. The accuracy of the measurement is as good as the displayed resolution on the screen and printout, which indicates 1/10th of a millimetre' (personal correspondence from Zeiss Humphrey Systems Technical Support Specialist). It must be noted that pupil size is still liable to continual oscillation, and the results must be interpreted with this in mind.

### 2.2.2 Experimental protocol

The subject's head was steadied in position at 30cm from the light box, using a chin rest see Figure 2.2-10. The height and lateral position of the chin rest were adjusted until the subject could comfortably view the two squares (with edge lengths of 5cm, equivalent to  $10^\circ$ ) of light through the filters. A light proof shade with internal matt black walls encased the apparatus and excluded any distracting reflections, and meant that normal room lighting could be used. As for the contrast threshold measurements, the ambient temperature in the room was maintained between  $16^\circ$  and  $22^\circ$  Centigrade.

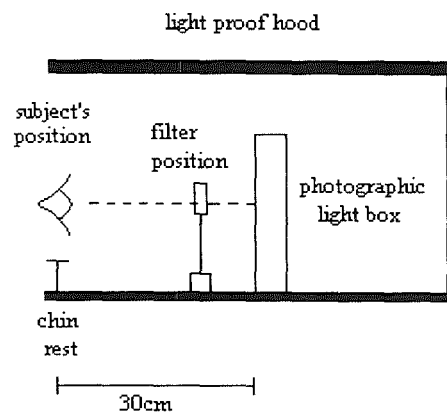


Figure 2.2-10 Schematic representation of SBR equipment (viewed from side) showing the position of the light box and filters through which the subject viewed the squares of light at 30cm, encased by light proof hood.

The starting position of the graduated filter was alternated between the two extremes: 0.2 log units (maximally bright) and 1.1 log units (maximally dark) for comparison with the fixed strength reference filter (usually 0.6 log units). Another method had been explored; however, in agreement with Borgmann *et al.*, it was found that if the initial position of the variable filter was transmitting the maximum amount of light, the SBR determination was not reproducible (Borgmann *et al.*, 1991). It was found that this could be avoided by alternating the start position between maximally bright and maximally dark.

With the subject viewing the filters appropriately (i.e. binocularly for inter-ocular tests, and monocularly for intra-ocular tests), he / she was asked which square appeared brighter. If the answer corresponded with the square covered by the less dense filter, the experiment continued. If the subject reported no difference, or that the square with the greater filter density in front appeared brighter, the fixed strength filter was amended. A different fixed

strength filter was chosen to provide a range for adjustment of the graduated filter. For example, if the graduated filter was at the bottom end of the scale (0.2 log units) and yet the square viewed through the 0.6 log unit fixed strength filter was perceived as being brighter, then the fixed strength filter would be exchanged for one of a higher density e.g. 0.9 log units. This increase continued until the subject saw the graduated filter as being brighter, thus allowing enough adjustment to achieve a match with the fixed strength filter.

### 2.2.2.1 Inter-ocular SBR

Once the appropriate fixed strength filter was in position, the subject was instructed to look straight ahead (with both eyes open) through the Wheatstone stereoscope (shown from above in Figure 2.2-7). The position of the prisms was adjusted for each individual in order that one square of light could be viewed with each eye (left eye viewing through the fixed strength filter, and right eye viewing through the graduated filter) shown in sketch form in Figure 2.2-11.

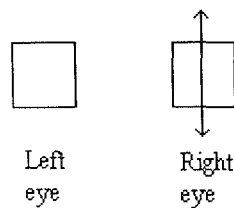


*Figure 2.2-11 Sketch of test squares for inter-ocular SBR testing – double-sided arrow indicates that the graduated filter was positioned over the square stimulating right eye. This will be used later for clarity on graphs and tables.*

When both eyes were open, both squares were visible, positioned side by side. Fusion of the squares did not occur in any subjects. The subject then adjusted the position of the graduated filter using the control dial until the perceived brightness of the graduated filter matched the brightness seen through the fixed strength filter. The position of the graduated filter at this point was recorded. Six readings were taken, with the initial position of the graduated filter alternated between the extreme positions, as previously described.

### 2.2.2.2 Intra-ocular SBR

The equipment was then rearranged to permit measurements of the nasal / temporal intra-ocular SBR, as shown in Figure 2.2-6: this is shown in sketch form in Figure 2.2-12.

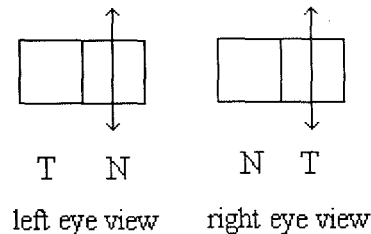


*Figure 2.2-12 Sketch of test squares for nasal / temporal intra-ocular SBR testing - double-sided arrow indicates that the graduated filter was positioned over the square stimulating the temporal field (T) for right eye, and the nasal field (N) for the left eye. These will be used later for clarity on graphs and tables.*

The subject was asked to look directly at the fixation point between the squares with one eye, the other eye being kept closed or occluded by an eye patch. If the subject reported correctly which was the brighter one (as previously described), he / she was then instructed to alter the graduated filter position until it matched the brightness of the fixed strength filter. With the filters positioned either side of the fixation spot, a simultaneous, parafoveal matching of the squares was undertaken rather a consecutive, central matching, which would have occurred if the eye flicked from one to the other. As before, 6 readings were taken, with alternate starting positions of the graduated filter. This was repeated for the companion eye. The equipment was adjusted to the form shown in Figure 2.2-5 for testing upper / lower intra-ocular SBR - shown in sketch form in Figure 2.2-13. The same testing procedure, described above, was followed.

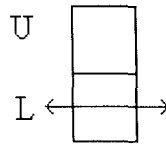


*Figure 2.2-13 Sketch of test squares for upper / lower intra-ocular SBR testing - double-sided arrow indicate that the graduated filter was positioned over the square stimulating the lower field (L), (U indicates square stimulating the upper field). These will be used later for clarity on graphs and tables.*

## **SUMMARY**

The experiment consisted of 5 SBR tests: one set of 6 inter-ocular readings and a set of 6 intra-ocular readings for both eyes in both upper / lower and nasal / temporal comparisons. With a co-operative subject, this took roughly 20 to 25 minutes from beginning to end, including time for giving instruction and rearranging the equipment. For all SBR measurements, the subject was regularly encouraged to blink or look away from the stimuli, as a more consistent match was achieved in this way. The subject was encouraged to move the graduated filter back and forth either side of the match point, as this tended to improve their confidence in the resulting end point. The position of the filter at the point of the perceived brightness match was then converted into a density value, and the difference between this and the fixed strength filter was converted to a percentage difference in sensitivity to light (see Appendix section 5.4 for further details).

### **2.2.2.3 Repeatability of SBR measurements**

A brief pilot test was undertaken to check the repeatability of SBR measurements. This was tested in one subject by taking repeated measurements of the inter-ocular SBR every 10-15 minutes for over one hour. All experiments involved matching the graduated filter to the 0.6 log unit fixed filter.

**RESULTS**

Figure 2.2-14 shows the mean SBR  $\pm$  one SE at 7 different times in one day for one subject (the author).

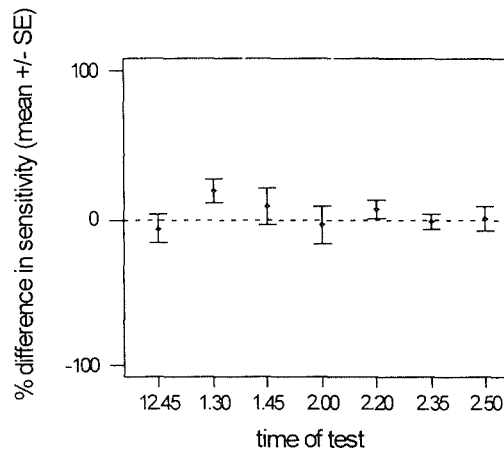


Figure 2.2-14 Mean inter-ocular SBR  $\pm$  SE, repeated every 10 to 15 minutes over 65 minutes, dotted line indicates the point of absolute match of the brightness sensitivity of each eye.

For a value of zero, the left and right eyes match in brightness sensitivity. Moving towards +100, the right eye is more sensitive by the stated percentage, moving towards -100, the left eye is more sensitive by the stated percentage. All subsequent SBR graphs follow the same format. The mean SBR in Figure 2.2-14 ranged from -6% to +19% in terms of the difference between the subject's eyes. Regression analysis on the mean SBR value over time showed no statistically significant change ( $R^2 = 4.2\%$ ,  $P = 0.7$ ).

### 2.2.3 Conventional visual field analysis

As previously stated 23 of the 24 older control subjects completed visual field testing on the Humphrey Visual Field Analyser. Where possible the gaze and blind spot fixation tracking programme was used as this also provided a standardised measurement of their pupil diameter. The results from the pupil diameter measurements are given in Table 3.1-2 and are described in Results section 3.1.2.1.

Regions of the Friedmann visual field that corresponded to the areas stimulated by the 5 SBR tests were quantified in the same way as previously described in relation to contrast threshold testing (Methods section 2.1.4). Masks appropriate to the SBR test areas were placed over the Friedmann Visual Field Charts. An example of the Friedmann charts for the left and right eyes of patient 15-g is shown in Figure 2.2-15. These are superimposed by the masks revealing nasal / temporal regions (A) and upper / lower SBR test regions (B).

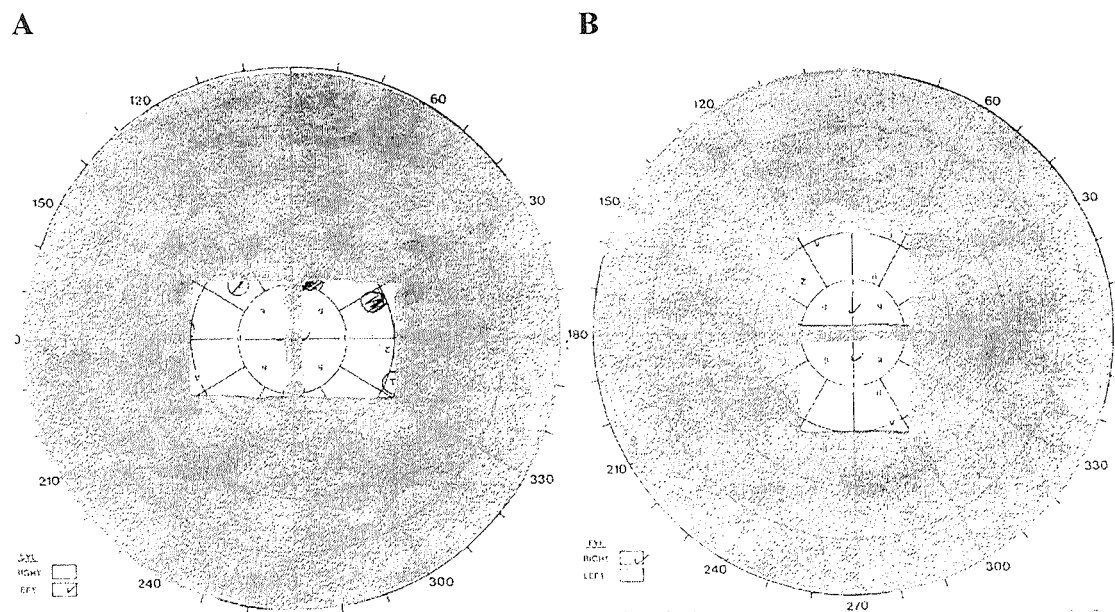


Figure 2.2-15 Friedmann plots for patient 15-g, indicating masks used to reveal points falling within SBR test regions; A: nasal / temporal comparisons in left eye, B: upper / lower comparisons in right eye.

In accordance with the calculation of the SBR as detailed in Appendix section 5.4 the visual field ratio was worked out. The score for each test region (i.e. upper, lower, nasal, temporal, or central right or central left) was divided by the total score possible and multiplied by 100. The difference between the values for percentage sensitivity in paired regions was then calculated as for the SBR (i.e. nasal – temporal; upper – lower; right eye

– left eye). As outlined with regard to the SBRs, when the visual field ratio was 0%, this indicated perfect balance in the sensitivity of the compared areas.

Occasionally, a sensitivity score of zero occurred on the denominator of the ratio – this was dealt with by counting a score of one rather than zero, which minimally increased the sensitivity and avoided an invalid result. This affected patients 5-g and 7-g, and resulted in a default score of 700% in favour of the sensitive region. The corresponding plot of quantified percentage visual losses for patient 15-g is shown in Figure 2.2-16.

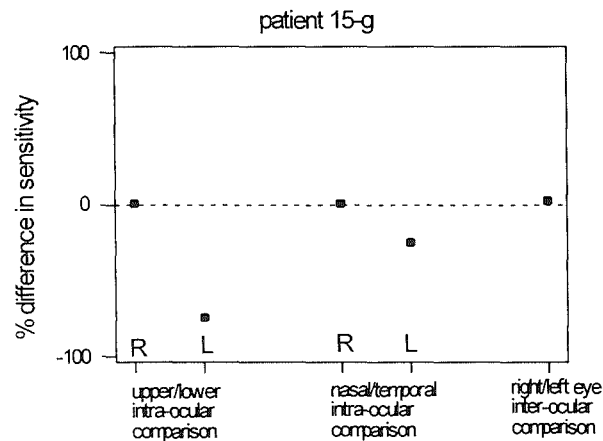


Figure 2.2-16 Mean percentage differences in sensitivity in Friedmann visual field plot for regions of visual field stimulated in SBR testing for patient 15-g (R = right eye, L = left eye).

In this patient's right eye, there was no difference in the sensitivity between the upper and lower regions whereas, in the left eye, the lower field was more sensitive by 74%. In the right eye, there was no difference in the sensitivity between the nasal and temporal regions whereas, in the left eye, the temporal region was more sensitive by 26%. For central inter-ocular comparisons the right eye was more sensitive than the left by 3%.

### **2.2.4 Analysis of results**

For each subject who completed the experiment, a mean value was calculated from the 6 readings and plotted for each of the 5 SBR tests. Graphs were plotted with error bars which indicated  $\pm$  one SE. For the purposes of defining a prediction limit for normal, we have used the convention of mean  $\pm$  2 SD which, as already stated, equates to a confidence limit of 97.7%.

One-sample t-tests were used to identify any difference between the mean SBR and zero. Where groups of data were being compared, two-sample t-tests were used. In all cases statistical significance was taken when  $P < 0.05$ . All calculations and statistical analysis were completed using Minitab 11.

In glaucoma patients, the mean SBRs were plotted against the ratios of quantified visual field results from conventional analysis, as described above, and linear regression analysis was applied. Since only 5 points are available, the importance of the regression will be interpreted with due caution.

## 3 Results

### 3.1 Contrast threshold results

#### 3.1.1 *Stationary versus flickering display*

In response to a stationary, green, concentric ring pattern, 6 contrast threshold readings were taken for up to 4 truncated quadrants in 19 subjects aged 24 to 59 years. The field size was 40° in diameter, with a 20° diameter central occluder. The stationary contrast thresholds were compared to values obtained in response to patterns flickering at 4Hz, 8Hz or 10Hz. The relative levels of these results (i.e. if the stationary image gave rise to thresholds which were higher than, lower than or equal to those obtained to the flickering image) are described in the following pages. As previously described, statistical analysis was carried out on the effect of each flicker speed against contrast threshold obtained to the stationary image using a balanced ANOVA (or an unbalanced ANOVA using the General Linear Model where there were unequal numbers of variables). In the text these will both be referred to as ANOVA.

For each experiment the flicker was generated using either

- a rotating mirror / polarizer or
- a solid vane windmill or
- a diffuser windmill,

as described in Methods section 2.1.2.6. Each set of results is described in turn.

**ROTATING MIRROR / POLARIZER**

Several experiments were undertaken in 9 subjects using the rotating mirror / polarizer, comparing at least one flicker speed to the stationary image. As can be seen from the two examples (from two different subjects) in Figure 3.1-1, the relative levels of contrast threshold in response to stationary and flickering images did not follow a predictable pattern in these subjects. In 4 cases the contrast threshold to the stationary image was lower than that obtained to the flicker (4Hz, 8Hz or 10Hz) ( $P \leq 0.001$ , ANOVA) (Figure 3.1-1 left). In 5 cases the contrast thresholds obtained in response to the stationary image were significantly higher than those for the flickering images (at either 4Hz or 10Hz,  $P \leq 0.02$ , ANOVA) (Figure 3.1-1 right). Within two of these results the level of contrast threshold to stationary image and those flickering at 10Hz were similar, however there was still a significant difference between stationary and the other flicker speed tested.

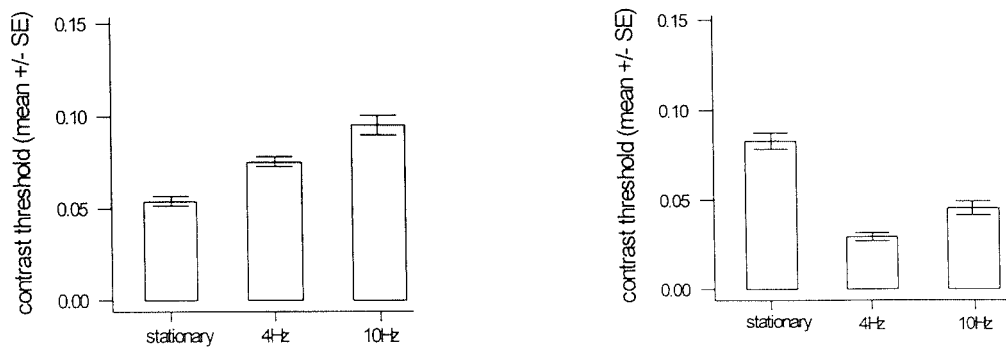


Figure 3.1-1 Mean contrast threshold  $\pm$  SE to a stationary image and an image flickering at 4Hz and 10 Hz using the rotating mirror / polarizer for two different subjects, left shows increased contrast thresholds in response to both 4Hz and 10Hz, right shows reduced contrast thresholds in response to both 4Hz and 10Hz.

**SOLID-VANE WINDMILL**

The second method, using the simple solid-vane windmill, was tested on 10 subjects in anticipation of producing more repeatable results, however, this was not the case. In 4 cases contrast thresholds to the stationary image were lower than to the flickering images at 4Hz or 8Hz ( $P \leq 0.03$ , ANOVA) (Figure 3.1-2 left). In 1 case there was no significant difference between contrast thresholds in response to the stationary image or one flickering at 4Hz ( $P = 0.7$ , ANOVA). In 5 cases the contrast thresholds obtained to the stationary image were significantly higher than those for the flickering images ( $P \leq 0.02$ , ANOVA) (Figure 3.1-2 right).

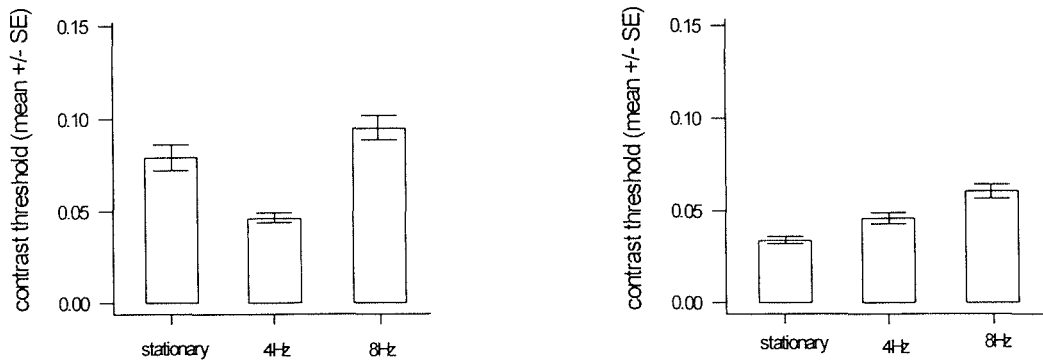


Figure 3.1-2 Mean contrast threshold  $\pm$  SE to a stationary image and an image flickering at 4Hz and 8Hz using the solid vane windmill for two different subjects, left shows reduced contrast threshold in response to 4Hz and similar contrast threshold in response to 10Hz, right shows increased contrast thresholds in response to both 4Hz and 8Hz.

## DIFFUSER WINDMILL

The third method was attempted in order to try to reduce the effect of the luminance flicker by allowing the transmission of light through the vanes while disrupting the transmission of the interference pattern. This method gave the most consistent results with the contrast threshold in response to the stationary image being lower than those in response to the 4Hz flicker in all 3 subjects ( $P < 0.001$ , ANOVA), an example is shown in Figure 3.1-3.

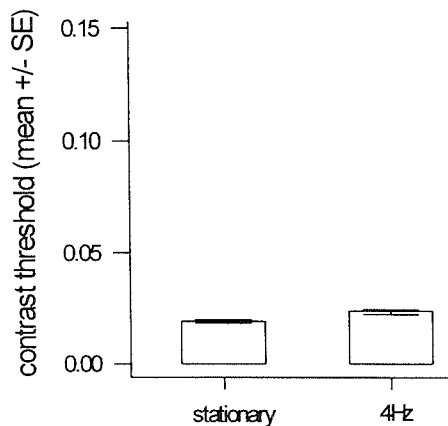


Figure 3.1-3 Mean contrast threshold  $\pm$  SE to a stationary image and an image flickering at 4Hz using the diffuser windmill, showing a small but statistically significant increased contrast threshold in response to 4Hz.

Intuitively, this outcome was puzzling, as it might have been expected that a flickering image would be perceived at lower contrast than a stationary one, as shown previously (Tolhurst, 1973).

As it did not provide a solid base-line against which to compare the results of a visually abnormal group, it was reasoned therefore, that it was therefore inappropriate to use this type of stimulus as part of this project, particularly as subjects preferred the stationary image. On the basis of these results, therefore, we decided to employ the stationary pattern as the final protocol.

### **3.1.2 Final protocol**

Contrast thresholds were obtained in response to a green sinusoidal grating pattern of one cycle per degree presented as a stationary image. The grating was viewed in 4 truncated quadrants oriented obliquely, subtending 20 to 40° in diameter. Both eyes were tested, with the subject's preferred eye first, 6 readings were taken for each quadrant. Three groups of subjects were recruited for testing: a control group, approximately age-matched with the patient group (the suffix -n is used as the subject identifier (ID) indicating *non-glaucoma*); a glaucoma patient group (for whom the suffix -g is used as the patient ID); and a young control group (for whom the suffix -y is used as subject ID). The older control group includes 6 visually abnormal eyes which are dealt with separately in Results sections 3.1.2.7 and 3.1.2.8. The abnormalities were unrelated to glaucoma; hence the suffix -n is used for both normal and abnormal eyes of these subjects.

### 3.1.2.1 Older control group subject details

Contrast thresholds were obtained from 18 subjects in whom both eyes were tested and from a further 6 subjects who provided results for one eye. The subjects' ages ranged from 49 to 81 years, with a mean of 66.0 years  $\pm$  8.5 SD. For the purposes of comparison with the glaucoma patient group, however, the results for the 3 youngest subjects (16-n: 51 years, 17-n: 52 years, 18-n: 49 years) were excluded in order to achieve a statistically significant age-match ( $P = 0.1$ , two-sample t-test). The mean of the age-matched control group used to compare to the patient group was therefore 67.5 years  $\pm$  6.7 SD (Figure 3.1-4).

All 18 control subjects have been described, however, as their results have been used for comparison with the visually abnormal control group and with the young control group.

N.B. In subsequent sections, the term 'age-matched control group' will apply to the group with the 3 youngest subjects excluded (for comparison with the glaucoma patient group), whereas 'older control group' will apply to the whole group of 18 binocular subjects and 6 monocular subjects (for comparison with the younger control group and the visually abnormal control sub-group).

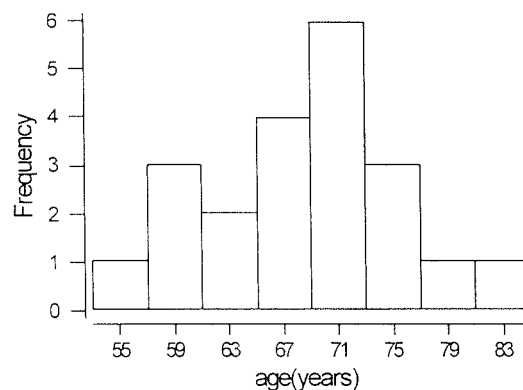


Figure 3.1-4 Distribution of ages for age-matched control group (i.e. older control group excluding the 3 youngest subjects: 16-n, 17-n and 18-n),  $n = 21$ . (Compare with age distribution of glaucoma group: Figure 3.1-8.)

The 42 visually normal eyes had best corrected Snellen acuities of 6/6 or better, except for both eyes of the eldest subject which were 6/12 (subject 12-n shown in Table 3.1-2), and

one eye of one subject (7-n) which was 6/7.5. The group consisted of 9 females and 15 males. Seven of the subjects (1-n, 3-n, 6-n, 16-n, 17-n, 23-n, 24-n) had recently attended their own optometrist for a full ophthalmic examination, and were judged to be visually healthy, except for the right eyes of 6-n and 23-n, which have been excluded for reasons discussed in Results section 3.2.1.7. Subject identifier (ID), age, gender and visual acuity are shown in Table 3.1-1. The 3 subjects for whom results are not included for comparison with the glaucoma patient group are prefixed with a cross.

Table 3.1-1 Subject details for older control group

SUBJECT ID	AGE (yrs)	GENDER	VISUAL ACUITY	
			Left eye	Right eye
1-n	70	M	6/5	6/5
2-n	78	F	*	6/4
3-n	70	M	6/6	6/5
4-n	65	F	6/5	6/5
5-n	59	F	6/4	6/5
6-n	63	M	6/5	*
7-n	69	F	*	6/7.5
8-n	61	F	6/5	6/5
9-n	76	M	6/4	*
10-n	71	M	6/6	6/5
11-n	66	M	6/5	6/5
12-n	81	M	6/12	6/12
13-n	69	F	6/5	6/6
14-n	73	M	6/5	6/6
15-n	73	F	6/5	*
X 16-n	51	M	6/4	6/4
X 17-n	52	F	6/4	6/4
X 18-n	49	M	6/4	6/4
19-n	69	M	6/5	6/6
20-n	66	M	6/6	6/4
21-n	65	M	6/4	6/4
22-n	55	M	6/4	6/4
23-n	59	F	6/6	*
24-n	59	M	6/5	6/5

Abbreviations and symbols used in Table

- F = female
- M = male
- n = non-glaucoma subject ID suffix
- X = subject's data not used for comparison with glaucoma patient group
- yrs = years
- \* = indicates abnormal eye – analysed in Results section 3.1.7.

### CONVENTIONAL VISUAL FIELD ANALYSIS

Humphrey visual field analysis was completed for 23 subjects in the older control group (all except 12-n), therefore 40 normal eyes were tested. The mean deviation (MD) for each individual eye as calculated by the field analyser ranged from  $-3.5$  dB to  $+2.3$  dB and these values are shown in Table 3.1-3. Mean MD for the group was  $-0.3$  dB  $\pm$  1.3 dB SD. While the analyser's results indicated that the MD was outside normal limits in 8 of the 40 eyes tested ( $P < 0.05$ ) marked with bold type on Table 3.1-2, examination of the visual fields by Dr Jay, consultant ophthalmologist at Gartnavel General Hospital led to the conclusion that they were normal. A number of anomalies were identified by the analyser affecting 14 eyes, including areas of diffuse or localised low or high sensitivity, 'abnormal' or 'borderline' results to the glaucoma hemifield test or lack of a blind spot. However these were all judged to be either unrelated to any ophthalmologic disorder, or were unrepeatable. These are thought to have been due to drooping eyelids or the trial lens frame blocking the subject's view of the stimuli, inaccurate responses of the subject or the high sensitivity of the machine. All the visual fields obtained for the older control group are included in the Appendix section 5.2 as Figures 5.2-1 to 5.2-23.

In subjects with two visually normal eyes, the pupil measurement by the visual field analyser was completed in both eyes of 13 individuals, in one eye of 3 individuals, and in neither eye of one individual. The measurements are indicated in Table 3.1-2. For subjects for whom the calculation of the inter-pupillary difference was not possible, a dash is marked in the table. In the subjects for whom measurements were obtained in both eyes, 9 had inter-pupillary differences less than 0.5mm, while 4 had pupil diameters with differences of 0.6mm to 0.9mm. These results are used in Figure 3.1-7 where subjects with whom inter-pupillary difference greater than 0.5mm are indicated with open symbols to distinguish them from the rest of the group.

Table 3.1-2 Humphrey visual field analysis for older control group

SUBJECT ID	VISUAL FIELDS		MEAN DEVIATION (dB)		PUPIL DIAMETER (mm)		
	Left eye	Right eye	Left eye	Right eye	Left eye	Right eye	Inter-pupillary difference
1-n	✓	GHT	+0.2	<b>-2.1</b>	4.8	5.5	0.7
2-n	*	✓	*	-0.5	*	3.1	-
3-n	✓	GHT	0.0	-1.0	3.4	3.4	0.0
4-n	✓	✓	+1.3	+1.1	2.8	3.7	0.9
5-n	✓	✓	0.0	+0.8	4.4	4.8	0.4
6-n	✓	*	-0.7	*	4.6	*	-
7-n	*	✓	*	-0.7	*	5.4	-
8-n	GHT	GHT	+0.2	+1.1	4.3	4.7	0.4
9-n	GHT	*	<b>-2.5</b>	*	-	*	-
10-n	✓	BS	<b>-1.4</b>	-0.5	-	4.9	-
11-n	✓	GHT	+0.9	+1.2	4.3	5.2	0.9
12-n	-	-	-	-	-	-	-
13-n	HS	GHT	+2.3	-0.6	-	4.9	-
14-n	✓	GHT BS	-1.0	+0.4	3.2	3.3	0.1
15-n	✓	*	+1.4	*	-	*	-
X 16-n	✓	✓	0.0	+1.0	-	5.0	-
X 17-n	✓	✓	+0.8	+0.6	4.7	5.0	0.3
X 18-n	✓	✓	-1.2	-1.3	-	-	-
19-n	✓	✓	+0.9	0.0	5.4	5.2	0.2
20-n	✓	GHT	<b>-2.2</b>	<b>-3.5</b>	4.1	4.7	0.6
21-n	✓	✓	-0.2	+2.1	3.1	3.1	0.0
22-n	BS	GHT	<b>-2.8</b>	-0.8	4.0	4.1	0.1
23-n	✓	*	<b>-2.0</b>	*	2.9	*	-
24-n	GHT	GHT	<b>-1.7</b>	-0.3	3.7	3.6	0.1

Abbreviations used in table

BS = no blind spot apparent in Humphrey visual field plot

GHT = glaucoma hemifield test result abnormal or borderline, indicated where diffuse or localised low sensitivity was apparent

HS = abnormally high sensitivity

- = no data from Humphrey visual field analyser

\* = abnormal eye – analysed in Results section 3.1.2.7.

**bold** = mean deviation stated to be outside normal age-matched limits by Humphrey

✓ = normal visual field

### 3.1.2.2 Older control group contrast threshold determinations

Contrast thresholds were obtained in response to the one c/deg vertical, sinusoidal grating pattern presented in truncated quadrants extending 10° to 20° into the peripheral field for the left and right eyes of 18 subjects and for one eye each of 6 subjects. Mean contrast threshold values  $\pm$  SE for 6 contrast threshold determinations for 4 control subjects are shown in Figure 3.1-5 to illustrate the range of results obtained.

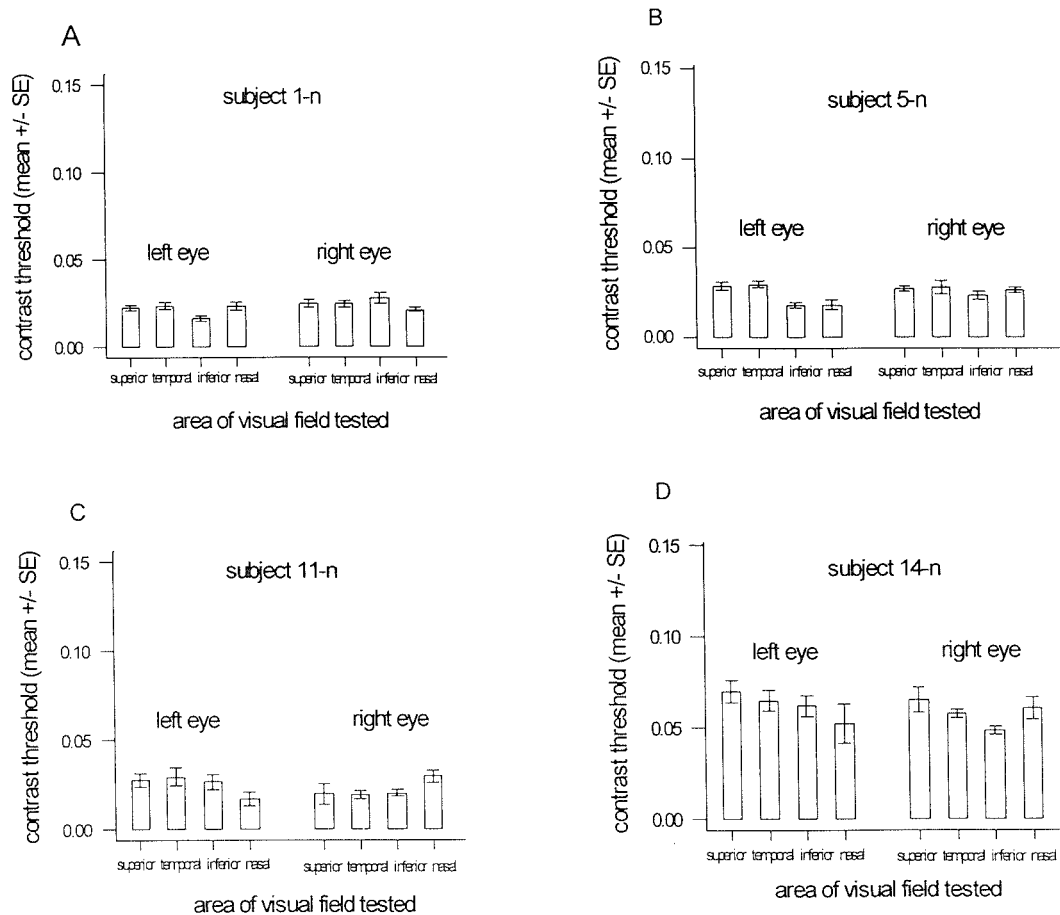


Figure 3.1-5 Four individual examples of mean contrast threshold  $\pm$  SE in control subjects for the named truncated quadrants, A: 1-n, 70 year old male, B: 5-n, 59 year old female, C: 11-n, 66 year old male, D: 14-n, 73 year old male.

In subject 1-n mean contrast thresholds ranged from 0.016 to 0.028 contrast units, in subject 5-n mean contrast threshold ranged from 0.018 to 0.030 contrast units, in subject 11-n mean contrast threshold ranged from 0.017 to 0.030 contrast units, and in subject 14-n mean contrast threshold ranged from 0.048 to 0.070 contrast units.

Throughout the group there was some variation in mean contrast threshold measured in all 4 truncated quadrants. Although the temporal quadrant did stimulate the typical location

for the blind spot, there was no consistent evidence of an elevated threshold there, when compared to the other 3 quadrants. Of 42 eyes tested, 6 had a clearly elevated contrast threshold in the temporal quadrant, in 3 eyes it was slightly elevated in the temporal quadrant and in 33 eyes the temporal quadrant contrast threshold was not elevated with respect to the others. There was no statistically significant effect of quadrant on contrast threshold, when both eyes were taken together in 8 of 18 subjects for whom both eyes were studied ( $P > 0.05$ , one-way ANOVA). In the 10 out of 18 subjects in whom a difference was present ( $P < 0.04$ ) there was no quadrant or quadrants which were consistently elevated.

### GROUP SUMMARY

For a general comparison with glaucoma patient's results, the individual results for the **age-matched** control group, i.e. excluding subjects 16-n, 17-n and 18-n were then combined as shown in Figure 3.1-6.

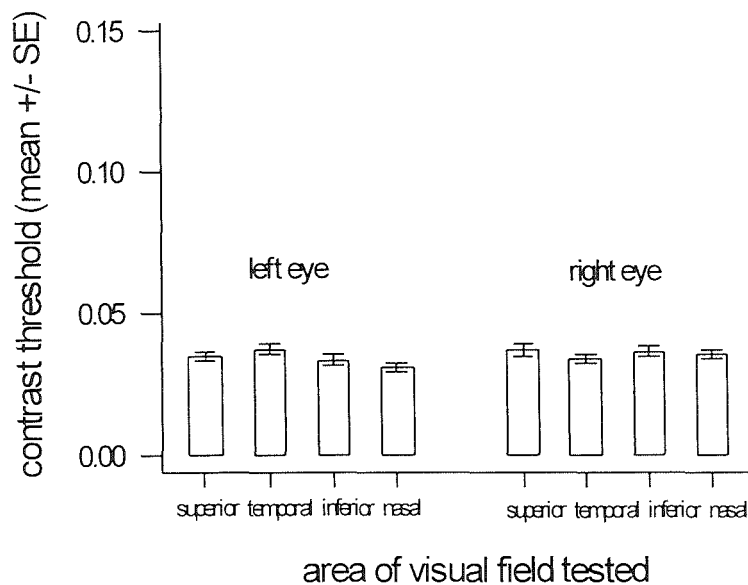


Figure 3.1-6 Mean contrast threshold  $\pm$  SE for age-matched control group i.e. older control subjects excluding 16-n, 17-n and 18-n ( $n = 21$ ).

These data showed very good consistency across the quadrants. The overall group data displayed no significant effect on contrast threshold of quadrant when the data from both eyes were aggregated ( $P = 0.6$ , one-way ANOVA).

The mean contrast threshold for a total of 168 quadrants (4 quadrants in 42 eyes) was  $0.033$  contrast units  $\pm 0.019$  SD. An upper prediction limit for normal (mean + 2 SD) has therefore been defined as  $0.071$  contrast units. As already stated, however, data for 3 of the subjects was excluded to maintain the age-match profile with the glaucoma patient group. Therefore the upper prediction limit for **age-matched** normal controls (using contrast threshold determinations from 4 quadrants in 36 eyes) was  $0.073$  contrast units (i.e. where the mean was  $0.035 \pm 0.019$  SD). The limit for normal using the whole control group will be referred to only in relation to the abnormal eyes within the control group and the young control group, while the age-matched control group will be used in any comparisons with the glaucoma group.

**DOES MEAN PERIPHERAL CONTRAST THRESHOLD CORRELATE WITH CENTRAL VISUAL SENSITIVITY AS MEASURED BY CONVENTIONAL ANALYSIS?**

For all 23 control subjects who completed the Humphrey visual field analysis, the mean deviation was obtained. This value was plotted against mean contrast threshold for each eye and regression analysis applied (Figure 3.1-7).

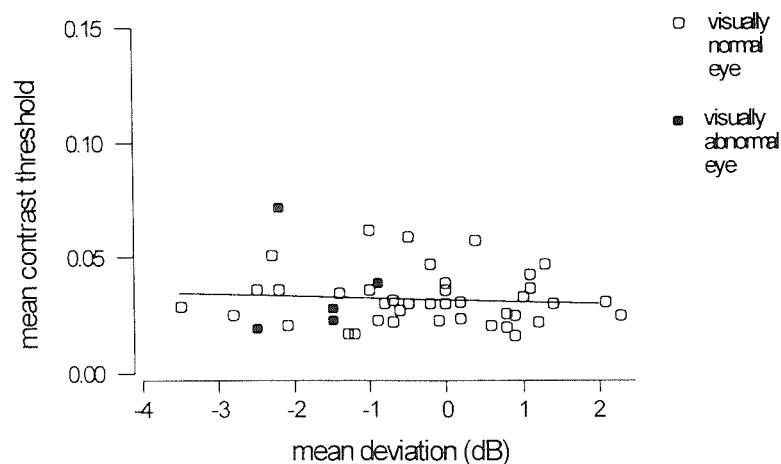


Figure 3.1-7 Mean contrast threshold plotted against MD for each eye of each control subject, visually abnormal eyes marked as filled symbols. Regression best-fit line is marked:  $y = 0.03 - 0.001x$ ,  $R^2 = 0.7\%$ ,  $P = 0.6$ .

There was no correlation between the central visual sensitivity as measured by the Humphrey Visual Field Analyser and mean peripheral contrast threshold in this group of subjects.

### 3.1.2.3 Glaucoma group patient details

Seventeen patients receiving treatment at the glaucoma clinic at Gartnavel General Hospital were recruited for the study between February 1999 and June 2000. The distribution of ages is 54 to 90 years (mean  $72.6 \pm 10.0$  SD) (Figure 3.1-8). This is not significantly different from the age-matched normal control group ( $P = 0.1$ , two-sample t-test).

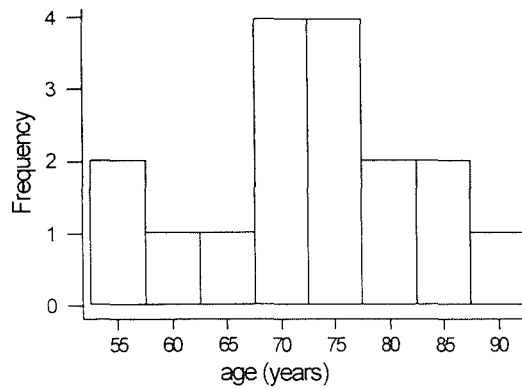


Figure 3.1-8 Distribution of ages for glaucoma patient group, (n = 17).

They had best corrected Snellen acuities of 6/9 or better, except one eye of each of 3 individuals, which ranged from 6/12 to 6/36. The group consisted of 4 females and 13 males. Six patients had POAG in both eyes (1-g, 3-g, 4-g, 6-g, 14-g, 16-g), one had narrow angle glaucoma in both eyes (13-g), one patient had OHT in both eyes (12-g), 3 patients had secondary glaucoma paired with a normal eye (8-g, 15-g, 17-g), 2 had POAG paired with a normal eye (9-g, 11-g), one patient had an unspecified type of glaucoma paired with a normal eye (10-g), one patient had glaucoma with pseudo-exfoliation in both eyes (7-g), one patient had one eye affected by POAG and the other by LTG (5-g), and one patient had LTG in one eye and retinal detachment in the other eye (2-g). Table 3.1-3 shows the patient identifier, specified diagnosis taken from glaucoma clinic case notes, age, gender and visual acuity.

Visual field testing was carried out on this group using the Friedmann Visual Field Analyser. Pupil diameter measurements are not available for the patient group as they did not complete Humphrey Visual Field testing and the other methods attempted to record pupil diameter, as described in Methods section 2.2.1.3 were unsatisfactory.

Table 3.1-3 Patient details for glaucoma group including specified diagnosis of glaucoma type from case notes.

PATIENT ID	SPECIFIED DIAGNOSIS		AGE (YRS)	GENDER	VISUAL ACUITY	
	Left eye	Right eye			Left eye	Right eye
1-g	POAG *	POAG	72	M	6/5	6/4
2-g	retinal detachment	LTG	54	M	6/12	6/5
3-g	POAG	POAG	73	M	6/6	6/7.5
4-g	POAG °	POAG	81	F	6/6	6/9
5-g	POAG	LTG	67	M	6/6	6/9
6-g	POAG	POAG	76	M	6/6	6/7.5
7-g	Glaucoma with pseudo-exfoliation	Glaucoma with pseudo-exfoliation	83	M	6/9	6/9
8-g	normal	Sarcoid induced secondary glaucoma	55	F	6/6	6/6
9-g	POAG	Normal +	68	M	6/6	6/5
10-g	normal	glaucoma	75	M	6/5	6/9
11-g	POAG	normal	87	F	6/36	6/9
12-g	OHT	OHT	70	M	6/5	6/5
13-g	Narrow angle Glaucoma	Narrow angle Glaucoma	61	F	6/9	6/9
14-g	POAG	POAG	90	M	6/9	6/24
15-g	Trauma related secondary glaucoma	normal	79	M	6/9	6/9
16-g	POAG	POAG	71	M	6/6	6/6
17-g	Ischaemia related secondary glaucoma	normal	73	M	6/9	6/9

Abbreviations and symbols used in Table

- F = female
- g = glaucoma patient ID suffix
- LTG = low tension glaucoma
- M = male
- POAG = primary open angle glaucoma
- OHT = ocular hypertension

- \* = contradiction in case notes stating both 'narrow angle' and 'open angle' stated – most recent information used
- ° = contradiction in case notes: POAG specified, however patient has normal visual fields as measured by Friedmann Visual Field Analyser
- + = contradiction in case notes stating both 'no detectable abnormality' and '0.6 cup to disc ratio' – most recent information used

Nine of the patients were on medication to control their intra-ocular pressure at the time of completing our experiments, 11 of the 17 patients had previously had surgery for glaucoma (see Appendix, Table 5.4-1).

### **3.1.2.3 Glaucoma patients contrast threshold determinations**

Contrast thresholds were again obtained in response to the one c/deg vertical, sinusoidal grating pattern presented in truncated quadrants in the peripheral field for the left and right eyes. Of the 17 patients with glaucoma who were recruited initially, one was excluded due to the inability to fixate centrally with the glaucomatous eye (10-g) and 3 were physically unable to complete the test (4-g, 11-g, and 14-g) due to immobility. With the equipment in its current format the subject must to move him or herself to view the image as the equipment cannot be adjusted to suit them. Where a patient could view the fixation spot, but was unable to perceive any pattern in a specific test region at the highest possible level of contrast, a default value of 1.0 contrast units was allocated (this affected 2 patients' results: 7-g and 13-g). Thirteen experiments were completed successfully and 4 examples are shown in Figure 3.1-9: data shown are mean contrast threshold values  $\pm$  SE for 6 contrast threshold determinations.

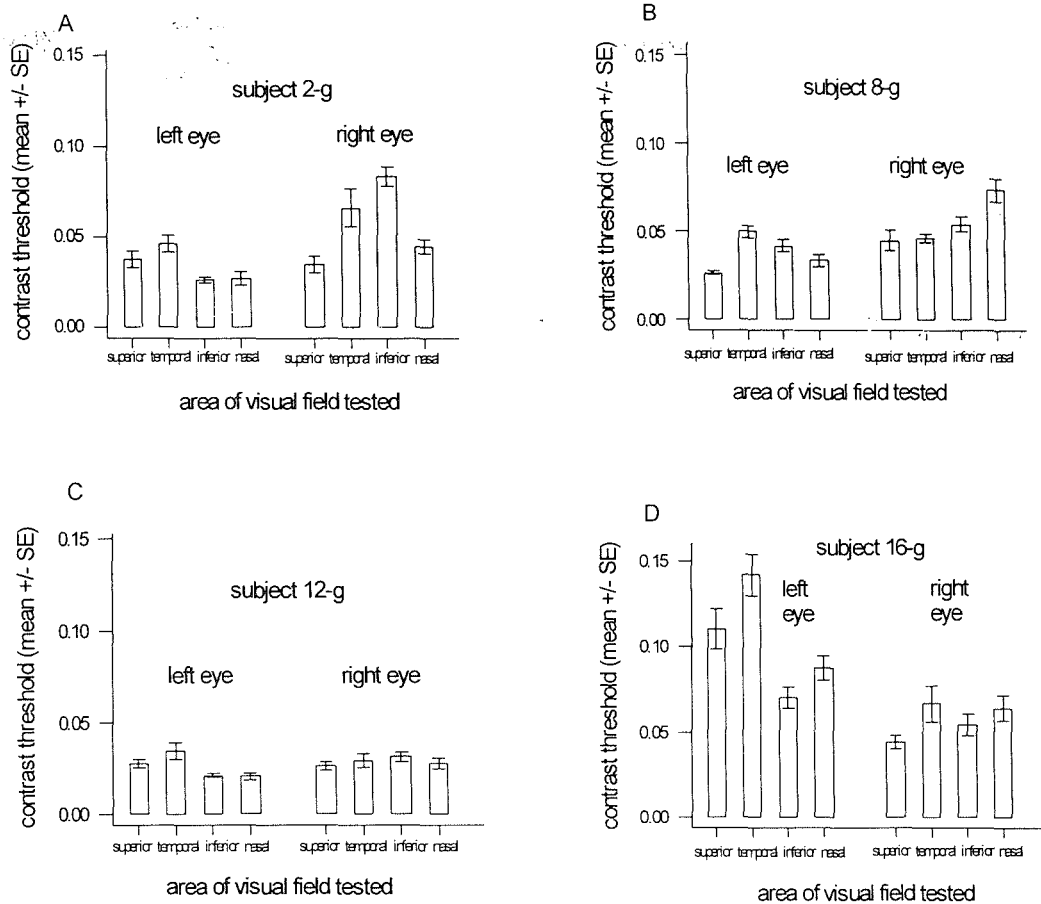


Figure 3.1-9 Four individual examples of mean contrast threshold  $\pm$  SE in patients with glaucoma for the named truncated quadrants, A: 2-g, 54 year old male with LTG in right eye, B: 8-g, 55 year old female with glaucoma in right eye, C: 12-g, 70 year old male with OHT both eyes, D: 16-g, 71 year old male with POAG in both eyes.

In patient 2-g the mean contrast threshold readings ranged from 0.026 to 0.083 contrast units, in patient 8-g the range was from 0.029 to 0.058 in patient 12-g the range was from 0.020 to 0.034 contrast units, and in patient 16-g the range was from 0.044 to 0.14 contrast units.

The graphs shown in Figure 3.1-9 suggest that there was a tendency towards greater variation in the contrast thresholds of many of the glaucoma patient group than in the age-matched controls (Figure 3.1-5).

**DOES MEAN CONTRAST THRESHOLD EXCEED THE NORMAL PREDICTION LIMIT?**

With the upper prediction limit for normal defined as 0.073 contrast units, **of the patients shown in Figure 3.1-9**, 2-g, 8-g and 16-g had one or more mean contrast threshold values which exceeded that limit. For patient 12-g (Figure 3.1-9 C), who had OHT in both eyes, all 8 mean contrast threshold values were within the normal limit.

The mean contrast thresholds for all 4 quadrants tested in both eyes for all patients (i.e. 8 values for each patient) are displayed in Figure 3.1-10, which has also been marked with a horizontal dashed line indicating the upper prediction limit for normal. Those patients who did not complete the test or were excluded are marked with an open circle and the 2 patients for whom a default score of 1.0 contrast unit was recorded are marked with triangles above the level of the broken y-axis.

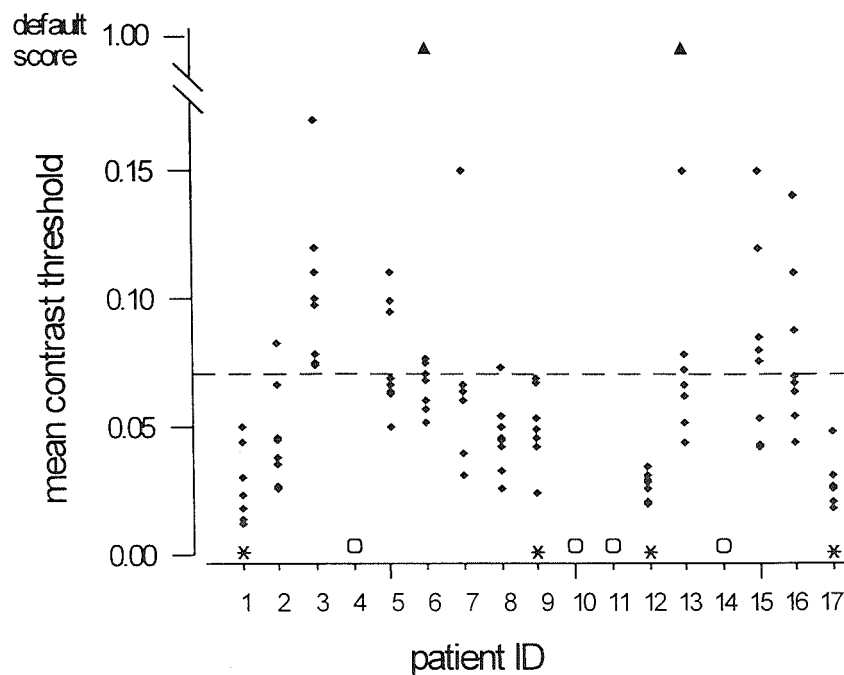


Figure 3.1-10 Mean contrast threshold in each quadrant for both eyes of all patients in glaucoma group. Dashed line indicates a contrast threshold value of 0.073 – the upper prediction limit for normal. Open symbol indicates patients who did not complete the experiment; asterisk indicates patients for whom all mean contrast threshold values were within normal limits, triangles indicate default scores of 1.0.

Overall, 9 of the 13 patients had one or more mean contrast threshold value which exceeded the upper limit for normal. For the remaining 4 patients (1-g, 9-g, 12-g, 17-g, marked with an asterisk on Figure 3.1-10) the mean contrast threshold in all 4 quadrants for both eyes was within normal limits.

### **LEVEL OF CONTRAST THRESHOLDS IN DIFFERENT QUADRANTS**

An analysis was undertaken to determine whether there was a common pattern of deficits in the glaucoma group which may be uncovered regardless of the actual level of contrast threshold. ANOVA statistical testing was performed on the effect of eye and quadrant on contrast threshold for each individual to identify any possible significant differences. Despite statistically significant differences in all patients with glaucoma ( $P < 0.03$ ), there was no obvious pattern to the variation between the quadrants. In the patients for whom contrast threshold was elevated above the prediction limit for normal, the elevation occurred in each of the 4 quadrants (superior, temporal, inferior and nasal) in at least one patient. However, in the OHT patient (12-g) there was no such significant difference between the quadrants ( $P = 0.1$ , ANOVA).

In the patients with unilateral glaucoma (2-g, 8-g, 9-g, 15-g, 17-g), the quadrant or quadrants with the highest contrast threshold were always in the affected eye. For these 5 patients, ANOVA testing revealed that the difference in contrast thresholds for their glaucomatous eye versus their non-glaucomatous eye was statistically significant ( $P < 0.001$ ).

Of the 4 patients for whom all contrast threshold values were within normal limits (1-g, 9-g, 12-g, 19-g), there was a significant difference between the eyes in 3 patients ( $P \leq 0.001$ , ANOVA). In patients 1-g, 9-g and 17-g the contrast threshold in the left eye was higher than in the right. Patient 1-g had POAG in both eyes, patient 9-g had POAG in the left eye only, and patient 17-g had POAG in his left eye. There was no significant difference between the contrast thresholds of right and left eyes in patient 12-g, who had OHT in both eyes ( $P = 0.2$ , ANOVA).

### **DOES CONTRAST THRESHOLD RELATE TO QUANTIFIED VISUAL FIELD LOSS BY CONVENTIONAL ANALYSIS?**

The patients' mean contrast threshold values for each quadrant were plotted against the quantified visual field scores from the Friedmann charts described in Methods section 2.1.4 and regression analysis was applied.

Of the 13 patients who completed the contrast threshold tests, 5 displayed a significant positive relationship (1-g, 2-g, 7-g, 8-g, 9-g) indicating a direct correlation between the elevation of contrast threshold and the location and extent of the visual field loss ( $R^2 \geq 55\%$ ,  $P \leq 0.04$ ). An example is shown in Figure 3.1-11 for patient 1-g, for whom the contrast threshold results are shown at the top, indicating elevated levels (although still within normal limits) for the left eye. The middle section of the Figure shows patient 1-g's Friedmann visual fields indicating considerable deficits in the left eye, and an almost fully sensitive right eye. The bottom of the Figure shows the relationship between these two sets of data and the regression best fit line which indicates a direct correlation.

In 5 patients there was no linear relationship between mean contrast threshold and visual field loss (3-g, 6-g, 13-g, 15-g and 16-g) ( $R^2 \leq 31\%$ ,  $P \geq 0.1$ ). An example is shown in Figure 3.1-12 for patient 16-g, indicating high levels of contrast threshold in the left eye including 3 which are well above the prediction limit for normal (top). Visual field deficits were present in both eyes, more severely in the left as shown in the middle of the Figure. The lack of relationship between these data is shown in the regression analysis featured at the bottom of the Figure with the best fit line.

For 2 patients, the relationship between mean contrast threshold and visual field results fell into a third group which could be described as statistically borderline (5-g and 17-g) ( $R^2 = 48 - 49\%$ ,  $P = 0.05$ ). An example is shown in Figure 3.1-13 for patient 17-g, indicating low levels of contrast threshold with elevation in the inferior quadrant of the left eye. The middle part of the Figure indicates visual field deficits in the left eye and a fully sensitive right eye. The regression analysis at the bottom of the Figure does suggest a tendency towards a positive relationship, however this did not reach statistical significance.

The data for one patient (12-g, OHT in both eyes) were unsuitable for regression analysis due to clustering of points at zero visual field loss, thus not providing a sufficient range against which to compare contrast threshold. These data are shown in Figure 3.1-14. As this patient was OHT in both eyes, and had therefore normal visual fields *by definition*, therefore this is interpreted as a good correlation between contrast threshold and visual field. This patient was indistinguishable from normal.

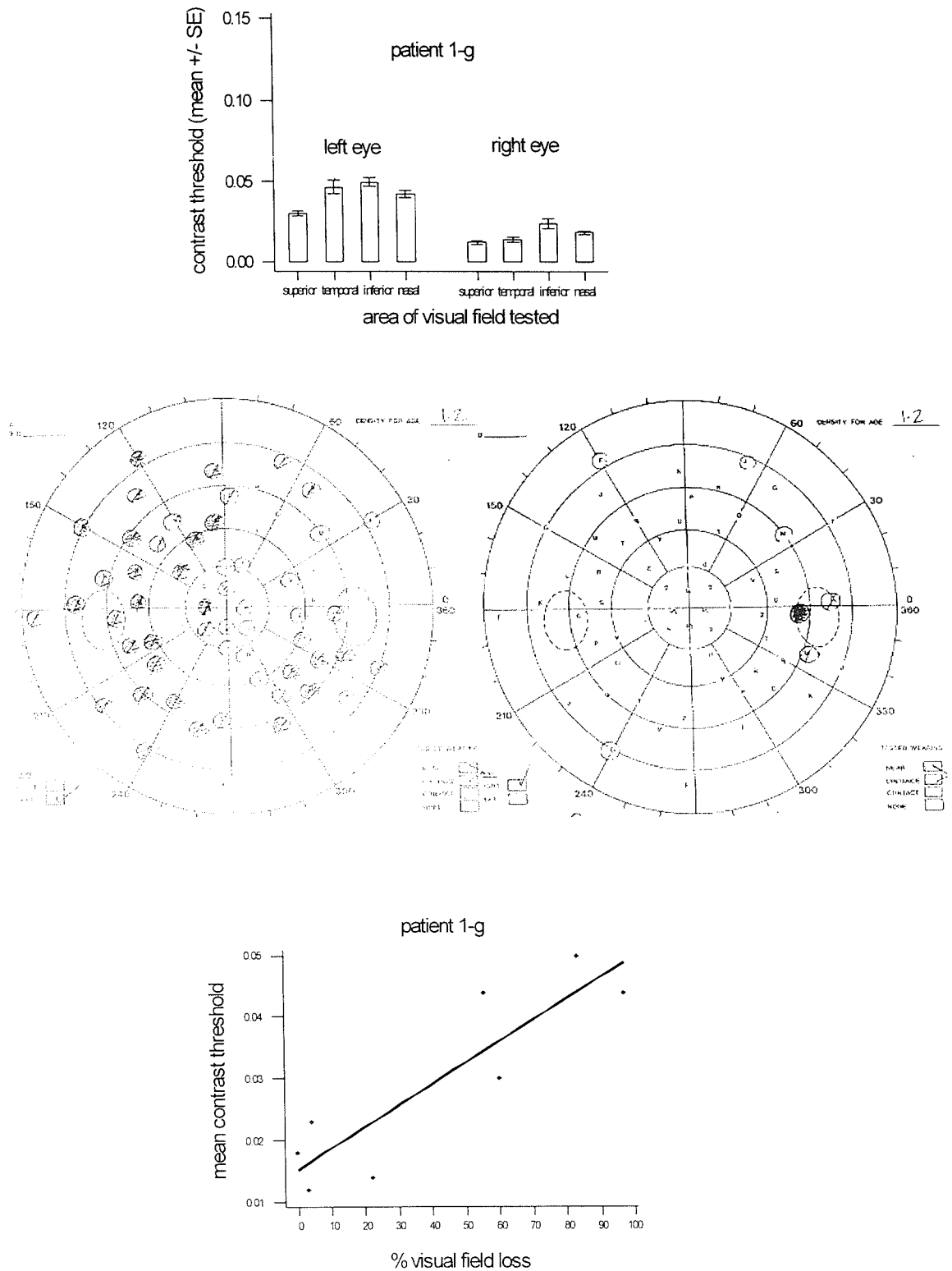


Figure 3.1-11 Top: mean contrast thresholds  $\pm$  SE. Middle: Friedmann Visual Field plots (left = left eye, right = right eye). Bottom: regression plot of mean contrast thresholds against quantified visual field loss, regression equation:  $y = 0.01 + 0.0003x$ ,  $R^2 = 79\%$ ,  $P = 0.003$ , for patient 1-g, a 72 year old male with POAG in both eyes.

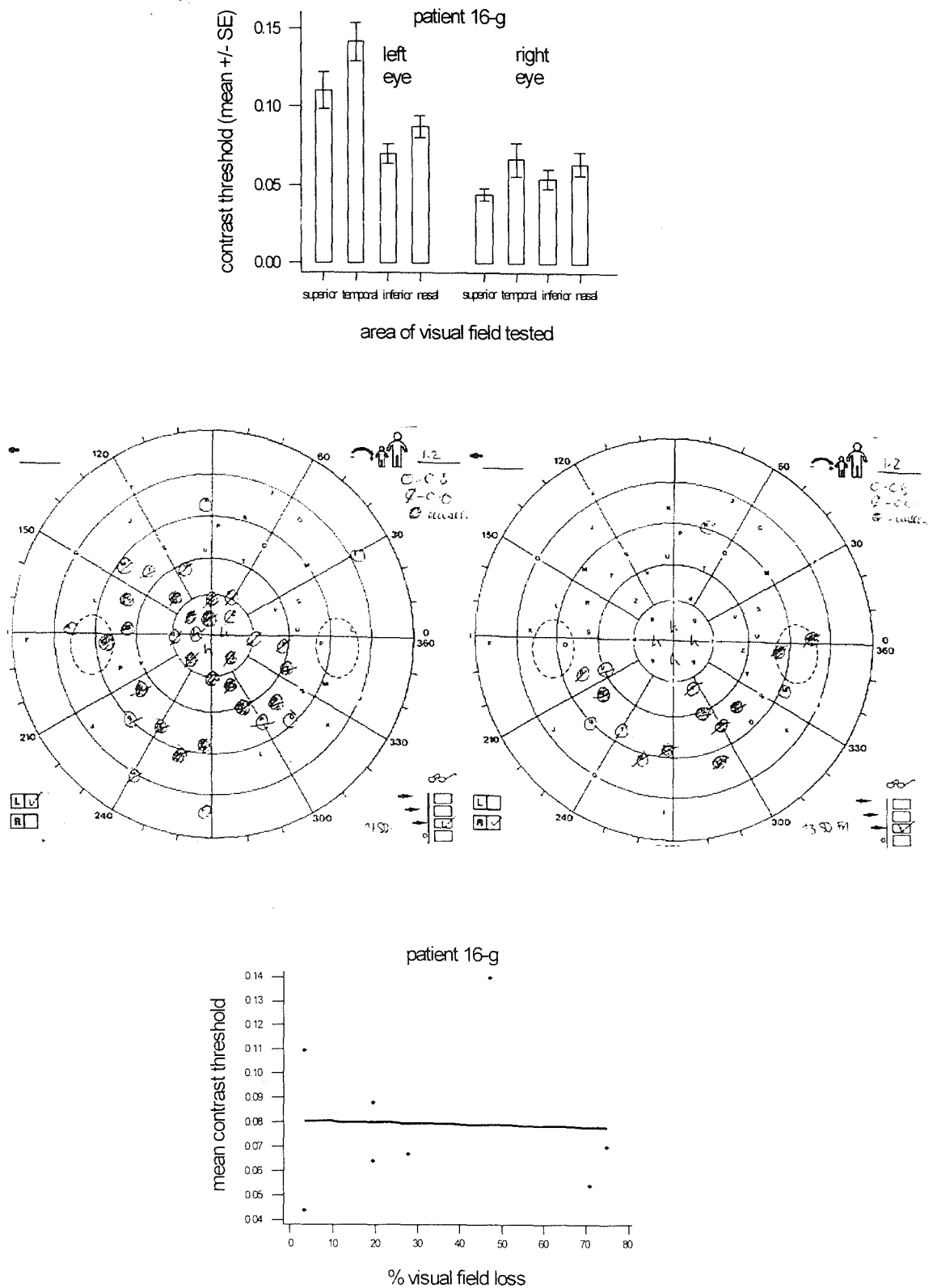


Figure 3.1-12 Top: mean contrast thresholds  $\pm$  SE. Middle: Friedmann Visual Field plots (left = left eye, right = right eye). Bottom: regression plot of mean contrast thresholds against quantified visual field loss, regression equation:  $y = 0.08 - 0.0003x$ ,  $R^2 = 0.1\%$ ,  $P = 0.9$ , for patient 16-g, a 71 year old male with POAG in both eyes.



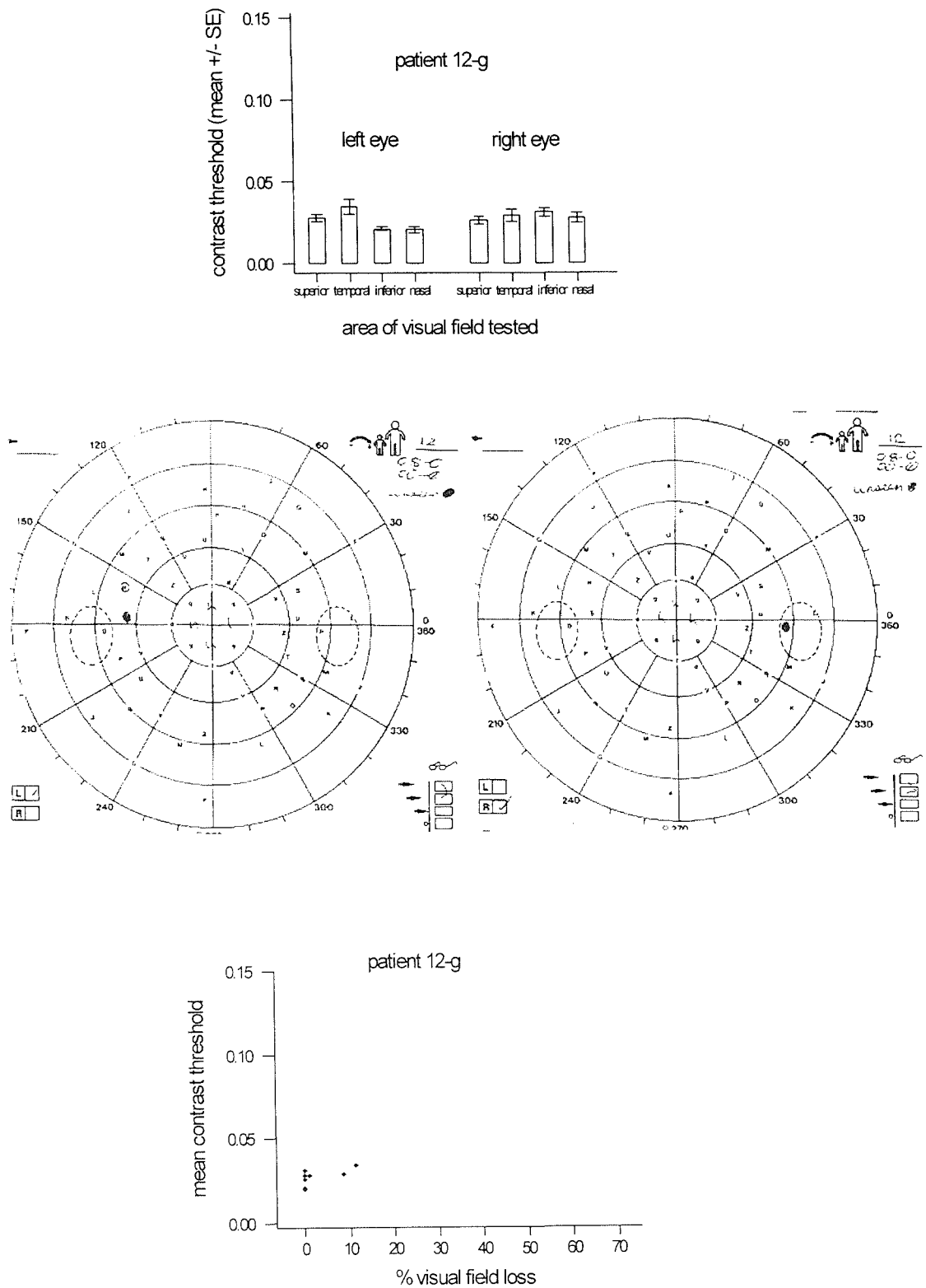


Figure 3.1-14 Top: mean contrast thresholds  $\pm$  SE. Middle: Friedmann Visual Field plots (left = left eye, right = right eye). Bottom: mean contrast thresholds against quantified visual field loss data unsuitable for regression analysis, for patient 12-g, a 70 year old male who has OHT in both eyes.

## **GROUP SUMMARY**

As the previous four Figures show there was a range of relationships between contrast threshold and conventional measures of visual field loss in this group of patients. To further explore these different types of relationships, the mean percentage field loss in each eye (as measured by the Friedmann analyser) was calculated using the percentage visual field loss in the 4 truncated quadrant areas. The severity of each patient's field loss for each eye therefore fell into one of the following groups: mild if the mean visual field loss was less than 33%; moderate if between 33 and 66% and severe if greater than 66%. None was recorded if the only points of reduced sensitivity in the entire field occurred in the temporal quadrant at the level of the blindspot. The percentage loss and category of visual field loss for both eyes of all patients who completed the contrast threshold experiments are shown in Table 3.1-4 with the visual health status of each eye. Alongside this are the numbers of contrast thresholds which exceeded the normal limit for each subject (between 0 and 4) and whether there was a significant relationship between mean contrast threshold readings and visual field loss ('yes'), no significant relationship ('no') or a statistically borderline relationship ('?').

Table 3.1-4 Patient's ID with indication of whether relationship between contrast thresholds and visual field is positive ( $P < 0.05$ ), negative ( $P > 0.05$ ) or borderline ( $P = 0.05$ ) using regression analysis, number of mean contrast thresholds which exceeded the normal limit, visual health and severity of visual field loss in each eye for all patients who completed contrast threshold experiments (i.e. not 4-g, 10-g, 11-g or 14-g).

PATIENT ID	CT CORRELATES WITH VF ?	ABNORMAL CTS		VISUAL HEALTH		VISUAL FIELD LOSS	
		L	R	L	R	L	R
1-g	Yes	0	0	G	G	Severe	Mild
2-g	Yes	0	1	RD	LTG	None	Moderate
3-g	No	4	4	G	G	Moderate	Moderate
5-g	?	1	2	G	LTG	None	Moderate
6-g	No	2	1	G	G	Mild	Moderate
7-g	Yes	0	3	G	G	None	Moderate
8-g	Yes	0	1	Normal	G	Mild	Moderate
9-g	Yes	0	0	G	Normal	Mild	None
12-g	Yes *	0	0	OHT	OHT	None	None
13-g	No	3	1	G	G	Mild	None
15-g	No	4	1	G	Normal	Moderate	Mild
16-g	No	3	0	G	G	Moderate	Mild
17-g	?	0	0	G	Normal	Moderate	None

Abbreviations and symbols used in Table

- CT = contrast threshold
- G = glaucoma
- L = left eye
- LTG = low tension glaucoma
- OHT = ocular hypertension
- R = right eye
- RD = retinal detachment
- VF = visual field

- bold** = indicates patients' eyes in which one or more contrast threshold exceeded normal limit
- 0-4 = number of quadrants in which contrast threshold exceeded normal limit
- ? = statistically borderline result
- \* = not appropriate for regression analysis

As indicated previously, there was a positive correlation between contrast threshold in each truncated quadrant and the percentage loss of visual field in 6 of the 13 patients who completed the test (including the patient with OHT). In these patients the amount of mean field loss in the test regions for each eye for each patient ranged from none through to severe. In the group of 5 patients where there was a lack of a relationship between visual field and contrast threshold and for the 2 in whom the significance of the relationship could

be described as borderline statistically, the mean percentage loss of field for each eye ranged from none to moderate. This will be discussed in more detail later.

### ANALYSIS OF THE GLAUCOMA PATIENT GROUP AS A WHOLE

The mean contrast threshold for each truncated quadrant in both eyes for every patient was plotted against the percentage visual field loss in the related area, see Figure 3.1-15. A broken y-axis is used to indicate the default scores of 1.0 contrast units without obscuring the detail at the lower end of the contrast threshold range.

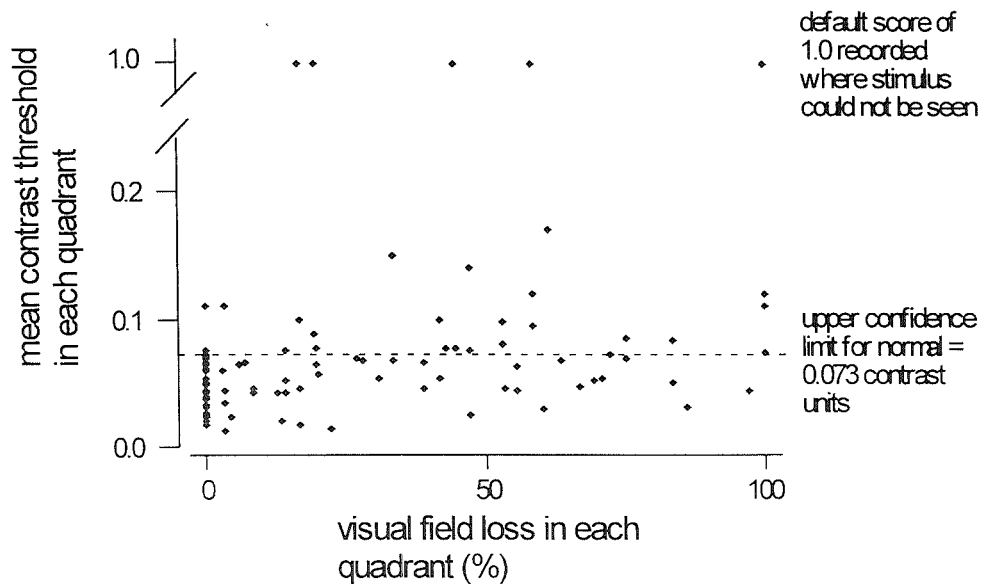


Figure 3.1-15 Plot of mean contrast threshold for *each quadrant in each eye* of patients in glaucoma group against percentage visual field loss in same quadrant as measured by Friedmann perimetry, dotted line indicates upper prediction limit for normal.

As the data are not normally distributed, regression analysis cannot be applied, however it would appear that *for the group as a whole*, there was no obvious linear correlation between contrast threshold and percentage visual field loss as measured by a conventional method. This was despite the fact that 75% of patients with known visual field loss had one or more mean contrast threshold value above the prediction limit for normal. This may be due in part to the accuracy of the conventional analysis itself, which, as has been discussed, is widely accepted to be a fairly insensitive measure of visual field loss. If, as is

anticipated, these two methods of measuring visual sensitivity do so by stimulating different components of the neural visual pathway then it is perhaps expected that no direct correlation between them would be found.

### 3.1.2.5 Young control group subject details

A third group which consisted of 20 control subjects, under the age of 35, was tested to provide a comparison with the older control group. Their ages ranged from 21 to 33 years (mean 26.4 years  $\pm$  2.7 SD) (Figure 3.1-16).

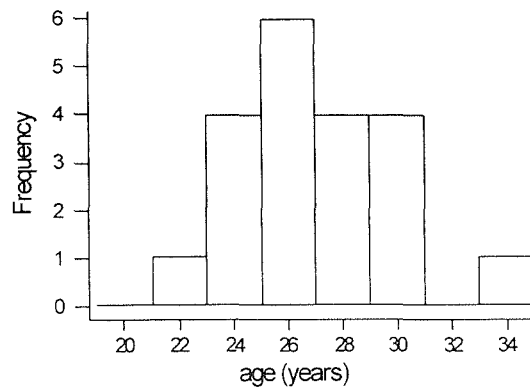


Figure 3.1-16 Distribution of ages for young control group (n = 20).

Subjects' best corrected Snellen acuities were 6/5 or better, except one eye of the eldest subject in this group which was 6/6. The group comprised 14 females and 6 males, (Table 3.1-5). Pupil diameter and visual fields were not recorded for this group.

Table 3.1-5 Subject details for young control group

SUBJECT ID	AGE (YEARS)	GENDER	VISUAL ACUITY	
			Left eye	Right eye
1-y	24	F	6/4	6/4
2-y	30	F	6/4	6/5
3-y	21	F	6/4	6/4
4-y	23	F	6/4	6/4
5-y	27	F	6/4	6/5
6-y	27	M	6/5	6/4
7-y	27	M	6/4	6/4
8-y	25	F	6/4	6/4
9-y	24	F	6/4	6/4
10-y	29	F	6/4	6/5
11-y	26	M	6/4	6/4
12-y	26	F	6/5	6/4
13-y	33	M	6/6	6/5
14-y	29	M	6/4	6/4
15-y	27	F	6/4	6/4
16-y	24	F	6/4	6/4
17-y	29	F	6/6	6/4
18-y	26	F	6/4	6/4
19-y	26	M	6/4	6/5
20-y	25	F	6/4	6/4

Abbreviations used in Table

F = female  
M = male  
-y = young subject ID suffix

**3.1.2.6 Young control group contrast threshold determinations**

Contrast thresholds were obtained in response to a one c/deg vertical, sinusoidal grating pattern presented in truncated quadrants in the peripheral field for the left and right eyes in 20 young control subjects. Data shown are mean contrast thresholds plotted with  $\pm$  one SE for 6 determinations. Four examples are shown in Figure 3.1-17.

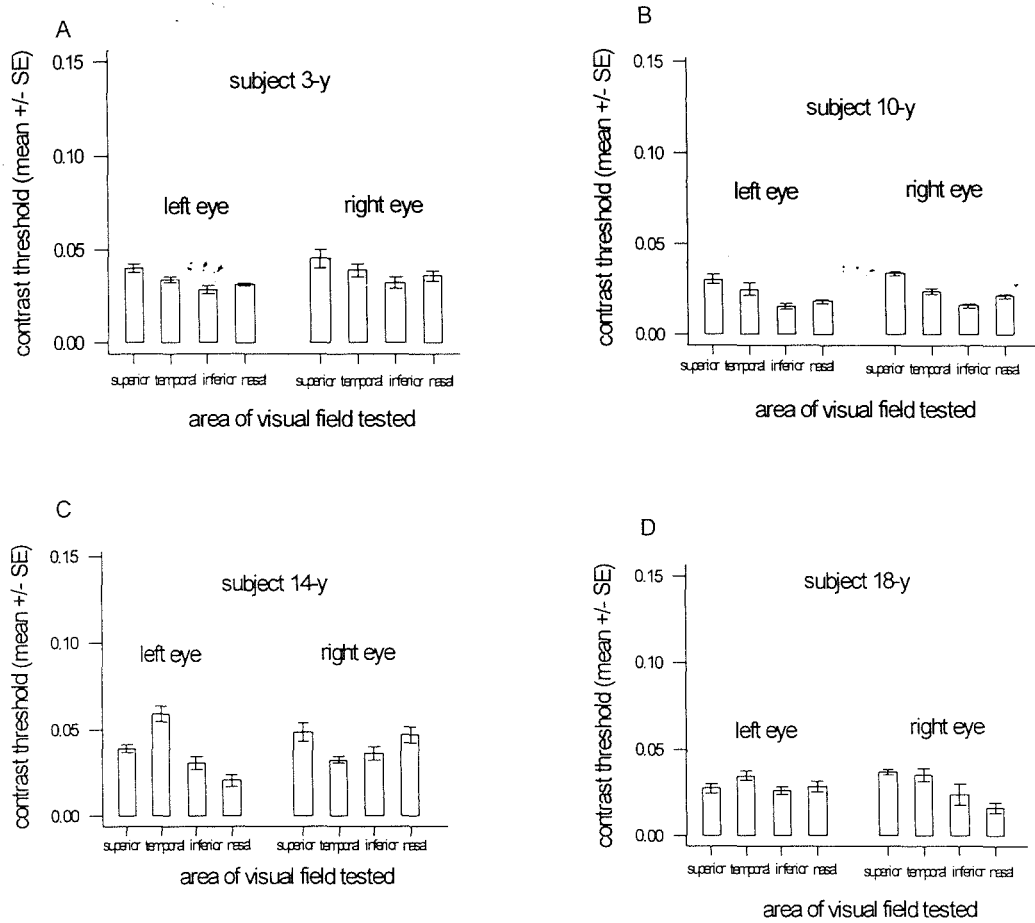


Figure 3.1-17 Four individual examples of mean contrast threshold  $\pm$  SE in young control subjects for the named truncated quadrants, A: 3-y, 21 year old female, B: 10-y, 29 year old female, C: 14-y, 29 year old male, D: 18-y, 26 year old female.

In subject 3-y mean contrast threshold readings ranged from 0.028 to 0.045 contrast units, in subject 10-y the range was from 0.016 to 0.033 contrast units, in subject 14-y the range was from 0.020 to 0.059 contrast units, and in subject 18-y the range was from 0.016 to 0.037 contrast units.

It was noted that the spread of data for two individuals (1-y, a 24 year old female and 5-y, a 27 year old female) was distinctly different from that in all other experimental subjects (despite being visually normal), as can be clearly seen in Figure 3.1-18.

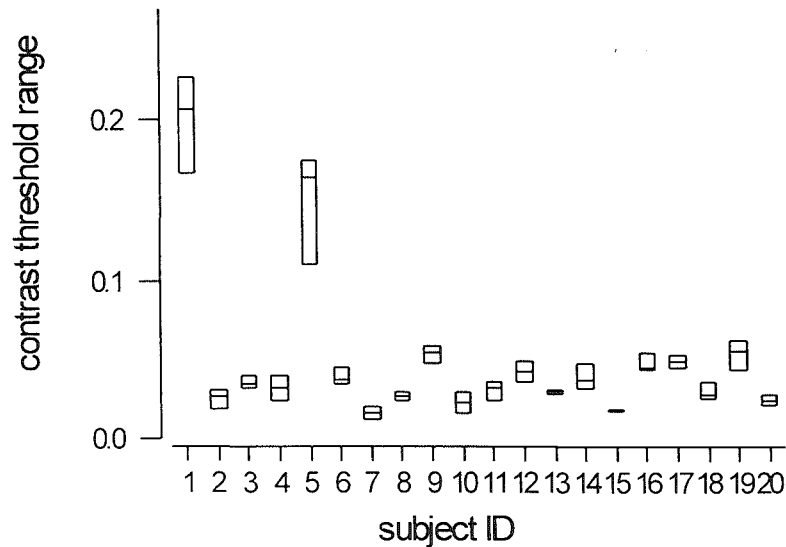


Figure 3.1-18 Box plots of the range of contrast thresholds in the young control group, the top of each box indicates the first quartile, the mid-line indicates the median and the bottom of the box indicates the third quartile. Note unusual spread of results for subjects 1-y and 5-y.

The mean contrast thresholds for these two subjects were between 3 and 10 times the level of the other control subjects. Comparing the results for each of these two subjects against the 18 other members of the group, indicated that the difference from the rest of the group was highly statistically significant, ( $P < 0.001$ , t-test of the means). We have interpreted this as indicating that these two individuals did not find the point of genuine threshold and instead have repeatedly overshoot this point, perhaps misinterpreting the instructions. For this reason they have been excluded from the subsequent young control group analysis.

As in the older control group, there was some variation in mean contrast threshold between the quadrants but it was generally low in all of them. There was no evidence in these subjects of an elevated threshold in the temporal quadrant due to the blind spot.

All the results for the young control group were plotted on a single graph to give an overview of contrast threshold in the young visually normal individual (Figure 3.1-19).

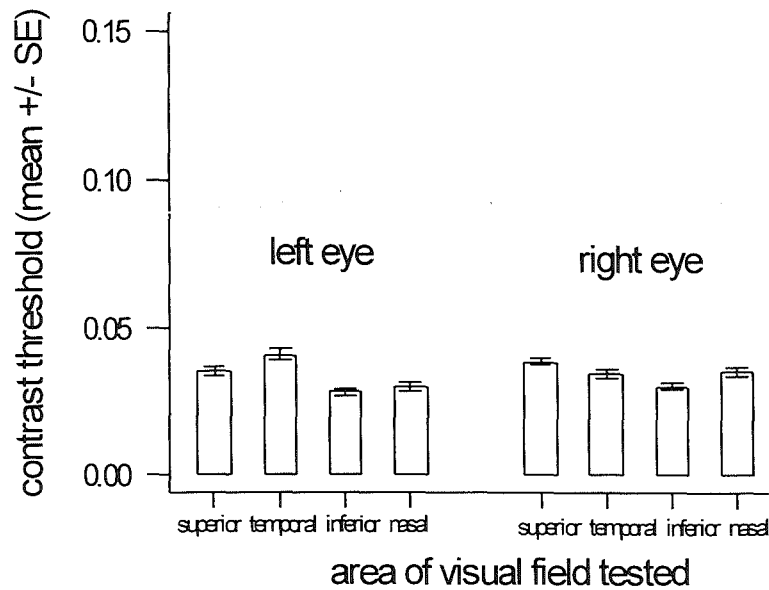


Figure 3.1-19 Mean contrast threshold  $\pm$  SE for the named truncated quadrants for young control group ( $n=18$ ).

The mean contrast threshold was 0.034 contrast units  $\pm$  0.015 SD. Therefore, an upper prediction limit for normal (mean + 2 SD) was defined as 0.064 contrast units, lower than for the older control group despite a mean which was marginally higher in the young control group, indicating that the variation in the readings was less extensive.

The effect of quadrant on contrast threshold (with both eyes taken together) was statistically significant ( $P < 0.001$ , one-way ANOVA), with superior and temporal quadrants apparently producing a higher threshold than inferior and nasal ones. However the differences are fairly small (0.037 and 0.038 compared to 0.029 and 0.032 respectively).

**COMPARISON WITH OLDER CONTROL GROUP**

For each of the two control groups the overall mean contrast threshold was calculated using data from all 8 quadrants in all subjects, i.e. the results for both eyes and the 4 quadrants tested are all taken together. The mean for the young control group (n = 18) was then compared to the mean for the older control group (n = 24) (Figure 3.1-20).

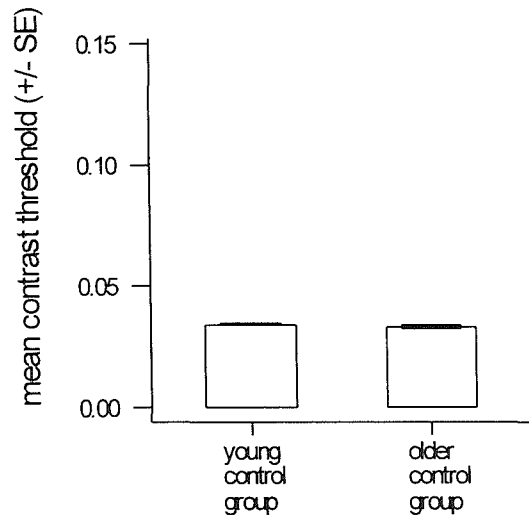


*Figure 3.1-20 Aggregated mean contrast threshold ± SE for all quadrants in the young and older control groups.*

The overall mean contrast threshold for these two control groups were shown to be statistically different ( $P = 0.001$ , two-sample t-test), however, the difference between the mean for the young control group (0.033 contrast units) compared with the mean for the older control group (0.029 contrast units) is extremely small.

**3.1.2.7 Older control group (abnormal eyes) subject details**

Within the older control group, 6 subjects had an abnormality in one eye. These have been included as special case studies as they provide information additional to that obtained from the glaucoma patients' results. The group consisted of 4 females and 2 males, whose ages ranged from 59 to 75 years. Table 3.1-6 shows the subject identifier, ocular problem, age, gender and visual acuity.

*Table 3.1-6 Subject details for those control subjects with visually abnormal eyes (subject identifiers relate to listing for older control group).*

SUBJECT ID	OCULAR HISTORY OF NON-NORMAL EYE	GENDER	AGE (YRS)	VISUAL ACUITY	
				Right eye	Left eye
2-n	Retinal scarring from infection, left eye	F	70	*	6/12
6-n	Retinal detachment (surgically reattached), right eye	M	63	6/12	*
7-n	Mild cataract, left eye	F	69	*	6/9
9-n	Unexplained poorer vision – possibly solar damage, right eye	M	76	6/18	*
15-n	Macular hole, right eye	F	73	6/36 (eccentric)	*
23-n	Amblyopia, right eye	F	59	6/12	*

Abbreviations and symbol used in Table

F = female

M = male

-n = non-glaucoma subject ID suffix

\* = normal eye (discussed in Results section 3.1.2.1)

It was not possible to have all subjects ophthalmologically examined, therefore some of these visual abnormalities are self-reported. Subject 2-n reported that her eye infection was caused by a nematode infection, while in East Africa. It is not known which area of retina had been detached in subject 6-n. Subject 9-n reported that he had an area of damage at the centre of his right eye, which was reported to have been caused by solar damage, however this was not confirmed. Each of five eyes had a visual acuity of between 6/9 and 6/18 and the eye with the macular hole had an eccentric visual acuity of 6/36.

**CONVENTIONAL VISUAL FIELD ANALYSIS**

All 6 subjects with a visually abnormal eye completed the conventional visual field analysis on the Humphrey analyser already described, however the eye with the macular hole was excluded, as her fixation could not be accurately held. There were abnormal results for 3 of these 5 visually abnormal eyes, including abnormal or borderline results on the glaucoma hemifield test and the lack of a blind spot. The MD was outwith normal limits in 4 eyes, indicated in Table 3.1-7 by bold type. The mean MD for these 6 eyes was  $-1.7\text{dB} \pm 0.5 \text{SD}$ . Comparison of this group of data with the MD for eyes in the visually normal control eyes, showed them to be significantly different ( $P = 0.02$ , t-test of the mean) with mean of  $-0.15\text{dB}$  and  $-1.6\text{dB}$  for normal and abnormal groups respectively.

*Table 3.1-7 Humphrey visual field analysis for each subject in control group with abnormal eyes.*

SUBJECT ID	VISUAL FIELDS		MEAN DEVIATION (dB)		PUPIL DIAMETER (mm)		
	Left eye	Right eye	Left eye	Right eye	Left eye	Right eye	Inter-pupillary difference
2-n	GHT	*	-2.2	*	3.8	3.1*	0.7
6-n	*	✓	*	<b>-1.5</b>	4.6*	4.3	0.3
7-n	GHT BS	*	<b>-1.6</b>	*	5.8	5.4*	0.4
9-n	*	✓	*	-0.9	-	-	-
15-n	*	-	*	-	-	-	-
23-n	*	GHT	*	<b>-2.1</b>	-	-	-

Abbreviations and symbols used in table

BS = no blind spot apparent

GHT = glaucoma hemifield test result abnormal or borderline, indicated where diffuse or localised low sensitivity was apparent

- = indicates no data from Humphrey visual field analyser

\* = indicates normal eye – analysed in Results section 3.1.2.1.

**bold** = mean deviation stated to be outside normal age-matched limits by Humphrey

✓ = normal visual field by Humphrey

### 3.1.2.8 Older control group (abnormal) contrast threshold determinations

#### SUBJECT 2-N

Subject 2-n (70 year old female) had a discrete scotoma in the temporal region of her left visual field (nasal retina) as a result of scarring due to an infection several decades ago. The visual acuity in the left eye was 6/12, and in the right eye was 6/4. Mean contrast thresholds  $\pm$  SE are shown in Figure 3.1-21.

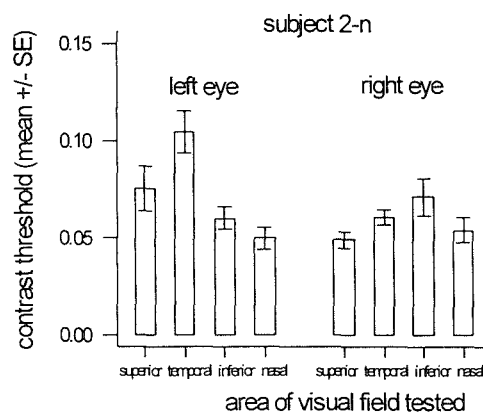


Figure 3.1-21 Mean contrast threshold  $\pm$  SE for subject 2-n (70 year old female with retinal scarring in her left eye).

Figure 3.1-21 shows that the mean contrast threshold was clearly elevated in the temporal quadrant of the subject's left eye with respect to the others. There was a significant difference between right and left eyes ( $P = 0.03$ , ANOVA) and a significant difference between the quadrants, with the temporal quadrant in the left eye at a higher level than the others ( $P = 0.01$ , ANOVA).

In subject 2-n therefore, the visual field defect in the temporal quadrant in her left eye has been reproduced in her contrast threshold results. The mean contrast threshold was above the normal limit normal in this quadrant and just above it in the left superior quadrant. This confirmed the results of the Humphrey visual field analyser (see Appendix, Figure 5.2-2), which showed an area of reduced sensitivity in the temporal region of her left eye. The Humphrey also indicated a significant difference in the MD of the affected eye with respect to normal and an abnormal glaucoma hemifield test in the left eye.

**SUBJECT 6-N**

Subject 6-n (63 year old male) had received surgery for retinal detachment in his right eye. The principal remaining visual problem, as perceived by the subject, were ‘floaters’ which occasionally caused temporary distraction during the experimental procedure. The visual acuity in the left eye was 6/12, and in the right eye was 6/5. The mean contrast thresholds  $\pm$  SE are shown in Figure 3.1-22.

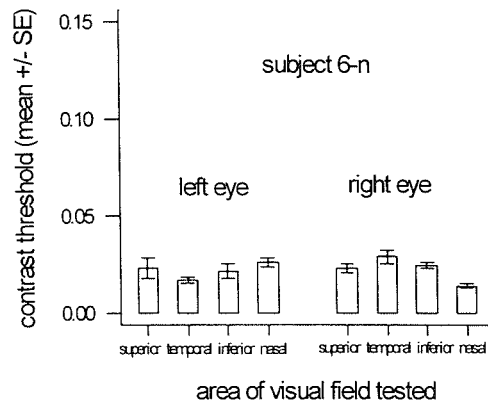


Figure 3.1-22 Mean contrast threshold  $\pm$  SE for subject 6-n (63 year old male with surgically treated retinal detachment in his right eye).

As can be seen from Figure 3.1-22, the patient’s retinal detachment has not caused any elevation of his contrast threshold relative to the other eye ( $P = 0.7$ , ANOVA). All contrast thresholds were comfortably within normal limits.

The Humphrey visual fields for this subject did not reveal any obvious areas of reduced sensitivity, (Appendix Figure 5.2-6), but the MD did vary between left and right eyes and it was statistically significantly different from normal in the right eye.

**SUBJECT 7-N**

Subject 7-n (69 year old female) had a mild cataract affecting her left eye, diagnosed at a recent visit to her optometrist. The visual acuity in the left eye was 6/9 and in the right eye it was 6/7.5. Mean contrast thresholds  $\pm$  SE are shown in Figure 3.1-23.

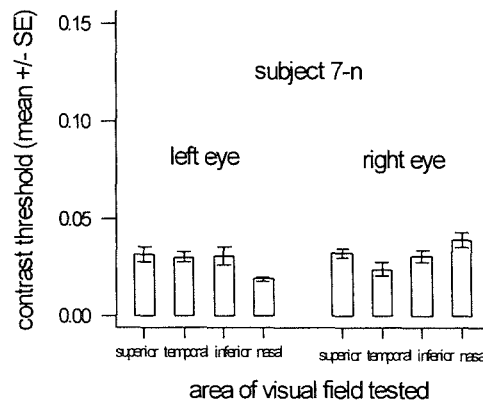


Figure 3.1-23 Mean contrast threshold  $\pm$  SE for subject 7-n (69 year old female with a mild cataract in her left eye).

All the mean contrast thresholds were comfortably within normal limits. There was no significant effect on contrast threshold by eye or quadrant ( $P = 0.2$ , ANOVA). The Humphrey visual fields for this subject did not reveal any obvious areas of reduced sensitivity, (Appendix Figure 5.2-7), but the MD did vary between left and right eyes and it was statistically significantly different from normal in the left eye. There was also no apparent blind spot and an abnormal glaucoma hemifield test in the left eye.

**SUBJECT 9-N**

Subject 9-n (76 year old male) had poorer vision in his right eye, the visual acuity in his left eye was 6/18 and in his right eye it was 6/4. Mean contrast thresholds  $\pm$  SE are shown in Figure 3.1-24.

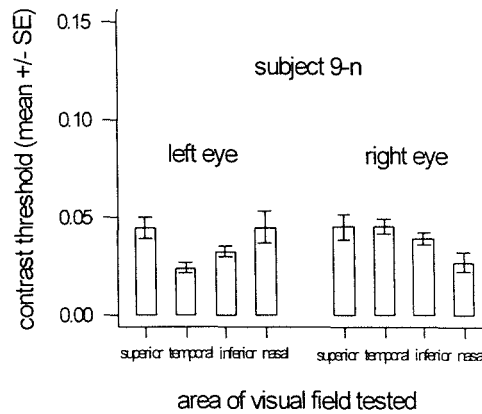


Figure 3.1-24 Mean contrast threshold  $\pm$  SE for subject 9-n (76 year old male with poorer vision in his right eye).

All mean contrast thresholds were comfortably within normal limits. There was no significant effect on contrast threshold by eye or quadrant ( $P = 0.3$ , ANOVA).

The Humphrey visual field plots are shown in the Appendix as Figure 5.2-9 showing that the right eye had normal levels of visual sensitivity. The upper field in the left eye, however, did reveal an area of significantly low sensitivity, shown up as the dark region. This was interpreted as being caused by a drooping eyelid. This apparent defect, which extends from roughly 15 to 25 in the upper field, would encroach on the most peripheral part of the superior quadrant in contrast threshold testing (which tests between 10 and 20 ). However the defect is not reflected in a high contrast threshold reading for that quadrant. The MD of the visually abnormal eye was not significantly different from normal.

**SUBJECT 15-N**

Subject 15-n (73-year old female) had a retinal hole at the macula in her left eye. The eccentric visual acuity in the left eye was 6/36 and central visual acuity in the right eye was 6/5. This prevented proper fixation on the contrast threshold stimulus fixation spot, and therefore no readings are available for the abnormal eye to compare to the normal eye (Figure 3.1-25).

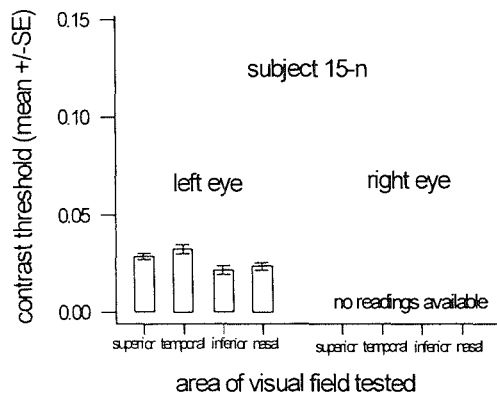


Figure 3.1-25 Mean contrast thresholds  $\pm$  SE for subject 15-n (73 year old female with a macular hole in her right eye).

The Humphrey visual field plot for the normal eye is shown in the Appendix Figure 5.2-14 and indicates normal sensitivity.

**SUBJECT 23-N**

Subject 23-n (59 year old female) had amblyopia in her right eye due to a “lazy” eye in childhood. The visual acuity in the left eye was 6/12 and in the right eye it was 6/6. This did not appear to cause any elevation to the subject’s contrast thresholds which are shown in Figure 3.1-26.

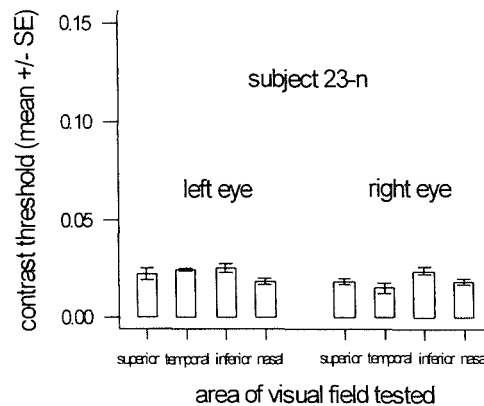


Figure 3.1-26 Mean contrast threshold  $\pm$  SE for subject 23-n (59 year old female with amblyopia in her right eye).

All values were comfortably within normal limits, which may have been expected since the subject’s abnormality is centrally located, well away from the contrast threshold test regions. A statistically significant increase was found in contrast thresholds for the left eye with respect to the right eye ( $P = 0.01$ , ANOVA) and for the effect of quadrant ( $P = 0.03$ , ANOVA), however, since all the contrast thresholds were very low these differences do not imply any abnormal visual sensitivity.

The Humphrey visual fields for this subject did not reveal any obvious areas of reduced sensitivity, (Appendix Figure 5.2-22), but the MD was statistically significantly different from normal in both eyes, there was an abnormal glaucoma hemifield test result for the right eye.

### **3.1.3 Apparatus investigations**

#### **3.1.3.1 Light intensity and contrast threshold**

Early in the development of the apparatus, it was identified that an area of instability, which could have a specific effect on the results, was that of the relationship between the intensities of the light beams (which were known to fluctuate). It was reasoned that contrast threshold for peripheral and foveal viewing of the quadrants would be dependent on the relative intensities of the laser and background illumination, i.e. low contrast thresholds would arise if the laser intensity were greater with respect to the background intensity and high contrast thresholds would arise if the laser intensity were lower with respect to the background intensity. As detailed previously, measurements were made of the intensities of the laser and background beams in order to achieve a match in their relative levels, however, it was acknowledged that there was still a possibility of fluctuation. In addition it was not always practicable to achieve a perfect match between the recorded levels, since the smallest possible step adjustment with an NDF filter was 0.1 log units (this represents a 20% reduction in intensity).

Therefore, although any differences were at a relatively low value in absolute terms (in the  $\text{nW/cm}^2$  range), and acceptance of some disparities within recorded values were tolerated, however, it was felt necessary to investigate these differences with respect to their possible effect on contrast threshold to check if, for example, high contrast threshold values were found when the imbalance was in the direction of higher laser intensities and vice versa. The mean contrast threshold for normal subjects in response to the green vertical sinusoidal grating was plotted against the respective value for the percentage difference in the two light beams measured immediately prior to the two light beams, and regression analysis applied (Figure 3.1-27).

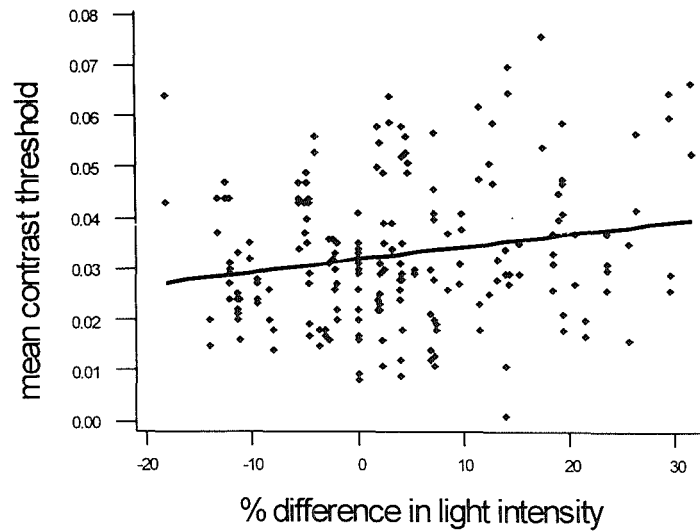


Figure 3.1-27 Regression plot of mean contrast threshold (in response to the vertical sinusoidal grating pattern) against the respective value for the percentage difference in intensity between background and laser beams. Regression equation is:  $y = 0.03 + 0.0002 x$ ,  $R^2 = 4\%$ ,  $P = 0.004$ ,  $F = 8$ , ( $n = 200$ ).

The mean percentage difference between laser and background beams, for all experiments using the vertical sinusoidal grating pattern, was  $3.9\% \pm 11.1$  (SD). The regression analysis revealed a weak relationship between mean contrast threshold and percentage difference in light intensity, ( $R^2 = 4\%$ ), though the slope of the best-fit line was significantly different from horizontal ( $P = 0.004$ ). Other types of regression, e.g. quadratic, or a log transformation of the data, did not improve the relationship greatly.

While the regression analysis revealed statistical significance, the relationship was very weak as shown above. The F-value was 8, considerably lower than the value of 22.8 required for the slope of regression to be accorded importance, as explained in Methods section 2.1.5 (Draper and Smith, 1981). Therefore it can be concluded that while errors between background and laser intensities had a weak effect on the contrast threshold, it was not felt to be of great importance.

In order to further explore this possible source of error, however, the readings of foveal contrast threshold, taken by the experimenter before every experiment, were utilised, as it was thought these may indicate the level of relative brightness of each light source and its effect on peripheral contrast threshold.

### 3.1.3.2 Psychophysical testing of illuminance of quadrants

As there is a limit to the precision of the measurement of light intensities at relatively low values (in the nW range), the radiometric measurements by the Optometer were backed up by psychophysical determinations of the foveal threshold.

The relationship between peripheral and foveal contrast threshold was investigated by plotting the peripheral contrast threshold readings for all the subjects taking part in the final protocol against the foveal contrast threshold readings (taken by the author) for each quadrant taken on the same day (Figure 3.1-28).

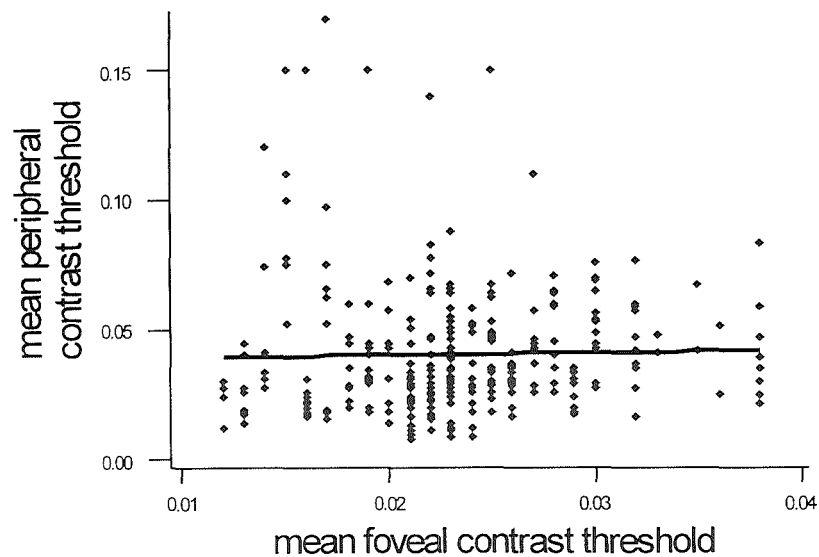


Figure 3.1-28 Regression plot of mean foveal contrast threshold for author against mean peripheral contrast threshold for subjects in final protocol in each quadrant. Regression equation  $y = 0.04 + 0.09x$ ,  $R^2 = 0\%$ ,  $P = 0.7$ , ( $n = 200$ ).

The regression analysis indicated that there was no relationship between peripheral and foveal contrast threshold ( $P = 0.7$ ); suggesting that the recorded results for peripheral contrast threshold are not related to differences in foveal contrast thresholds.

### 3.1.3.3 Repeatability

An experiment was undertaken to determine how repeatable the readings for contrast threshold were over a period of several hours. Four readings were taken for each of the 4 truncated quadrants in response to a stationary, green, vertical sinusoidal grating pattern of one c/deg. The field size was 40° in diameter, with a 20° diameter central occluder. The readings were repeated every hour for 6 hours for one visually normal subject (the author) who remained in the room under low light throughout (0.1 lux, as previously stated) (Figure 3.1-29).

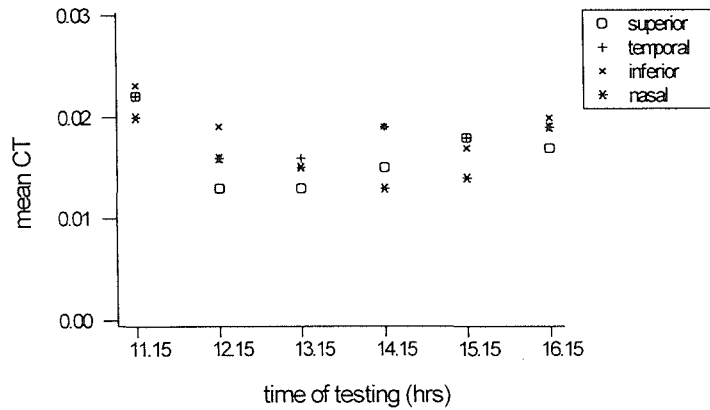


Figure 3.1-29 Mean contrast threshold in response to a stationary concentric grating pattern, 4 peripheral quadrants measured hourly for 6 hours (only 3 results are visible at each test time as one result is hidden by another).

It is apparent that there is some variation over time, with the highest values occurring during the first test session. This is possibly due to the effect of dark adaptation which occurs after the entry into the dark room or due to a learning effect.

For this reason, readings taken for the initial quadrant were retaken at the end, and the second set of readings was used for analysis. This approach was applied to all subjects, and the full experiment was completed in one continuous run after the subject had become adapted to the lighting levels (which remained constant throughout the experiment).

## **3.2 SBR results**

For all subjects, 6 determinations were taken for each of 5 SBR tests, namely upper / lower intra-ocular SBR (for each eye), nasal / temporal intra-ocular SBR (for each eye) and right / left eye inter-ocular SBR. The stimulus fields consist of squares of light, of 10° side lengths, viewed at 30cm. All SBR graphs are plotted with the same format: if the mean is a positive number, the first named area of field in each test i.e. upper, nasal or right eye is more sensitive by the stated percentage. Likewise if the mean is negative, the second named field area, i.e. lower, temporal or left eye is more sensitive by the stated percentage.

### ***3.2.1 Older control group subject details***

A control group comprising the same 24 subjects described in Results section 3.1.2.1 completed the SBR tests. For group evaluation, the abnormal eyes of those subjects with a known ocular problem have again been excluded, and are analysed separately in Results section 3.2.7. This affects the inter-ocular SBR for subjects 2-n, 6-n, 7-n, 9-n, 15-n and 23-n, the left intra-ocular SBRs of subjects 2-n and 7-n, and the right intra-ocular SBRs of subjects 6-n, 9-n, 15-n and 23-n. Also as before, for evaluation with the glaucoma patient group, data from the age-matched control group was used (i.e. the older control group excluding subjects 16-n, 17-n and 18-n).

### ***3.2.2 Older control group SBR determinations***

The mean values  $\pm$  SE for the percentage difference in sensitivity in the compared areas were plotted for each subject: 4 examples illustrating different types of results are shown in Figure 3.2-1.

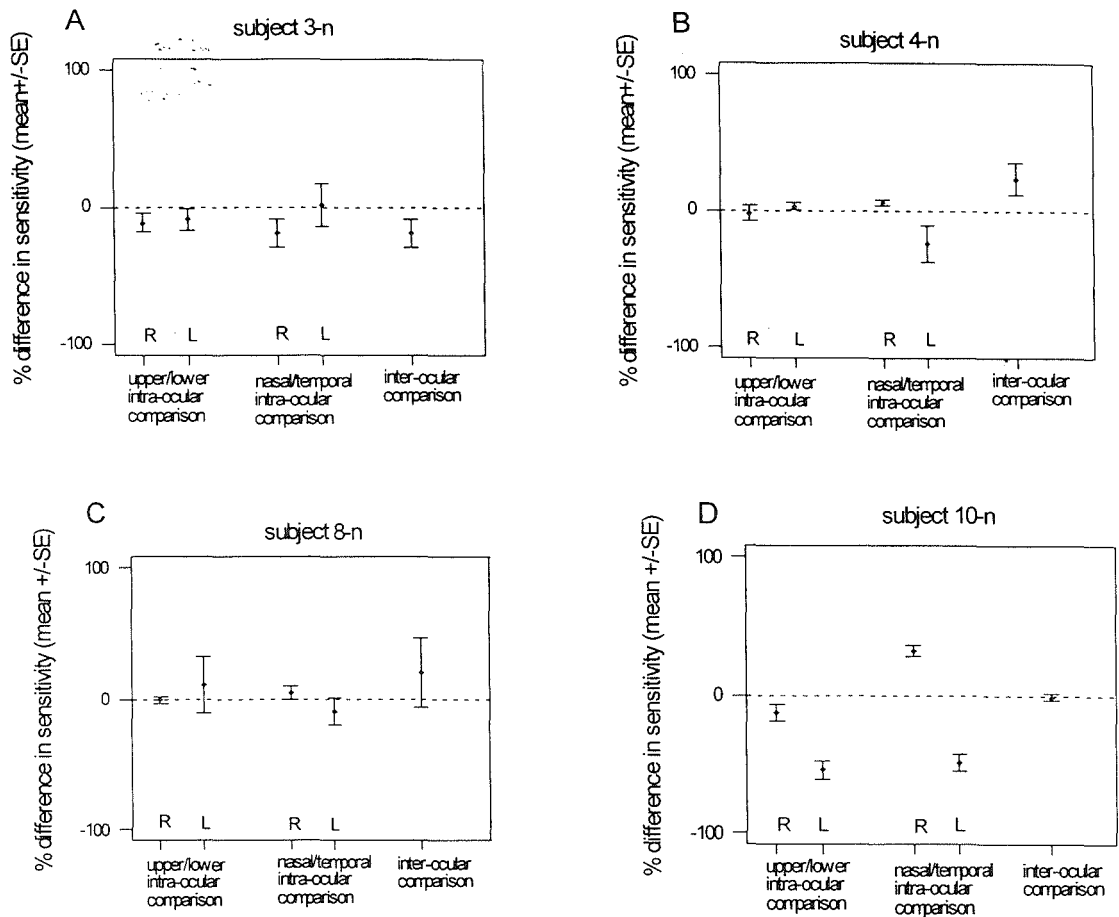


Figure 3.2-1 Four individual examples of mean SBRs  $\pm$  SE for upper / lower, nasal / temporal intra-ocular comparisons, and inter-ocular central comparisons in control subjects. A: 3-n, 70 year old male, B: 4-n, 65 year old female, C: 8-n, 61 year old female, D: 10-n, 71 year old male. R = right eye, L = left eye.

As the examples in Figure 3.2-1 indicate, there was some variation in the ratio of sensitivity between the different retinal areas tested for all subjects, rarely falling precisely on a value of perfect balance (0% difference in sensitivity).

In subject 3-n, the SBRs indicated that the lower field was more sensitive than the upper field in the right and left eyes by about 10%, the temporal field was more sensitive than the nasal field in the right eye by 20%, the nasal field was more sensitive than the temporal in the left eye by 2%, and that the central field was more sensitive in the left eye than in the right eye by 20%.

In subject 4-n, the SBRs indicated that the lower field was more sensitive in the right eye by 2%, the upper field was more sensitive in the left eye by 3%, the nasal field was more sensitive in the right eye by 6% the temporal in the left eye by 24%, and the central field was more sensitive in the right eye by 23%.

In subject 8-n, the SBRs indicated that the lower field was more sensitive in the right eye by 1%, the upper field was more sensitive in the left eye by 10%, the nasal field was more sensitive in the right eye by 5%, the temporal field in the left eye by 10%, and the central field was more sensitive in the right eye by 20%.

In subject 10-n, the SBRs indicated that the lower field was more sensitive in the right eye by 13% and in the left eye by 54%, the nasal field was more sensitive in the right eye by 32%, and the temporal field in the left eye by 48%, and the central field was more sensitive in the left eye by 1%.

To give an overview of the range of values in visually normal older control subjects, the mean SBR values for each subject were plotted on 5 separate graphs (Figure 3.2-3 A to E). The scale for the y-axis is slightly extended for graph A, to include one outlying point for subject 12-n. Open symbols on graph E indicate those subjects whose inter-pupillary difference was found to be greater than 0.5mm by the Humphrey Visual Field Analyser (this will be explored further in the following section).

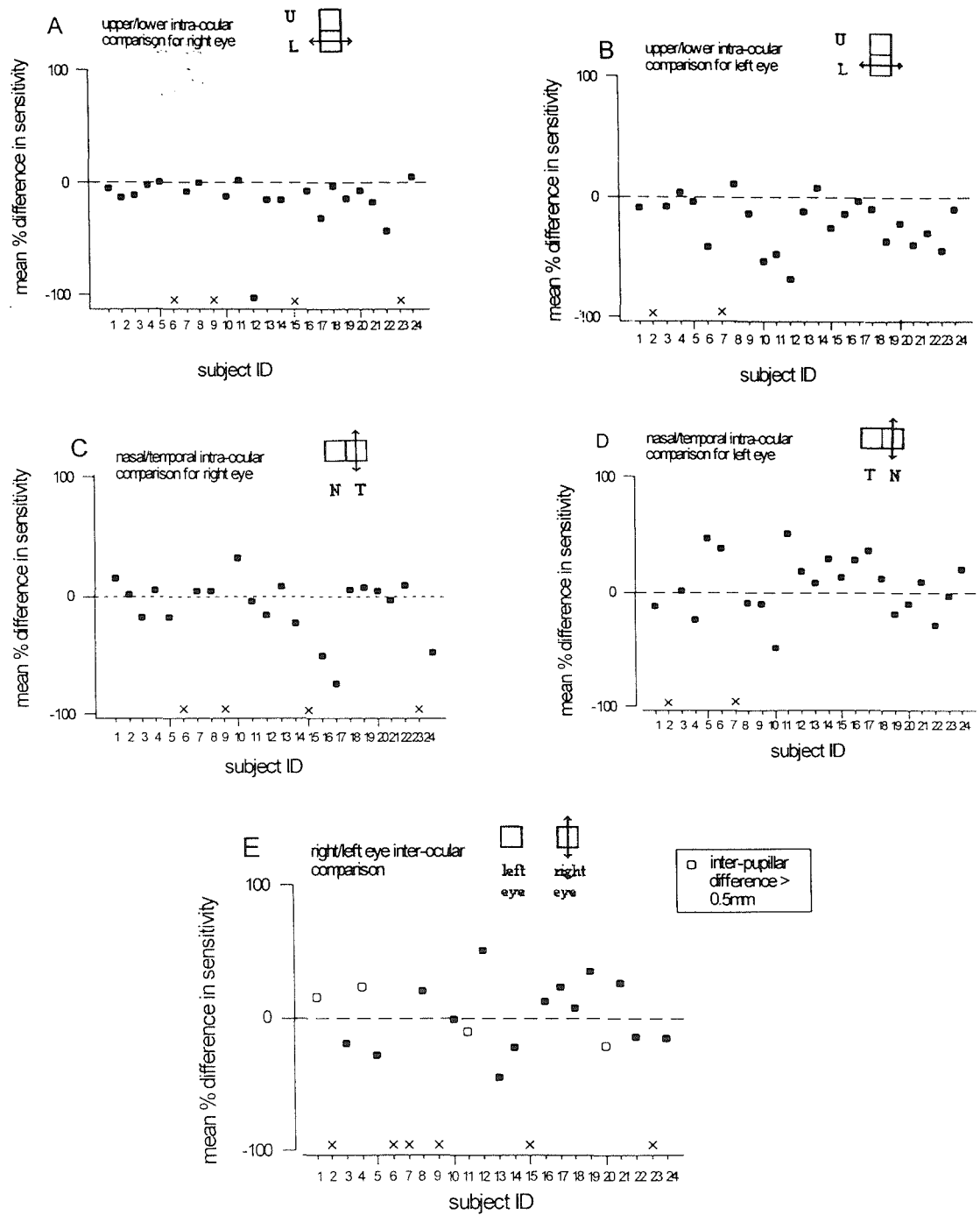


Figure 3.2-2 Graphs showing all mean SBR values for older control group by test, A: upper / lower right eye, B: upper / lower left eye, C: nasal / temporal right eye, D: nasal / temporal left eye, E: right / left eye inter-ocular. Crosses indicate subjects with visually abnormal eye results analysed in Results section 3.2.7, open symbols on graph E indicate subjects for whom inter-pupillary difference > 0.5mm, U = upper, L = lower, N = nasal, T = temporal.

The range of mean SBRs for each test for the older control subjects were as follows: upper / lower right intra-ocular: -104.0% to +5.3%; upper / lower left intra-ocular: -68.4% to +10.4%; nasal / temporal right intra-ocular: -74.6% to +31.9%; nasal temporal left intra-ocular: -48.5% to +50.6%; and right / left eye inter-ocular: -44.9% to +50.7%.



For comparison with the glaucoma patient group, SBR determinations for **the age-matched** control group (i.e. excluding subjects 16-n, 17-n and 18-n) are plotted in Figure 3.2-4.

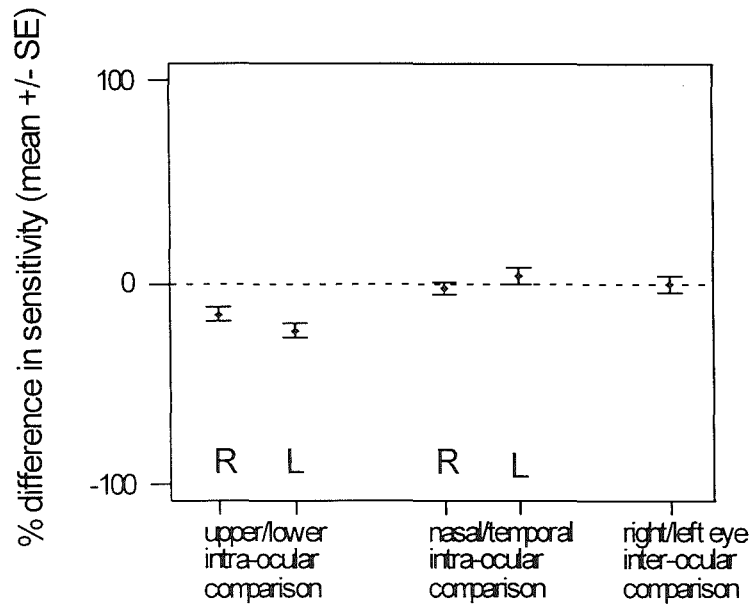
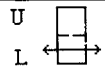
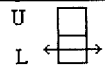
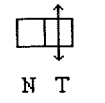
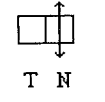
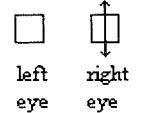


Figure 3.2-4 Mean SBR  $\pm$  SE for age-matched control group, R = right eye, L = left eye.

In the group as a whole, the SBRs indicated that the lower field was more sensitive in the right eye by 16%, and in the left eye by 24%. The temporal field was more sensitive in the right eye by 2% and the nasal field was more sensitive in the left eye by 4%. The central fields were almost precisely matched, with a marginal bias towards the left eye of 0.3%. This shows a tendency towards bias on the side of the apparatus with the graduated filter for intra-ocular tests, especially in the upper / lower tests where the bias was more pronounced, as shown in Figure 3.2-4. Hence the lower field was indicated as more sensitive for both eyes, the temporal field more sensitive for right eyes and nasal for left eyes). This finding was not repeated in the inter-ocular tests. Analysis of the group data to determine if the mean was significantly different from zero in each case, is shown in Table 3.2-1.

All SBR determinations for age-matched control subjects were used to calculate prediction limits for normal (mean  $\pm$  2 SD, equivalent to 97.7% confidence interval) as shown in Table 3.2-1. These upper and lower limits are indicated on the group graphs for the glaucoma patients in Figure 3.2-6.

Table 3.2-1 Mean SBRs for age-matched control group with prediction limits and P-value for difference between mean and zero using one-sample t-test.

TEST PERFORMED		MEAN (%)	PREDICTION LIMITS: MEAN $\pm$ 2 SD (%)	P-VALUE, ONE-SAMPLE T-TEST
Upper / lower	Right Eye 	-15.7	-87.1 to +55.7	0.02
	Left Eye 	-23.7	-103.3 to +55.9	0.0002
Nasal / temporal	Right Eye 	-2.3	-61.1 to +56.5	0.6
	Left Eye 	3.7	-88.5 to +95.9	0.6
Right / left eye		-0.3	-75.1 to +74.5	1.0

The equivalent confidence intervals were also calculated for the whole older control group for comparison with the young control group and are included in the Appendix as Table 5.4-1.

### 3.2.3 Glaucoma patient group details

Fifteen of the 17 of the glaucoma patient group described in Results section 3.1.2.3 were available to attempt the SBR tests (all except 8-g and 13-g). Of those 15, 14 successfully completed all 5 tests (all except 14-g). Patient 10-g, who could not centrally fixate with his right eye, successfully completed the intra-ocular tests using peripheral cues to orientate his vision, but was excluded from the inter-ocular test which tested central vision.

### 3.2.4 Glaucoma patient group SBR determinations

The mean values  $\pm$  SE for the percentage difference in sensitivity in the compared areas were plotted for each subject: 4 examples illustrating different types of results are shown in Figure 3.2-5.

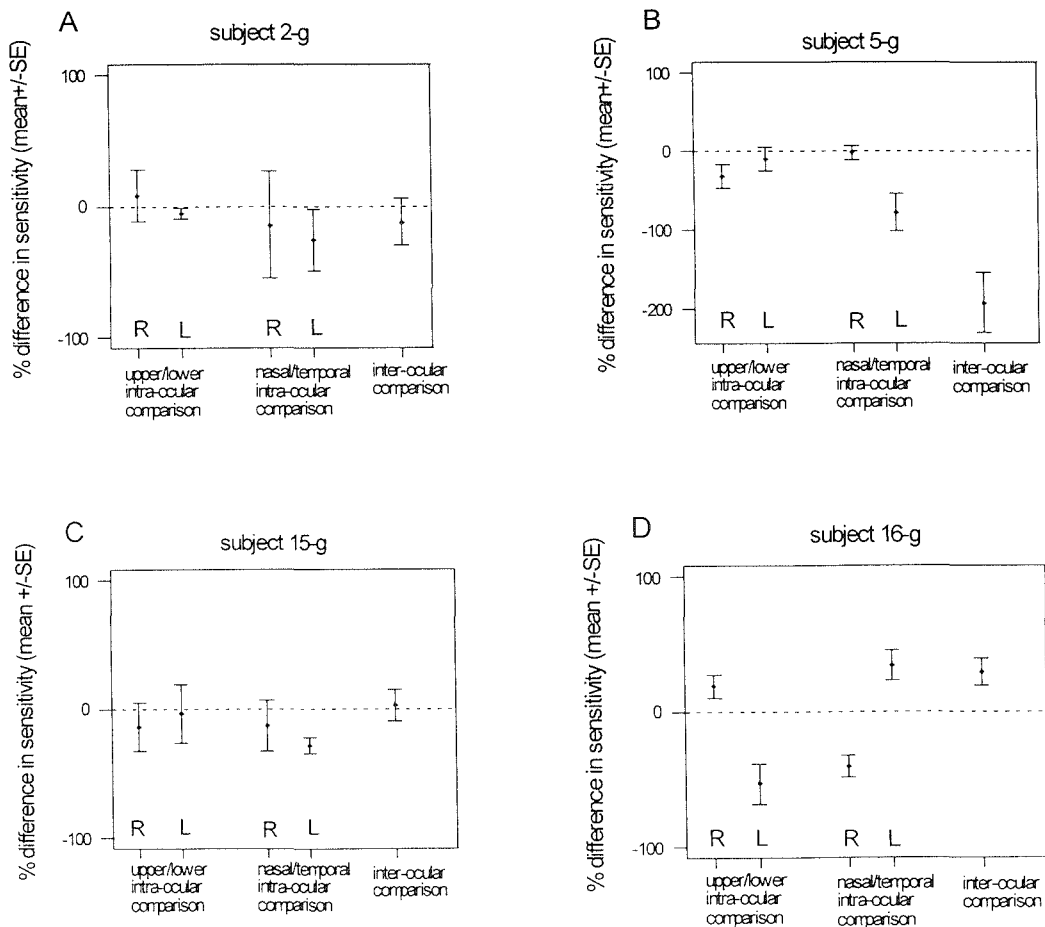


Figure 3.2-5 Four individual examples of the mean SBRs  $\pm$  SE for upper / lower, nasal / temporal intra-ocular comparisons, and inter-ocular central comparisons in glaucoma patients. A: 2-g, 54 year old male with LTG in his right eye, B: 5-g, 67 year old male with POAG in his left eye and LTG in right eye, C: 15-g, 79 year old male with glaucoma in his left eye, D: 16-g, 71 year old male with POAG in both eyes, R = right eye, L = left eye.

As the examples in Figure 3.2-5 indicate, there was a considerable amount of variation in the ratio of sensitivity between the different retinal areas tested in patients with glaucoma.

In patient 2-g (who had LTG in his right eye), the SBR indicated that the upper field was more sensitive in the right eye by about 8% and the lower field was more sensitive in the left eye by 6%, the temporal field was more sensitive in the right and left eyes by 15% and 26%, respectively, and the central field was more sensitive in the left eye than the right eye by 12%.

In patient 5-g (who had POAG in his left eye and LTG in his right eye), the SBR indicated that the lower field was more sensitive in the right and left eyes by 32% and 10% respectively, the temporal field was more sensitive in the right and left eyes by 2% and 78%, respectively, and the central field was more sensitive in the left eye by 193%.

In patient 15-g (who had glaucoma in his left eye), the SBR indicated that the lower field was more sensitive in the right and left eyes by 14% and 4%, respectively, the temporal field was more sensitive in the right and left eyes by 12% and 29%, respectively, and the central field was slightly more sensitive in the right eye by 2%.

In patient 16-g (who had POAG in both eyes), the SBR indicated that the upper field was more sensitive in the right eye by 19% and the lower field was more sensitive in the left eye by 53%, the temporal field was more sensitive in the right eye by 40%, and the nasal field was more sensitive in the left eye by 34%, and the central field was more sensitive in the left eye by 29%.

The mean SBR values for each glaucoma patient were plotted on 5 separate graphs for each of the SBR tests (Figure 3.2-6). For comparison, the prediction limits for the age-matched control group (as shown in Table 3.2-1) are marked on each graph as horizontal dashed lines.

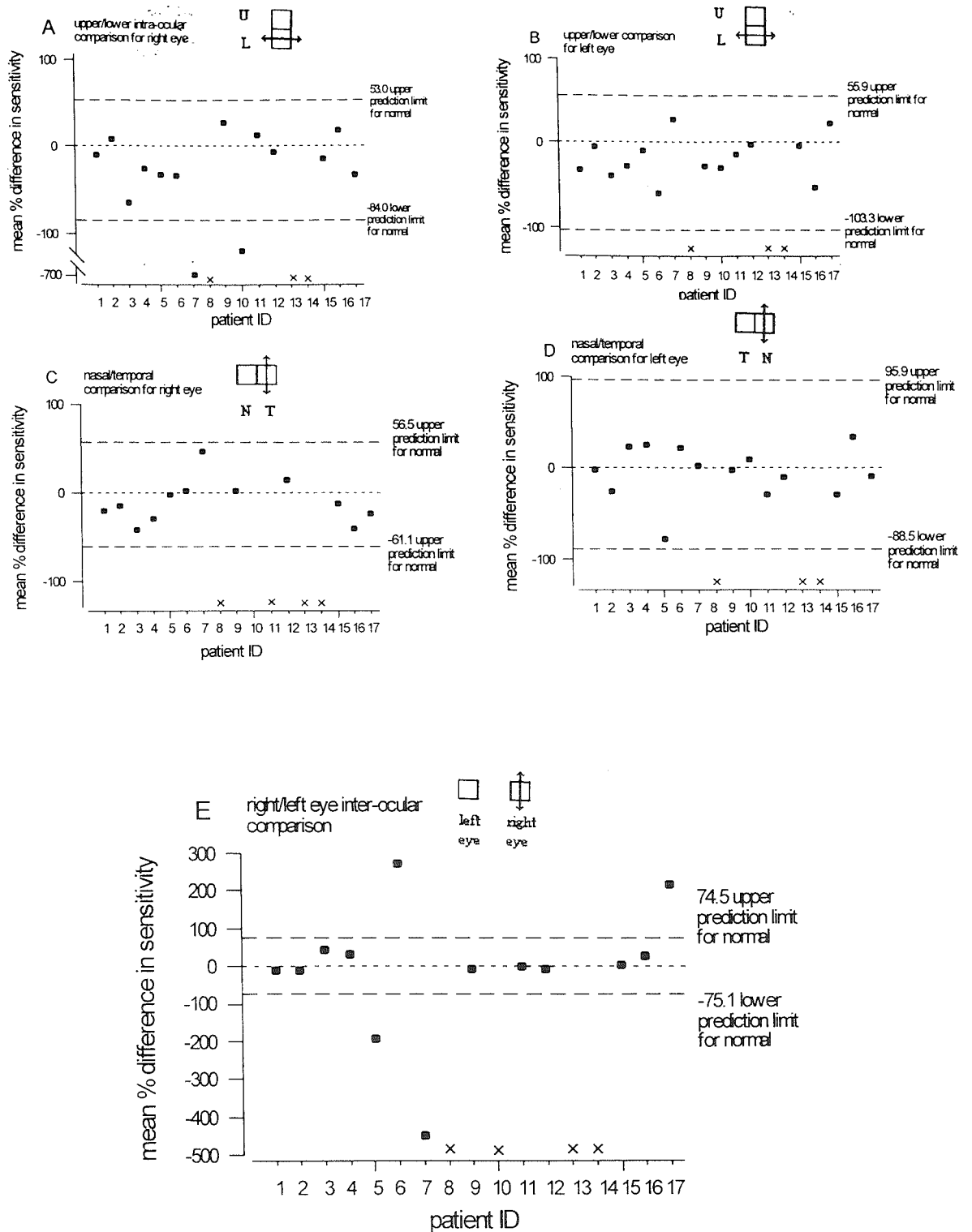


Figure 3.2-6 Graphs showing all mean SBR values for glaucoma patients (filled symbols) and prediction limits for age-matched normal subjects marked as dashed lines, (A): upper / lower right eye, (B): upper / lower left eye, (C): nasal / temporal right eye, (D): nasal / temporal left eye, (E): right / left eye inter-ocular. N.B. Y-scales have been adjusted to include large positive and negative values – not same on all 5 graphs. Crosses indicate patients who did not complete the test. U = upper, L = lower, N = nasal, T = temporal, broken axis on Graph A used to show default score without obscuring other values. More details in text.

Patient 7-g (an 83 year old male with glaucoma in both eyes) could not perceive the upper half of the stimulus when completing the upper / lower intra-ocular experiment. This related to a large area of deep scotoma in the upper half of his right eye field and is indicated on Figure 3.2-6 (A) by a default score. A default score of  $-700\%$  was used, calculated using the formula described in Methods section 2.2.3. The symbol is marked on the Figure using a broken y-axis. Patient 11-g (an 87 year old female with POAG in her left eye) was unable to complete the nasal / temporal intra-ocular comparison for her right eye, but could not clearly describe which parts of the field were missing, therefore it is marked as missing data with a cross on graph C.

As can be seen in Figure 3.2-6, there were wide limits for normal which led to 2 patients' intra-ocular SBRs and 4 patient's inter-ocular SBRs falling outwith the normal range. The range of mean SBRs for each test in the patient group were as follows: upper / lower right eye:  $-700\%$  to  $+27.6\%$ ; upper / lower left eye:  $-60.3\%$  to  $+27.4\%$ ; nasal / temporal right eye:  $-134.0\%$  to  $+47.2\%$ ; nasal / temporal left:  $-77.8\%$  to  $+34.1\%$ ; and right / left eye intra-ocular:  $-448.8\%$  to  $+274.4\%$ . In the 4 patients for whom inter-ocular SBR was outwith normal limits, 3 had glaucoma in both eyes (5-g, 6-g, 7-g), and one had glaucoma in the left eye paired with a normal right eye (17-g). The inter-ocular SBR suggested a more sensitive right eye in this patient. In the 2 patients for whom the upper / lower right eye intra-ocular SBR was outwith normal limits (7-g and 10-g), both eyes were affected by glaucoma and the lower field had less field loss by conventional analysis than the upper field. There were no patients for whom abnormal SBRs were obtained for upper / lower intra-ocular comparison in the left eye, or nasal / temporal comparisons in either eye.

### **Does SBR relate to the quantified visual field loss by conventional analysis?**

The quantified visual field scores from the Friedmann charts (as detailed in Methods section 2.2.3) were plotted against SBR values. An SBR value of zero indicates perfect balance in the brightness sensitivity of the compared regions, whereas a visual field ratio of zero indicates equal visual detection of the Friedmann test stimulus in the compared regions. Regression analysis was applied, although since only 5 points are available for each patient, the results will be interpreted with due caution.

There was no statistically significant linear relationship between SBRs and the visual field ratios in 11 patients (1-g, 2-g, 3-g, 5-g, 6-g, 9-g, 10-g, 11-g, 15-g, 16-g and 17-g) ( $R^2 < 61\%$ ,  $P > 0.1$ ). Although the best fit lines had  $R^2$  values greater than 50% in 3 cases, the significance of the regression is low. An example of one of these results is shown in Figure 3.2-7 with the SBRs at the top. The Figure shows a tendency towards greater sensitivity in the lower field of both right and left eyes with respect to the upper field; the temporal field of the right eye with respect to the nasal field; the nasal field of the left eye with respect to the temporal field; and the right eye with respect to the left eye. All 5 mean SBRs are within normal limits. The middle part of the Figure shows the patient's Friedmann visual field plots, indicating defects which include those in the upper half of both eyes and the temporal part of the left eye. The range of visual field loss ratio extends from  $-300\%$  to  $-18\%$ , which compares with a SBR range of  $-64\%$  to  $+45\%$ . At the bottom of the Figure is the plot of the relationship between these two sets of data. The data can be reasonably well described by the best-fit line, hence  $R^2 = 64\%$ ; however the high  $P$  value of 0.1 indicates that the relationship is not statistically significant.

The relationship for one set of data was statistically significant (7-g) ( $R^2 = 92\%$ ,  $P = 0.01$ ). These data are shown in Figure 3.2-8. There is a semblance of a correlation between SBR and visual field ratio due to 3 values close to zero for both, together with the default value of  $-700\%$  (procedure described in Methods section 2.2.2).

The data for 2 patients were unsuitable for regression analysis because all 5 ratios of conventional visual field regions were zero, as there was no visual field loss in each of the test regions (4-g and 12-g). These results, therefore, do not provide a range against which to compare SBR and so no regression analysis can be performed or statistics supplied. For the purposes of analysis, therefore, these are marked as 'yes' with asterisks on Table 3.2-2 because there is agreement between normal fields and SBRs close to zero. An example of one of these is shown in Figure 3.2-9 for patient 12-g.

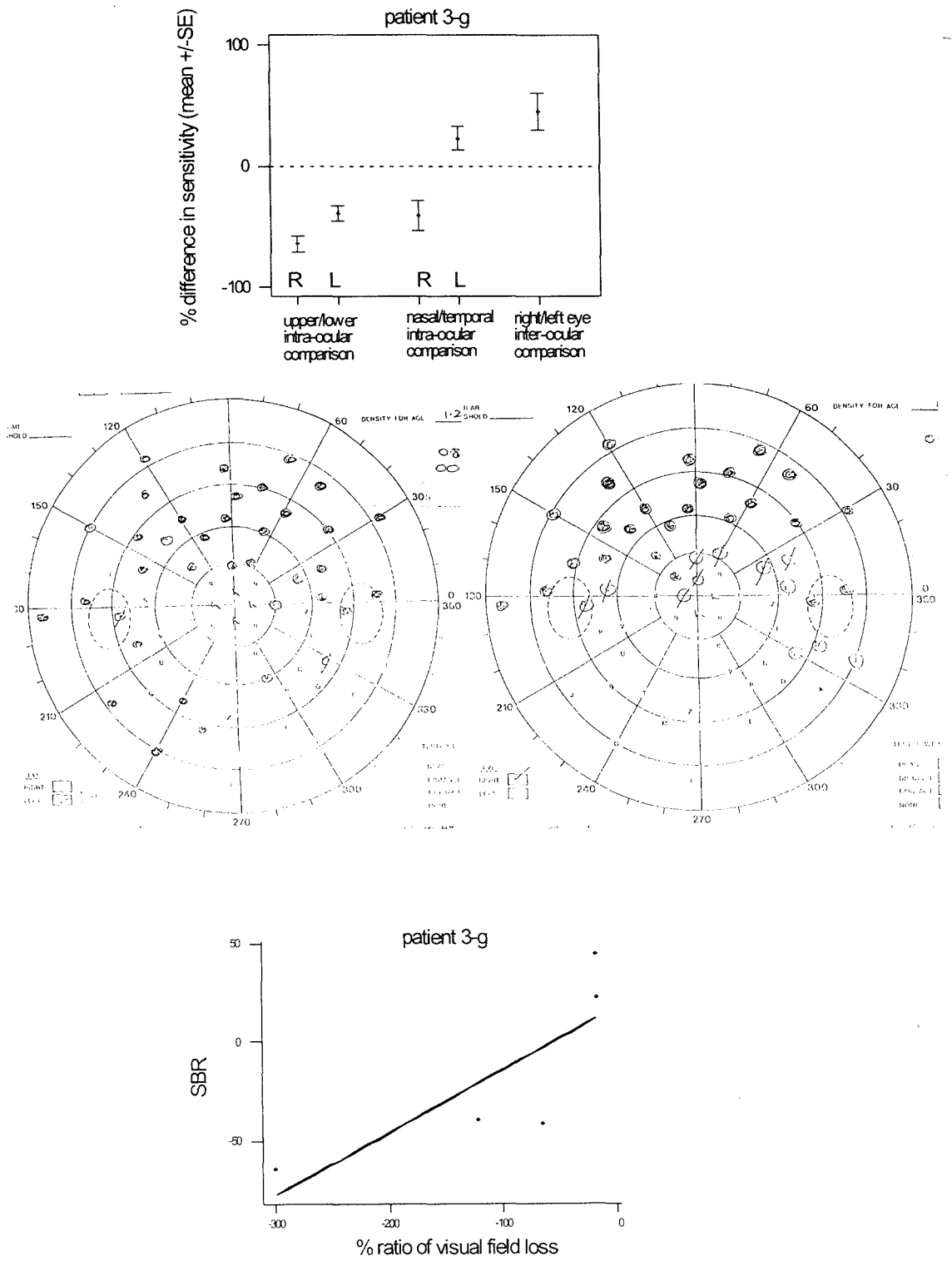


Figure 3.2-7 Top: mean SBR  $\pm$  SE for each of the 5 tests. Middle: Friedmann visual fields. Bottom: regression plot of mean SBR plotted against the ratio of visual fields (%), regression equation is:  $y = 17 + 0.3x$ ,  $R^2 = 63\%$ ,  $P = 0.1$ , for patient 3-g – a 73 year old male with POAG in both eyes.

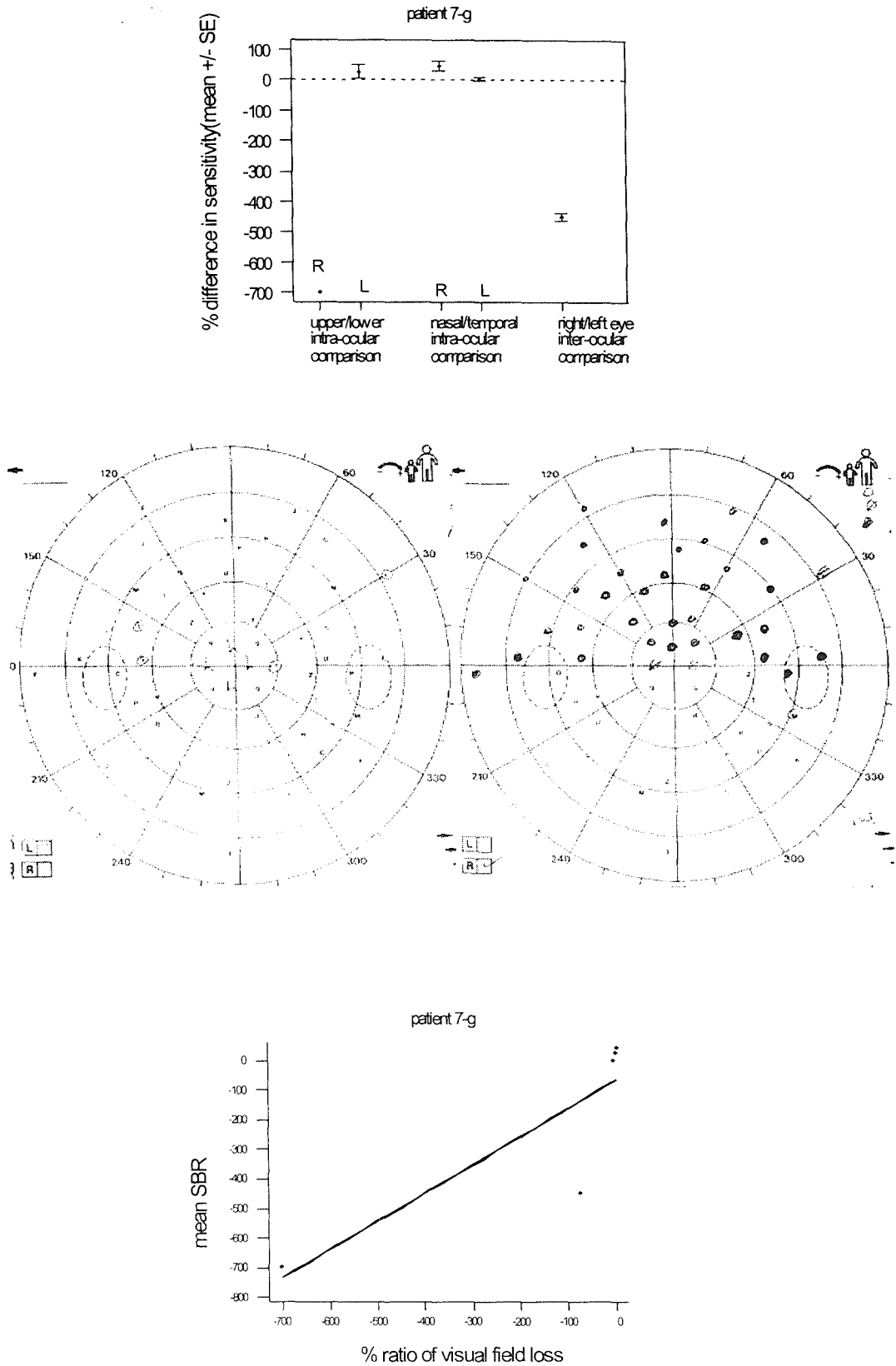


Figure 3.2-8 Top: mean SBR  $\pm$  SE for each of the 5 tests. Middle: Friedmann visual fields. Bottom: regression plot of mean SBR plotted against the ratio of visual fields (%), regression equation is:  $y = -34 + 2.5x$ ,  $R^2 = 92\%$ ,  $P = 0.01$ , for patient 7-g -- an 83 year old male with glaucoma in both eyes. N.B. this graph includes default SBR and VF loss values of -700% for area of total visual field loss.

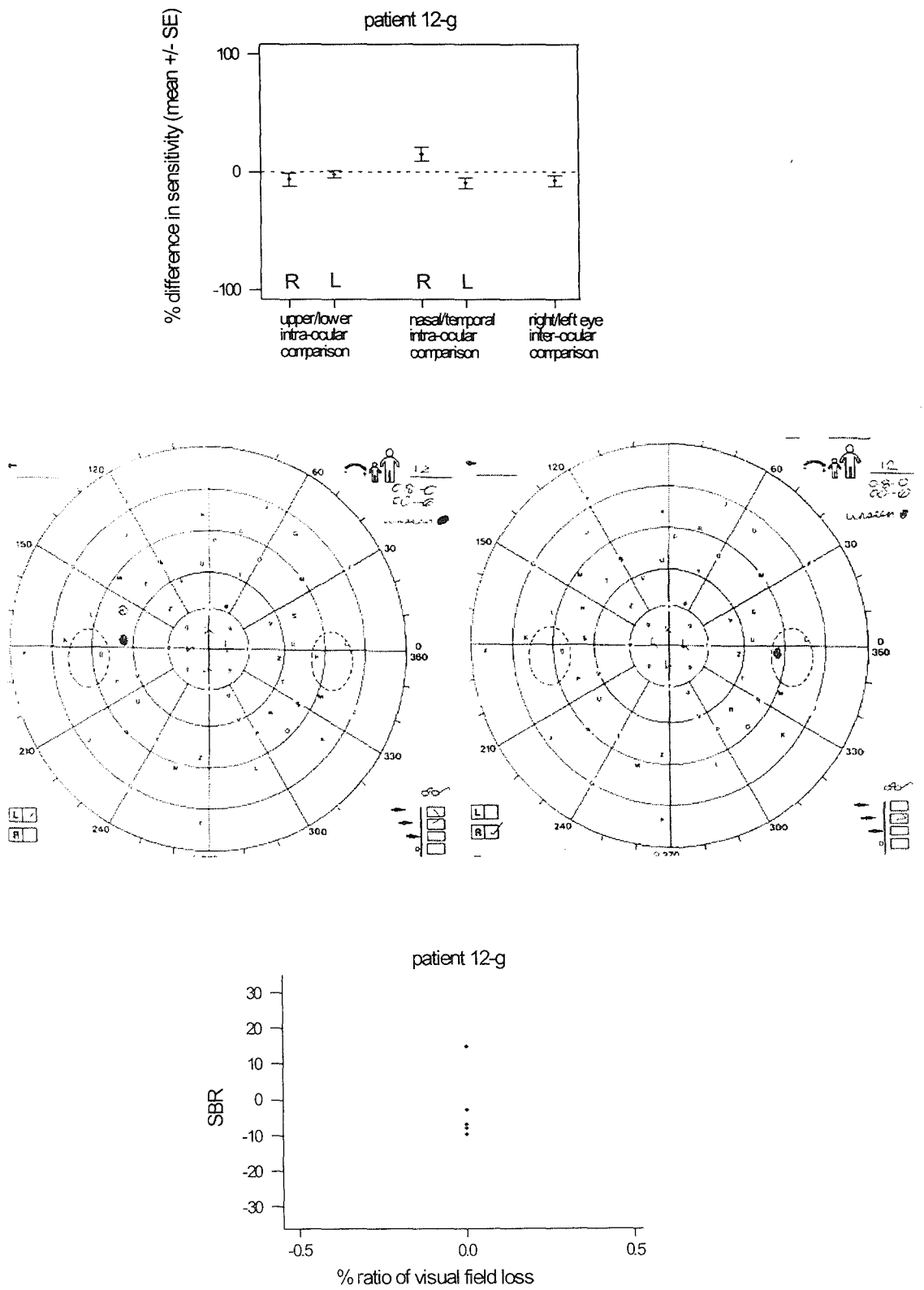


Figure 3.2-9 Top: mean SBR  $\pm$  SE for each of the 5 tests. Middle: Friedmann visual fields. Bottom: mean SBRs plotted against ratio of visual fields (%) of related areas from visual fields, data not suitable for regression analysis, for patient 12-g -- a 70 year old male with OHT in both eyes.

## GROUP SUMMARY

As the previous Figures show there is some evidence for a few different types of relationships between SBR and conventional measures of visual field loss in this group of patients, with the majority indicating a lack of correlation between the two measures overall. The results are summarised in Table 3.2-2, where the right-hand column indicates the patients for whom there was a positive, significant relationship between mean contrast threshold readings and visual field loss or those for whom there was no significant relationship. The centre column indicates the number of SBR tests which were identified as being abnormal.

*Table 3.2-2 Patient group's normal and abnormal SBRs, and whether relationship between SBRs and visual field is positive ( $P < 0.05$ ) or negative ( $P > 0.05$ ).*

<b>GLAUCOMA PATIENT IDENTIFIER</b>	<b>ABNORMAL SBRs</b>	<b>CORRELATION BETWEEN MEAN SBR AND VISUAL FIELDS</b>
1-g	0	no
2-g	0	no
3-g	0	no
4-g	0	yes*
5-g	1	no
6-g	1	no
7-g	2	yes
9-g	0	no
10-g	1	no
11-g	0	no
12-g	0	yes*
15-g	0	no
16-g	0	no
17-g	1	no

### Symbols used in Table

- 0-2 = number of mean SBRs outwith normal limit  
 \* = not appropriate for regression analysis

To further explore these relationships and discover if there were any common features of the patients whose results were described by each type of relationship, the ratio of field loss in each test region (as measured by the Friedmann analyser) was calculated, using the quantified visual field loss values. The modulus of the values for visual field loss ratio was averaged for each patient. Patient's field loss ratio was then placed into one of the following groups: none, mild if the visual field loss ratio was less than 33%; moderate if between 34 and 66% and severe if greater than 67%. Only one field ratio fell close to the boundary of two categories, the right / left eye ratio for patient 15-g, which was 33% and is recorded as mild, all others were clearly within one category. The severity of these ratios for all patients who completed the SBR experiments are shown in Table 3.2-3 with the visual health status of each eye.

Table 3.2-3 Visual health and the severity of the imbalance in ratio of visual field loss (as measured by the Friedmann visual field analyser) in paired regions relating to SBR tests of all patients who completed the SBR experiments (i.e. not 8-g, 13-g or 14-g), patient 10-g did not complete the inter-ocular test (R/L).

GLAUCOMA ID	VISUAL HEALTH		RANGE OF SEVERITY OF FIELD LOSS RATIOS				
	LEFT EYE	RIGHT EYE	RIGHT EYE		LEFT EYE		R/L
			U/L	N/T	U/L	N/T	
1-g	G	G	None	None	Mild	Severe	Moderate
2-g	RD	LTG	Mild	Mild	None	None	None
3-g	G	G	Severe	Moderate	Severe	Mild	Mild
4-g	G	G	None	None	None	None	None
5-g	G	<b>LTG</b>	Severe	Severe	None	None	<b>Severe</b>
6-g	G	<b>G</b>	Severe	Mild	None	None	<b>Moderate</b>
7-g	G	<b>G</b>	<b>Severe</b>	Mild	None	None	<b>Severe</b>
9-g	G	Normal	None	None	None	None	Mild
10-g	<b>Normal</b>	<b>G</b>	<b>Severe</b>	<b>Moderate</b>	None	None	Severe*
11-g	G	Normal	None	None	Severe	Mild	Mild
12-g	OHT	OHT	None	None	None	None	None
15-g	G	Normal	Severe	None	None	Severe	Mild
16-g	G	G	Moderate	None	Mild	Moderate	Severe
17-g	G	Normal	severe	None	none	Moderate	<b>Severe</b>

Abbreviations and symbols used in Table

- G = glaucoma
- LTG = low tension glaucoma
- N/T = nasal / temporal regions compared
- OHT = ocular hypertension
- RD = retinal detachment
- R/L = central regions of right and left eyes compared
- U/L = upper / lower regions compared

\* = this patient did not complete the corresponding SBR test, due to the inability to centrally fixate

**bold** = this indicates the corresponding SBRs which were abnormal

As indicated previously, there was a statistically significant relationship between SBR and the percentage visual field loss ratio of in 1 of the 14 patients who completed the tests and agreement between levels in 2 others (7-g, 4-g, 12-g respectively). In the latter 2 patients, little is gained from the SBRs or visual field ratios, which are all zero. In the former patient, there is a range of field loss ratio between none and severe. In the remaining patients although the abnormal SBRs did all occur in patients for whom there was at least moderate imbalance in the visual field loss ratio, there were 18 other incidences where a normal SBR was produced in spite of moderate or severe imbalance in the visual field loss as measured by the Friedmann.

### 3.2.5 Young control group subject details

A young control group comprising the 20 subjects described in Results section 3.1.2.5 completed the SBR tests.

### 3.2.6 Young control group SBR determinations

The mean values  $\pm$  SE for the percentage difference in sensitivity in the compared areas were plotted for each subject: 4 examples illustrating different types of results are shown in Figure 3.2-10.

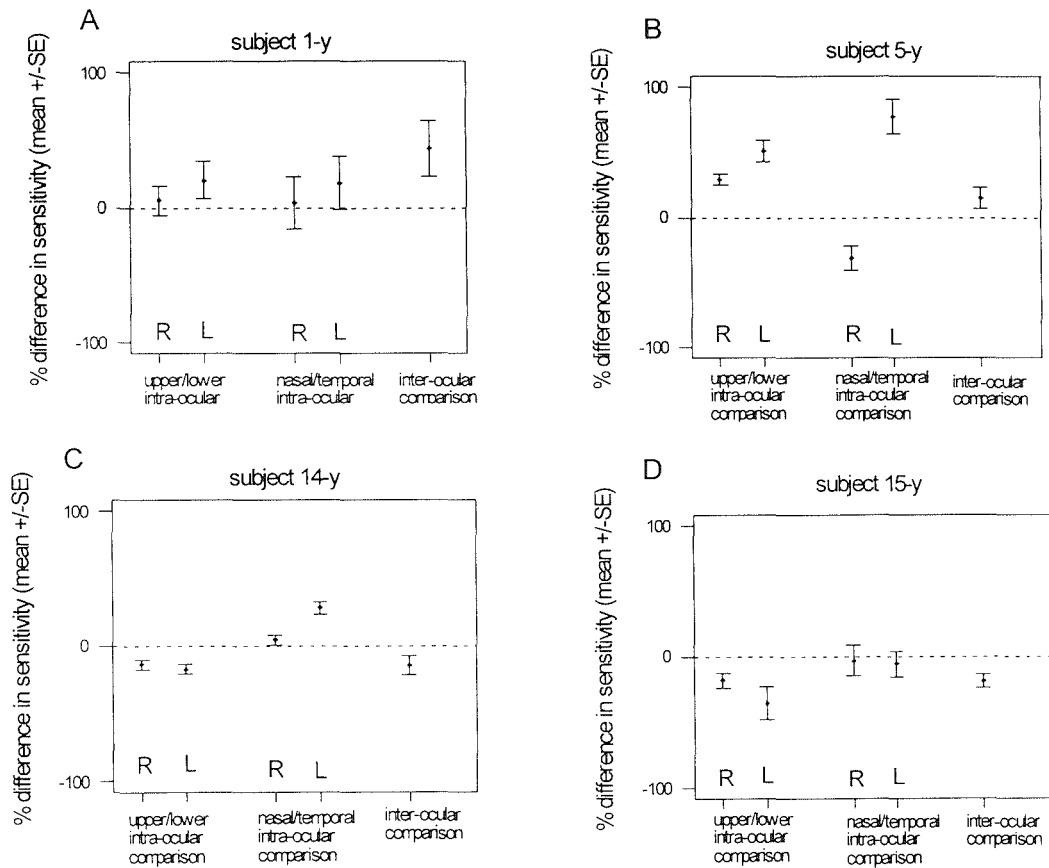


Figure 3.2-10 Four individual examples of mean SBRs  $\pm$  SE for upper / lower and nasal / temporal intra-ocular comparisons, and central inter-ocular comparisons in young control subjects. A: 1-y, 24 year old female, B: 5-y, 27 year old female, C: 14-y, 29 year old male, D: 15-y, 27 year old female, R = right eye, L = left eye.

In subject 1-y, the SBR indicated a more sensitive upper field in the right and left eyes by 5% and 20%, respectively, a more sensitive nasal field in the right and left eyes by 3% and 18%, respectively and for the central field the right eye was more sensitive than the left eye by 43%.

In subject 5-y, the SBR indicated that the upper field was more sensitive in the right and left eyes by 30% and 51%, respectively, the temporal field was more sensitive in the right eye by 31% and the nasal more sensitive in the left eye by 77%. The central field was more sensitive in the right eye by 15%.

In subject 14-y, the SBR indicated that the lower field was more sensitive in right and left eyes by 14 and 18%, respectively, the nasal field was more sensitive in the right and left eyes by 4 and 28%, respectively, and that the central field was more sensitive in the left eye by 15%.

In subject 15-y, the SBR indicated that the lower field was more sensitive in the right and left eyes by 18 and 35%, respectively, the temporal field was more sensitive in the right and left eyes by 3% and 6% and that the central field was more sensitive in the left eye by 19%.

As with the older control group, to give an overview of the range of values obtained for each test in young control subjects, the mean SBR values for each subject were plotted on 5 separate graphs – one for each different test (Figure 3.2-11).

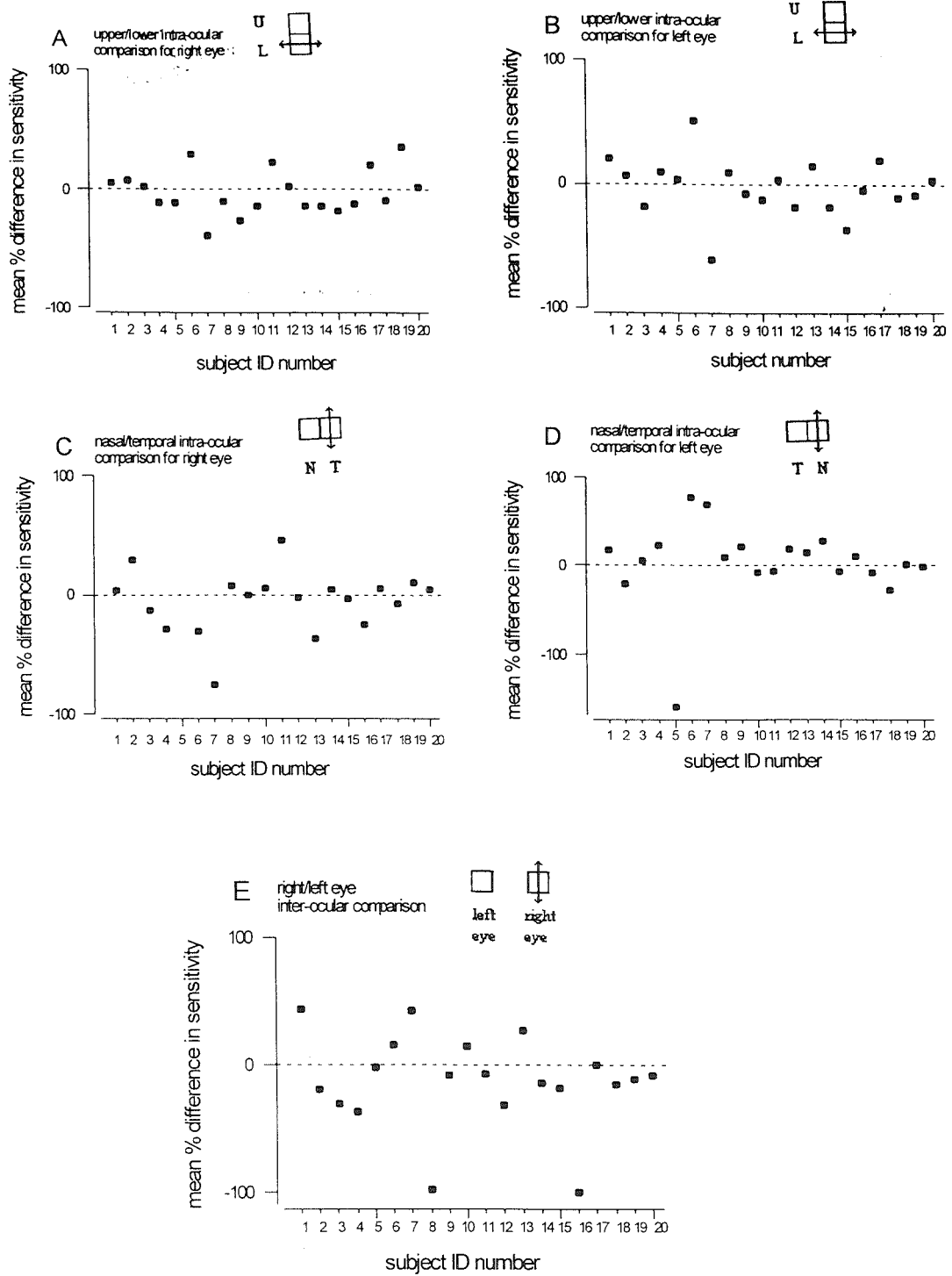


Figure 3.2-11 Mean SBR values for young control group by test, A: upper / lower right eye, B: upper / lower left eye, C: nasal / temporal right eye, D: nasal / temporal left eye, E: right / left eye inter-ocular. N.B. The y-axis scale is extended on graph D to include an outlying point.

The range of mean SBRs for each test for young visually normal subjects were as follows: upper / lower right: -38.0% to +35.0%; upper / lower left: -60.2% to +51.1%; nasal / temporal right: -75.6% to +45.9%; nasal / temporal left: -161.0% to +77.5%; and right / left eye inter-ocular: -100.9% to +43.2%.

From the results shown in Figure 3.2-11, the mean SBR  $\pm$  one SE was then calculated for each of the compared areas for all young visually normal subjects and plotted in Figure 3.2-12.

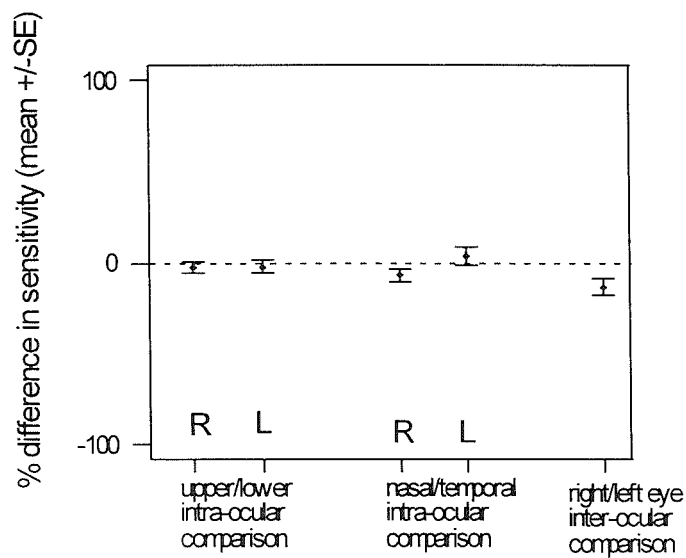


Figure 3.2-12 Mean SBR  $\pm$  SE for young control group, R = right eye, L= left eye.

In the group as a whole the SBR indicated a more sensitive lower field in the right eye by 3%, and in the left eye by 2%. The temporal field was shown to be more sensitive in the right eye by 7% and the nasal field was more sensitive in the left eye by 3%. The left central field was more sensitive than the right by 13%. All SBR determinations for these 20 young subjects were used to calculate prediction limits for normal (mean  $\pm$  2 SD) as shown in Table 3.2.4. The prediction limits were used to compare to those obtained with the older control group data. As for the older control group, one-sample t-tests were used to determine whether the mean values for the group were statistically significantly different from zero, *P*-values are shown in the Table.

Table 3.2-4 Mean SBR values for young control group with prediction limits and P-values for difference between mean and zero using one-sample t-test.

TEST PERFORMED			MEAN (%)	PREDICTION LIMITS: MEAN ± 2 SD (%)	P-VALUE, ONE-SAMPLE T-TEST
Upper / lower	Right Eye	U L	-2.8	-68.8 to +74.4	0.5
	Left Eye	U L	-2.1	-86.5 to +82.3	0.6
Nasal / temporal	Right Eye	N T	-7.1	-92.1 to +77.9	0.3
	Left Eye	T N	3.4	-113.4 to +120.2	0.8
Right / left eye		left eye right eye	-13.4	-110.8 to +84.0	0.1

The prediction limits obtained using the young control group data were wider than those obtained using the older control group data. This was particularly so for nasal / temporal intra-ocular comparisons (right eye: -92% to +78% compared with -76% to +60%; left eye: -113% to +120% compared with -81% to +94%) and also the inter-ocular comparison (-111% to +84% compared with -70% to +75%). The older control group data can be seen in more detail in Table 5.4-1 of the Appendix.

### 3.2.6.1 Comparison with older control group

All SBR values were plotted for each test for the young and older control groups (Figure 3.2-13).

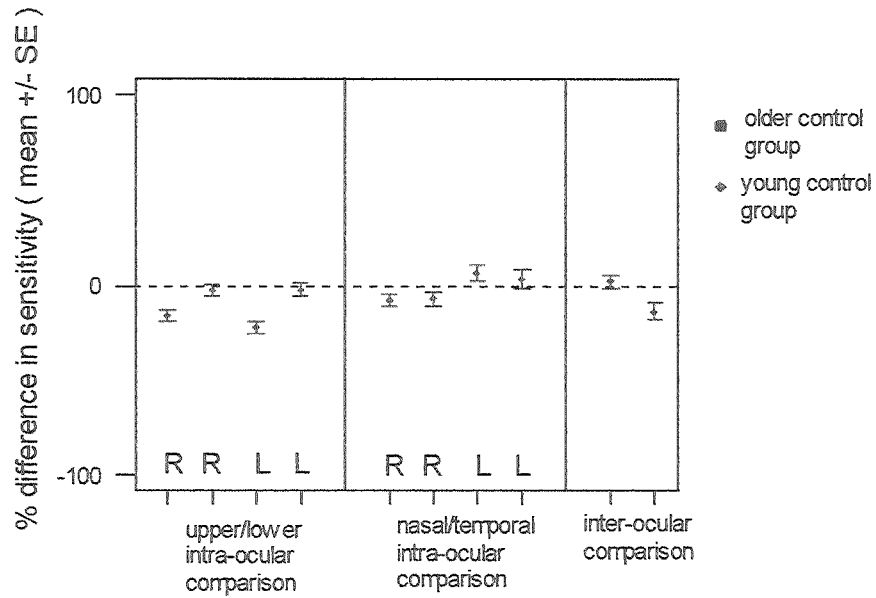


Figure 3.2-13 Mean SBR  $\pm$ SE for both young and older control groups for each test, R = right eye, L = left eye.

The mean SBR for each test and all subjects in the two groups were compared by two-sample t-test. This revealed that for there was no significant difference between the two groups in 4 of the 5 tests completed ( $P > 0.1$ ). In the upper / lower SBR for the left eye, the older control group had a greater imbalance, in favour of the lower field by 14% compared to the young control group of 1% ( $P = 0.008$ , two-sample t-test).

### 3.2.7 Older control group (abnormal eyes) SBR determinations

#### SUBJECT 2-N

SBRs were plotted for subject 2-n (70 year old female) who had retinal scarring which caused an area of scotoma in the temporal region of her left visual field (i.e. nasal retina), as revealed in her Humphrey fields as an area of scotoma (see Appendix, Figure 5.2-2). Mean SBRs  $\pm$  SE are shown in Figure 3.2-14.

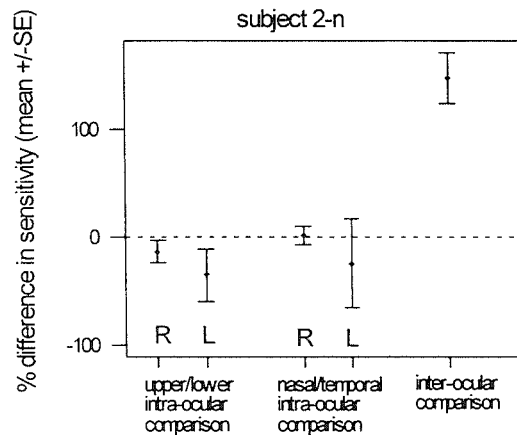


Figure 3.2-14 Mean SBR  $\pm$  SE for subject 2-n (70 year old female with retinal scarring in her left eye) R = right eye, L = left eye.

The intra-ocular SBRs for the left eye had a larger spread of data than for the right eye, indicated by the error bars on Figure 3.2-14. The lower field was more sensitive in the right eye by 13% and in the left eye by 35%. The nasal field was more sensitive in the right eye by 1% and the temporal field was more sensitive in the left eye by 24%. These mean values were comfortably within normal limits, however, the inter-ocular SBR for this subject was clearly outwith the normal limit of  $-70.6\%$  to  $+74.8\%$  with her right eye being more sensitive than the left by 148%. This subject's Humphrey Visual Field Plot (Figure 5.2-2) also revealed an abnormally low MD and an abnormal glaucoma hemifield test in the left eye.

**SUBJECT 6-N**

SBRs were plotted for subject 6-n (63 year old male) who has received surgery for retinal detachment in his right eye (Figure 3.2-15).

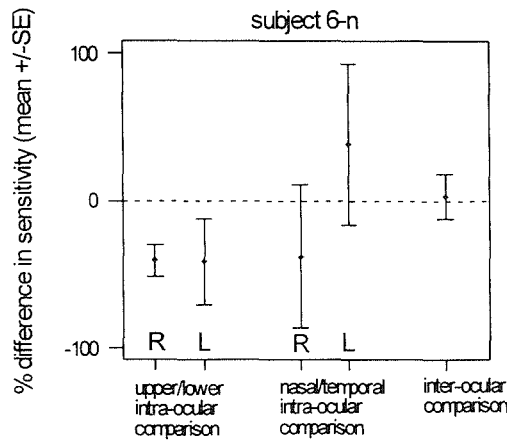


Figure 3.2-15 Mean SBR ± SE for subject 6-n (63 year old male with retinal detachment in right eye), R = right eye, L= left eye.

The SBRs indicated that the lower field was more sensitive in the right eye by 41%, and in the left eye by 42%. The temporal field was more sensitive in the right eye by 38% and the nasal field was more sensitive in the left eye by 38%. The central field was more sensitive in the right eye by 2%. Mean SBRs for all 5 tests which were well within normal limits (it is notable that the inter-ocular SBR was particularly well balanced). However, the spread of all SBRs is unusually large. During the experiment, the subject had reported considerable lack of confidence over the end-point when matching the brightness of the stimuli. The subject's Humphrey visual field plots (Figure 5.2-6) are normal apart from an abnormally low MD in the right eye.

**SUBJECT 7-N**

SBRs were plotted for subject 7-n (69 year old female) who had a mild cataract in her left eye (Figure 3.2-16).

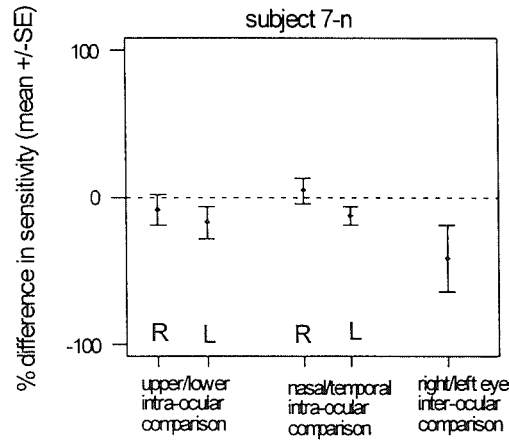


Figure 3.2-16 Mean SBR  $\pm$  SE for subject 7-n (a 69 year old female with mild cataract in her left eye), R = right eye, L = left eye.

The SBRs indicated that the lower field was more sensitive in the right eye by 9% and in the left eye by 17%. The nasal field was more sensitive in the right eye by 4% and the temporal field was more sensitive in the left eye by 13%. The central field was more sensitive in the left eye by 41%. Hence, mean SBRs for all 5 tests were well within normal limits, suggesting that the cataract has not adversely affected the retinal sensitivity to brightness. The subject's Humphrey visual field plots (Figure 5.2-7) indicate a normal right eye, but an abnormally low MD in the left eye with no apparent blind spot and an abnormal glaucoma hemifield test also in the left eye.

**SUBJECT 9-N**

SBRs were plotted for subject 9-n (76 year old male) who had poor vision affecting his right eye (Figure 3.2-17).

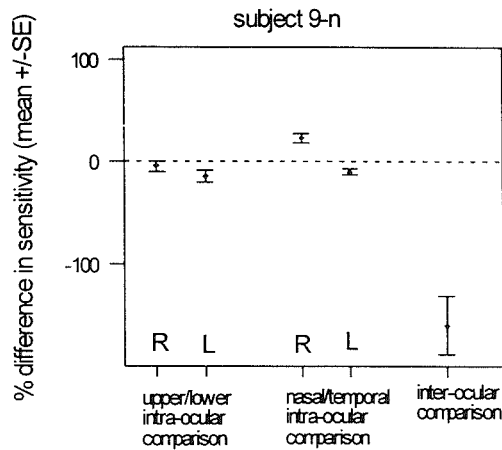


Figure 3.2-17 Mean SBR ± SE for subject 9-n (76 year old male with poor vision in his right eye), R = right eye, L = left eye.

The lower field was more sensitive in the right eye by 4%, and in the left eye by 14%. The nasal field was more sensitive in the right eye by 23% and the temporal field was more sensitive in the left eye by 10%. These are all comfortably within normal limits. However, the inter-ocular SBR for this subject was clearly out with the normal prediction limits of -70.6% to +74.8%: his left eye being more sensitive than the right by 160%. The subject's Humphrey visual field plots are shown in the Appendix Figure 5.1-9. As with the contrast threshold results, the SBR results for this subject do not show any evidence to support the apparent defect in the superior field of the subject's left eye detected by the Humphrey plot which led to an abnormally low MD and an abnormal glaucoma hemifield test.

**SUBJECT 15-N**

SBRs are plotted for subject 15-n (73 year old female) who had a macular hole (Figure 3.2-18). The subject was able to complete the SBRs in her right eye using peripheral vision to locate and steady her fixation. She could not however, maintain an accurate gaze for inter-ocular comparisons.

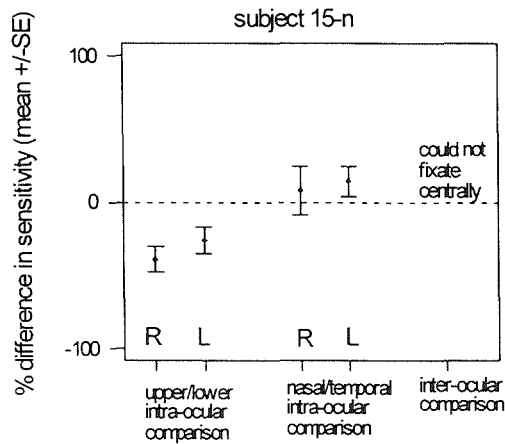


Figure 3.2-18 Mean SBR ± SE for subject 15-n (73 year old female with a macular hole in her right eye), R = right eye, L = left eye.

The lower field was more sensitive in the right eye by 39%, and in the left eye by 26%. The nasal field was more sensitive in the right eye by 8% and in the left eye by 14%. The mean SBRs were within normal limits for all 4 tests. The Humphrey visual field plot for this subject's left eye is shown in Figure 5.2-14 of the Appendix and is normal.

**SUBJECT 23-N**

SBRs are plotted for subject 23-n (59 year old female) who had amblyopia in her right eye due to a “lazy” eye in childhood (Figure 3.2-19).

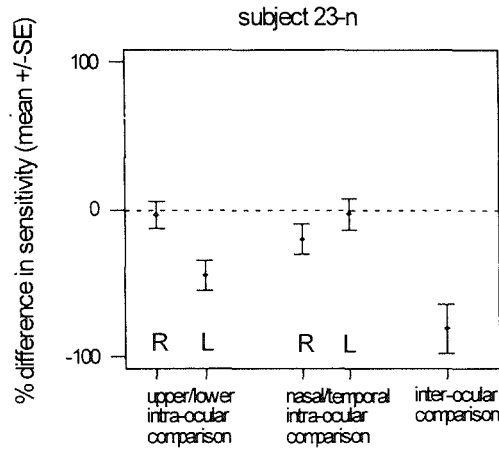


Figure 3.2-19 Mean SBR ± SE for subject 23-n (59 year old female with amblyopia in her right eye), R = right eye, L = left eye.

The lower field was more sensitive in the right eye by 3% and in the left eye by 45%. The temporal field was more sensitive in the right eye by 20% and in the left eye by 3%. The mean SBRs were all therefore within normal prediction limits. However, the inter-ocular comparison indicated that the left eye was more sensitive than the right eye by 81%, which is outwith the limit for normal. The Humphrey visual field plots are shown in Figure 5.2-22 of the Appendix, and in both eyes there was a low MD, in the right eye there was also an abnormal glaucoma hemifield test.

**SUMMARY**

In this small group, therefore, it appears that inter-ocular SBR testing has successfully identified abnormalities in 3 of the these 5 subjects who each had one visually abnormal eye and one normal eye. In all 3 cases the more sensitive eye indicated by the SBR was the normal one. Although some of the intra-ocular SBRs appeared unusual with a larger standard errors than most visually normal eyes' results, there were no mean SBRs which exceeded the normal limits.

## **4 Discussion**

By undertaking this project we aimed to develop and validate a form of visual field assessment, which would go some way to meeting the needs created by shortfalls in current methods, used in the diagnosis of glaucoma. A major proportion of the work involved devising the most useful form of the two tests investigated. First, contrast threshold measurements, which targeted peripheral retina and second, simultaneous brightness ratios (SBR) measurements, which targeted central and paracentral retina. Once the optimal format for each was established, testing was undertaken on a group of patients attending the glaucoma clinic at Gartnavel General Hospital, a group of visually normal age-matched controls and a group of visually normal controls of a younger age. Of the age-matched control group, 6 subjects also had a visually abnormal eye, not affected by glaucoma.

### **4.1 Contrast thresholds**

#### ***4.1.1 Concentric ring pattern***

The image was presented in the Maxwellian view as this creates the possibility of generating a large field that is independent of refraction. Initially (as described in Methods section 2.1.2.1) we presented a green, stationary concentric pattern of rings to subjects with the intention of testing the contrast threshold of increasingly peripheral regions of the retina, which may be important in glaucoma. This, however, proved to be impracticable since the contrast threshold values were always dominated by the sensitivity of the central region of retina.

Following a series of experiments using the concentric ring pattern (cf. Methods section 2.1.2.2), it also became apparent from subjects' feedback that the combination of bold rings, with additional fine rings, created some uncertainty in the detection of the image. This occurred since the two components of the image became visible at different levels of contrast, i.e. the fine rings appeared at lower contrast than the bold ones but were harder to resolve.

Exploration of the optimal colour of the image led to the use of a red laser for comparison with the contrast threshold results in response to the image created by the green laser (cf. Methods sections 2.1.2.4 and 2.1.2.5). Despite the fact that the green and red displays were matched to be at equivalent amounts above photopic threshold, the contrast thresholds in response to the green display were lower than those obtained in response to the red display. Subjects also reported a distinct preference for the green image. The differences in the contrast thresholds may be a reflection of more numerous packing of green cone photoreceptors in the retina, which constitute 60% of the total number as opposed to the less numerous red cones, which constitute 35% of the total number (Marc and Sperling, 1977). As the intensities were made photopically equal, using filters to determine equal levels of threshold, the luminance advantage of the greater absolute number of cones had been removed. Therefore it would appear that the only factor to account for the results is the more dense packing of photoreceptors which has aided better resolution of the green grating pattern.

#### **4.1.2 Stationary versus flickering grating pattern**

Previous work published on contrast sensitivity using laser interference grating patterns did not involve flickering stimuli (Isayama *et al.*, 1980; Tagami *et al.*, 1981; Motolko and Phelps, 1984); therefore to the best of the author's knowledge the generation of a flickering pattern using a laser as a light source without a luminance flicker has not previously been described.

Three methods of generating flicker were tested: a rotating mirror / polarizer, a solid-vane windmill and a diffuser windmill (the methods are described in section 2.1.2.6 and the results in section 3.1.1). When using the rotating mirror / polarizer, both increased and decreased contrast threshold were revealed in different subjects (cf. Figure 3.1-1). In the solid-vane windmill, again both increases and decreases in contrast threshold in response to flicker were recorded, as well as one experiment in which there was no change (cf. Figure 3.1-2). Finally, with the diffuser windmill (which was the method to induce flicker with the least amount of luminance flicker), lower thresholds were obtained in response to the stationary pattern in all subjects (cf. Figure 3.1-3). This has also been confirmed in separate experiments involving central viewing of a low spatial frequency grating pattern (Morrison, personal communication, 2001).

These results were unexpected because there is a considerable body of evidence which indicates that moving gratings are detected with lower contrast (Westheimer, in Moses and Hart, 1987). Our findings with the laser interferometer, therefore, contrast with the more predictable results described previously by authors using CRT displays who showed that flicker of the pattern induces a lower contrast threshold (Lundh, Lennerstrand and Derefeldt, 1983).

This is understandable on the basis that a flickering image selectively stimulates magnocellular ganglion cells, which are more sensitive to temporal modulation than parvocellular ganglion cells. The results may be due to the fact that stimulation of more peripheral parts of the retina leads to a leftwards shift of the contrast sensitivity function. For direct viewing, the contrast sensitivity function peak is at 3 c/deg, but at a nominal eccentricity of 12° used in the paper, the peak is between 0.75 and 1 c/deg (Kelly, 1984). In this paper, there was no difference in the contrast threshold in response to 1 c/deg between temporal modulation at 0.5Hz and at 10Hz, unlike for central viewing when the contrast threshold is much reduced for the faster temporal modulation (Kelly, 1984). The leftwards shift of the contrast sensitivity function has another consequence in that the contrast threshold in response to 2 c/deg at a peripheral location is elevated compared with that for central viewing. For laser interferometric sinusoidal patterns, the contrast sensitivity at 16° eccentricity is over 40% lower than for central viewing. The difference actually becomes smaller as the field size becomes larger (Hilz and Cavonius, 1974). Therefore, for central viewing, temporal modulation increases contrast sensitivity at low spatial frequencies up to 5 or 6 c/deg (Tolhurst, 1973). Due to the leftward shift of the contrast sensitivity function for the adoption of more peripheral locations, contrast sensitivity measurements taken in response to a pattern of one c/deg effectively means that the point at which temporal modulation has a facilitatory effect on the detection of the grating pattern is exceeded.

All the methods we used to produce flicker in the laser generated interference pattern, unavoidably, had a luminance flicker component in addition to a pattern flicker which can be avoided using CRT displays. However, the effect of this additional flicker stimulus is not clear, as it may have been expected that it would enhance the visibility of the pattern and thus produce lower thresholds, rather than higher ones. Additionally it is thought that the variation in the display may have generated stimuli of inconsistent quality, which would therefore elicit different responses in subjects during each experiment. One cannot also rule out that different subjects interpreted the instructions differently and therefore used different cues to determine the point of threshold.

Although admittedly it is difficult to draw conclusions from these experiments due to the small number completed on each flicker method. One of the studies previously mentioned, showed that a grating pattern presented as a stationary stimulus was more useful than a flickering one in identifying glaucomatous damage in patients (Ross, Bron, and Clarke, 1984), and since subjects tended to prefer it, the use of the flickering stimulus was discontinued in favour of the more readily identifiable stationary grating pattern.

### **4.1.3 Final protocol**

Previous work has, almost exclusively, involved presenting a grating pattern to central or peripheral regions of retina in small squares or circles of around  $5^\circ$  in diameter (see Table 1.6-1). Since there is a well-established pattern of common visual field defects in glaucoma (Aulhorn and Karmeyer, 1977), it was reasoned that new and useful information might be obtained about glaucomatous retinae if the pattern could be targeted at such areas, i.e. the arcuate region. Furthermore, there is widespread support for the concept of selectively testing the sensitivity of one population of ganglion cells in order to identify early glaucoma, detailed in Introduction sections 1.4.3.2 and 1.4.3.3, albeit some dispute over the most appropriate population to choose. This theory of reduced redundancy (attributed to Glovinsky *et al.*, 1991 and developed by Johnson, 1994), suggests that the earliest diagnosis of glaucoma may arise from the measurement of the deterioration of specific aspects of visual sensitivity which can be attributed to just one type of ganglion cell, assuming that that particular type of ganglion cell is the first to be adversely affected by the disease process. This would work equally well if the targeted cell type were affected specifically at the earliest stages, as some authors suggest with regard to the parasol (magnocellular) ganglion cell population, or if the targeted cell type was one of a group of cell types affected early. The difference in these scenarios would remain that the patient's overall visual function would be more likely to be noticeably damaged in the latter case where several types of ganglion cell were lost in the early stages. However, the diagnostic procedure followed would not change. It would remain desirable to identify a test which could allow observation of the subtle early changes in visual sensitivity as the first ganglion cells are beginning to be lost. Clearly problems would arise if there were indeed a selective loss of a specific type of ganglion cell, and the targeted type was among the last to be damaged. In this case, clearly such a test would be ineffective for the purposes of the initial identification of glaucoma.

With this in mind, the characteristics chosen for our test were that of a low spatial frequency grating pattern targeted at peripheral retina which may preferentially stimulate the parasol (magnocellular) ganglion cell population, particularly when viewed at low contrast. It was reasoned that a test, which did target one specific type of ganglion cell would be appropriate and after reviewing the evidence it was clear that even if the parasol ganglion cells are not selectively lost in the glaucomatous process, then they are likely to be at least among those lost early.

In summary, therefore, a stationary, green, vertical sinusoidal grating of one c/deg was presented in truncated quadrants extending from 10 to 20° radius.

#### **4.1.3.1 Older and young control groups**

For visually normal eyes (in both the age-matched and young control groups), the mean contrast threshold was around 0.03 contrast units in both right and left eyes, with no definite consistent pattern of elevated thresholds in a specific quadrant or quadrants (see Figures 3.1-6 and 3.1-19, respectively). Some individuals did show small elevations or depressions, which were interpreted to be 'noise' in the system. The blind spot, which is estimated to occupy about 8% of the area of the quadrant (details of calculation shown in Appendix section 5.3), did not lead to elevated contrast thresholds in the temporal quadrant in the majority of subjects. Of 42 normal eyes in the older control group, 6 showed an elevation in the temporal quadrant, 3 showed a slight elevation, and in 33 there was no elevation. This implies that surrounding retina within that quadrant region may sufficiently compensate for the insensitive region. This should be borne in mind when considering discrete pathological regions of retina: if they are adjacent to fully sensitive areas, the contrast threshold for the region may reflect the most sensitive cells within it, rather than revealing the least sensitive ones.

Although there was no significant difference between the contrast thresholds in the young and older control groups, it is still considered essential to match the control group with the patient group for age. The observed lack of difference may be due to the choice of a low spatial frequency which is not the most sensitive to age-related changes in contrast sensitivity (McGrath and Morrison, 1981). It may also be the case that our group of glaucoma patients and age-matched controls comprised too wide an age range (54 to 90 years and 55 to 81 years, respectively). If the three youngest subjects were excluded from

the older control group for comparison with the young control group, then the difference was still very small, but with the age-matched control group marginally higher at 0.035 contrast units.

It was thought possible that the shape of the quadrant may constitute a different stimulus when presented in its different locations, i.e. in the superior and inferior quadrant, there were shallow gratings which were more numerous than the longer length gratings which appeared in the nasal and temporal quadrants, see Figure 2.1-21. However, in the age-matched control group, the older control group in its entirety, and also the young control group there was no difference in the contrast thresholds to these two sets of quadrants ( $P \geq 0.05$ , ANOVA). Also the number of cycles in both types of stimulus still exceeds the minimum number required before there is an effect of cycle number on contrast threshold (Hoekstra *et al.*, 1973).

### **CONVENTIONAL VISUAL FIELD ANALYSIS FOR THE OLDER CONTROL GROUP**

The results obtained on the Humphrey Visual Field Analyser for the 40 visually normal eyes of the older control group (both eyes of 17 subjects and one eye of 6 subjects) revealed 25 'normal' results and 15 apparent anomalies. All the anomalies were examined by a consultant ophthalmologist and were judged to be unlikely to reflect any underlying visual abnormality. The anomalies included the lack of a blind spot, abnormally high or low sensitivity, and abnormal or questionable glaucoma hemifield test results. The mean deviation was outwith the age-matched normal limit (as judged by the field analyser) in 8 eyes. However, despite these apparent defects all these eyes do appear to be normal suggesting that the Humphrey generates a considerable number (almost 40%) of false positive results for visual defects.

Where one eye was identified as having a defect by the Humphrey analyser (e.g. abnormal MD, abnormal glaucoma hemifield test) in control subjects with two normal eyes, statistical testing revealed no significant difference between the contrast thresholds in any of the 6 individuals ( $P \geq 0.05$ , ANOVA). In the 12 normal eyes in which the glaucoma hemifield test was abnormal or borderline, a significant difference between the contrast thresholds to the superior and inferior quadrants was identified in 3 eyes (the left eye of 8-n, where the contrast thresholds in response to the inferior quadrant were higher than the superior quadrant, and both right and left eyes of 24-n where the reverse was true),

whereas the remaining 9 eyes showed no difference. All these mean contrast thresholds were within the normal prediction limit. In the subjects with abnormally high sensitivity, no distinct blind spot, or an abnormal MD there was no correlation with the contrast threshold results.

#### 4.1.3.2 Glaucoma patient group

With the equipment in its early prototype layout which was quite awkward for some subjects to use, there was a fairly high proportion of the elderly subjects who were unable to finish the test. This led to 4 of the 17 patients recruited to the study being unable to comfortably view the image and control the rotatable polarizer simultaneously. It is feasible that these same patients would have struggled with other visual field analysers, which involve some flexibility and manual dexterity, e.g. the Humphrey Visual Field Analyser, although it is acknowledged that such machines are capable of being adjusted for height etc. In further developments of the apparatus, this would have to be taken into account.

In the patient group, there was considerably more variation in contrast thresholds across the quadrants than in the age-matched control group. With the upper prediction limit for normal defined as mean plus two standard deviations (97.7% confidence limit) using the age-matched control group data (where  $n = 21$ ), 9 of the 13 individuals (69%), in the patient group were identified as having one or more mean contrast threshold above that limit cf. Figure 3.1-10. Of the 4 patients for whom all mean contrast thresholds were within normal limits, one had OHT in both eyes, two had unilateral glaucoma and one had bilateral glaucoma. Excluding the patient with OHT who had no visual field loss, this gives a sensitivity value for contrast threshold testing in this format of 75% (i.e. 9 true positives and 3 false negatives) (equations for calculating sensitivity and specificity are given in Appendix section 5.6).

When analysed by eye, 19 of the 26 eyes in the patient group who completed the contrast threshold experiments had glaucoma (10 with POAG, 2 with LTG, 3 with secondary glaucoma, 2 with narrow angle glaucoma and 2 with glaucoma with pseudo-exfoliation) (Table 3.1-3). Three of these (5-g left eye, 7-g left, 13-g right), however, had no visual field loss recorded during their most recent Friedmann Visual Field test despite glaucoma being recorded in their case notes. These patients have significant cupping of both optic

discs and patient 13-g was known to have had raised IOP in both eyes, (see Appendix Table 5.5-1 for additional details from patients' case notes). As detailed in Table 3.1-3, in the eye without visual field loss in patients 5-g and 13-g, there was one abnormal mean contrast threshold, while all mean contrast thresholds were within the prediction limit for normal in patient 7-g's eye.

The remaining 7 out of the 26 eyes in the patient group did not have glaucoma (including 4 normal eyes, 2 eyes with OHT and one with retinal detachment). Although 2 of the normal eyes (8-g left eye and 15-g right) did record mild field loss on the Friedmann Visual Field Analyser, the deficits were recorded in the temporal and inferior quadrants which indicate that they may not be glaucomatous defects. They may be due to large or unusually placed blind spots which can arise with inaccurate fixation of the patient during the test. The other two visually normal eyes were the right eye of patient 15-g in which there was one abnormal mean contrast threshold, and the right eye of patient 9-g in which all mean contrast thresholds were normal. In patient 12-g, who had OHT in both eyes, there were no abnormal mean contrast thresholds and both visual fields were normal. As with the control subject in the visually abnormal group with retinal detachment (6-n), whose eye did not produce an abnormal contrast threshold reading, the left eye of patient 2-g which was also affected by retinal detachment had contrast threshold readings in the normal range. In patients with unilateral glaucoma, the glaucomatous eye had higher mean contrast thresholds in all 5 patients who completed the experiment. These were all highly statistically significant.

In summary, therefore, a mean contrast threshold above the prediction limit occurred in 13 of the 19 glaucomatous eyes, including 2 of the 3 without field loss as recorded on their most recent Friedmann field plot (Table 3.1-3). All the mean contrast thresholds were below the prediction limit in 6 of the 7 non-glaucomatous eyes including one with apparent mild field loss. In the seventh eye, mean contrast threshold was above the normal prediction limit in one quadrant. Therefore if a true positive is defined as an eye with glaucoma in which one or more mean contrast threshold is above the normal limit, and a false negative as an eye with glaucoma where all mean contrast thresholds are below the normal limit, this gives a sensitivity for the test of 68% (i.e. 13 true positives and 6 false negatives). Accordingly if a true negative is defined as an eye without glaucoma in which all mean contrast thresholds are below the normal limit, and a false positive as an eye without glaucoma in which one or more mean contrast threshold is above the normal limit, this relates to a specificity of 86% (i.e. 6 true negatives and 1 false positive) when analysing the eyes individually rather than each patient as a whole.

It does become increasingly complicated as how to define a positive or negative result (true or otherwise) when one attempts to use the available information for each patient. For example, does one require field defects on the Friedmann to satisfy the definition of 'glaucoma', in which case there are 3 less glaucomatous eyes than stated in their case notes? Or is it enough that a patient has ever had recorded field defects which may be subject to long-term fluctuation or may have improved following surgery or medication, in which case one must examine all previously recorded visual field charts? This would therefore inevitably include anomalous visual field abnormalities which are known to be generated by some field analysers and would give an over estimate of actual visual field loss. Additionally we know that different modalities of visual function do not deteriorate in a fixed sequence for all patients (cf. Introduction section 1.6.3 and Ruben *et al.*, 1994). Conversely is an eye in which mild field losses are recorded in a different quadrant from the blind spot with no other sign of glaucoma really a normal eye, in which case the field analyser must be judged to be inaccurate or at least unhelpful?

Clearly, the patient numbers are small and therefore the significance of these figures remains to be seen if a larger trial were to be conducted. In such a trial, the control population should be increased in order to produce more meaningful prediction limits for normal. Additionally, if a greater number of glaucoma patients were tested more conclusive insights into the relationship between visual field defects and contrast threshold increases may be possible. It has been shown, as summarised in Table 1.6-1, that the measurement of contrast threshold in patients with glaucoma can highlight those who require further investigation in various ways: either with higher than normal contrast threshold readings, or with uneven levels of contrast threshold between eyes. These measures may relate to visual sensitivity as measured conventionally.

### **CONTRAST THRESHOLD VS CONVENTIONAL ANALYSIS OF VISUAL FIELD IN GLAUCOMA PATIENTS**

A further problem is the interpretation of the data for those glaucoma patients whose contrast thresholds fell within the normal range but who showed a positive correlation between contrast threshold and percentage visual field loss. With respect to patient 1-g, for whom there was a relationship between mean contrast threshold and visual field loss ( $R^2 = 79\%$ ,  $P = 0.003$ ) but for whom all contrast thresholds were within normal limits, it is possible that this may be attributable to the adeptness of the patient. In its current format

the mechanism for altering the contrast in the image in combination with the layout of the equipment requires a certain amount of dexterity, which may influence the fineness of the judgement by the patient concerned. Therefore someone very adept might produce very accurate, low values especially when coupled with an acute ability to discriminate the grating pattern. Whereas someone with difficulty in the use of their arm or fingers in actions requiring very fine movements may produce more blunt turns of the polarizer and therefore more variable or higher readings for contrast thresholds. This could be dealt with in practical alterations or additions to future equipment layouts, e.g. a movable optical bench, or a remote control for the polarizer rather than one on top of the table. However, the experience of the individual, and the range of skills should still be considered to be a factor. It is anticipated that the age-matching of the control group and the range of experience in each of the two groups (in each group at least 90% of the subjects were naive to the set up, where the others had experience of the laboratory set up) would balance out the effect of this on the overall results. Therefore, one has to resort to more refined analysis to uncover the significance and meaning of the results. This was done using regression analysis which itself is limited by the need for an adequate spread of data, i.e. there must be a range of visual field losses against which to compare the test data. The limited number of points (i.e.  $n = 8$ ) in each individual experiment puts constraints on the likelihood of a statistical significance. So an individual showing a strong correlation here cannot be dismissed even if all the contrast threshold values fall within the normal prediction limit.

As indicated in Table 3.1-4, when regression analysis was applied to the mean contrast thresholds for each test area against the visual field loss as measured conventionally in each area, there was a statistical significance in 5 patients (1-g, 2-g, 7-g, 8-g, 9-g) (cf. Figure 3.1-11). In the OHT patient (12-g) there was a correlation, reflected in low contrast thresholds and normal visual fields (cf. Figure 3.1-14). In two subjects (5-g, 17-g) there was a statistically borderline correlation (cf. Figure 3.1-13), and in 5 patients there was a complete absence of a relationship between the two measures (cf. Figure 3.1-12).

The concept that the range of the extent of visual field loss within a group may relate to these types of relationship between contrast threshold and conventional visual field was then explored, and it was found that the group with the strongest correlation comprised the widest range of visual field loss, details are in Table 3.1-4. In other words when field loss in the group ranged from none to severe there was a strong correlation between contrast threshold and visual field loss. However when the range of field loss in the group was more limited, e.g. when it varied from mild to moderate there was a poor correlation. This

reflects the conditions for regression analysis, and therefore may be a consequence of statistics rather than a difference in visual field sensitivity.

If we exclude the OHT patient (with normal fields by definition), the contrast threshold test identified abnormal results in two patients' eyes, which appeared normal by the Friedmann visual field analysis (i.e. 5-g left eye, 13-g right eye). At first glance this suggests that contrast threshold testing may have identified visual field abnormalities prior to their detection by conventional machines, or that the perceived recovery of the visual field when measured by the Friedmann was not concealed in the contrast threshold readings. Either way this would imply that contrast threshold testing may be more sensitive to defects of the visual field in glaucoma.

When evaluating contrast threshold as a screening test, the number of false negatives (6) described above creates difficulties and must be more fully explored. It is possible the field defects being measured by the Friedmann were not comparable to the defects identified by the contrast threshold test. It is known that conventional perimeters measure sensitivity to light in a non-specific way, i.e. they identify defects when there is a lack of responsive ganglion cells (of any type) at the location that is being stimulated. Therefore, severe loss (by the categorisation previously used in Table 3.1-4) was identified in a quadrant region where more than 66% of the test locations do not elicit a response. In fact, each truncated quadrant, when applied to the Friedmann visual fields, includes between 8 and 12 test points, as seen in Figure 2.1-22. Therefore if 6 to 8 of these points are missed, the region would be revealed as having severe loss. In contrast threshold testing, the test stimulus, as shown in Figure 2.1-21, is a truncated quadrant shape which stimulates each quarter of the arcuate region simultaneously, therefore it is feasible that 6 to 8 small regions of very poor sensitivity may be compensated for by the remaining 2 to 4 areas which are still responsive to the stimulus. This may need to be evaluated in the choice of the stimulus characteristics of future protocols, i.e. its shape, size and location.

It is necessary to consider whether the Friedmann visual field test is an adequate standard against which to compare the results of a new test. It is simpler than the Humphrey visual field analyser, and this may lead to as many benefits (e.g. less false positives or anomalous results) as drawbacks (less sensitive information). When the Humphrey Analyser was used to test 40 apparently visually normal eyes in the older control group, 15 were identified as abnormal by the glaucoma hemifield test, the lack of a blind spot, or an abnormal MD. Despite being in use for many years, the Humphrey Analyser is still subject to ongoing

development to adjust its sensitivity level, it may be fair, therefore, to assume that the Friedmann analyser was at the least no worse than the Humphrey.

The range of intervals between the recording of the conventional visual field and the completion of the contrast threshold experiments was between a few hours and 22 weeks. It was possible that the lack of a correlation between the two measures were exacerbated by that variation within the group. When the data were examined by eye, it was not, however, the case that the longer the gap (detailed in Methods section 2.1.4), the poorer the correlation between contrast threshold and visual sensitivity as measured by the Friedmann, so the mismatch in the contrast threshold and visual field sensitivity are not attributable to simple linear changes over time. For example in patient 2-g there were 22 weeks between the two tests and yet a positive correlation between the measures. Whereas in patient 16-g the tests were done on the same day and yet there was no correlation between the measures. However it is feasible that the visual field of each patient was changing at different rates, and that the time passing between the two tests was significant in an unpredictable way. The lack of correlation may also be inevitable when the conventional field is used in comparison, as if it were a 'gold standard', when it is, in fact, not adequately repeatable or sensitive as already outlined (Sample *et al.*, 1994). This is due in part to the widely acknowledged fluctuation in the glaucomatous visual field which can produce an unrepresentative, or possibly even inaccurate, picture of the extent of the individual's visual field defects against which to compare the contrast threshold results.

#### **4.1.3.3 Older control group (abnormal eyes)**

The 6 abnormal eyes of subjects in the older control group added a further dimension to the analysis of this form of contrast threshold testing, although one subject was excluded as she was unable to centrally fixate, due to a macular hole (15-n, right eye). The group included one individual with retinal scarring from an infection, one individual with surgically treated retinal detachment, one with mild cataract, one with poorer vision reportedly because of solar damage and one with amblyopia.

The mean contrast thresholds of all quadrants in the latter 4 of these eyes were within normal prediction limits, while there were abnormal readings in subject 2-n, whose left retina had scarring as a result of an infection. The location of the retinal defect in subject 2-n, which occurred in the temporal quadrant of the left eye, corresponded well with the

region of abnormally high contrast threshold, as can be seen in Figures 3.1-21 and 5.2-2. The Humphrey visual field chart also revealed a significant deviation in this eye, and an abnormal glaucoma hemifield test (Table 3.1-2). The infection has apparently left a localised region of defective retina that has shown up on both tests. The Humphrey also identified an abnormal MD in the abnormal eye.

Since no defects revealed by the contrast threshold testing for subject 6-n, it would appear that the repair of the retinal detachment has been successfully achieved with respect to his sensitivity to contrast and light (Figure 3.1-22). However, since his visual acuity is 6/12, it would appear that there has been some impact on his central vision and this may also be reflected in the significantly low MD recorded by the Humphrey analyser (Table 3.1-2 and Figure 5.2-6) for the abnormal eye.

It would appear that the mild cataract affecting subject 7-n did not adversely affect viewing of the contrast threshold stimulus (Figure 3.1-23). However her Humphrey visual field reveals a certain amount of reduced sensitivity centrally, shown in Figure 5.2-7 and highlighted a significantly low MD and an abnormal glaucoma hemifield test (Table 3.1-2). An imbalance in the MD between right and left eyes was also identified, and the difference from normal was significant in the subject's abnormal eye. The difference between the results obtained to these two forms of testing may be ascribed to the fact that the subject views the contrast threshold grating pattern in the Maxwellian View, which is known to bypass minor lens opacities, as previously described in Methods section 2.1.1.1 and illustrated in Figure 2.1-2, while conventional perimeters are sensitive to lens opacity.

The poorer vision in the right eye of subject 9-n does not appear to have caused any significant impairment to contrast threshold (Figure 3.1-24) or conventional analysis (Figure 5.2-9). The solar damage was reported to have happened to the subject's central vision while he was concentrating at a conference and was unable to avoid bright sunlight while looking straight ahead, although the nature and extend of the damage could not be independently confirmed. He was able to maintain fixation comfortably throughout the experiment, and his peripheral contrast thresholds were normal indicating normal function in his peripheral retina. The subject's left eye revealed a profound area of visual field loss in the upper hemifield during the Humphrey Visual Field Analysis, which was interpreted as being due to a drooping eyelid, which generated an abnormal glaucoma hemifield test and an abnormal mean deviation.

Subject 23-n's amblyopia also did not cause any impairment to her perception of the grating pattern (Figure 3.1-26) despite a visual acuity of 6/12. There was, however, a significantly reduced MD as recorded by the Humphrey analyser and a borderline glaucoma hemifield test result (Table 3.1-7). The visual fields are shown in Figure 5.1-22. It appears that although this subject was unable to perceive fine details at high contrast, as is tested using the Snellen eye chart, her peripheral retina was adequately sensitive to contrast at low spatial frequencies.

It may therefore be concluded that contrast threshold measurements were successfully and usefully applied in a limited number of cases with mild cataract, retinal detachment and amblyopia. The subject with the macular hole could not be tested due to the inability to centrally fixate. The test has also been shown to successfully detect a scotoma arising from a cause other than glaucoma.

#### ***4.1.4 Contrast threshold as a screening device***

The results are promising in that it has been shown that contrast threshold, even in a layout which was not adjustable, can be successfully completed by the majority of elderly subjects with a range of visual problems, and that abnormalities are consistently identified.

If this device were to be further developed as a primary screening device, the technique could be improved by being arranged into a more robust and yet more flexible layout, which could be adapted to suit the individual patient or subject without risk of unpredictable change to the image if bumped or interfered with in some way. For example, it is important to be confident about where the subject or patient was fixating, and since the fixation should not alter throughout the experiment, this could be dealt with by installing a fixation monitor which could be checked throughout by the experimenter. The time to complete the test may be reduced by taking fewer contrast threshold readings taken for each retinal region tested, if these could be shown to have significant diagnostic meaning. The test could be limited to the upper and lower quadrants (identified as the most commonly affected regions of the glaucomatous visual field) (Aulhorn and Karmeyer, 1977), thus reducing the testing time by half. A digital readout from the rotatable polarizer would appreciably reduce the time needed for the test, in terms of the necessary intervention of the experimenter in the course of the tests. The apparatus used in this form of testing can also be easily modified to extend the test area more peripherally,

in order to explore areas beyond the conventional visual field. Additionally the shape of the field is by no means fixed, and could be arranged to any desirable shape.

This visual testing system has been newly created, tested on real people with a range of physical and visual characteristics and useful results have been produced. Clearly it is difficult to say how diagnostically helpful these results would be, because more patients and control subjects are needed and an absolute benchmark against which to compare visual sensitivity is still lacking. It has been extremely useful to have the opportunity to attempt an analysis of conventional visual field analysers from an experimental starting point and it is certainly the case that dissatisfaction with the signal to noise ratio of conventional perimeters persists. In the case of the Humphrey Visual Field Analyser, this has led to ever more complex software being devised to improve it, or in other words to dampen down its sensitivity, as it still appears to generate high numbers of false positive results even after its continued use for many years.

This form of contrast threshold testing has shown the potential to address some of the desirable attributes of a future glaucoma test which were specified earlier. It has been shown that it can be carried out by the majority of a group of elderly subjects, and this proportion would certainly be improved, now that the physical difficulties which its inflexible layout caused have been identified. Further testing or analysis may identify areas of visual field which are affected early in glaucoma in all patients, and these tests could be targeted at those areas and thus carried out more quickly. It is a simple test which is easy to explain and understand. It is not necessary to correct for refractive error, and is not adversely affected by mild lens opacities. It has been able to identify a range of types of visual field loss, and although two eyes with moderate or severe damage were rated as normal, the range of visual field loss in one of those patients correlated strongly with the range of contrast threshold (it was borderline statistically in the other). Therefore contrast threshold measurements have described visual sensitivity as being abnormal in a group of patients with a range of visual field defects, albeit in not resolutely identifying 100% of abnormal cases. Since there has been a widespread inability to find distinct dividing lines between glaucoma patients, suspects and normal subjects in many tests this may be an acceptable condition applied to visual field tests for glaucoma in the future, assuming it is fully acknowledged. The search for an absolute dividing line beyond which an individual is said to definitely have glaucoma may be in vain.

## 4.2 Simultaneous Brightness Ratio

A new method of testing inter-ocular SBR was developed and evaluated in age-matched controls (as before including 6 non-glaucomatous visually abnormal eyes), glaucoma patients and young control subjects. For the first time, intra-ocular SBRs were also tested in the same subjects comparing upper and lower retina, and also nasal and temporal retina. These comparisons were carried out using a pair of squares of light (whose edges were  $10^\circ$ ), which were viewed by the subjects either centrally, for inter-ocular SBR, or each at  $\pm 10^\circ$  into peripheral retina for intra-ocular SBR.

### 4.2.1 Inter-ocular SBR

#### 4.2.1.1 Older and young control groups

The percentage difference in brightness sensitivity was seldom balanced precisely for the paired retinal regions stimulated. In fact, it varied quite considerably in all groups tested, including both older and young control groups. The large spread of results in age-matched control subjects (cf. Figure 3.2-2 E and Table 3.2-1) generated wide prediction limits for normal (mean  $\pm 2$  SD or a 97.7% confidence interval):  $-75\%$  to  $+74\%$  for inter-ocular SBR. Previous work has defined inter-ocular limits for normal ( $n = 91$ ) as  $68\%$  to  $131\%$  (where the point of exact balance between the eyes was taken to be  $100\%$  rather than  $0\%$ ) (MacMillan *et al.*, 1994). These authors also defined their confidence interval using mean  $\pm 2$  SD.

We were also able to evaluate the effect of differences in pupil diameter, as measured by the Humphrey Visual Field Analyser, on inter-ocular SBR. We found no significant relationship between the two variables in 13 subjects for whom inter-pupillary difference ranged from  $-0.2\text{mm}$  to  $+0.9\text{mm}$  and inter-ocular SBR ranged from  $-30\%$  to  $+35\%$  (regression analysis,  $R^2 = 0\%$ ,  $P = 0.98$ ) (cf. Figure 3.2-3). Therefore it would appear that anisocoria of up to  $1\text{mm}$  did not affect inter-ocular SBR when tested in this format. This agrees with the published results of Sadun and Lessell, 1985 who also stated that there was no effect of anisocoria on inter-ocular SBR, but was in contrast to those of MacMillan *et al.*, 1994 who stated that SBR was highly sensitive to inter-ocular differences greater than  $0.5\text{mm}$  (the range tested was roughly zero to  $3\text{mm}$  difference between eyes).

In the young control group there was an apparent difference to the older group (cf. Figure 3.2-13), where the mean error from zero in the inter-ocular SBR for the young group was greater although the difference was also not statistically significant.

#### **4.2.1.2 Glaucoma patient group**

The SBRs obtained for inter-ocular SBR in the age-matched control group deviated quite considerably from the point of perfect balance, and therefore produced wide prediction limits. Perhaps unsurprisingly then, abnormal results were revealed in few patients. Of the 13 patients who completed the inter-ocular SBR tests, 10 had an imbalance in the inter-ocular ratio of their Friedmann visual fields and 4 of these produced an inter-ocular SBR which was outside the prediction limit for normal, shown in Figure 3.2-6 E and summarised in Table 3.2-3. The identification of 4 in 10 patients compares with a previous study in which all 20 of the POAG patients tested were identified as abnormal by brightness sense testing (Cummins *et al.*, 1994). As discussed in Methods section 2.2.1.3, pupil diameter measurements were not available for the patient group.

#### **SBR VS CONVENTIONAL VISUAL FIELD ANALYSIS IN GLAUCOMA PATIENTS**

As stated above 10 patients were found to have uneven central visual field loss from visual field measurements (cf. Table 3.2-3) and among these were the 4 identified as abnormal from their inter-ocular SBR (5-g, 6-g, 7-g and 17-g). These 4 patients had either moderate or severe visual field loss imbalances. Of the remaining 9 patients, 4 had mild imbalance in their visual fields as measured conventionally, in one patient the imbalance was moderate, in one it was severe and the other 3 had balanced visual fields.

(The inter-ocular SBRs for visually abnormal eyes within the older control group will be discussed in Discussion section 4.2.2.3 by subject.)

## 4.2.2 Intra-ocular SBR

### 4.2.2.1 Older and young control groups

To the best of the author's knowledge no data are available on intra-ocular SBRs against which to compare. The mean intra-ocular SBRs for the age-matched control group showed a tendency to indicate the region of retina with the graduated filter over it as the more sensitive region. The mean SBR for the age-matched control group was significantly different from zero ( $P \leq 0.02$ , one-sample t-test) for the upper / lower comparisons in both eyes, however, for the nasal / temporal comparisons, they were not significantly different from zero ( $P \geq 0.6$ , one-sample t-test).

This suggests that in these subjects there was a tendency towards the upper retina being more sensitive to brightness than the lower retina. The significance of this should not be overstated based on the results of a small sample. However, if this did actually represent a genuine difference in the brightness sensitivity of these retinal regions, then such a difference may reflect the human visual experience. In simple terms, visual representations of our environment involve the sky being presented in the upper field (i.e. the lower retina) and darker more detailed images presented in the lower field (i.e. the upper retina). In theory therefore, the more brightness sensitive upper retina would be better able to resolve detail in the images it perceives in the lower field. It is feasible, therefore, that this may confer some evolutionary advantage, or indeed be as a direct consequence of the exposure to different types of visual stimulus in the upper and lower fields during the development of visual neurones. There is, however, no evidence for asymmetry of rods in the upper and lower retina (Østerberg, 1935)

A similar result in the group results was obtained for the young control group with a very slight tendency to indicate the retinal region that was covered by the graduated filter as being the more sensitive one of the two being compared. In the young control group, however, the spread of data generated even wider prediction limits (cf. Figure 3.2-12 and Table 3.2-4). The mean SBRs were much closer to zero than in the older control group, however, and none of them were significantly different from zero ( $P > 0.1$ , one-sample t-test). Therefore in these subjects there was no indication that there was an imbalance in the sensitivity of opposing halves of the retinae, which therefore discounts the aforementioned theory of this as a consequence of exposure during development. This difference from the older group raises the possibility that asymmetry of hemi-retinae

sensitivity is an age-related change, which emphasises the importance of using age-matched control groups in visual studies.

Regardless of the underlying physiological causes, these results imply that, particularly in older subjects, the subject tended to identify a match point on the graduated filter at a position which was stronger than necessary than to match with the fixed strength filter. In other words, the area of retina being stimulated by the variable filter required less light to match with the retina being stimulated by the fixed strength filter. If it is interpreted as an experimental error caused by the difference between the two stimuli (one of which was changing over time) this may be due to an effect of light adaptation, whereby the two halves are adapting at differing rates. Since this occurred in older subjects, it may reflect a change in the composition of the older retina. It is known that retinal ganglion cells are lost throughout life (Balazsi *et al.*, 1984; Johnson *et al.*, 1987; Gao and Hollyfield, 1992). One interpretation of the evidence is that it indicates that the losses are not evenly spread in the retina, and in fact may be preferentially lost in the lower retina, although clearly this is conjecture based on a small study population. The direction of the emphasis in this apparent difference would appear to depend on which area the level of brightness is changeable and on which side it is fixed. The result is that the perceived brightness of the fluctuating area is enhanced relative to the stable side. It is also worth noting that these theoretical differences are limited to the intra-ocular SBRs and not to the inter-ocular comparisons for either group.

Although this apparent difference did indeed occur in the age-matched control group when the upper and lower fields were being compared, this was not the case in the comparisons of the nasal and temporal fields, their inter-ocular comparisons, or any of those for the young control group. If the tests were to be repeated or developed in some way, it would be useful to alternate the position of the graduated filter, or carry out a repeat experiment in individuals with the graduated filter in the opposing position to observe if the more sensitive region did reflect its location. Since a physiological explanation (asymmetric sensitivity or rates of adaptation) is eroded by the lack of consistency in the younger control group, and yet the mechanical explanation (position of graduated filter) is inconsistent with the results within the older control group inter-ocular results, it may suggest that the observed differences are, in fact, simply a reflection of noise in this insensitive testing system.

#### **4.2.2.2 Glaucoma patients**

As with the inter-ocular SBR, there was a large amount of variation in the intra-ocular SBR in the older and young control groups. The large prediction limits for normal led to two patients being identified as abnormal from one of their mean intra-ocular SBR scores: 7-g and 10-g (by upper / lower intra-ocular comparison for right eye); 10-g (by upper / lower intra-ocular comparison for left eye) as shown in Figure 3.2-6 A to D. This indicates that intra-ocular SBR is not a useful test for glaucomatous field loss in this format.

#### **SBR VS CONVENTIONAL VISUAL FIELD ANALYSIS IN GLAUCOMA PATIENTS**

Overall, there were 12 patients with uneven visual field sensitivity (in the SBR test regions) as measured by the Friedmann field analyser. The two patients for whom an abnormal intra-ocular SBR was identified, had severe or moderate visual field imbalances in the affected eye. However, this leaves 14 eyes of 10 patients with moderate or severe visual imbalance who were indistinguishable from normal by their intra-ocular SBRs (cf. Table 3.2-3).

As a further step in analysis, the percentage difference in visual field loss in the corresponding areas of the visual field was quantified using their conventional field measurements. As only 5 points were available for regression analysis, however, there is limited statistical significance in the results. It transpired that the only results which generated a statistically significant relationship, were those of patient 7-g in whom default scores were necessary for both SBR and visual field quantification. Although the patient with OHT in both eyes did produce SBRs which were close to zero, this did correlate with the well balanced ratios for percentage field loss by conventional analysis. It would appear however, that in this format, an individual's SBR does not accurately reflect the ratio of sensitivity in the paired retinal areas tested, as measured by conventional methods.

#### **4.2.2.3 Older control group (abnormal eyes)**

Subject 2-n who had retinal scarring in her left eye produced a clear abnormality in the brightness sense between the two eyes, with the right eye measured as being more

sensitive. This was despite the peripheral location of her defect which was at the level of the blind spot i.e.  $15^{\circ}$  to  $20^{\circ}$ , this suggests that the area of damaged retina, with respect to brightness perception, was more extensive than expected. However, the difference was not reproduced in the nasal / temporal comparison for that eye. This may reflect a difficulty of the subject to fixate accurately, or that the brightness sense involved greater areas than those specifically stimulated due to light scatter by the  $10^{\circ}$  light squares with healthy retina compensating around this region. What did appear, however, was a large spread of results shown by the large error bars on Figure 3.2-14, which occurred for the left eye only. This suggests that the brightness sense of the left eye was impaired and that this was detected in two ways (as a clear difference between the eyes, and as an increase in the variability of the SBR within the abnormal eye). The borderline glaucoma hemifield test result revealed by the Humphrey analyser (Table 3.1-7 and Figure 5.2-2) was not reflected in a mismatch in the upper / lower SBR in the left eye.

The retinal detachment in subject 6-n's right eye, also appeared to generate a large amount of variability in the intra-ocular SBR apparent in the large error bars (particularly for the nasal / temporal comparisons) (see Figure 3.2-15). However, this large spread of results was repeated in his left eye and the inter-ocular SBR was indistinguishable from that of a normal control result, therefore one cannot say that this was specifically due to the subject's eye condition.

The results for subject 7-n are entirely normal, and it would appear that her mild cataract has had no significant effect on her brightness sense, as tested in this format (Figure 3.2-16). As with subject 2-n, the borderline glaucoma hemifield test result indicated by the Humphrey analyser (Table 3.1-7 and Figure 5.2-7) was not reflected by any obvious abnormality in the upper / lower comparison for the left eye.

Subject 9-n had normal intra-ocular SBRs for both eyes, however the inter-ocular SBR was abnormal and indicated that the left eye was more sensitive by 160% (see Figure 3.2-17), which is consistent with the damage in his right eye.

The macular hole in her right eye prevented subject 15-n from completing the inter-ocular SBR test, but she was able to complete the intra-ocular tests. These indicated that the brightness sense in both eyes was within normal limits (Figure 3.2-18). This is feasible since the macular lesion is well localised and therefore not impinging on the function of the parafoveal retina.

Amblyopia in the right eye of subject 23-n (Figure 3.2-19) and a normal left eye produced an intra-ocular SBRs which were all within normal limits. However, the inter-ocular SBR was abnormal and indicated that the left eye was more sensitive to brightness. This is consistent with a non-localised amount of reduced sensitivity throughout the amblyopic eye, which would lead to balanced intra-ocular SBRs but would however, show up as a significant difference when compared to a normal eye.

SBR testing in this format has therefore been unable to resolve any intra-ocular abnormality in any of the abnormal eyes within the older control group, although without more detailed evaluation of each individual abnormality it is difficult to take the analysis further. In a group of limited sample size this may not be surprising, however there appears to be enough evidence to require a further evaluation of the stimulus format. One possible improvement would be to use more widely separated fields in which case one could have more confidence that direct fixation would be avoided, or at least would be easier to monitor.

#### ***4.2.3 SBR as screening device***

The above results suggest that in this format, intra-ocular SBR has limited use as a screening device for glaucoma or other visual abnormalities. The inter-ocular SBR was slightly more successful at identifying abnormalities but, while substantial deviation from the point of perfect balance in visually normal subjects is so common, its ability to distinguish glaucomatous individuals from age-matched controls remains poor.

Several difficulties arose with the SBR testing including the physical impracticalities of this particular set up. These made the process more time consuming and physically awkward than would be desirable. The adjustment to the graduated filter involved many turns of a small dial meaning that the subject was exposed to the light squares for relatively extended periods of time, and thus vulnerable to adaptation effects, for minutes at a time rather than seconds. Also, despite the filters used in the graduated and fixed apparatus being of similar materials and their density carefully measured using a spectrophotometer, some subjects reported a distinct colour difference between the two squares. This affected 9 of the 24 control subjects and 8 of the 15 glaucoma patients who completed the SBR tests, and included two (self-reported) colour blind individuals and those with normal colour vision. This unexpected colour difference, which some subjects found distracting,

was described as 'greyish pink', 'creamy', 'yellow', 'green' or 'lilac'. The perceived colour was often, but not always, in the graduated filter and 3: subjects saw a different colour in each of the two filters they were viewing simultaneously. This perceived colour discrepancy did apparently make the task of matching the brightness of the squares more difficult, as even at the point of equal brightness match, there may have been a residual colour difference which the subject was instructed to try and disregard. When the results were examined by eye, however, this difficulty did not lead to unusually mismatched results in those subjects, and there was no obvious correlation between the perception of a colour mismatch between the filters and SBRs. This may be a factor which merits more detailed analysis in the future.

One area of difficulty which arose regularly was that of maintaining constant and steady fixation between the stimulus squares for obtaining intra-ocular SBRs. Subjects reported how difficult it was to avoid looking directly at the squares. Although, one would imagine that if subjects were viewing them directly, then the SBRs would be more closely matched rather than the opposite. In inter-ocular SBRs, each square was only visible to one eye, therefore fixating on the wrong one was not physically possible if the set up were arranged correctly. However it is feasible that subjects did not fixate on the squares directly as this involved allowing the eyes to diverge. It is also possible that the squares were not viewed simultaneously, rather that subjects may have viewed each in turn, which would give central viewing, but would be consecutive. In such a scenario the way in which the brightnesses would be judged relative to one another would be different. These two issues would be dealt with were a fixation monitor added to the set up. As with the contrast threshold testing, there are other technical improvements which could make the test more 'user-friendly', which may have the side effect of more useful results. For example, a more convenient arrangement for recording the end point of each observation, a digital read out and a more robust layout of the equipment which could be altered between each test orientation quickly and easily.

The smoothly graduated filter was employed, and control over the change in brightness of the test squares given to the subject, as it was anticipated that this may lead to a more finely tuned end point in the match between the two squares. This is as opposed to other testing methods whereby step changes in the brightness caused by filter changes of 0.2 log units, are 'offered' to the subject by the experimenter who chooses the nearest match (Martin and Robison, 1994). However, one interpretation of our results (i.e. the wide normal limits shown in Table 3.2-1) may be that the continual fluctuation in brightness involved in such a method makes the matching more difficult rather than less so, and may

be responsible for the resulting high numbers of false negatives achieved. Perhaps an improved mechanism could be developed for altering the position of the graduated filter, allowing both gross and fine adjustments to the filter strength quickly. In theory this might combine the perceived advantages of the smooth change in the filter strength (over the blunt step changes) without the disadvantage of the extended time required to view the image while those changes are achieved and the resulting adaptation effects that this incurs. It may also be necessary to test more peripheral locations for intra-ocular SBRs, which may make fixation less of a struggle as mentioned above.

As brightness appreciation is carried by both magnocellular and parvocellular ganglion cell pathways, the likelihood of identifying early defects by this method may be low, if the theory of reduced redundancy is to be adhered to when producing the most sensitive tests.

### 4.3 Conclusions

The aim of the work described in this thesis was to develop and analyse two visual field tests which have been identified by previous authors as having potential in glaucoma diagnosis. It has been shown here that sensitive information can be obtained about the visual fields of patients with glaucoma and individuals with non-glaucomatous visual abnormalities using tests other than conventional tests.

The optimal way of characterising the glaucomatous visual field in order that it can be identified and distinguished from normal remains elusive, however the following points have been demonstrated:

- contrast threshold has some potential in making the diagnosis, or describing the extent of glaucomatous visual field loss. Contrast threshold testing would be deemed successful if it reliably identified a normal visual field, with any anomaly requiring a full visual field test or further investigation. However, it has also been shown that the definition of a normal field has not been straightforward when using conventional testing.
- the intra-ocular SBR (both upper / lower and nasal / temporal comparisons) appear to depend on many factors which we have been unable to resolve and therefore in this format it may have limited usefulness as a primary visual field analysis method. Many cases of moderate or severe imbalance in visual field loss were not identified. The fact that several factors seem to influence SBR may conspire to conceal sensitive information about the abnormal or normal visual field. Since it is suspected that there are several different visual modalities which underlie glaucoma, such a non-specific test would not make an ideal diagnostic test.
- and finally, although inter-ocular SBR has been shown in the past to be highly sensitive to glaucomatous damage, we have been unable to reproduce these results. Four of 6 cases with moderate or severe imbalance in the corresponding visual field regions, were identified as abnormal, although none of the 4 with mild visual sensitivity imbalance were identified by this test.

It is necessary to increase the size of the test groups to investigate more fully the relationship between the processes of degeneration and the subsequent different types of observed visual field defects. The ideal diagnostic tool for glaucoma is still elusive despite decades of investigations, and the concept of such a tool as a single test seems increasingly unlikely. For this reason the search for a test of the visual field in the future may need to focus on being able to describe borderline cases with more sensitivity or accuracy rather than obsessing about the separation of 'normal' and 'abnormal' patients. The concept of an 'abnormal' field, IOP or optic disc may need to be sidelined in the study of glaucoma, so that such a defining characteristic is not sought to the cost of the overall understanding of each patient's status and therefore is not overly relied upon in evaluating the necessary management of each individual's disease.

It is, however, the case that individuals at risk can be identified successfully if thorough and age-appropriate primary screenings are carried out, and of course if the individual presents themselves regularly for such screening. Therefore the target of identifying people at risk as early as possible in order to initiate the necessary treatment, (which is, after all, effective in the majority of cases) is still dependent upon the tests being used and the population being able and willing to undergo them.

The experience of carrying out these investigations suggests that peripheral contrast thresholds measurements have again showed potential to fulfil both the investigators and clinicians' requirements for a primary screening test, while the format itself has been endorsed by the participants.

## 5 Appendix

### 5.1 Lens equations

*Equation 5.1-1 To calculate combined power of 2 lenses*

$$F = F_1 + F_2 - d \cdot F_1 \cdot F_2$$

- $F_1$  = power of first lens in sequence  
 $F_2$  = power of second lens in sequence  
 $d$  = the distance between principal planes of lenses

*Equation 5.1-2 To calculate combined power of 3 lenses*

$$F = F_1 + F_2 + F_3 - (d_1 \cdot F_1 \cdot F_2) - d_2 \cdot F_2 \cdot F_3 - ((d_1 + d_2) \cdot F_1 \cdot F_3) + (d_1 \cdot d_2 \cdot F_1 \cdot F_2 \cdot F_3)$$

- $F_1$  = strength of first lens in sequence  
 $F_2$  = strength of second lens in sequence  
 $F_3$  = strength of third lens in sequence  
 $d_1$  = distance between lenses  $F_1$  and  $F_2$   
 $d_2$  = distance between lenses  $F_2$  and  $F_3$

### 5.2 Humphrey Visual Field plots – older control subjects

Humphrey visual field plots were obtained for 23 of the 24 control subjects (except subject 12-n). The plots were taken using the Central 24-2 Threshold programme except for subject 18-n and 24-n for whom the Central 30-2 threshold programme was used. On all Figures 5.1-1 to 5.1-24, the left half shows the dot plot for the subject's left eye, and the right half shows the plot for the subject's right eye. The sensitivity of the subject's retina is related to the density of the dots in each area, i.e. the blind spot or areas of minimal sensitivity are indicated by black region surrounded by dense dots. Highly sensitive areas are lightly dotted. The mean deviation (MD) in decibels (in decades) (dB) of each eye is given in the legend in the order of the plots, i.e. left eye first, right eye second.

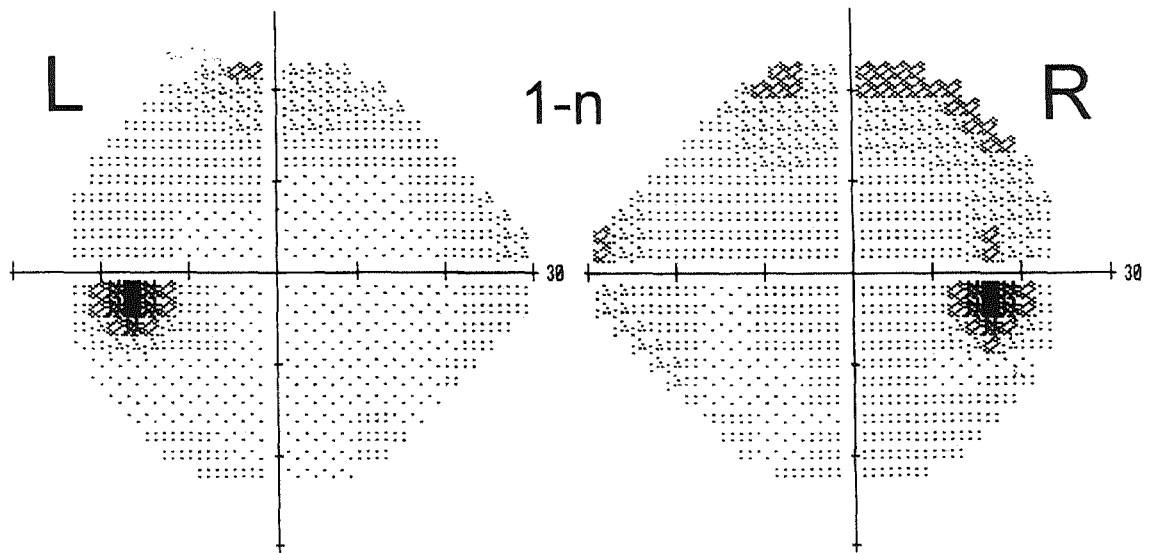


Figure 5.2-1 Humphrey visual field plot using the Central 24-2 programme for subject 1-n, 70 year old male, MD = +0.2dB, -2.1dB, L = left eye, R = right eye.

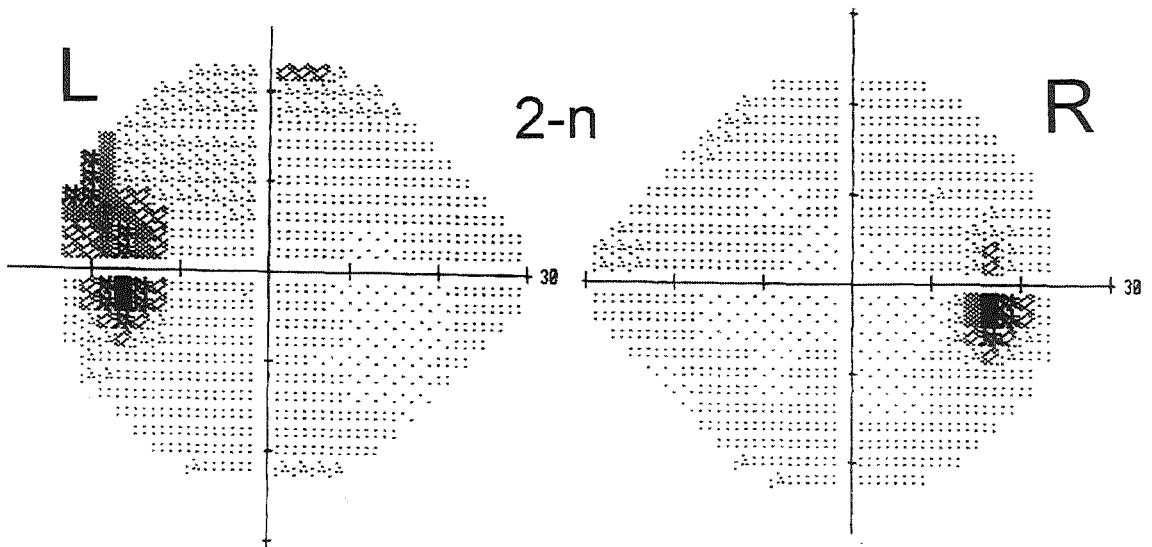


Figure 5.2-2 Humphrey visual field plot using the Central 24-2 programme for subject 2-n, 78 year old female with retinal scarring in left eye, MD = -2.2dB, -0.5dB, L = left eye, R = right eye.

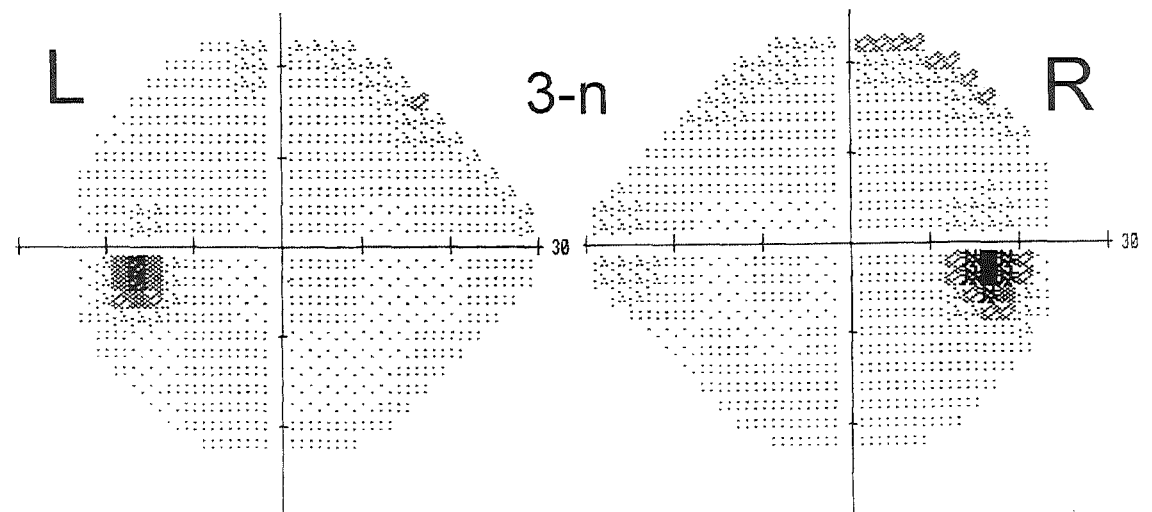


Figure 5.2-3 Humphrey visual field plot using the Central 24-2 programme for subject 3-n, 70 year old male, MD = 0.0dB, -1.0dB, L = left eye, R = right eye.

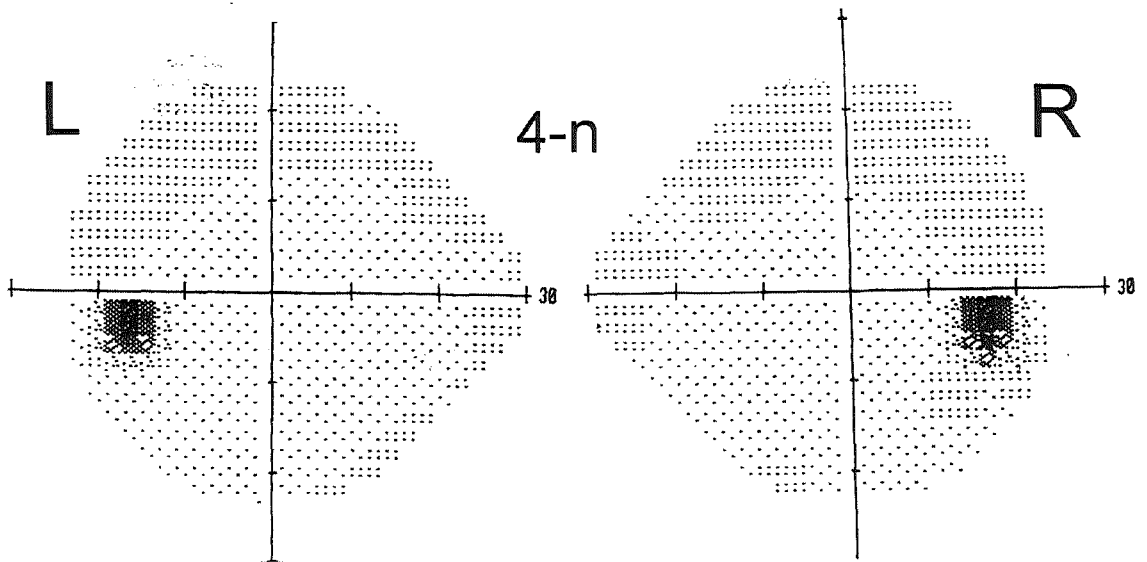


Figure 5.2-4 Humphrey visual field plot using the Central 24-2 programme for subject 4-n, 65 year old female, MD = +1.3dB, +1.1dB, L = left eye, R = right eye.

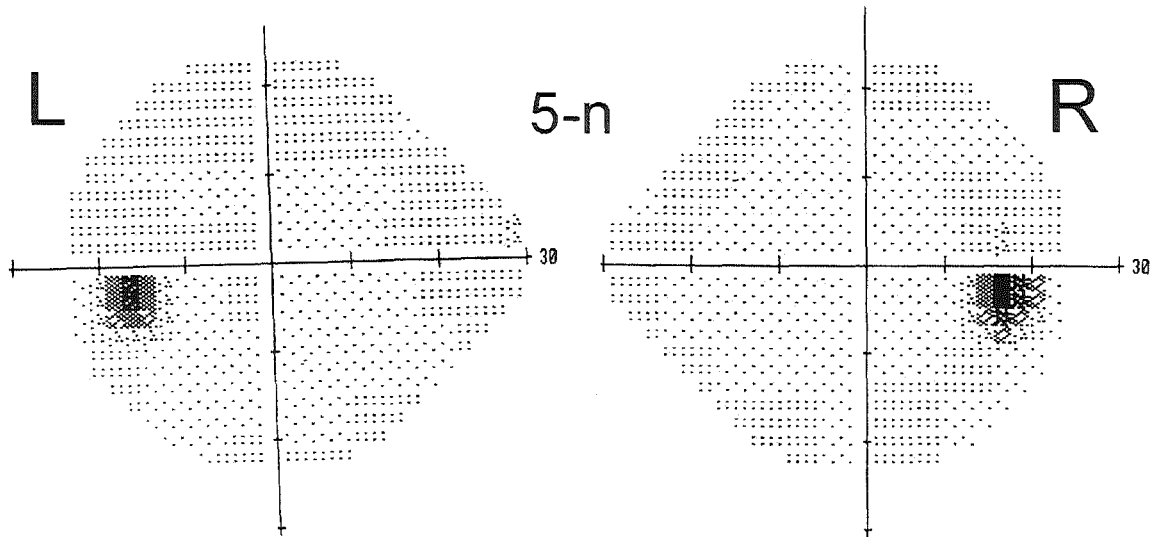


Figure 5.2-5 Humphrey visual field plot using the Central 24-2 programme for subject 5-n, 59 year old female, MD = 0.0dB, +0.8dB, L = left eye, R = right eye.

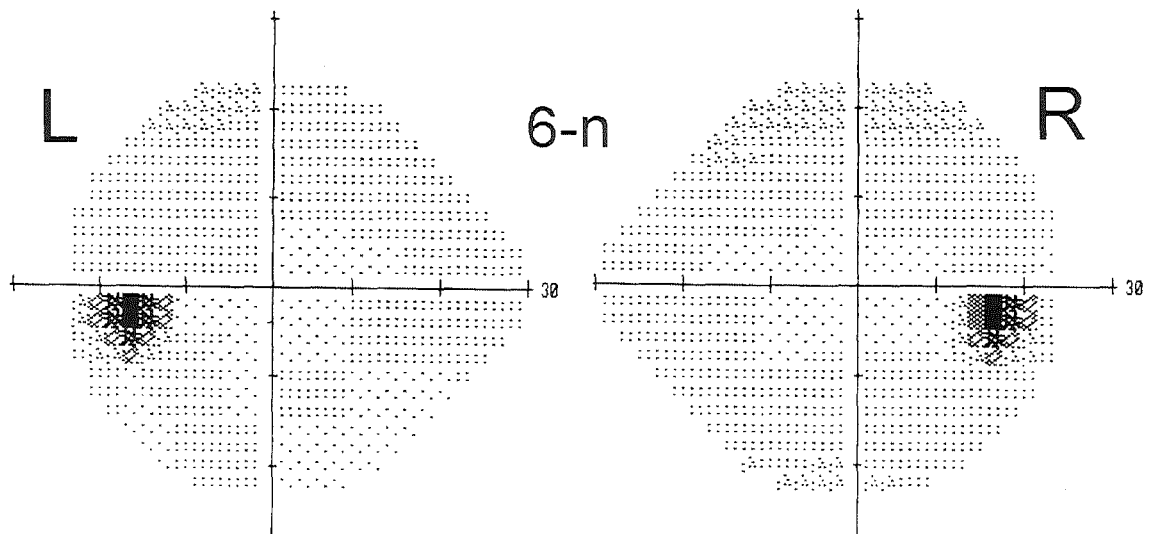


Figure 5.2-6 Humphrey visual field plot using the Central 24-2 programme for subject 6-n, 63 year old male with surgically corrected retinal detachment in right eye, MD = -0.7dB, -1.5dB, L = left eye, R = right eye.

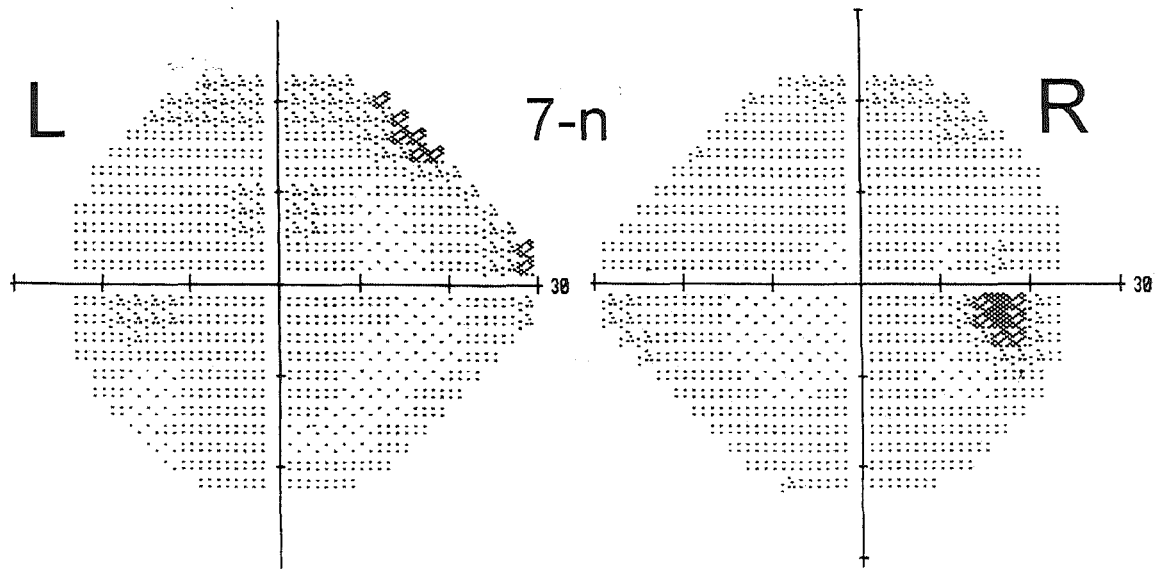


Figure 5.2-7 Humphrey visual field plot using the Central 24-2 programme for subject 7-n, 69 year old female with mild cataract in left eye, MD = -1.6dB, -0.7dB, L = left eye, R = right eye.

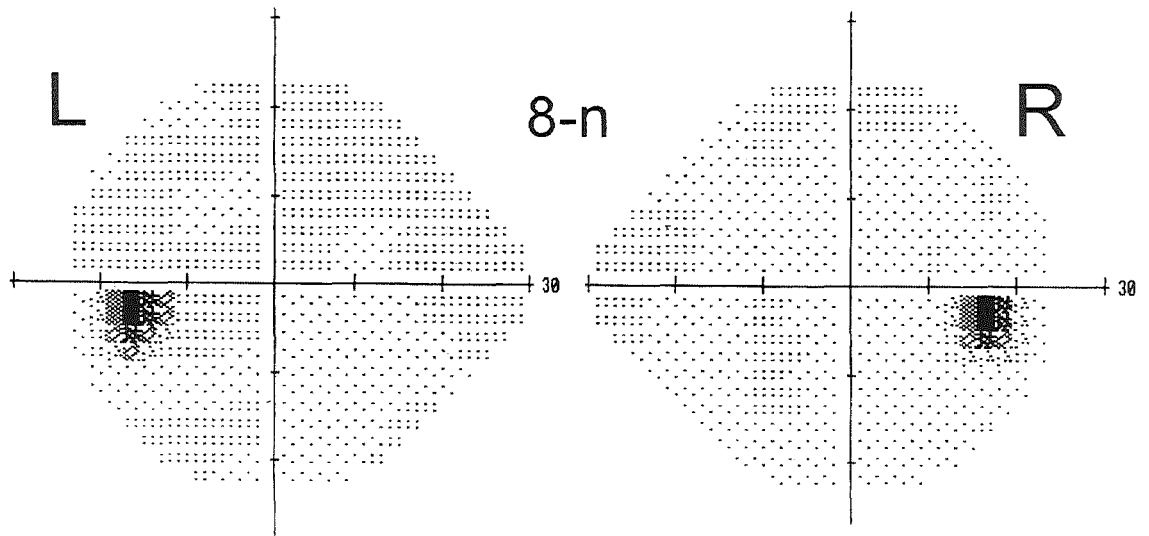


Figure 5.2-8 Humphrey visual field plot using the Central 24-2 programme for subject 8-n, 61 year old female, MD = +0.2dB, +1.1dB, L = left eye, R = right eye.

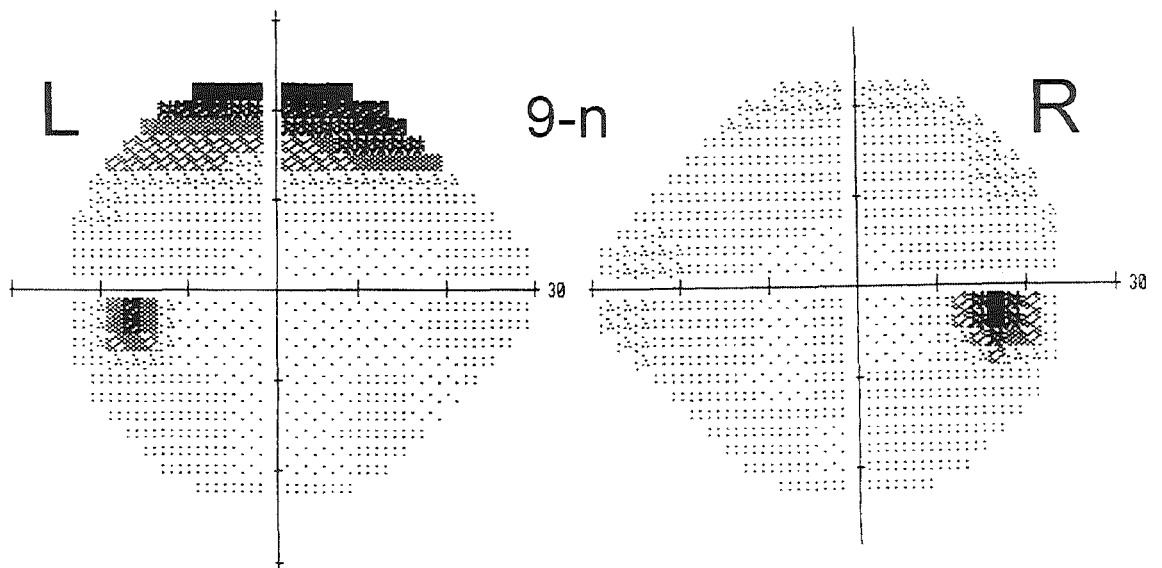


Figure 5.2-9 Humphrey visual field plot using the Central 24-2 programme for subject 9-n, 76 year old male with retinal scarring in right eye, MD = -2.5dB, -0.9dB, L = left eye, R = right eye. Left eye shows loss of sensitivity in upper field.

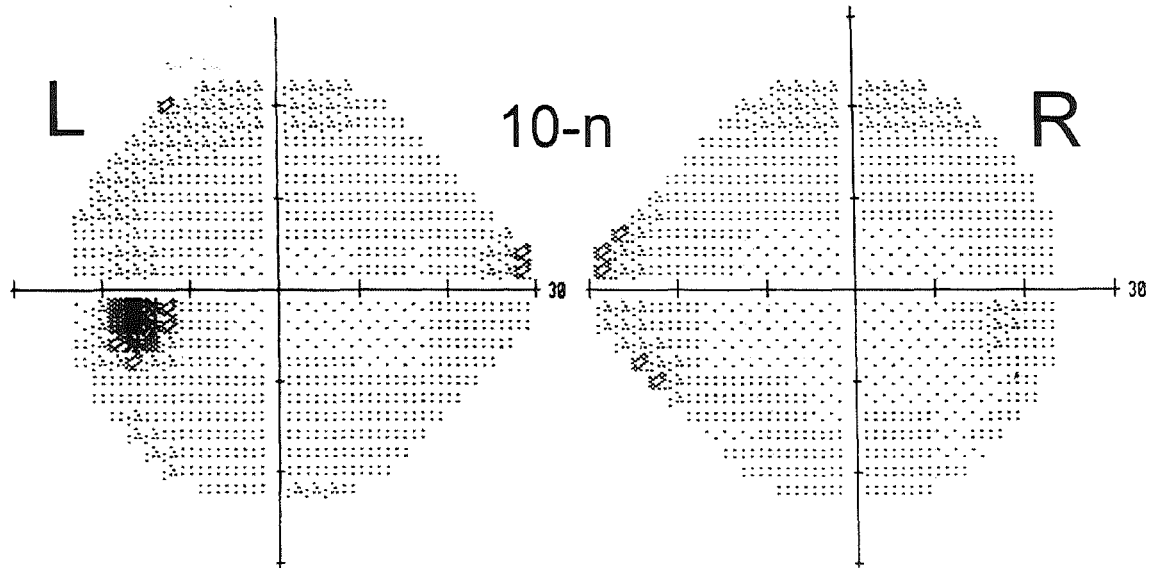


Figure 5.2-10 Humphrey visual field plot using the Central 24-2 programme for subject 10-n, 71 year old male, MD = -1.4dB, -0.5dB, L = left eye, R = right eye.

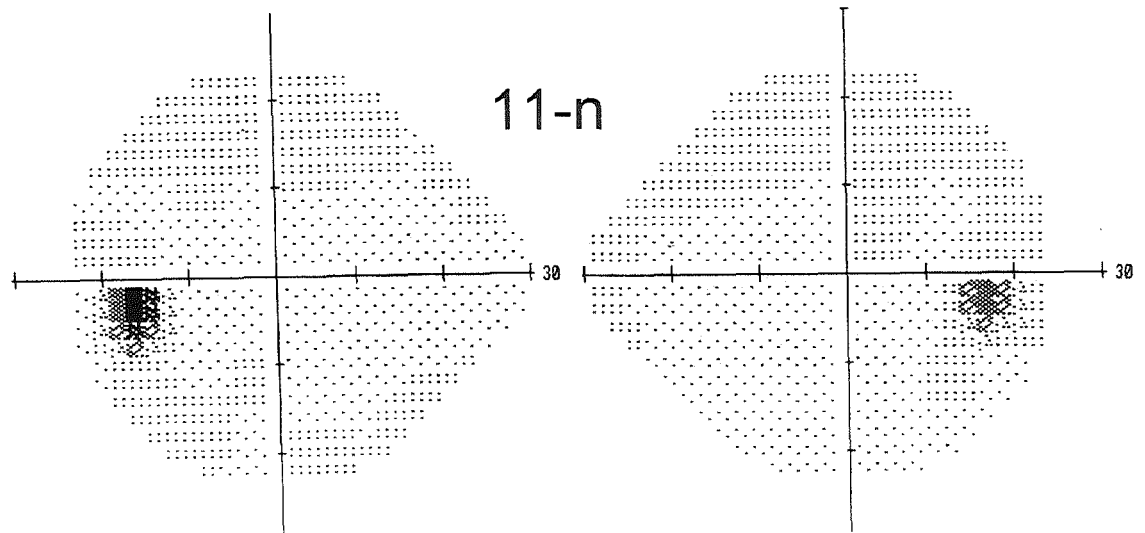


Figure 5.2-11 Humphrey visual field plot using the Central 24-2 programme for subject 11-n, 66 year old male, MD = +0.9dB, +1.2dB, L = left eye, R = right eye.

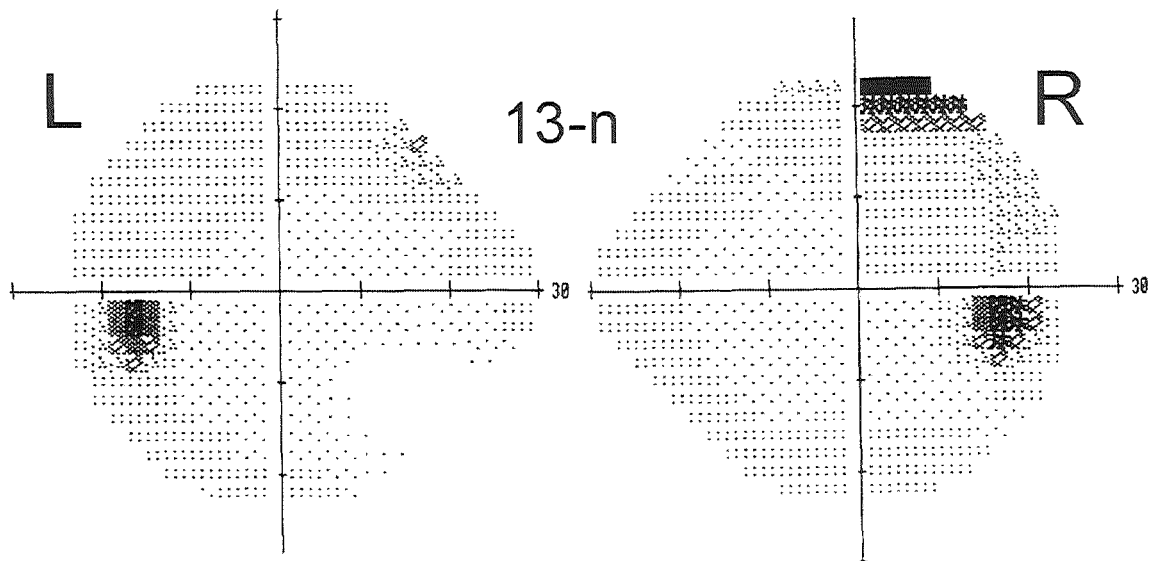


Figure 5.2-12 Humphrey visual field plot using the Central 24-2 programme for subject 13-n, 69 year old female, MD = +2.3dB, -0.6dB, L = left eye, R = right eye. Left eye shows hypersensitivity, right eye shows area of reduced sensitivity.

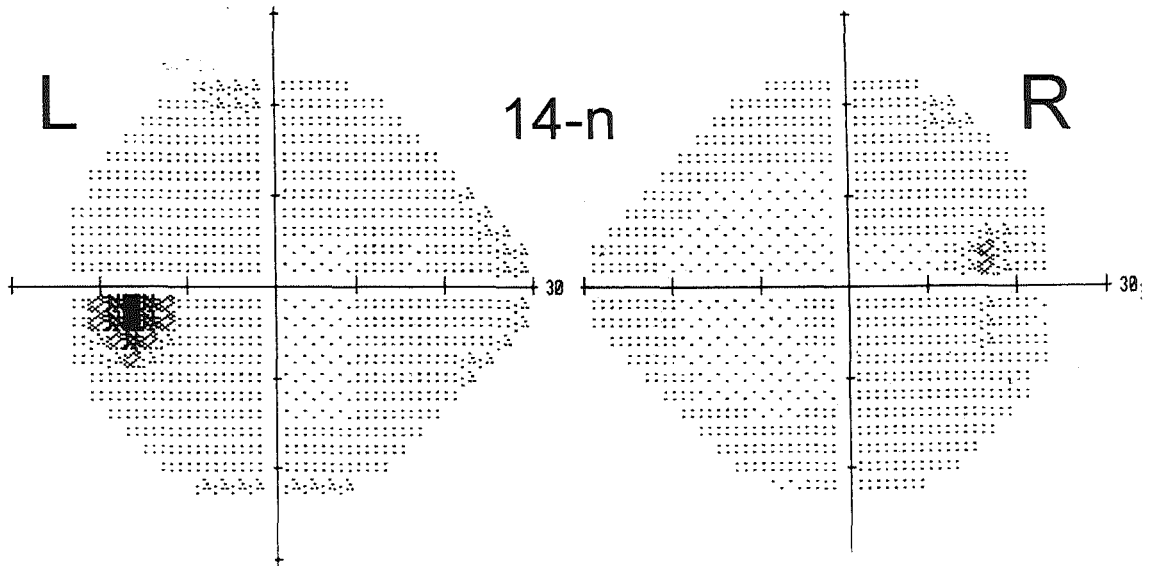


Figure 5.2-13 Humphrey visual field plot using the Central 24-2 programme for subject 14-n, 73 year old female, MD = -1.0dB, +0.4dB, L = left eye, R = right eye.

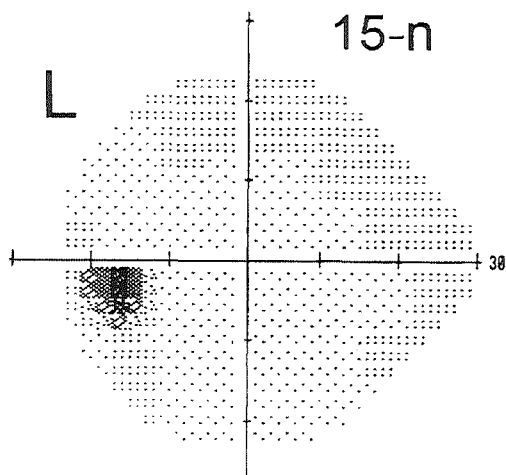


Figure 5.2-14 Humphrey visual field plot using the Central 24-2 programme for subject 15-n, 73 year old female with macular degeneration in right eye - therefore unable to fixate, MD = +1.4dB, L = left eye.

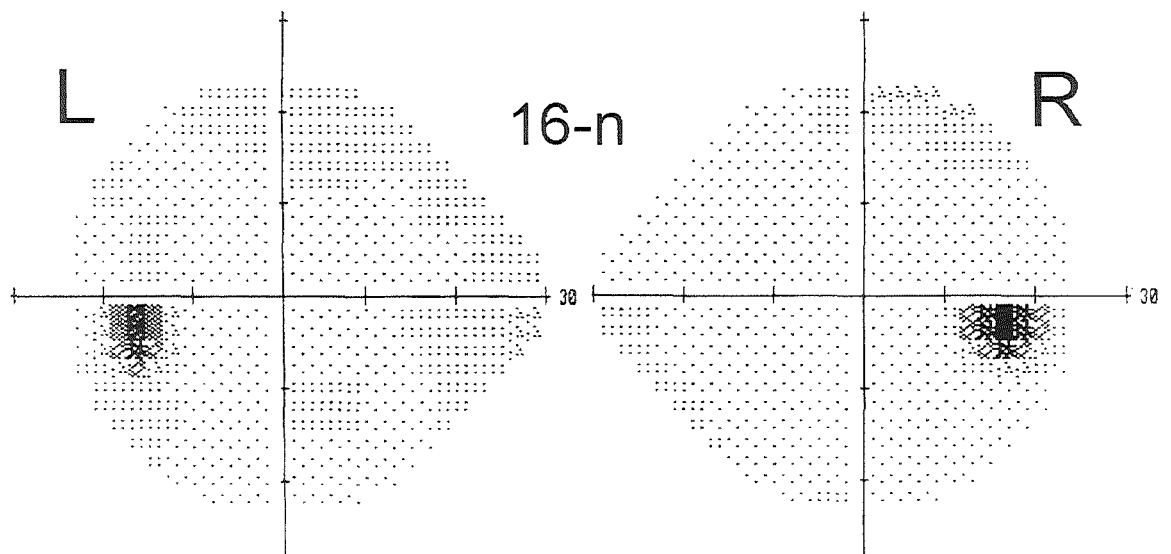


Figure 5.2-15 Humphrey visual field plot using the Central 24-2 programme for subject 16-n, 51 year old male, MD = 0.0dB, +1.0dB, L = left eye, R = right eye.

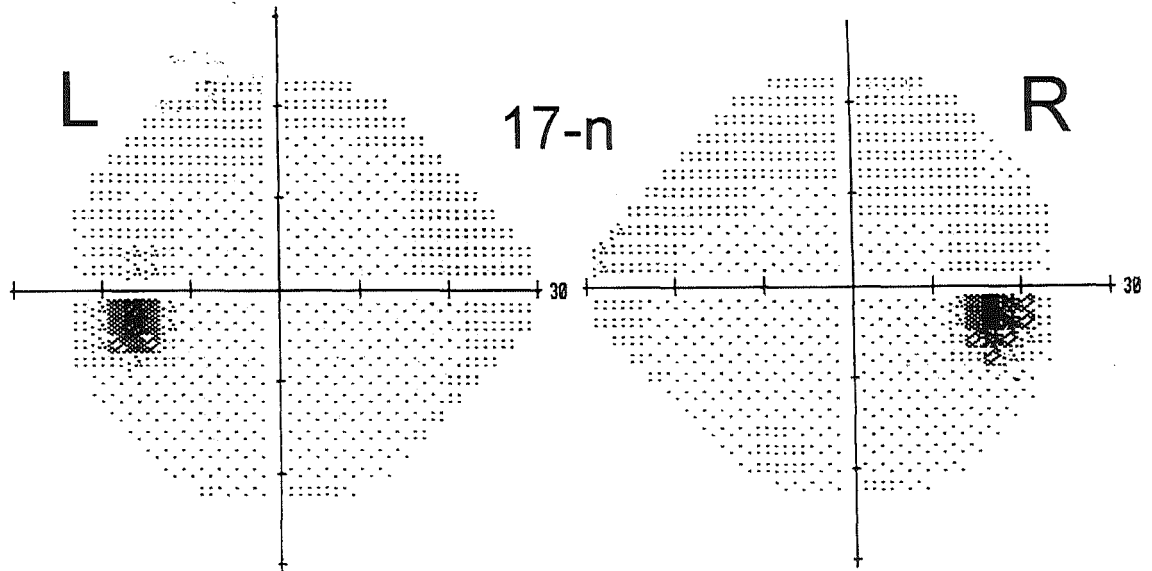


Figure 5.2-16 Humphrey visual field plot using the Central 24-2 programme for subject 17-n, 69 year old female, MD = +0.8dB, +0.6dB, L = left eye, R = right eye.

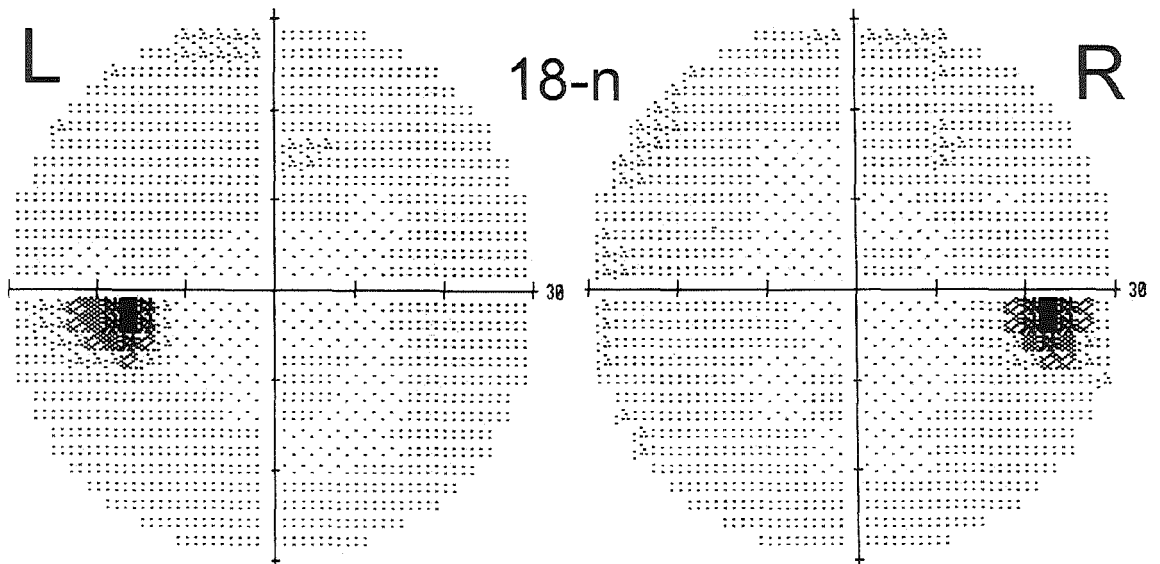


Figure 5.2-17 Humphrey visual field plot using the Central 30-2 programme for subject 18-n, 49 year old male, MD = -1.2dB, -1.3dB, L = left eye, R = right eye.

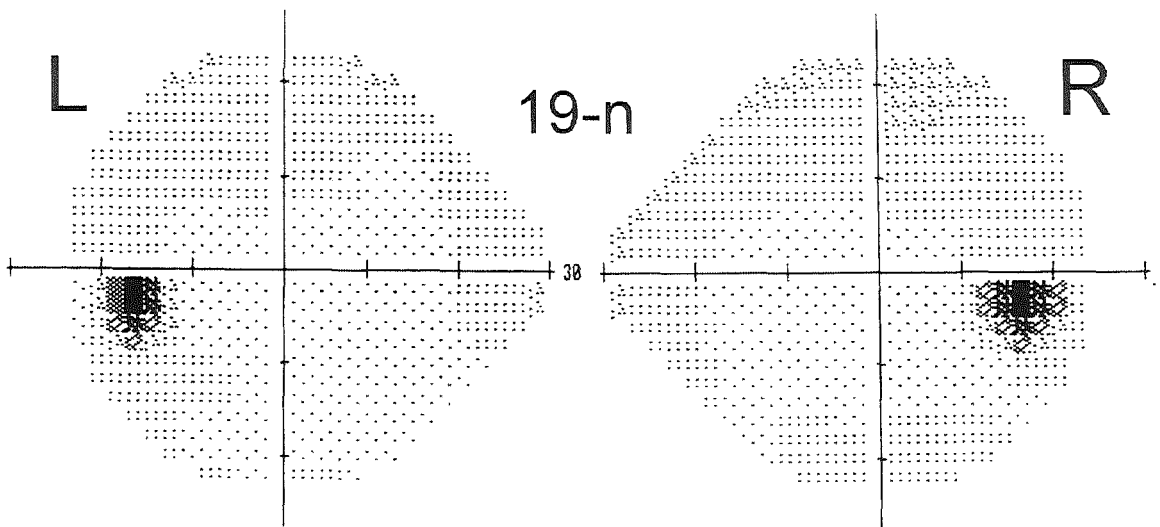


Figure 5.2-18 Humphrey visual field plot using the Central 24-2 programme for subject 19-n, 52 year old male, MD = +0.9dB, 0.0dB, L = left eye, R = right eye.

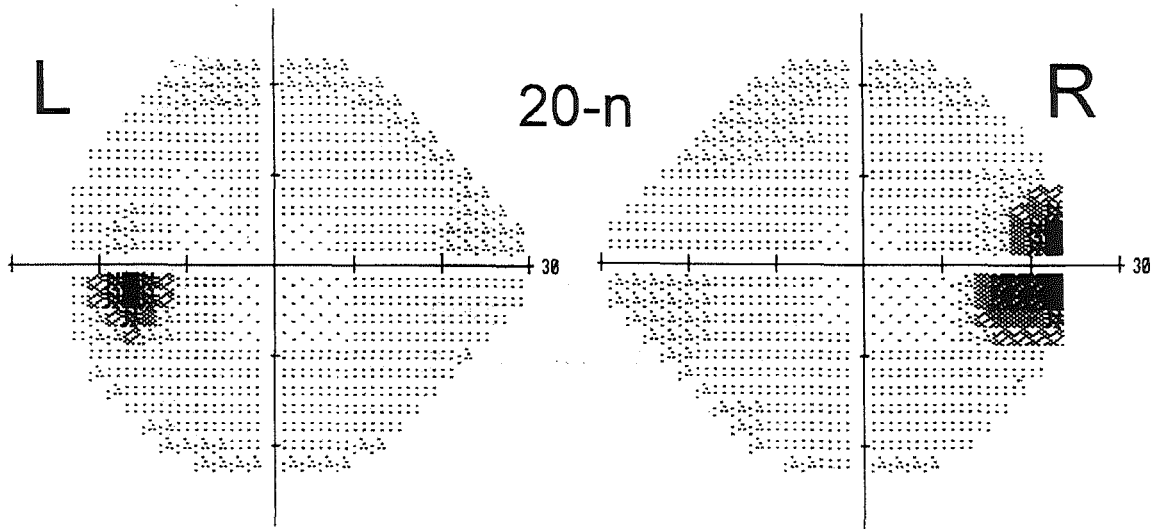


Figure 5.2-19 Humphrey visual field plot using the Central 24-2 programme for subject 20-n, 66 year old male, MD = -2.2dB, -3.5dB, L = left eye, R = right eye.

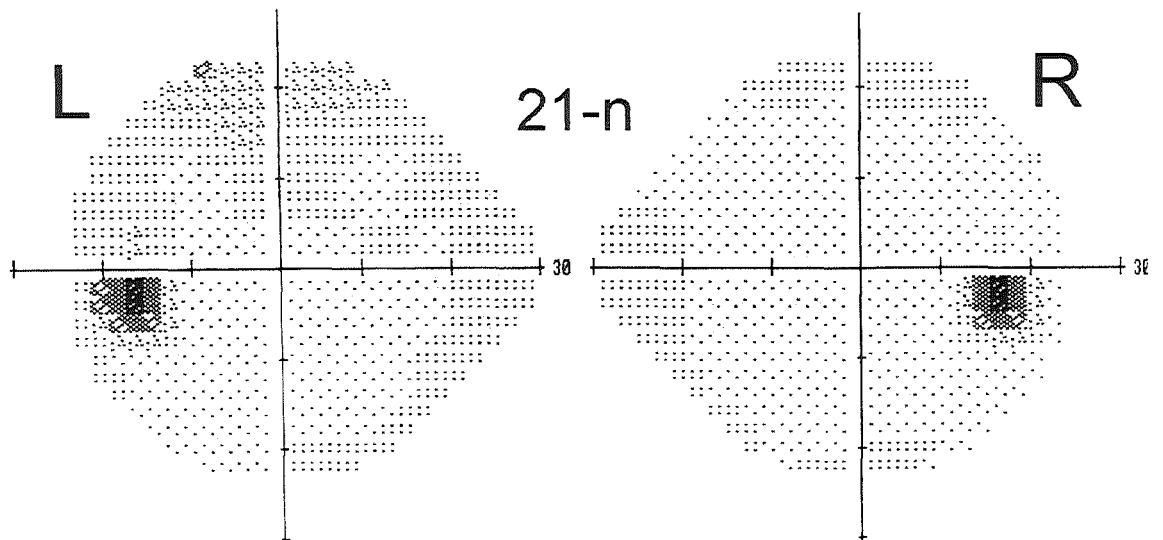


Figure 5.2-20 Humphrey visual field plot using the Central 24-2 programme for subject 21-n, 65 year old male, MD = -0.2dB, +2.1dB, L = left eye, R = right eye.

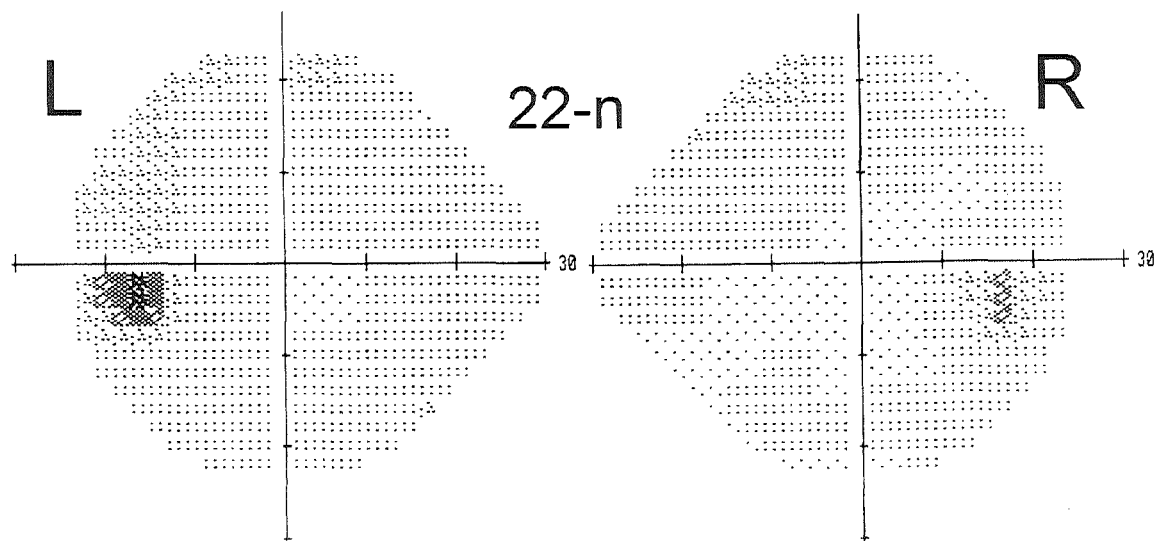


Figure 5.2-21 Humphrey visual field plot using the Central 24-2 programme for subject 22-n, 55 year old male, MD = -2.8dB, -0.8dB, L = left eye, R = right eye.

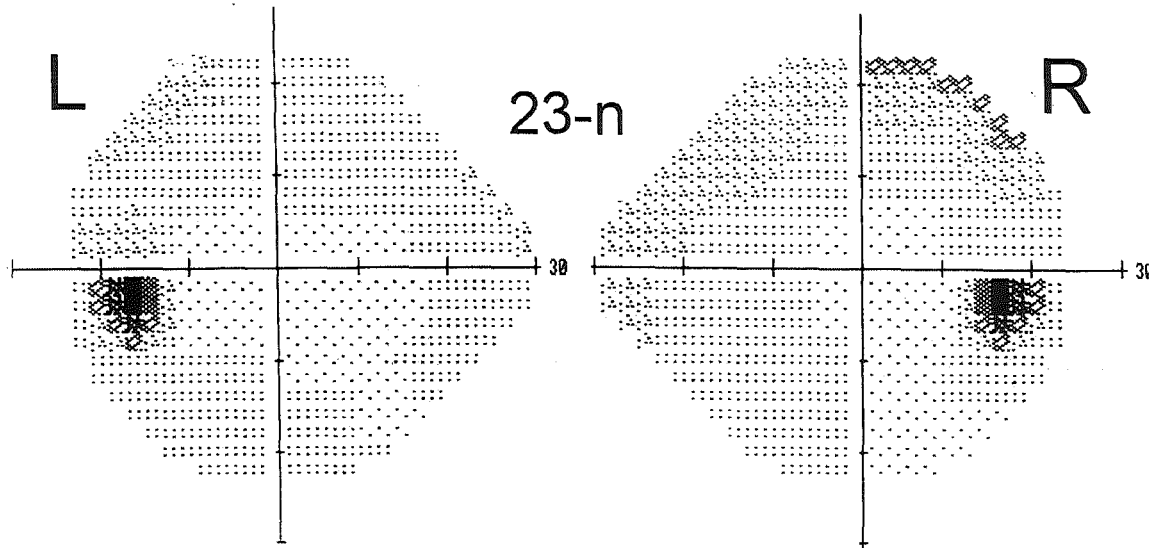


Figure 5.2-22 Humphrey visual field plot using the Central 24-2 programme for subject 23-n, 59 year old female with amblyopia in her right eye, MD = -2.0dB, -2.1dB, L = left eye, R = right eye.

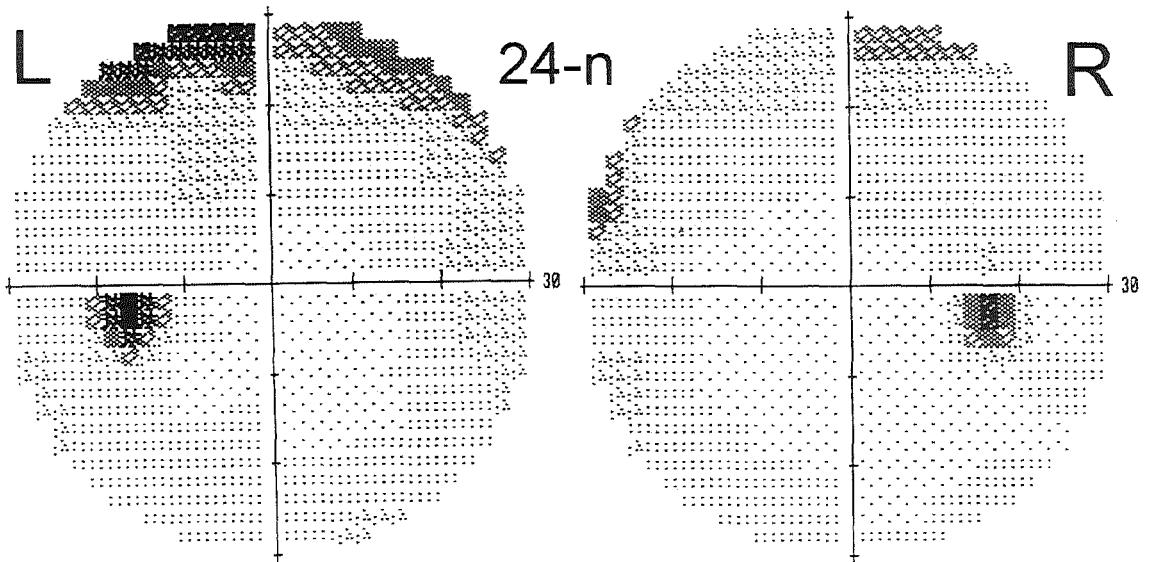


Figure 5.2-23 Humphrey visual field plot using the Central 30-2 programme for subject 24-n, 59 year old male showing loss of sensitivity in upper field (especially in left eye), repeat testing showed similar results, but ophthalmologic examination identified no abnormality, MD = -1.7dB, -0.3dB, L = left eye, R = right eye.

### 5.3 Calculation of blind spot as fraction of quadrant area

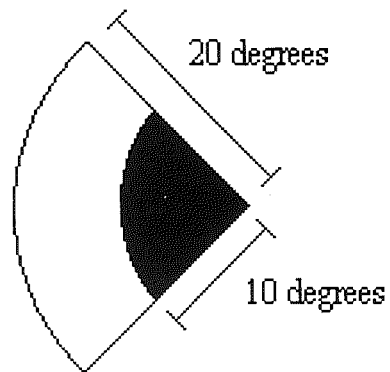
Area of truncated quadrant

$$\begin{aligned}
 &= \frac{1}{4} \pi r_o^2 - \frac{1}{4} \pi r_i^2 \\
 &= \frac{1}{4} \pi (20)^2 - \frac{1}{4} \pi (10)^2 \\
 &= \frac{300\pi}{4}
 \end{aligned}$$

where :

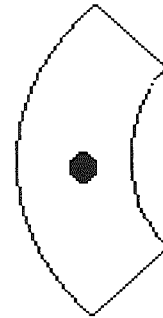
$r_o$  is outer radius

$r_i$  is inner radius



Area of blind spot -  $5^\circ$  in diameter

$$\begin{aligned}
 &= \pi \left(\frac{5}{2}\right)^2 \\
 &= \left(\frac{25\pi}{4}\right) / \left(\frac{300\pi}{4}\right) \\
 &= \frac{25}{300} \times 100 \\
 &= 8\% \text{ area of quadrant}
 \end{aligned}$$



## 5.4 Conversion equations for SBR readings

All 6 readings for inter-ocular, and 6 readings each for both eyes of both intra-ocular tests (5 sets of results in all) were individually converted into a value for percentage difference in sensitivity. This was achieved by the following steps, using the Minitab 11 statistical package:

- The raw value for filter position in mm, at the subject's chosen point of matching brightness, was converted to NDF strength using the calibration equation, (previously stated in Methods section 2.2):

*Equation 2.2-1* 
$$y = 0.12 + 0.009 x$$

- The NDF strength was converted to a difference in strength between the variable and fixed filter (the latter was usually 0.6 log units, but occasionally a stronger or weaker filter was necessary).
- The sign of this difference was stored in a separate Minitab worksheet column as +1 or -1
- The sign of the difference was then removed from the column of NDF difference
- The NDF difference (without sign) was converted to a % difference in sensitivity by using the equation:

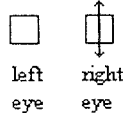
*Equation 5.3-1* 
$$\% \text{ difference} = ((\text{anti log } (x) * 100) - 100)$$

where x is the NDF difference

- The sign was re-applied by multiplying the percentage difference sensitivity data against the stored +1 / -1 value

The mean  $\pm$  SE for the percentage difference in sensitivity to brightness for each pair of test regions (i.e. central vision of both eyes; upper and lower vision for each eye or nasal and temporal vision for each eye) was then be calculated.

Table 5.4-1 Mean SBRs for older control group with prediction limits and P-value for difference between mean and zero using one-sample t-test.

TEST PERFORMED		MEAN (%)	PREDICTION LIMITS: MEAN ± 2 SD (%)	P-VALUE, ONE-SAMPLE T-TEST
Upper / lower	<b>Right Eye</b> 	-15.5	-84.1 to +53.1	0.009
	<b>Left Eye</b> 	-21.8	-97.2 to +53.6	0.0001
Nasal / temporal	<b>Right Eye</b> 	-7.9	-75.9 to +60.1	0.2
	<b>Left Eye</b> 	6.7	-80.9 to +94.3	0.4
<b>Right / left eye</b>		2.1	-70.4 to +74.9	0.3

## 5.5 Glaucoma patient details

Table 5.5-1 Further details of patients glaucoma, medications specific to glaucoma at the time of the experiments, surgery for glaucoma prior to the experiments, recorded cup to disc ratio and IOP history, and any other relevant details from case notes relevant to visual health.

Patient ID	Glaucoma medication	Glaucoma surgery	Cup to disc ratio (right eye / left eye, year recorded)	IOP	Other relevant details
1-g	Betagan 0.5% both eyes, 1994 onwards	Trabeculectomy both eyes, 1993	pathological cupping, both discs	Peaked at 32/40mmHg 1992, below 20mmHg since 1994	—
2-g	None	None	0.7/0.4, 1998	Below 20mmHg both eyes	Retinal detachment left eye, brother has glaucoma
3-g	None	Trabeculectomy both eyes, 1993	0.7/0.9, 1994	Peaked at 28/30 mmHg, 1993, below 20mmHg since then	Cataracts both eyes
4-g	Trusopt, three times daily	None	0.5/0.7, 1997	Peaked at 31/30, 1996	Strong family history of glaucoma
5-g	Cosopt, twice daily, both eyes	None	0.9/0.8, 1989	Currently well controlled at 19/20mmHg	Repaired retinal detachment, right eye, 1982
6-g	None	Trabeculectomy both eyes, prior to 1997, right trabeculectomy, 1997	0.95/0.8, 1997	Peaked at 21/36 mmHg, 1997, 20 or below since	—
7-g	None	Trabeculectomy both eyes, 1993	0.75.0.7	—	Cataract (1993) and intra-ocular lens implantation (1996) surgery, both eyes
8-g	Cosopt, twice daily, right eye	Trabeculectomy right eye – multiple operations, 1971 - 1981	advanced cupping, right eye	Peaked at 34mmHg, right eye 1999	Long history of glaucoma
9-g	Cosopt twice daily, left eye	None	0.6/0.8, 1999	'top end of normal'	—
10-g	None	Trabeculectomy right eye. 1992 and 1998	—	Peaked at 30 mmHg, 1992	—
11-g	Bet/chlor/cyclo	Trabeculectomy left eye, 1999	0.7/1.0	Peaked 24/19 mmHg, 1999	—
12-g	Betagan, twice daily, both eyes	None	'asymmetric cupping' 0.4/0.3	Peaked 30/25 mmHg, 1991, controlled since	—
13-g	Cosopt, both eyes	YAG, both eyes 1998	0.8/0.8	30/32 mmHg on several occasions	Father had glaucoma

Patient ID	Glaucoma medication	Glaucoma surgery	Cup to disc ratio (right eye / left eye, year recorded)	IOP	Other relevant details
14-g	None	Trabeculectomy both eyes	0.7/0.7	Peaked at 25/46 mmHg, 1993, 19/20 mmHg, 1999	Cataract extraction, left eye 1992
15-g	None	Trabeculectomy left eye, 1990 and 1995	0.6	20/8, 1999	Cataract extraction left eye 1992
16-g	Cosopt and Xalatan, left eye	Trabeculectomy both eyes	'End stage pathological cupping, both discs' 0.7/0.7	—	—
17-g	None	None	'left disc pale' 0.4/0.5	Peaked at 20/22 mmHg	—

Abbreviations and symbol used in Table

-g = glaucoma patient identifier

IOP = intra-ocular pressure

mmHg = millimetres of mercury

— = indicates that patient's case notes did not contain this information

## 5.6 Equations used in Discussion

*Equation 5.6-1 To calculate the sensitivity of a test, which is the ability of the test to produce a negative test result in an individual who does not have the disease.*

$$\text{Sensitivity} = \frac{\text{true positives}}{\text{false negatives} + \text{true positives}}$$

(Wald, 1994)

*Equation 5.6-2 To calculate the specificity of a test, which is the ability of the test to produce a positive test result in an individual who does have the disease.*

$$\text{Specificity} = \frac{\text{true negatives}}{\text{true negatives} + \text{false positives}}$$

(Wald, 1994)

## 5.7 Additional analysis – monocular data

### 5.7.1 Contrast threshold

Where both eyes were normal in control subjects, or both eyes had glaucoma in the patient group, one eye was chosen using a random number table from the internet web site: <http://www.mrs.umn.edu/~sungurea/introstat/public/instruction/ranbox/randomnumbersII.html>, where odd numbers were taken to indicate the left eye, and even numbers the right. Where one eye was normal in the control group or one eye had glaucoma in the patient group, only the values from that eye have been used.

The mean contrast threshold in the **age-matched control group** using monocular data was 0.034 contrast units, and the SD was 0.018. This gave rise to an upper confidence limit of 0.070 contrast units; this is marked with a dotted line on the graph below (Figure 5.7-1). The Figure shows the mean contrast threshold readings for one eye each of the glaucoma patient group in relation to the upper confidence limit. The contrast thresholds of three patients with glaucoma were within the normal range (1-g, 7-g, 17-g), and the OHT patient's thresholds were normal (12-g).

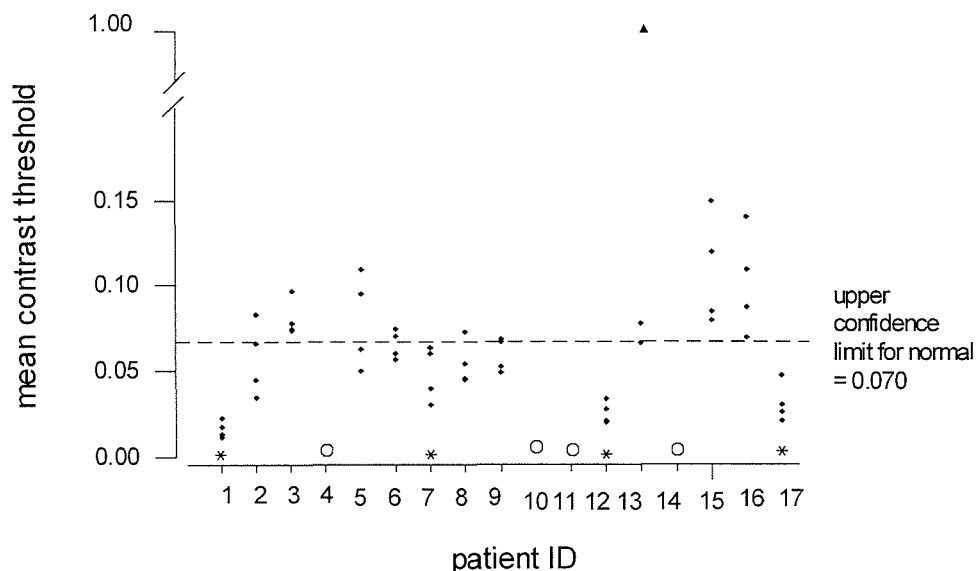


Figure 5.7-1 Contrast threshold readings for one eye each of patient group as compared to the upper confidence limit for age-matched normal group (dotted line), default score of 1.0 indicated by triangle, open circles indicate subjects who did not complete the experiment, asterisks indicate readings which are all within normal range.

The upper confidence limit for normal was slightly lower when monocular data from the older control group was used (0.070 compared to 0.073 contrast units using binocular data), and this led to a minor change in the results. All mean contrast thresholds of glaucoma patients 1-g and 17-g and OHT patient 12-g were normal by both methods, however, using monocular data the readings of patient 7-g were all in the normal range, whereas those of patient 9-g included 2 readings which just exceeded the limit. The reverse result had been obtained using binocular data. Therefore, the same number of patients were identified as abnormal by each analytical method.

The same method for random choice of eye was also applied to the young control group, and a mean contrast threshold of 0.034 units (SD 0.015) was obtained. This gives an upper confidence limit of 0.065 contrast units. This can be compared with the monocular data from the **older control group** in which the mean contrast threshold was 0.033 contrast units  $\pm$  0.018 SE, giving an upper confidence limit of 0.069 units. Mean contrast thresholds for these two groups are shown in Figure 5.7-2.

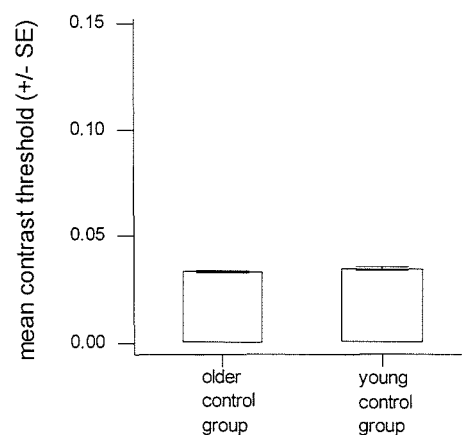


Figure 5.7-2 Mean contrast threshold ( $\pm$ SE) in older control group and young control group using monocular data.

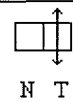
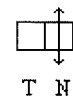
A two-sample t-test on the group means indicated no significant difference  $P = 0.2$ , in contrast to the result using the binocular data which had demonstrated a significantly higher mean contrast threshold in the younger control group.

### 5.7.2 Simultaneous Brightness Ratio

As described above, one eye of each patient and subject was randomly selected and the mean intra-ocular SBRs were determined in those eyes. As there is a difference between the perception of the fixed and changeable filters for the nasal / temporal comparison (during which, the position of the fixed filter changed, according to which eye was being used) the data were kept 'eye-specific' with nasal / temporal data for both right and left eyes individually.

The mean SBRs in the age-matched control group were similar whether monocular or binocular data was used, although the confidence limits were wider using the monocular analysis, probably due the reduced amount of data, as shown in Table 5.7-1. There remained evidence of a statistically significant difference between the mean SBR and zero in the upper / lower comparisons. Additionally there was also a significant difference in the nasal / temporal comparison for the right eye.

Table 5.7-1 Mean SBRs for age-matched control group with prediction limits and P-value for difference between mean and zero using one-sample t-test.

TEST PERFORMED		MEAN (%)	PREDICTION LIMITS: MEAN ± 2 SD (%)	P-VALUE, ONE-SAMPLE T-TEST
Upper / lower	Both Eyes 	-23.1	-95.7 to +49.5	0.001
	Right Eye 	-9.2	-74.2 to +55.8	0.010
Nasal / temporal	Left Eye 	-0.9	-109.1 to +107.3	0.90

The prediction limits for the age-matched control group were used to define the glaucoma patient results as normal or abnormal, and are marked on Figure 5.7-3: the abnormal results are indicated with a cross on the Figure.

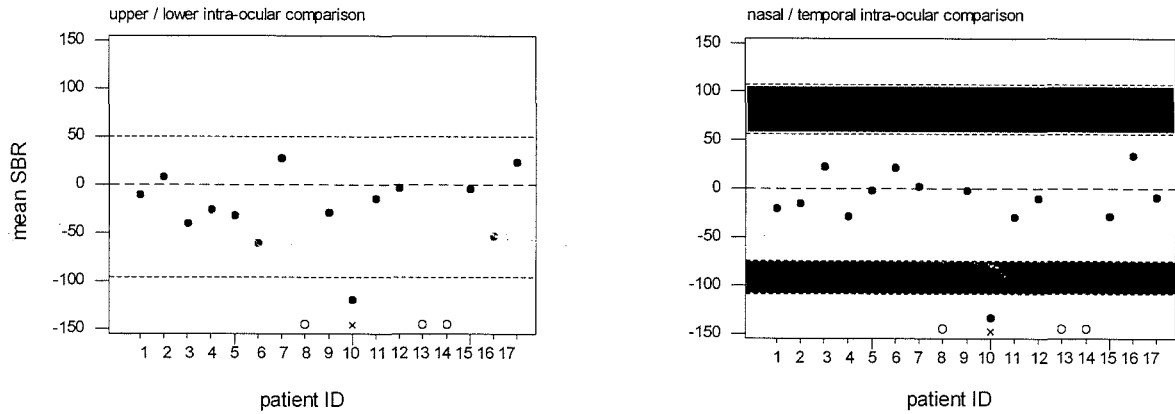


Figure 5.7-3 Mean intra-ocular SBRs for upper / lower (left) and nasal / temporal (right) comparisons in one eye each of glaucoma patients. Prediction limits marked by dotted lines – hatched area on right graph indicates both right and left eye limits. Crosses indicate those SBRs which fall outside confidence limit for age-matched group for that eye, open circles indicate those who didn't complete this test.

As the Figure shows, using monocular prediction limits from the age-matched control subjects, 1 patient (10-g) was identified as abnormal by both his upper / lower intra-ocular and nasal / temporal comparisons. This confirms SBR, as measured by this method, as a poor indicator of individuals with visual field loss.

The **older control group** in its entirety was used to define confidence limits against which to compare the young control group SBR results. As before, monocular data was used and the mean, prediction limits and one-sample t-test results are shown in Table 5.7-2.

Table 5.7-2 Mean SBRs for older and young control groups with prediction limits and P-value for difference between mean and zero using one-sample t-test.

TEST PERFORMED		CONTROL GROUP	MEAN (%)	PREDICTION LIMITS: MEAN ± 2 SD (%)	P-VALUE, ONE-SAMPLE T-TEST
Upper / lower	Both Eyes U L	OLDER	-21.7	-92.7 to +49.3	0.0001
		YOUNG	-0.8	-87.2 to +85.6	0.83
Nasal / temporal	Right Eye N T	OLDER	-9.2	-74.1 to +55.7	0.024
		YOUNG	0.6	-90.7 to +92.0	0.98
	Left Eye T N	OLDER	0.2	-107.7 to +108.2	0.97
		YOUNG	17.9	-57.1 to +93.0	0.024

The mean SBR was significantly different from zero in the upper / lower and nasal / temporal comparison in the right eye for the older group, but only the nasal / temporal left eye comparison in the young group.

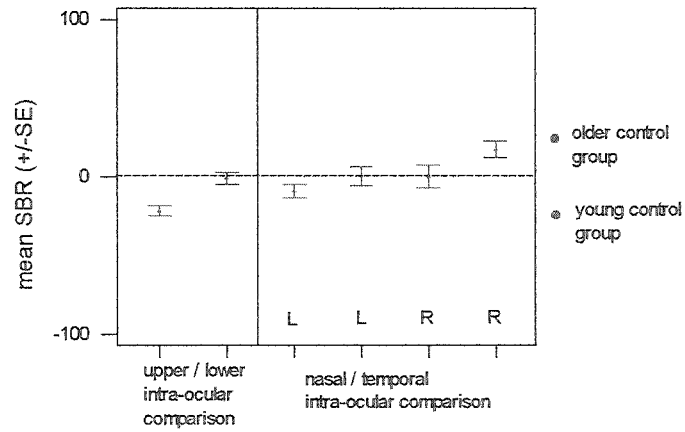


Figure 5.7-4 Mean SBRs  $\pm$ SE of young and older control group

This form of analysis did not significantly alter the relationship between the young and older control groups, when investigated using a two-sample t-test, as there was a significant difference between the groups in the upper / lower comparisons, ( $P < 0.05$ ), but no difference in the nasal / temporal comparisons – similar to the result as obtained using binocular data.

## 6 Bibliography

- ABE, H., HASEGAWA, S. & IWATA, K. (1987). Contrast sensitivity and pattern visual-evoked potential in patients with glaucoma. *Documenta Ophthalmologica* **65** 65 – 70
- ABRAMS, L.S., SCOTT, I.U., SPAETH, G.C., QUIGLEY, H.A. & VARMA, R. (1994). Agreement among optometrists, ophthalmologists and residents in evaluating the optic disc for glaucoma. *Ophthalmology* **101** 1662 - 1667
- ANDERSON, R.S. & O'BRIEN, C. (1997). Psychophysical evidence for a selective loss of M ganglion cells in glaucoma. *Vision Research* **37** 1079-1083
- ARAIE, M., YAMAGAMI, J. & SUZUKI, Y. (1993). Visual field defects in normal-tension and high tension glaucoma. *Ophthalmology* **100** 1808 - 1814
- ARDEN, G.B. & JACOBSON, J.J. (1978). A simple grating test for contrast sensitivity: preliminary results indicate value in screening for glaucoma. *Investigative Ophthalmology and Visual Science* **17** 23-32
- ASMAN, P. & HEIJL, A. (1994). Diffuse visual field loss and glaucoma. *Acta Ophthalmologica* **72** 303-308
- AULHORN, E. & KARMEYER, H. (1977). Frequency distribution in early glaucomatous visual field defects. *Documenta Ophthalmologica Proceedings Series* **14** 75-83
- AZUMA, I. (1996). Glaucoma and the autoregulation. *NeuroOphthalmology Japan* **13** 3-6  
N.B. article is in Japanese, quoting only from abstract
- BACH, M. & SPEIDEL-FIAUX, A. (1989). Pattern electroretinogram in glaucoma and ocular hypertension. *Documenta Ophthalmologica* **73** 173-181
- BALAZSI A.G., ROOTMAN J. DRANCE S.M., SCHULZER M. & DOUGLAS G.R. (1984). The effect of age on the nerve fiber population of the human optic nerve. *American Journal of Ophthalmology*. **97** 760-766
- BALLON, B.J., ECHELMAN, D.A., SHIELDS, A.R. & OLLIE, A.R. (1992). Peripheral visual field testing in glaucoma by automated kinetic perimetry with the Humphrey visual field analyser. *Archives of Ophthalmology* **110** 1730-1732
- BATHIJA, R., GUPTA, N., ZANGWILL, L. & WEINREB, R.N. (1998). Changing definition of glaucoma. *Journal of Glaucoma* **7** 165-169
- BERNE, R.M. & LEVY, M.N. (2000). Principles of physiology. *St. Louis: C.V. Mosby co.* **3ed**
- BODIS-WOLLNER, I. (1979). Detection of visual defects using the contrast sensitivity function. *Investigative Ophthalmology and Visual Science* **20** 135-153
- BODIS-WOLLNER, I & BRANNAN, J.R. (1994). Assessment of current visual and psycho-physical testing methods with special reference to primary open angle glaucomatous disease. *Neuro-Ophthalmology* **14** 61-71
- BORGMANN, C., STEINER, H. & DUTTON, G.N. (1991). Optimum technique of light brightness assessment in control subjects and patients with ocular hypertension and glaucoma. *Ophthalmologica* **203** 126-132

- BOWMAKER, J.K. & DARTNALL, H.J.A. (1980). Visual pigments of rods and cones in a human retina. *Journal of Physiology* **298** 501-511
- BRANDT, J.D. & O'DONNELL, M.E. (1999). How does the trabecular meshwork regulate outflow? Clues from the Vascular Endothelium *Journal of Glaucoma* **8** 328 - 339
- BRETON, M.E., WILSON, T.W., WILSON, R., SPAETH, G.L. & KRUPIN, T. (1991). Temporal contrast sensitivity loss in primary open angle glaucoma and glaucoma suspects. *Investigative Ophthalmology and Visual Science* **32** 2931-2940
- CAPRIOLI, J. (1997). Neuroprotection of the optic nerve in glaucoma. *Acta Ophthalmologica Scandinavica* **75** 364-367
- CHIA, W-L.A., GOLDBERG, I. & BAUMAN, A. (1999). Evaluation of oculokinetic perimetry. *Australian and New Zealand Journal of Ophthalmology* **27** 306 - 311
- CRAWFORD, M.L.J., HARWERTH, R.S., SMITH, E.L. III, SHEN, F. & CARTER-DAWSON, L. (2000). Glaucoma in primates: cytochrome oxidase reactivity in parvo- and magnocellular pathways. *Investigative Ophthalmology and Visual Science* **41** 1791 - 1802
- CUMMINS, D., MACMILLAN, E.S., HERON, G. & DUTTON, G.N. (1994). Simultaneous interocular brightness sense testing in ocular hypertension and glaucoma. *Archives of Ophthalmology* **112** 1198-1203
- DACEY, D., PACKER, O.S., DILLER, L., BRAINARD, D., PETERSON, B. & LEE, B. (2000). Center surround receptive field structure of cone bipolar cells in primate retina. *Vision Research* **40** 1801-1811
- DACEY, D.M. (2000). Parallel pathways for spectral coding in primate retina. *Annual Reviews Neuroscience* **23** 743-775
- DANDONA, L., HENDRICKSON, A. & QUIGLEY, H.A. (1991). Selective effects of experimental glaucoma on axonal transport by retinal ganglion cells to the dorsal lateral geniculate nucleus. *Investigative Ophthalmology and Visual Science* **32** 1593-1599
- DAVSON, H. (1990). Physiology of the eye. *Macmillan Press, London* **5ed**
- DAWSON, W.W. & MAIDA, T.M. (1984). Relations between the human retinal cone and ganglion cell distribution *Ophthalmologica* **188** 216-221
- DE MONASTERIO, F.M. (1978). Properties of ganglion cells with atypical receptive-field organization in retina of macaques. *Journal of Neurophysiology* **41** 1435-1449
- DESATNIK, H., QUIGLEY, H.A. & GLOVINSKY, Y. (1996). Study of central retinal ganglion cell loss in experimental glaucoma in monkey eyes. *Journal of Glaucoma* **5** 46-53
- DEVOS, M., DEVOS, H., SPILEERS, W. & ARDEN, G.B. (1995). Quadrant analysis of peripheral colour contrast thresholds can be of significant value in the interpretation of minor visual field alterations in glaucoma suspects *Eye* **9** 751 - 756
- DODT, E. (1987). The electrical response of the human eye to patterned stimuli: clinical observations. *Documenta Ophthalmologica* **65** 271 - 286
- DRANCE, S.M. (1985). The early structural and functional disturbances of chronic open angle glaucoma: The Robert N. Shaffer lecture. *Ophthalmology* **92** 853-857

- DRANCE, S.M. (1996). The concept of chronic open angle glaucoma: a personal view. *Ophthalmologica* **210** 251-256
- DRAPER, N. & SMITH, H. (1981). Applied regression analysis. *John Wiley and Sons* **2ed**
- EMERY, J.M., LANDIS, D., PATON, D., BONIUK, M. & CRAIG, J.M. (1974). The lamina cribrosa in normal and glaucomatous human eyes. *Transactions American Academy of Ophthalmology and Otolaryngology* **78** 290-297
- FALCÃO-REIS, F., O'DONOGHUE, E., BUCETI, R., HITCHINGS, R.A. & ARDEN G. B. (1990). Peripheral contrast sensitivity in glaucoma and ocular hypertension. *British Journal of Ophthalmology* **74** 712-716
- FECHTNER, R.D. & WEINREB, R.N. (1994). Mechanisms of optic nerve damage in primary open angle glaucoma. *Survey of Ophthalmology* **39** 23-42
- FINDL, O., STRENN, K., WOLZT, M., MENAPACE, R., VASS, C., EICHLER, H. & SCHMETTERER, L. (1997). Effect of changes of intraocular pressure on human ocular haemodynamics. *Current Eye Research* **16** 1024-1029
- FITZKE, F.W., HITCHINGS, R.A. POINOOSAWMY, D., MCNAUGHT, A.I. & CRABB, D.P. (1996). Analysis of visual field progression in glaucoma. *British Journal of Ophthalmology* **80** 40-48
- FONTANA, L., POINOOSAWMY, D., BUNCE, C.V., O'BRIEN, C. & HITCHINGS, R.A. (1998). Pulsatile ocular blood flow investigation in asymmetric normal tension glaucoma and normal subjects. *British Journal of Ophthalmology* **82** 731-736
- FREEMAN, M.H. (1990). Optics *London: Butterworths* **10ed**
- GAASTERLAND, D., TANISHIMA, T. & KUWABARA, T. (1978). Axoplasmic flow during chronic experimental glaucoma. *Investigative Ophthalmology and Visual Science* **17** 838-846
- GAO, H. & HOLLYFIELD, J.G. (1992). Aging of the human retina. *Investigative Ophthalmology and Visual Science* **33** 1-17
- GARCIA-VALENZUELA, E. SHAREEF, S., WALSH, J. & SHARMA, S.C. (1995). Programmed cell death of retinal ganglion cells during experimental glaucoma. *Experimental Eye Research* **61** 33-44
- GARWAY-HEATH, D.F., WOLLSTEIN, G. & HITCHINGS, R.A. (1997). Aging changes of the optic nerve head in relation to open angle glaucoma. *British Journal of Ophthalmology* **81** 840-845
- GEIJSEN AND, H.C. & GREVE, E.L. (1995). Vascular concepts in glaucoma *Current Opinion in Ophthalmology* **6** 71 - 77
- GLOOR, B.P. AND VOKT, B.A. (1985) Long-term fluctuations versus actual field loss in glaucoma patients. *Developmental Ophthalmology* **12** 48-69
- GLOVINSKY, Y., QUIGLEY, H.A., DRUM, B., BISSET, R.A. & JANPEL, H.D. (1992). A whole field scotopic retinal sensitivity test for the detection of early glaucoma damage. *Archives of Ophthalmology* **110** 486-490
- GLOVINSKY, Y., QUIGLEY, H.A. & DUNKELBERGER, G.R. (1991). Retinal ganglion cell loss is size dependent in experimental glaucoma. *Investigative Ophthalmology and Visual Science* **32** 484-491

- GONZALEZ, I., PABLO, L.E., PUEYO FERRER, P.E., MELCON, B., ABECIA, E. & HONRUBIA, F.M. (1997). Assessment of diurnal tension curve in early glaucoma damage. *International Ophthalmology* **20** 113-115
- GRAHAM, S. L. (1997). Selective nerve fibre loss in glaucoma: magnocellular or parvocellular. *Australian and New Zealand Journal of Ophthalmology* **25** 189 - 191
- GRAHAM, S.L. & KLITORNER, A. (1998). Electrophysiology: A review of signal origins and applications to investigating glaucoma. *Australia and New Zealand Journal of Ophthalmology* **26** 71-85
- GRUNWALD, J.E. (1994). Intraocular Pressure and retinal blood flow in the normal human and glaucomatous eye. *Chibret International Journal* **10** 13-15
- GUYTON, A.C. AND HALL, J.E. (1996). Textbook of medical physiology *W.B. Saunders Company* 9ed
- HAWLINA, M., STRŪCL, M., STIRN-KRANJC, B., FINDERLE, Z. & BRECELJ, J. (1989). Pattern electroretinogram recorded by skin electrodes in early ocular hypertension and glaucoma. **73** 183 - 191
- HEALEY, P.R., MITCHELL, P., SMITH, W. & WANG, J.J. (1997). The influence of age and IOP on the optic cup in a normal population. *Journal of Glaucoma* **6** 274-278
- HENDRY, S.H.C & REID, R.C. (2000). The koniocellular pathway in primate vision. *Annual Reviews Neuroscience* **23** 127-153
- HENSON, D.B. (1993). Visual Fields. *Oxford : Oxford University Press*
- HERNDON, L.W., CHOUDRI, S.A., COX, T., DAUJI, K.F., SHIELDS, M.B. & ALLINGHAM, R.R. (1997). Central corneal thickness in normal, glaucomatous and ocular hypertensive eyes. *Archives of Ophthalmology* **115** 1137-1141
- HILZ, R. & CAVONIUS, C.R. (1974). Functional organization of the peripheral retina: sensitivity to periodic stimuli. *Vision Research* **14** 1333-1337
- HITCHINGS, R.A. (1997). Duke Elder lecture. Flying blind. *Eye* **11** 771-778
- HITCHINGS, R.A., POWELL, D.J., ARDEN, G.B. & CARTER, R.M. (1981). Contrast sensitivity gratings in glaucoma family screening. *British Journal of Ophthalmology* **65** 515-517
- HOEKSTRA, J., VAN DER GOOT, D.P.J, VAN DEN BRINK, G. & BILSEN, F.A. (1973). The influence of the number of cycles upon the visual contrast threshold for spatial sine wave patterns. *Vision Research* **14** 365 - 368
- HOLOPIGIAN, K., SEIPLE, W., MAYRON, C., KOTY, R. & LORENZO, M. (1990). Electrophysiology and psychophysical flicker sensitivity in patients with primary open angle glaucoma and ocular hypertension. *Investigative Ophthalmology and Visual Science* **31** 1863 - 1868
- HOOD, D.C., GREENSTEIN, V.C., HOLOPIGIAN, K., BAUER, R., FIROZ, B., LIEBMANN, J.M., ODEL, J.G. & RITCH, R. (2000). An attempt to detect glaucomatous damage to the inner retina with the multifocal ERG. *Investigative Ophthalmology and Visual Science* **41** 1570-1579
- HORN, F.K., KORTH, M. & MARTUS, P. (1994). Quick full-field flicker test in glaucoma diagnosis: correlations with perimetry and papillometry. *Journal of Glaucoma* **3** 206-213

- HOSKINS JR, H.D. & KASS, M. (1989). Becker - Shaffer's Diagnosis and therapy of the glaucomas. *St. Louis : Mosby*
- ISAYAMA, Y., MIZOKAMI, K. & TAGAMI, Y. (1980) Spatial contrast sensitivity in optic nerve disorders. Its relationship to the visual fields and the atrophy of retinal nerve fibre layer. *Japanese Journal of Ophthalmology* **34** 293-300  
N.B. article is in Japanese, read in abstract
- JANSSEN, P., NASKAR, R., MOORE, S., THANOS, S. & THIEL, H. (1997). Evidence for glaucoma-induced horizontal cell alterations in the human retina. *German Journal of Ophthalmology* **5** 378-385
- JAY, J.L. (1992 ) (a). Medical versus surgical treatment of primary open angle glaucoma. *Recent Advances in Ophthalmology* Churchill Livingstone **8ed**
- JAY, J.L. (1992 ) (b). Rational choice of therapy in primary open angle glaucoma. *Eye* **6** 243-247
- JAY, J.L. (1994). Computerised perimetry: the emperor's new clothes? *British Journal of Ophthalmology* **78** 513-515
- JAY, J.L. & MURDOCH, J.R (1993). The rate of visual field loss in untreated primary open angle glaucoma. *British Journal of Ophthalmology* **77** 176-178
- JAY, J.L. & MURRAY, S.B. (1980). Characteristics of reduction of intra ocular pressure after trabeculectomy. *British Journal of Ophthalmology* **64** 432-435
- JOHNSON, B.M., MIAO, M. & SADUN, A.A. (1987). Age related decline of human optic nerve axon populations. *Age* **10** 5-9
- JOHNSON, C.A. (1994). Selective versus non-selective losses in glaucoma. *Journal of Glaucoma* **3S1** 32-44
- KAHN, H.A. & MILTON, R.C. (1980). Alternative definitions of open angle glaucoma. *Archives of Ophthalmology* **98** 2172-2177
- KANSKI, J.J., MCALLISTER, J.A. & SALMON, J.F. (1996). Glaucoma. A colour manual of diagnosis and treatment. *Butterworth-Heinemann* **2 ed**
- KELLY, D.H. (1984). Retinal inhomogeneity. I. Spatiotemporal contrast sensitivity. *Journal of the Ophthalmologic Society of America A*. **1** 107-113
- KENDALL, K.R., QUIGLEY, H.A., KERRIGAN, L.A., PEASE, M.E. & QUIGLEY E.N. (1995). Primary open angle glaucoma is not associated with photoreceptor loss. *Investigative Ophthalmology and Visual Science* **36** 200-205
- KERR, J., NELSON, P. & O'BRIEN, C. (1998) A comparison of ocular blood flow in untreated primary open-angle glaucoma and ocular hypertension. *American Journal of Ophthalmology* **126** 42-51
- KITAZAWA, Y. & YAMAMOTO, T. (1997). Glaucomatous visual field defects: their characteristics and how to detect them. *Clinical Neuroscience* **4** 279-283
- KLINE, R.P., RIPPS, H. & DOWLING, J.E. (1978). Generation of b-wave currents in the skate retina. *Proceedings of the National Academy of Science USA* **75** 5727-5731

- KUYK T.K. & WESSON, M.D. (1991). Aging-related foveal flicker sensitivity losses in normal observers. *Optometry and Vision Science* **68** 786-789
- LAMPERT, P.W., VOGEL, M.H. & ZIMMERMAN, L.E. (1968). Pathology of the optic nerve in experimental acute glaucoma. *Investigative Ophthalmology* **7** 199-213
- LAQUIS, S., CHAUDHARY, P. & SHARMA, S.C. (1998). The patterns of retinal ganglion cell death in hypertensive eyes. *Brain Research* **784** 100-104
- LEE, B.B. (1996). Mini review: receptive field structure in the primate retina. *Vision Research* **36** 631-644
- LESKE, M. C. (1983). The epidemiology of open-angle glaucoma: a review. *American Journal of Epidemiology* **113** 606-613
- LEWIS, R.A., JOHNSON, C.A. & QUIGLEY, H.A. (1985). Early detection of glaucomatous damage. *Survey of Ophthalmology* **30** 111-126
- LIESGANG, T.J. (1996). Glaucoma: changing concepts and future directions. *Mayo Clinical Proceedings* **71** 689-694
- LIU, J.H.K., KRIPKE, D.F., TWA, M.D., HOFFMAN, R.E, MANSBERGER, S.L., REX, K.M., GIRKIN, C.A. & WEINREB, R.N. (1999). Twenty-four-hour pattern of intraocular pressure in the aging population. *Investigative Ophthalmology and Visual Science* **40** 2912 - 2917
- LUNDH, B.L. (1985). Central and peripheral contrast sensitivity for static and dynamic sinusoidal gratings in glaucoma. *Acta Ophthalmologica* **63** 487-492
- LUNDH, B.L. & GOTTVALL, E. (1995). Peripheral contrast sensitivity for dynamic sinusoidal gratings in early glaucoma. *Acta Ophthalmologica Scandinavica* **73** 202-206
- LUNDH, B.L. & LENNERSTRAND, G. (1981). Eccentric contrast sensitivity loss in glaucoma. *Acta Ophthalmologica* **59** 21-24
- LUNDH, B.L., LENNERSTRAND, G. & DEREFELDT, G. (1983). Central and peripheral normal contrast sensitivity for static and dynamic sinusoidal gratings. *Acta Ophthalmologica* **61** 171-182
- LUSTGARTEN, J.S., MARX, M.S., PODOS, S.M., BODIS-WOLLNER, I., CAMPEAS, D. & SERLE, J.B. (1990). Contrast sensitivity and computerised perimetry in early detection of glaucomatous change. *Clinical Vision Sciences* **5** 407-413
- MACMILLAN, E.S., CUMMINS, D., HERON, G. & DUTTON, G.N. (1994). The simultaneous interocular brightness sense test. *Archives of Ophthalmology* **112** 1190-1197
- MARAFFA, M., MANSOLDO, C., MORBIO, R., DE NATALE, R., TOMAZZOLI, L. & BONOMI, L. (1997). Does nerve fibre layer thickness correlate with visual field defects in glaucoma? *Ophthalmologica* **211** 338-340
- MARC, R.E. & SPERLING, H.G. (1977). Chromatic organization of primate cones. *Science* **196** 454-456
- MARTIN, T.J. & ROBISON, G.D. (1994). Instrument for measuring relative brightness perception. *American Journal of Ophthalmology* **117** 625-631
- MCGRATH, C. & MORRISON, J.D. (1981). The effect of age on spatial frequency perception in human subjects. *Quarterly Journal of Experimental Physiology* **66** 253-261

- MERIGAN, W.H., KATZ, L.M. & MAUNSELL, J.H. (1991). The effects of parvocellular lateral geniculate lesions on the acuity and contrast sensitivity of macaque monkeys. *Journal of Neuroscience* **11** 994-1001
- MERRITT, J.C., CRAWFORD, W.J., ALEXANDER, P.C. (1980). Effect of marijuana on intraocular and blood pressure in glaucoma. *Ophthalmology* **87** 222-228
- MIGDAL, C. (2000). Glaucoma medical treatment: philosophy, principles and practice. *Eye* **14** 515-518
- MIGLIOR, S., BRIGATTI, L., LONATI, C., ROSSETTI, L., PIERROTTET, C. & ORZALESI, N. (1996). Correlation between the progression of optic disc and visual field changes in glaucoma. *Current Eye Research* **15** 145-150
- MINCKLER, D.S., BUNT, A.H. & JOHANSON, G.W. (1977). Orthograde and retrograde axoplasmic transport during acute ocular hypertension in monkeys. *Investigative Ophthalmology and Visual Science* **16** 426-441
- MORGAN, J.E. (1994). Selective cell death in glaucoma: does it really occur? *British Journal of Ophthalmology* **78** 875-879
- MORGAN, J.E., UCHIDA, H. & CAPRIOLI, J. (2000). Retinal ganglion cell death in experimental glaucoma. *British Journal of Ophthalmology* **84** 303 - 310
- MORRISON, J.D. & REILLY, J. (1989). An assessment of decision-making as a possible factor in the age-related loss of contrast sensitivity. *Perception* **15** 541-552
- MOSES, R.A. & HART, W.M. (1987). Adler's physiology of the eye. *C.V. Mosby Company* 8ed
- MOTOLKO, M.A. & PHELPS, C.D. (1984). Contrast sensitivity in asymmetric glaucoma. *International Ophthalmology* **7** 45-50
- MUIR, J.A., BARLOW, H.L. & MORRISON, J.D. (1996). Invariance of the pattern electroretinogram evoked by psychophysically equivalent stimuli in human ageing. *Journal of Physiology* **497** 825-835
- MUNDORF, T.K., ZIMMERMAN, T.J., NARDIN, G.F. & KENDALL, K.S. (1989). Automated perimetry, tonometry and questionnaire in glaucoma screening. *American Journal of Ophthalmology* **108** 505-508
- MUTLUKAN, E. (1995). Campimetry with offset stimulus and dynamic fixation. *University of Glasgow thesis* **10163**
- NEIMA, D., LEBLANC, R. & REGAN, D. (1984). Visual field defects in ocular hypertension and glaucoma. *Archives of Ophthalmology* **102** 1042-1045
- NORDMANN, P. (1996). Early visual disturbances in glaucoma. *Current opinion in Ophthalmology* **7** 1090-1095
- NOURI-MAHDAVI, K., BRIGATTI, L., WEITZMAN, M. & CAPRIOLI, J. (1997). Comparison of methods to detect visual field progression in glaucoma. *Ophthalmology* **104** 1228-1236
- OAKLEY II, B. AND GREEN, D.G. (1976). Correlation of light-induced changes in retinal extracellular potassium concentration with c-wave of the electroretinogram. *Journal of Neurophysiology* **39** 1117-1133

- O'BRIEN, C. (1998) (a) Is there a role for computerised image analysis in glaucoma management? *British Journal of Ophthalmology* **82** 2-3
- O'BRIEN, C. (1998) (b) The optic disc in glaucoma *Ophthalmologic Physiological Optics* **18** 238-239
- ØSTERBERG, G. (1935) Topography of the Layer of Rods and Cones in the Human Retina. *Acta Ophthalmologica*. **s6** 102
- PAPST, N., BOPP, M. & SCHNAUDIGEL, O.E. (1984) (a). Pattern electroretinogram and visually evoked cortical potentials in glaucoma *Graefe's Archive for Clinical and Experimental Ophthalmology* **222** 29 – 33
- PAPST, N., BOPP, M & SCHNAUDIGEL, O.E. (1984) (b). The pattern electroretinogram associated with elevated intraocular pressure *Graefe's Archive for Clinical and Experimental Ophthalmology* **222** 34 – 37
- PARR, J. (1989). Introduction to ophthalmology. *Oxford Medical Publications* **3ed**
- PERKINS, E.S. (1973). The Bedford glaucoma survey, I: longterm follow up of borderline cases. *British Journal of Ophthalmology* **57** 179-185
- PETER, E., THOMAS, R. & MULIYIL, J. (1996). Brightness discrimination test is not useful in screening for open angle glaucoma. *Journal of Glaucoma* **5** 182-186
- POINTER, J.S. (1999). Human intraocular pressure and its diurnal variation in healthy subjects. *Ophthalmological Physiological Optics* **19** S43 – S48
- PORCIATTI, V., FALSINI, B., BRUNOI, S., COLOTTO, A. & MORETTI G. (1987). Pattern electroretinogram as a function of spatial frequency in ocular hypertension and early glaucoma. *Documenta Ophthalmologica* **65** 349-355
- PRESTON, D.S., BERNSTEIN, L. & SADUN, A.A. (1988). Office techniques for detecting optic neuropathies. *Neuro-Ophthalmology* **8** 245-250
- QUIGLEY, H.A. (1990). Advances in diagnosis and treatment of glaucoma. *Maryland Medical Journal* **39** 396- 398
- QUIGLEY, H.A. (1994). Commentary *British Journal of Ophthalmology* **78** 879-880
- QUIGLEY, H.A. (1995). Ganglion cell death in glaucoma: pathology recapitulates ontogeny. *Australia New Zealand Journal of Ophthalmology* **23** 85-91
- QUIGLEY, H.A., ADDICKS, E.M. & GREEN, W.R. (1982). Optic nerve in human glaucoma III. Quantitative correlation of nerve fibre loss and visual field defect in glaucoma, ischemic neuropathy, papilloedema and toxic neuropathy. *Archives of Ophthalmology* **100** 135-146
- QUIGLEY, H.A., ADDICKS, E.M., GREEN, R. & MAUMENEE, A.E. (1981). Optic nerve damage in human glaucoma: II the site of injury and susceptibility to damage. *Archives of Ophthalmology* **99** 635-649
- QUIGLEY, H.A., DUNKELBERGER, G.R. & GREEN, W.R. (1988). Chronic human glaucoma causing selectively greater loss of large optic nerve fibres. *Ophthalmology* **95** 357-363
- QUIGLEY, H.A., ENGER, C., KATZ, J., SOMMER, A., SCOTT, R. & GILBERT, D. (1994). Risk factors for the development of glaucomatous visual field loss in ocular hypertension. *Archives of Ophthalmology* **112** 644-649

- QUIGLEY, H.A., SANCHEZ, R.M., DUNKELBERGER, G.R., L'HERNAULT, N.L. & BAGINSKI, T.A. (1987). Chronic glaucoma selectively damages large optic nerve fibres. *Investigative Ophthalmology and Visual Science* **28** 913-920
- RASKER, M.T., VAN DEN ENDER, A., BAKKER, D. & HOYNG, P.G. (1997). Deterioration of visual fields in patients with glaucoma with and without optic disc haemorrhages. *Archives of Ophthalmology* **115** 1257-1262
- ROSE, K.A., LEVICK, W.R. & BURKE, W. (1997). Changes in the receptive fields of cat retinal ganglion cells affected by pressure on the optic nerve. *Australian and New Zealand Journal of Ophthalmology* **25S1** 61-63
- ROSS, J.E., BRON, A.J. & CLARKE, D.D. (1984). Contrast sensitivity and visual disability in chronic simple glaucoma. *British Journal of Ophthalmology* **68** 821-827
- ROYAL COLLEGE OF OPHTHALMOLOGISTS. (1997) Guidelines for the Management of Ocular Hypertension and Primary Open Angle Glaucoma. *The Invicta Press Ashford Kent and London*
- RUBEN, S.T., HITCHINGS, R.A., FITZKE, F. & ARDEN, G.B. (1994). Electrophysiology and psychophysics in ocular hypertension and glaucoma: evidence for different pathomechanisms in early glaucoma. *Eye* **8** 516-520
- SADUN, A.A. & LESSELL, S. (1985). Brightness-sense and optic nerve disease. *Archives of Ophthalmology* **103** 39-43
- SAMPLE, P.A., BOSWORTH, C.F. & WEINREB, R.N. (1997). Short-wavelength automated perimetry and motion automated perimetry in patients with glaucoma. *Archives of Ophthalmology* **115** 1129-1133
- SAMPLE, P.A., MADRID, M.E. & WEINREB, R.N. (1994). Evidence for a variety of functional defects in glaucoma suspect eyes. *Journal of Glaucoma* **3S** 5-18
- SANO, N. & ADACHI-USAMI, E. (1997). Decreased contrast sensitivity in normal tension glaucoma determined by pattern visually evoked cortical potentials. *Clinical Neuroscience* **4** 292-294
- SCHILLER, P.H. & MALPELI, J.G. (1977). Properties and tectal projections of monkey retinal ganglion cells. *Journal of neurophysiology* **40** 428 - 445
- SCHUMER, R.A. & PODOS, S.M. (1994). The nerve of glaucoma! *Archives of Ophthalmology* **112** 37 - 44
- SHAPLEY, R. & PERRY, V.H. (1986). Cat and monkey retinal ganglion cells and their visual functional roles. *Trends In NeuroScience* **9** 229-235
- SHIELDS, M.B. (1987). Textbook of glaucoma. *Baltimore London : Williams & Wilkins* **2 ed**
- SHIOSE, Y., KITAZAWA, Y., TSUKAHARA, S., AKAMATSU, T., MIZOKAMI, K., FUTA, R., KATSUSHIMA, H. & KOSAKI, H. (1991). Epidemiology of glaucoma in Japan - a nationwide glaucoma survey. *Japanese Journal of Ophthalmology* **35** 133-155
- SILVERMAN, S.E., TRICK, G.L. & HART, W.M. (1990). Motion perception is abnormal in primary open-angle glaucoma and ocular hypertension *Investigative Ophthalmology and Visual Science* **31** 722 - 729

- SOMMER, A. (1989). Intraocular pressure and glaucoma. *American Journal of Ophthalmology* **107** 186-188
- SOMMER, A. (1996). Doynne lecture. Glaucoma: facts and fancies. *Eye* **10** 295-301
- SOMMER, A., TIELSCH, J.M., KATZ, J., QUIGLEY, H.A., GOTTSCH, J.D., JAVITT, J. & SINGH, K. (1991). Relationship between IOP and POAG among white and black Americans. *Archives of Ophthalmology* **109** 1090-1095
- SPONSEL, W.E. (1985) Visual field quantification in the diagnosis and assessment of chronic open angle glaucoma *Bristol University Thesis* **M572**
- SPONSEL, W.E., DEPAUL, K.L., MARTONE, J.F., SHIELDS, M.B., OLLIE, A.R & STEWART, W.C. (1991). Association of Vistech contrast sensitivity and visual field findings in glaucoma. *British Journal of Ophthalmology* **75** 558-560
- STEWART, W.C. & CHAUHAN, B.C. (1995). Newer visual tests in the evaluation of glaucoma. *Survey of Ophthalmology* **40** 119-135
- SUDESH, S., MOSELEY, M.J. & THOMPSON, J.R. (1993). Accuracy of Goldmann tonometry in clinical practice. *Acta Ophthalmologica* **71** 185-188
- SUGIYAMA, T., MORIY, S., OKU, H. & AZUMA, I. (1995). Association of endothelin-1 with normal tension glaucoma: clinical and fundamental studies. *Survey of Ophthalmology* **39S1** 49-56
- TAGAMI, Y., ONUMA, T., MIZOKAMI, K. & ISAYAMA, Y. (1981). Comparison of spatial contrast sensitivity with visual field in optic neuropathy and glaucoma. *Documenta Ophthalmologica Proceedings Series* **26** 147-154
- TEOH, S.L., ALLAN, D., DUTTON, G.N. & FOULDS, W.S. (1990). Brightness discrimination and contrast sensitivity in chronic glaucoma - a clinical study. *British Journal of Ophthalmology* **74** 215-219
- TEZEL, G., KASS, M.A., KOLKER, A.E., BECKER, B. & WAX, M.B. (1997). Plasma endothelin levels in primary open angle glaucoma. *Journal of Glaucoma* **6** 83-89
- TIELSCH, J.M., KATZ, J., SINGH, K., QUIGLEY, H.A., GOTTSCH, J.D., JAVITT, J. & SOMMER A. (1991). A population-based evaluation of glaucoma screening: the Baltimore eye survey. *American Journal of Epidemiology* **134** 1102-1110
- TIELSCH, J.M., SOMMER, A., KATZ, J., ROYALL, R., QUIGLEY, H.A. & JAVITT, J. (1991). Racial variations in the prevalence of primary open-angle glaucoma. The Baltimore eye survey. *Journal of the American Medical Association* **266** 369-374
- TOLHURST, D.J. (1973). Separate channels for the analysis of the shape and the movement of a moving visual stimulus. *Journal of Physiology* **231** 385-402
- TORIS, C.B., YABLONSKI, M.E., WANG, Y-L. & CAMRAS, C.B. (1999). Aqueous humor dynamics in the aging human eye. *American Journal of Ophthalmology* **127** 407 - 412
- TRICK G.L. (1987 ). Pattern reversal retinal potentials in ocular hypertensives at high and low risk of developing glaucoma. *Documenta Ophthalmologica* **65** 79-85
- TUCK, M.W. & CRICK, R.P. (a) (1997). The cost-effectiveness of various modes of screening for primary open angle glaucoma. *Ophthalmic Epidemiology*. **4** 3-17

- TUCK, M.W. & CRICK, R.P. (b) (1997). Screening for glaucoma. Why is the disease underdetected? *Drugs and Aging* **10** 1-9
- TYLER, C.W. (1981). Specific deficits of flicker sensitivity in glaucoma and ocular hypertension. *Investigative Ophthalmology and Vision Science* **20** 204-213
- VAEGAN & HALLIDAY, B.L. (1982). A forced choice test improves clinical contrast sensitivity testing. *British Journal of Ophthalmology* **66** 477-491
- VO VAN TOI, V., GROUNAUER, D.A. & BURCKHARDT, C.W. (1990). Artificially increasing intra-ocular pressure causes flicker sensitivity losses. *Investigative Ophthalmology and Visual Science* **31** 1567-1574
- VRABEC, F. (1976). Glaucomatous cupping of the human optic disc: a neuro histologic study. *Graefe's Archive for Clinical and Experimental Ophthalmology* **198** 223-224
- WALD, N.J. (1994). Guidance on terminology. *Journal of Medical Screening* **1** 76
- WALSH, J.W.T. (1958) The principles of Photometry. *Dover Publications Inc* **3ed**
- WEALE, R.A. (1992). The senescence of human vision. *Oxford Medical Publications* **edition**
- WORMWALD R.P.L., BASAURI, E., WRIGHT, L.A. & EVANS J.R. (1994). The African-Caribbean eye survey: risk factors for glaucoma in a sample of African Caribbean people living in London. *Eye* **8** 315-320
- YAMADA, N., CHEN, P.P., MILLS, R.P., LEEN, M.M., LIEBERMAN, M.F., STAMPER, R.L. & STANFORD, D.C. (1999). Screening for glaucoma with frequency-doubling technology and Damato campimetry *Archives of Ophthalmology* **117** 1479 – 1484
- ZULAUF, M. & FLAMMER, M. (1993). Correlation of spatial contrast sensitivity and visual fields in glaucoma. *Graefe's Archive for Clinical and Experimental Ophthalmology* **231** 146-150